



**THE EFFECT OF POLYMER MATERIALS ON THE
FRACTURE CHARACTERISTICS OF HIGH
PERFORMANCE CONCRETE (HPC)**

By

MOHMED ALKILANI YAHYA

A thesis submitted in partial fulfilment of the requirements of
Edinburgh Napier University, for the award of

Doctor of Philosophy

School of Engineering and the Built Environment
Edinburgh Napier University
Edinburgh, Scotland, United Kingdom

November 2015

DECLARATION

I hereby declare that this thesis together with work contained herein was produced entirely by myself, and contains no materials that have been accepted for the award of any other degree or diploma in any university. To the best of my knowledge and belief, this thesis contains no material previously published or written by another person except where due acknowledgment to others has been made.

Signature:

Mohmed Yahya

DEDICATION

This thesis is dedicated to:

My Father

My head crown (My mother)

My love (My Wife)

My heart (My Children):

Sajida, Mahdi, Solwan, Sarah and Aisha

My Brothers and Sisters:

Souad, Hashem, Nafisa and Iman

ABSTRACT

Compared with most construction materials, concrete is considered as a brittle material, and its brittleness increases with the compressive strength. For super-high-strength concrete, failure can be sudden, explosive and disastrous. Also the tensile strength is not proportionally increased. Therefore, it is necessary to carry out research on the brittleness of concrete in order to establish parameters for assessing the brittleness, find ways to improve the brittleness and tensile strength, and eventually design and manufacture concrete materials with high strength and low brittleness. In this study, strengthening and toughening effects of polymer materials on the high performance concrete (HPC) were investigated. The HPC was manufactured using ordinary Class 52.5 N Portland cement, silica fume and superplasticizer. The adopted polymers included the styrene-butadiene-rubber (SBR) latex, polyvinylidene chloride (PVDC), linear low density polyethylene (LLDPE) and high density polyethylene (HDPE) with contents of 1.5%, 3% and 5% in weight of cement content. The measured material and fracture properties included compressive and tensile strengths, modulus of rupture, Young's modulus, fracture energy, fracture toughness and brittleness. The test results at 28 days indicate that the addition of 1.5% and 3% SBR, PVDC, LLDPE and HDPE into the HPC could largely improve the compressive strength by up to 15.7%, while the addition of 5% SBR, LLDPE and HDPE did not show any enhancement except for 5% PVDC which increased the compressive strength by 10.9%. The tensile strength was considerably increased for all dosages of polymers, with the maximum increases of 72.7% and 83.2% for 3% SBR and 1.5% LLDPE, respectively. The fracture energy were also enhanced by adding 1.5% SBR and all dosages of LLDPE, with a maximum increase of 24.3%, while there were no indications of enhancement for other dosages of polymers. The modulus of rupture, fracture toughness and Young's modulus were not improved for lower dosages of polymers but slightly decreased for higher dosages. The brittleness decreased monotonically with increasing amount of LLDPE, but it increased with increasing amounts of SBR, PVDC and HDPE.

ACKNOWLEDGEMENTS

This study has started since January 2011 under the guidance and supervision of Dr. Binsheng (Ben) Zhang with Dr. Michael Baker as the Second Supervisor. In January 2013, Dr. Zhang moved to Glasgow Caledonian University and as a result the Supervisors exchanged roles. Dr. Barker became the first Supervisor and Dr. Zhang became the Second Supervisor. During the course of the study, Dr. Zhang has given so much invaluable advice, encouragement, and support, and the author is indeed indebted to him. I would like to express my deep gratitude and sincere appreciation to my supervisor, Dr. Michael Barker for his kind support, help and advice.

Thanks are also extended to all staff members in the School of Engineering and the Built Environment at Edinburgh Napier University, in particular, the technical staff of the Heavy Structural Laboratory. Special gratitude is expressed to Mr. Roshan Dhonju. Thanks also go to Ms. Lynn Chalmers of the Advanced Material Laboratory.

Deep gratitude is expressed to my lovely wife, Hend, for her unlimited patience, encouragement and love. I am deeply indebted to her continuous support and extraordinary efforts to take full responsibilities of all shopping and home duties including supporting our five lovely kids, Sajida, Mahdi, Solwan, Sarah and Aisha. My sincere gratitude also goes to my great parents, brother and sisters who always wished me every success.

TABLE OF CONTENTS

DECLARATION	II
DEDICATION	III
ABSTRACT	IV
ACKNOWLEDGEMENTS	V
TABLE OF CONTENTS	VI
LIST OF FIGURES	XI
LIST OF TABLES	XVI
ABBREVIATIONS AND NOTATIONS	XIX
CHAPTER 1 INTRODUCTION	1
1.1 Introduction	1
1.2 Significance of the Study	3
1.3 Aims	3
1.4 Objectives	3
1.5 Research Methodologies	4
1.6 The Outline of the Dissertation	5
CHAPTER 2 LITERATURE REVIEW	7
2.1 High Performance Concrete (HPC).....	7
2.1.1 Introduction	7
2.1.2 Normal strength concrete (NSC)	7
2.1.3 Reactive powder concrete (RPC)	8
2.1.4 High strength concrete (HSC)	8
2.1.5 High performance concrete (HPC).....	9
2.1.5.1 Advantages and disadvantages of HPC with silica fume	9
2.1.5.2 History of development and applications of high performance concrete	10
2.1.6 Lightweight high performance concrete (LHPC).....	10
2.1.7 Ultra-high strength concrete (UHSC).....	11
2.1.8 Mix design methods of HPC	11

2.1.8.1	ACI 211-1 Standard practice for selecting proportions for normal, heavyweight and mass concrete	11
2.1.8.2	The proposed method (Aïtcin, 2004)	13
2.1.8.3	Method suggested in ACI 363 Committee on high strength concrete	15
2.1.8.4	Larrard method (de Larrard, 1990)	16
2.1.8.5	Mehta and Aïtcin simplified method.....	17
2.2	Polymer Modified Cement, Mortar and Concrete.....	18
2.2.1	General	18
2.2.2	Polymer-modified mortar and concrete (PMM and PMC)	19
2.2.3	The workability of concrete modified with polymers	21
2.2.4	Compressive, tensile and flexural strengths	22
2.2.5	Durability.....	23
2.2.6	Adhesion strength of SBR modified concrete	25
2.2.7	Polyethylene-vinyl acetate (EVA).....	25
2.2.8	Effects of vinyl acetate (VA/veova) powder on physical and mechanical properties of cement mortar	26
2.2.9	Effects of styrene-acrylic ester (SAE) on physical and mechanical properties of cement mortar.....	26
2.2.10	Applications of latex blend modified concrete.....	27
2.3	Fracture Characteristics of Concrete	28
2.3.1	History of fracture mechanics	28
2.3.2	Linear elastic fracture mechanics (LEFM).....	30
2.3.3	Quasi-brittle fracture mechanics of concrete.....	32
2.3.4	The fracture process zone	33
2.3.5	The fictitious crack model (FCM).....	36
2.3.6	The size effect model.....	38
2.3.7	The two-parameter fracture model	39
2.3.8	The effective crack model.....	40
2.3.9	Using three-point bending test to determinate fracture energy	43
2.3.10	Analytical models for test results	45
2.3.11	Brittleness index for concrete	47
2.3.12	Factors influencing the brittleness of concrete.....	49
2.3.12.1	Chemical bonds in cement paste	49

2.3.12.2	Porosity in cement paste.....	49
2.3.12.3	Water-cement ratio (W/C).....	49
2.3.12.4	Aggregate type	49
2.3.12.5	Aggregate size	50
2.3.12.6	Aggregate-cement ratio (A/C).....	50
2.3.12.7	Sand-cement ratio (S/C).....	50
2.3.12.8	Silica fume.....	50
2.3.12.9	Polymers additives	50
2.4	Elastic Modulus.....	51
2.5	Summary	51

**CHAPTER 3 CHARACTERISTICS OF MATERIALS FOR
MANUFACTURING HIGH PERFORMANCE CONCRETE 54**

3.1	Cement	54
3.2	Silica Fume.....	55
3.3	Coarse Aggregate	56
3.3.1	Specific gravity and absorption of coarse aggregate.....	56
3.3.2	Grading of coarse aggregates	57
3.3.3	Aggregate impact value.....	58
3.4	Fine Aggregate	59
3.4.1	Specific gravity and absorption of fine aggregate.....	59
3.4.2	Grading of fine aggregate.....	60
3.5	Superplasticizer	60
3.6	Polymers.....	62
3.6.1	Styrene-Butadiene Rubber (SBR) latex.....	63
3.6.2	Polyvinylidene Chloride (PVDC).....	65
3.6.3	Linear Low Density Polyethylene (LLDPE).....	66
3.6.4	High Density Polyethylene (HDPE).....	67
3.7	Water	68
3.8	Summary	69

CHAPTER 4 MIX DESIGNS..... 70

4.1	Introduction	70
4.2	Summary of the Proposed Method (Aitcin, 2004)	71
4.2.1	Water/binder ratio.....	72

4.2.2	Water content.....	72
4.2.3	Super-plasticizer dosage.....	73
4.2.4	Coarse aggregate content.....	73
4.2.5	Air content.....	73
4.2.6	Calculations on the mix design sheet.....	74
4.3	Specimens.....	92
4.4	Batching and Curing.....	93
4.5	Summary.....	95
CHAPTER 5 THE EXPERIMENTAL PROGRAMME.....		96
5.1	Introduction.....	96
5.2	Fundamental Mechanical Tests.....	96
5.2.1	Workability testing.....	96
5.2.2	Compression testing.....	96
5.2.3	Splitting tensile testing.....	99
5.2.4	Dynamic and static elastic modulus testing.....	100
5.2.5	Unit weight (density) testing.....	102
5.3	Fracture Testing.....	103
5.3.1	Test apparatus and data acquisition.....	105
5.3.2	Three-point bending testing.....	105
5.3.3	Testing for modulus of rupture.....	108
5.3.4	Testing for fracture energy.....	108
5.3.5	Fracture energy related fracture toughness.....	110
5.3.6	Brittleness.....	111
5.4	Summary.....	111
CHAPTER 6 TEST RESULTS AND DISCUSSION.....		112
6.1	Workability.....	112
6.2	Unit Weight (Density).....	114
6.3	Compressive Strength.....	116
6.3.1	Compression test results at 7 days.....	119
6.3.2	Compression test results at 28 days.....	121
6.3.3	Compression test results at 90 days.....	123
6.4	Splitting Tensile Strength.....	125
6.5	Modulus of Rupture.....	130

6.6	Fracture Toughness	132
6.7	Fracture Energy	136
6.8	Static Elastic Modulus.....	140
6.9	Brittleness	144
6.10	Summary	153
CHAPTER 7 CONCLUSIONS AND FUTURE WORK.....		155
7.1	Conclusions	155
7.2	Future Work	159
REFERENCES.....		161
APPENDIX A MIX DESIGN.....		172
APPENDIX B LOAD VERSUS DISPLACEMENT CURVES		182

LIST OF FIGURES

Figure 1-1 Thesis structure.....	5
Figure 2-1 Step-by-step procedure of mix design according to ACI 211-1 (ACI, 2009).....	13
Figure 2-2 Proposed method (Aitcin, 2004)	14
Figure 2-3 Polymeric admixtures or modifiers (Ohama, 1997).....	20
Figure 2-4 Shear testing methods (Chmielewska, 2008)	25
Figure 2-5 Linear, nonlinear and quasi-brittle fractures (Trussoni, 2009).....	29
Figure 2-6 Different failure modes of engineering materials (Trussoni, 2009)	29
Figure 2-7 Stress near crack tip (Trussoni, 2009).....	32
Figure 2-8 Crack tip and stress distribution (Trussoni, 2009).....	32
Figure 2-9 K_{IC} versus specimen depth W (Trussoni, 2009).....	33
Figure 2-10 Enlarged fracture process zone (Trussoni, 2009).....	34
Figure 2-11 Varying sizes of FPZ (Nemati et al, 1998).....	34
Figure 2-12 Edge effect on FPZ (Hu and Wittmann, 1992).....	35
Figure 2-13 Plane stress – strain effects on fracture (Hu and Wittmann, 1992).....	35
Figure 2-14 Tension test with deformation measurements (Hillerborg, 1985).....	36
Figure 2-15 Linear approximation of a $\sigma - \varepsilon$ curve (Hillerborg, 1985).....	37
Figure 2-16 Linear approximation of a $\sigma - w$ curve (Hillerborg, 1985).....	37
Figure 2-17 Bi-linear approximation of a $\sigma - w$ curve (Hillerborg, 1985).....	38
Figure 2-18 A three-point bending test (Hillerborg, 1985).....	38
Figure 2-19 Typical unloading curve for two-parameter fracture model (Bordelon, 2005)	40
Figure 2-20 Effective notch concept (Karihaloo and Nallathambi, 1989).....	41
Figure 2-21 Three-point bending test on a notched beam specimen.....	44
Figure 2-22 A typical load versus load-point deflection curve.....	44

Figure 2-23 K_{IC} versus f'_c for hardened cement (Shah, 1988)	46
Figure 2-24 G_F versus f'_c for concrete (Shah, 1988).....	46
Figure 2-25 A complete load– displacement curve for a notched beam (Zhang et al, 2002).....	47
Figure 3-1 Sample of granite aggregate	56
Figure 3-2 Grading of coarse granite aggregates	58
Figure 3-3 Grading of fine aggregates	62
Figure 3-4 Chemical structure of SBR.....	63
Figure 3-5 SBR latex.....	65
Figure 3-6 Chemical structure of the PVDC used in this study	65
Figure 3-7 PVDC Powder	66
Figure 3-8 Chemical structure of LLDPE	67
Figure 3-9 The LLDPE powder used in this study.....	67
Figure 3-10 Chemical structure of HDPE	68
Figure 3-11 HDPE powder.....	68
Figure 4-1 Proposed compressive strength – W/B relationship (Aitcin, 2004)	72
Figure 4-2 Determination of the minimum water dosage (Aitcin, 2004).....	73
Figure 4-3 Coarse aggregate content (Aitcin, 2004)	73
Figure 4-4 Beam samples with notches at mid-span.....	93
Figure 4-5 Typical cube specimens of polymer modified concrete for first 24 hours after casting and second 24 hours to complete the polymerisation process...	94
Figure 5-1 Slump testing	97
Figure 5-2 The 3000 kN Avery Denison testing machine	97
Figure 5-3 Compression tests	98
Figure 5-4 Arrangement of splitting tensile testing	99
Figure 5-5 Splitting tensile testing	100
Figure 5-6 Pundit ultrasonic tester for measuring the dynamic elastic modulus	101

Figure 5-7 Density testing apparatus (weight-in-air/weight-in-water method)	103
Figure 5-8 Fracture toughness testing in the 5500 R Instron testing machine	104
Figure 5-9 The linear variable differential transducer (LVDT)	105
Figure 5-10 Illustration of three-point bending test set-up	106
Figure 5-11 Three-point bending test set-up	107
Figure 5-12 A notched beam during three-point bending testing	107
Figure 5-13 A typical load versus deflection curve	109
Figure 5-14 Standard three-point-bending notched concrete beam	109
Figure 5-15 Typical failure pattern in a three-point bending test	110
Figure 6-1 Measured slump values for the HPC modified with different types and contents of polymers	114
Figure 6-2 Densities of the HPC modified with different types and contents of polymers at 28 days	116
Figure 6-3 Shapes of the crushed SBR modified HPC cubes at failure	117
Figure 6-4 Shapes of the crushed PVDC modified HPC cubes at failure	117
Figure 6-5 Shapes of the crushed LLDPE modified HPC cubes at failure	118
Figure 6-6 Shapes of the crushed HDPE modified HPC cubes at failure	118
Figure 6-7 Compressive strength of the HPC modified with different types and contents of polymers at 7 days with standrad deviations	120
Figure 6-8 Compressive strength of the HPC modified with different types and contents of polymers at 28 days with standrad deviations	123
Figure 6-9 Compressive strength of the HPC modified with different types and contents of polymers at 90 days with standrad deviations	125
Figure 6-10 Splitting tensile strengths of the HPC modified with different types and contents of polymers at 28 days with standrad deviations	127
Figure 6-11 Fracture surfaces of the HPC samples modified with SBR in splitting	128

Figure 6-12 Fracture surfaces of the HPC samples modified with PVDC in splitting	128
Figure 6-13 Fracture surfaces of the HPC samples modified with LLDPE in splitting.....	129
Figure 6-14 Fracture surfaces of the HPC samples modified with HDPE in splitting	129
Figure 6-15 Failure patterns of the HPC specimens under splitting tension.....	130
Figure 6-16 Modulus of rupture of the HPC modified with different types and contents of polymers at 28 days	130
Figure 6-17 Fracture toughness of the HPC modified with different types and contents of polymers	134
Figure 6-18 Fracture toughness with the standard deviations.....	135
Figure 6-19 Fracture energy of the HPC modified with different types and contents of polymer	138
Figure 6-20 Fracture energy with the standard deviations.....	139
Figure 6-21 Static elastic modulus of the HPC modified with different types and contents of polymers	143
Figure 6-22 Static elastic modulus E versus compressive strength f_{cu}	143
Figure 6-23 Elastic displacement of the HPC with different types and contents of polymers	151
Figure 6-24 Failure displacement of the HPC with different types and contents of polymers	151
Figure 6-25 Brittleness of the HPC with different types and contents of polymers	152
Figure A-1 Proposed W/B – compressive strength relationship.....	172
Figure A-2 Determination of the minimum water dosage.....	173
Figure A-3 Coarse aggregate content.....	173
Figure B-1 Load – displacement curves for the HPC control mix.....	182

Figure B-2 Load – displacement curves for the HPC modified with 1.5% SBR....	183
Figure B-3 Load – displacement curves for the HPC modified with 3.0% SBR....	184
Figure B-4 Load – displacement curves for the HPC modified with 5.0% SBR....	185
Figure B-5 Load – displacement curves for the HPC modified with 1.5% PVDC.	186
Figure B-6 Load – displacement curves for the HPC modified with 3.0% PVDC..	187
Figure B-7 Load – displacement curves for the HPC modified with 5.0% PVDC..	188
Figure B-8 Load – displacement curves for the HPC modified with 1.5% LLDPE.....	189
Figure B-9 Load – displacement curves for the HPC modified with 3.0% LLDPE.....	190
Figure B-10 Load – displacement curves for the HPC modified with 5.0% LLDPE.	191
Figure B-11 Load – displacement curves for the HPC modified with 1.5% HDPE.....	192
Figure B-12 Load – displacement curves for the HPC modified with 3.0% HDPE.....	193
Figure B-13 Load – displacement curves for the HPC modified with 5.0% HDPE.....	194

LIST OF TABLES

Table 2-1 Specimen dimensions specified by RILEM.....	45
Table 3-1 Chemical compositions of the cement used.....	54
Table 3-2 Physical characteristics of the cement used	54
Table 3-3 Physical Properties and chemical compositions of silica fume used	55
Table 3-4 Typical sieve analysis results of natural coarse granit aggregates.....	57
Table 3-5 Impact test results of aggregates	59
Table 3-6 Typical sieve test results of fine aggregates.....	61
Table 3-7 Characteristics of the superplasticizer Structuro 11180.....	62
Table 3-8 Formulations for emulsion polymerisation of typical SBR latexes as cement modifiers (ACI, 1991)	64
Table 3-9 Physical and chemical properties of the SBR used.....	64
Table 3-10 Physical and chemical properties of the PVDC used.....	66
Table 3-11 Physical and chemical properties of the LLDPE used.....	67
Table 3-12 Physical and chemical properties of the HDPE used.....	68
Table 4-1 Mix designs of polymers modified HPCs.....	71
Table 4-2 Calculations on mix design sheet (Aitcin, 2004).....	74
Table 4-3 Mix design sheet for the control mix of HPC	77
Table 4-4 Mix design sheet for the HPC modified with 1.5% SBR	78
Table 4-5 Mix design sheet for the HPC modified with 3% SBR	79
Table 4-6 Mix design sheet for the HPC modified with 5% SBR	80
Table 4-7 Mix design sheet for the HPC modified with 1.5% PVDC	81
Table 4-8 Mix design sheet for the HPC modified with 3% PVDC	82
Table 4-9 Mix design sheet for the HPC modified with 5% PVDC	83
Table 4-10 Mix design sheet for the HPC modified with 1.5% LLDPE.....	84
Table 4-11 Mix design sheet for the HPC modified with 3% LLDPE.....	85

Table 4-12 Mix design sheet for the HPC modified with 5% LLDPE.....	86
Table 4-13 Mix design sheet for the HPC modified with 1.5% HDPE.....	87
Table 4-14 Mix design sheet for the HPC modified with 3% HDPE.....	88
Table 4-15 Mix design sheet for the HPC modified with 5% HDPE.....	89
Table 6-1 Slumps of concrete mixes investigated.....	113
Table 6-2 Density test results at 28 days.....	115
Table 6-3 Compression test results at 7 days.....	119
Table 6-4 Compression test results at 28 days.....	122
Table 6-5 Compression test results at 90 days.....	124
Table 6-6 Indirect tension test results at 28 days.....	126
Table 6-7 Modulus of rupture test results at 28 days.....	131
Table 6-8 Fracture toughness of the SBR modified high performance concrete	132
Table 6-9 Fracture toughness results of the PVDC modified high performance concrete.....	133
Table 6-10 Fracture toughness results of the LLDPE modified high performance concrete.....	133
Table 6-11 Fracture toughness results of the HDPE modified high performance concrete.....	134
Table 6-12 Fracture energy results of the SBR modified high performance concrete	136
Table 6-13 Fracture energy results of the PVDC modified high performance concrete	137
Table 6-14 Fracture energy results of the LLDPE modified high performance concrete.....	137
Table 6-15 Fracture energy results of the HDPE modified high performance concrete	138
Table 6-16 Elastic modulus results of the SBR modified high performance concrete	141

Table 6-17 Elastic modulus results of the PVDC modified high performance concrete	141
Table 6-18 Elastic modulus results of the LLDPE modified high performance concrete	142
Table 6-19 Elastic modulus results of the HDPE modified high performance concrete	142
Table 6-20 Elastic displacements of the SBR modified high performance concrete	145
Table 6-21 Elastic displacements of the PVDC modified high performance concrete	145
Table 6-22 Elastic displacements of the LLDPE modified high performance concrete	146
Table 6-23 Elastic displacements of the HDPE modified high performance concrete	146
Table 6-24 Failure displacements of the SBR modified high performance concrete	147
Table 6-25 Failure displacements of the PVDC modified high performance concrete	147
Table 6-26 Failure displacements of the LLDPE modified high performance concrete	148
Table 6-27 Failure displacements of the HDPE modified high performance concrete	148
Table 6-28 Brittleness values of the SBR modified high performance concrete	149
Table 6-29 Brittleness values of the PVDC modified high performance concrete .	149
Table 6-30 Brittleness values of the LLDPE modified high performance concrete	150
Table 6-31 Brittleness values of the HDPE modified high performance concrete .	150
Table A-1 The amount of concrete to make the trial batch	175
Table A-2 Mix design sheet of abbreviations.....	176
Table A-3 Mix design sheet of abbreviations.....	179

ABBREVIATIONS AND NOTATIONS

A	Mass of oven-dry sample in air
ACI	American Concrete Institute
a	Crack length; Length of specimen
a_c	Critical crack length
a_e	Effective notch length
a_0	Notch length
B	Beam width; Mass of saturated surface-dry sample in air
C	Apparent mass of saturated sample immersed in water
C_n	Geometry coefficient
C_V	Coefficient of variance
$C_I + \dots$	Higher order terms
CC	Conventional concrete
$CMOD_c$	Critical crack mouth opening displacement
$CTOD_c$	Critical crack tip opening displacement
d_{max}	Maximum size of aggregate in mm
E	Modulus of elasticity in GPa
E_d	Dynamic modulus of elasticity in GPa
EVA	Ethylene-vinyl acetate
F_t	Maximum tensile load in N
f_t	Tensile strength of concrete in MPa
f_t'	Splitting tensile strength in MPa
f_r	Modulus of rupture in MPa
FCM	Fictitious crack model
FM	Fracture mechanics
FPZ	Fracture process zone
G	Strain energy release rate in N/m
G_F	Fracture energy in N/m
G_P	Plastic dissipation portion of the strain energy release rate in N/m
G_{SSD}	Bulk specific gravity
g	Gravity acceleration and $g = 9.81 \text{ m/s}^2$
H	Depth of the beam in mm

HDPE	High Density Polyethylene
HPC	High performance concrete
HSC	High strength concrete
K_{IC}	Critical stress intensity factor in MN/m ^{1.5}
k	Shear coefficient
L	Length of specimen in mm
l_{ch}	Characteristic length in mm
LDPE	Low-Density Polyethylene
LEFM	Linear elastic fracture mechanics
LLDPE	Linear Low Density Polyethylene
LVDT	Linear variable differential transducer
LWAC	Lightweight aggregate concrete
M	Specimen mass in gram
m	Moment in Nm
OCC	Ordinary cement concrete
P	Mid-span concentrated load in N
P_C	Peak load in N
P_l	Arbitrary load level in N
PC	Polymer concrete
PET	Polyethylene terephthalate
PIC	Polymer impregnated concrete
PM	Polymer mortar
PMC	Polymer-modified concrete
PMM	Polymer-modified mortar
PVDC	Polyvinylidene chloride
r	Distance
RPC	Reactive powder concrete
S	Span in mm
SAE	Styrene-Acrylic Ester
SBR	Styrene-Butadiene Rubber
SCC	Self-compacting concrete
SEM	Size effect method
SHSC	Super high strength concrete

t	Beam depth in mm; Time the ultrasonic wave travels in micro-second
U	Elastic energy in Nm
V	Velocity of the ultrasonic wave in m/s
VA	Vinyl acetate
W	Specimen depth in mm
W_{air}	Mass of concrete in the air in gram
W_{water}	Mass of concrete under the water in gram
W_{abs}	Water absorption
w	Self-weight of the beam per unit length in N/m
WFM	Work-of-fracture method
W/C	Water cement ratio
δ_i	Deflection corresponding to the peak load P_c in mm
δ_p	Deflection corresponding to the arbitrary load P_i in mm
Δl	Deformation of the specimen in mm
ε	Strain along the beam length
γ	Traction-free crack surface
$\gamma(a)$	Correction function
λ	Correction factor
ν	Poisson's ratio
θ	Angle
ρ_c	Concrete density in kg/m ³
σ	Applied stress in MPa
σ_c	Critical stress in MPa
σ_{ij}	Stress field
σ_n	Nominal tensile stress in MPa

CHAPTER 1 INTRODUCTION

1.1 Introduction

The modern world largely depends on concrete as a most excellent material for construction. Developments in concrete technology have fostered larger use and paralleled a better understanding of its application in contemporary systems of construction. Compared with most construction materials like steel and timber, concrete is regarded as a brittle material.

Brittle material has a synthetic characteristic of the deformation and fracture, or a characteristic of abrupt fracture at small deformation. It is the opposite of ductility. The mechanics of materials were not understood in ancient times, and simple constructions with brittle materials were primarily used in compression to avoid cracking and failure. Incorporate ductile metal armatures in concrete in the nineteenth century recouped the low tensile strength and cracking characteristics that developed into the modern form as a structural system of reinforced concrete with concrete resisting compression and steel providing tensile strength.

When numerous failures in steel structures occurred and when such failures were not accounted for by traditional stress analysis, the development of material fracture theories was initiated. Ultimately the study of these metal failures led to the improvement of theories and development of fracture mechanics (FM) as a tool for engineering analysis and design with metals.

The compressive strength has traditionally been the fundamental design parameter in concrete structural design. However, the basic concepts of FM have been advanced by the concrete research community for studying the fracture characteristics of concrete at the peak load or over the whole fracture process.

Some design applications of reinforced concrete with high performance concrete (HPC) have dynamically led to super structures, e.g. long span prestressed concrete bridges, off-shore structures, pipelines and earthquake resistant tall buildings and can benefit from enhanced fracture properties of the concrete.

The advantage of high performance concrete (HPC) in practical applications comes from the dramatic increase of concrete strength. However, the brittleness of concrete increases with strength, and for super-high-strength concrete, failure can be sudden, explosive and disastrous.

Therefore, it is necessary to carry out research on the brittleness of concrete in order to establish parameters for assessing the brittleness, to find ways to improve the brittleness, to design procedures and to eventually manufacture concrete materials with high strength and low brittleness. Strength, stiffness, toughness and fracture energy are all the fracture properties for such purpose.

Previous research shows that the addition of polymers to the normal strength concrete mixture could lead to a reduction in water cement ratio (w/c), an increase in porosity due to plasticizing effect of polymer, a delayed setting (for a high amount of polymer) and a reduction in shrinkage (Chmielewska, 2008). In this study, strengthening and toughening effects of polymer materials on the high performance concrete (HPC) will be investigated.

There are two methods which are currently used to determine the fracture energy of concrete. The first method was proposed by RILEM and is known as the work-of-fracture method (WFM). The second method proposed by Bažant and Pfeiffer (1986) is a procedure known as the size effect method (SEM), and it is used for geometrically similar beams but is not as popular as the first one. The critical stress intensity factor K_{IC} and the fracture energy G_F are the effective parameters used to study the fracture process with respect to the stress intensity around the crack tip when crack extension is initiated and the energy absorbed by the material during crack extension.

Energy is absorbed in a region of the concrete that is in front of the crack tip known as the fracture process zone (FPZ). The size or volume of the FPZ leads to the understanding of the failure mechanism and energy absorption capabilities of concrete. Compared with normal strength concrete, high strength concrete normally has higher compressive strength, not highly increased tensile strength, lower deformation at peak load and at failure, and higher brittleness. The fracture properties of high performance concrete containing polymers will be investigated and determined in this dissertation, for which the following questions must be answered:

1. What fracture mechanics parameters should be utilised?
2. Will the fracture properties of high performance concrete be enhanced by adding polymers?
3. What are the additional effects of the polymer on the fracture characteristics of the HPC?
4. What is the difference between the fracture properties of polymer modified high performance concrete and normal high performance concrete?

1.2 Significance of the Study

Research on fracture characteristics of concrete, especially with a wide range of compressive strengths, still needs to be conducted. Some researchers have studied the effect of the coarse aggregates (Wu et al, 2001), high temperatures (Zhang, 2011), varying silica fume and fly hash contents (Zhou et al, 1995; Bharatkumar et al, 2005) on the fracture characteristic of high performance concrete. However, from a review of current literature, it was considered that the amount of published data on improving the fracture characteristic in high performance concrete is rather limited. Therefore, information on the performance of high performance concrete without and with polymer materials needs to be obtained. Such performance includes the fracture characteristic of high performance concrete in addition to compressive and tensile strengths, modulus of rupture and dynamic elasticity modulus.

1.3 Aims

The purpose of the present research project is to investigate the effects of polymer materials on the fundamental mechanical and fracture characteristics of high performance concrete through extensive experimental testing and analysis on the test results in order to enhance the fracture and mechanical properties and to design and manufacture high performance concrete with high strength and low brittleness.

1.4 Objectives

The objectives and scope of the research program are summarised as follows:

- To establish the state-of-the-art of high performance concrete without and with polymers;
- To review fracture mechanics and its application for assessing the performance of high strength concrete;
- To examine the available methods used in designing high performance concrete without and with polymers and identify a suitable method that can be used;
- To review the test methods used for determining fracture properties and other most available testing methods;
- To determine the experimental procedures for measuring the fracture characteristics of high performance concrete modified with different types of polymers;
- To experimentally measure the mechanical and fracture properties of HPC modified by polymers, e.g. compressive strength, tensile strength, flexural strength, modulus of elasticity, dynamic modulus of elasticity, fracture energy, fracture toughness, brittleness, etc.;
- To compare the results obtained from four types of polymer enhanced concrete and determine the best polymer that can provide good performance.

1.5 Research Methodologies

The research methods in this study mainly include:

- Obtaining information through reading books, technical reports and papers, and searching on the internet;
- Appreciating the theories that define the fracture characteristics in concrete;
- Exploring the applications of polymers to practical use for improving concrete properties;
- Conducting experimental investigations on fracture characteristics of polymer enhanced concrete;
- Analysing the test results using commercial software and drawing conclusions.

1.6 The Outline of the Dissertation

The dissertation is structured as shown in Figure 1-1 and is divided into a total of seven chapters with two appendixes.

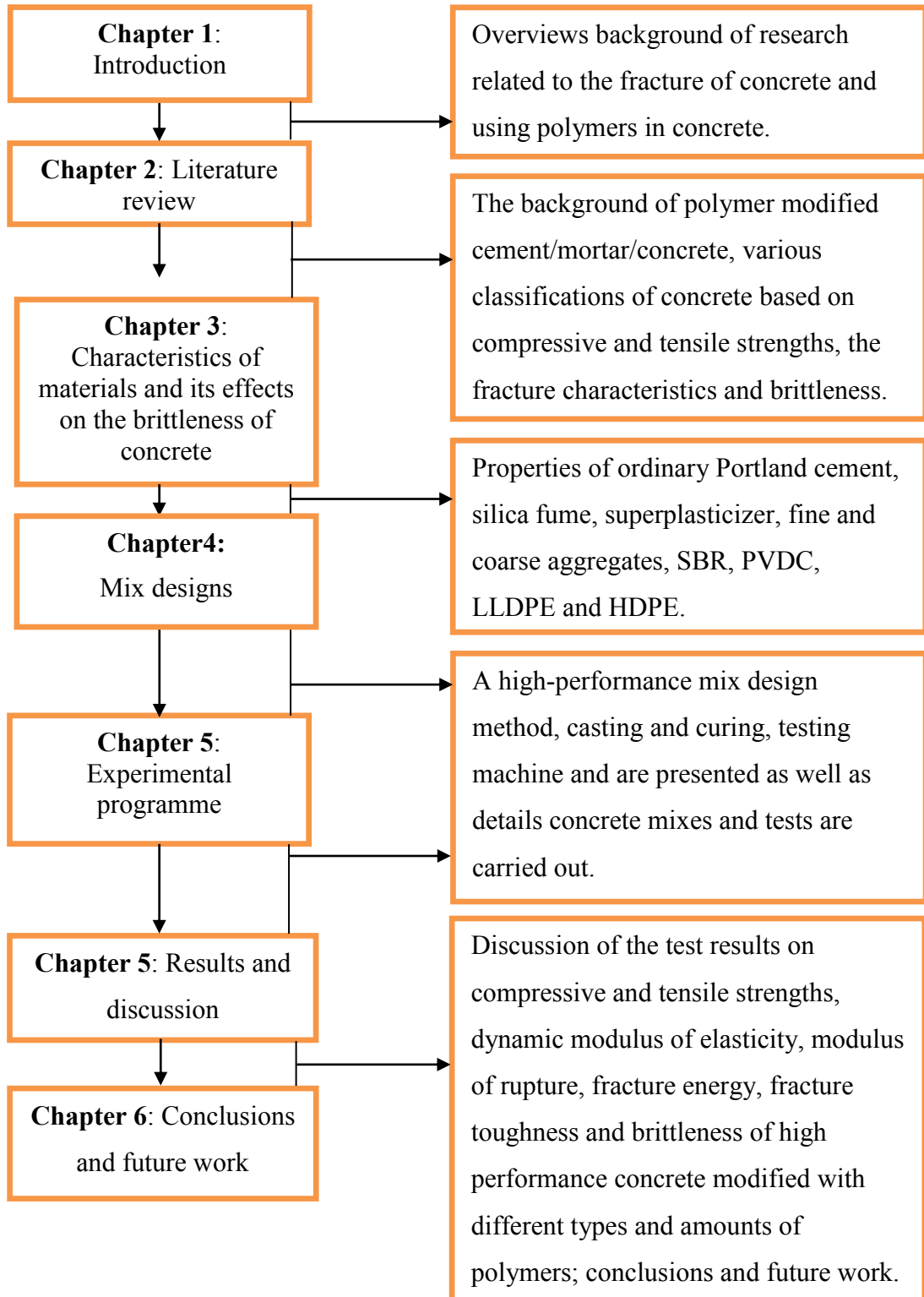


Figure 1-1 Thesis structure

Chapter 1 of this dissertation overviews the background, aims, objectives, scope and outline of research related to the brittleness of concrete and methods for determining the fracture parameters of concrete. Utilisation of polymers in concrete is discussed. This chapter also describes various significances of the study.

Chapter 2 reviews the literature on the polymer modified cement/mortar/concrete, including polymer modified mortar (PMM) and concrete (PMC), adhesion strength of SBR modified concrete, the effects of vinyl acetate (VA/veova) powder on the physical and mechanical properties of cement mortar, and the effects of styrene-acrylic ester (SAE) on the physical and mechanical properties of cement mortar and latex blend modified concrete. It also summarises various classifications of concrete based on its compressive strength, including normal strength concrete (NSC), HPC, reactive powder concrete (RPC), lightweight HPC (LHPC) and mix design of HPC. This chapter extensively describes the fracture characteristics of concrete.

Chapter 3 summarises the characteristics of materials for manufacturing HPC, e.g. properties of ordinary Portland cement, silica fume, superplasticizer, fine and coarse aggregates, Styrene – Butadiene Rubber (SBR), Polyvinylidene Chloride (PVDC), Linear Low Density Polyethylene (LLDPE) and High Density Polyethylene (HDPE).

Chapter 4 details the mix designs carried out in this research. A high-performance concrete mix design method, summary of the utilised method, and casting and curing of specimens are presented.

Chapter 5 describes the details of the experimental programme carried out in this research. Details on testing machines and conventional and fracture testing are presented, together with details of concrete mixes and tests carried out.

Chapter 6 presents the test results and discusses the characteristics of HPC, e.g. compressive and tensile strengths, modulus of rupture, static and dynamic modulus of elasticity, fracture energy, fracture toughness and characteristic length of high performance concrete modified with different types and amounts of polymers.

Chapter 7 summarises the overall conclusions drawn from previous chapters, together with recommendations for future research. Finally, the references used in the introduction of this thesis and those used in the literature review, experimental programme and discussions are all listed.

CHAPTER 2 LITERATURE REVIEW

2.1 High Performance Concrete (HPC)

2.1.1 Introduction

Concrete is a principal construction material today. There are some problems such as bleeding, segregation and honeycomb which sometimes happen. To solve these problems, concretes with high workability and high durability, such as high-performance concrete (HPC), self-compacting concrete (SCC) and polymers concrete (PC) have recently been developed. The American Concrete Institute (ACI) published guidelines for concrete mix design in 1991. The Total Volume Method for mix design is described by ACI Committee 211 (ACI Committee, 2009). The present classification of concrete based on its compressive strength is presented as follows.

2.1.2 Normal strength concrete (NSC)

Normal strength concrete (NSC) consists of cement, water, and coarse and fine aggregates. It has relatively good compressive strength up to 40 MPa. To obtain better mechanical properties, additives are incorporated in the original mix.

Two major disadvantages for normal concrete are low tensile strength and low strain at fracture. The rapid propagation of numerous micro cracks existing in normal concrete under applied stress is responsible for the low tensile strength of the material (Ramakrishnan, 1995).

When concrete is subjected to loads the initiation and propagation of pre-existing micro cracks governed the mechanical behaviour of concrete. These micro cracks remain stable under loading up to approximately 30% of the peak load. Randomly distributed micro crack networks begin to increase in length, width and number with increasing load. This stage is known as slow crack propagation (Neville, 1995).

Before the maximum load is reached there is a substantial non-linearity. When the load approaches 70% to 90% of the peak load the micro cracks coalesce and

localisation occurs. This is known as the fast crack propagation stage. After the peak load softening behaviour occurs under steady-state crack propagation (Ansari, 1989).

The propagation of cracks in NSC is due to the bond failure at the aggregate-paste interface, which is partially a result of stress concentration caused by the incompatibility of the elastic moduli of cement paste and the aggregate (Newman, 1965). Normally, cracks run around aggregates through the cement-aggregate bonds (Bentur and Mindess, 1986). Thus, the weak aggregate-matrix interface is the main factor limiting the strength development of NSC (Struble et al, 1980).

2.1.3 Reactive powder concrete (RPC)

Reactive Powder Concrete (RPC) displays very high mechanical and durable properties. The mix composition includes ordinary Portland cement, silica fume, aggregates with very tiny grains, sand with an average grain diameter of 250 μm and crushed quartz (average grain diameter of 10 μm). Silica fume reduces concrete porosity so as to enhance the strength and durability. Metallic fibres can be added in order to increase the ductility and flexural strength of concrete (Cheyrezy et al, 1995).

2.1.4 High strength concrete (HSC)

To improve properties of concrete and get highly specific needs and requirements such as high strength, Neville and Aitcin (1998) stated that the strength can be required at a very early age in order to put the structure into service. However, high strength concrete tends to be brittle when loaded to failure, which is due to the lack of plastic deformation.

The size of the inherent flaws of HSC is smaller and more uniform and the microstructure is more homogeneous. Moreover, the difference between the elastic moduli of the concrete matrix and aggregate for HSC is smaller than that for NSC, resulting in lower stress concentrations at the transition zone (Nevile, 1997). Cracks in HSC are relatively uniform in size and are activated approximately simultaneously under loading, resulting in a more linear stress-strain relation and increased brittleness (Reinhardt, 1995). Usually relatively smooth fracture surface is resulted from the path travelling through the cement paste and aggregate (Tasdemir and Tasdemir, 1995).

2.1.5 High performance concrete (HPC)

In general, high performance concrete contains ordinary Portland cement, good quality aggregate at high content (about 450-550 kg/m³), silica fume (about 5-15% by volume) and superplasticizers. Other cementations materials, such as fly ash or ground granulated blast furnace slag (ggbs) may be used depending on the application. Because the high performance concrete has other enhanced properties such as stiffness, abrasion resistance and durability, Domone, Soutsos and Sabir considered that high strength concrete (HSC) could be a particular case of high performance concrete (HPC) (Sabir, 1995; Domone and Soutsos, 1995). However, Neville and Aitcin stated that high performance concrete is different from high strength concrete. This emphasis has moved from very high strength to other properties desirable under some circumstances such as high modulus of elasticity, high density, low permeability and high resistance to some forms of chemical attack. In spite of the superior characteristics of HPC, there are some problems which seem not to have been overcome such as low tensile strength and low failure strain (Neville and Aitcin, 1998).

To achieve high performance concrete, the main parameters to be considered can be summarised as follows (Nawy, 2001):

- quality and type of cement,
- proportion of cement in relation to water in the mixture,
- strength, size and cleanliness of aggregate,
- interaction or adhesion between cement paste and aggregate,
- type of admixture chosen,
- adequate mixing of the ingredients,
- proper placing, finishing and compaction of the fresh concrete,
- curing at a temperature not below 50°F (10°C) while the placed concrete gains strength.

2.1.5.1 Advantages and disadvantages of HPC with silica fume

The main advantages of HPC with silica fume are:

- increasing early-age strength development of concrete,
- producing low permeable concrete with enhanced durability,

- reducing the ingress of chlorides and other chemicals in the concrete (Khan, 2006).

The main disadvantages of HPC are:

- increasing water demand when using silica fume in HPC, which reduces workability and needs to add in superplasticizers to maintain the given workability (Khan, 2006),
- increasing brittleness with the compressive strength,
- causing sudden, explosive and disastrous failure for super-high-strength concrete,
- not proportionally increasing tensile strength.

2.1.5.2 History of development and applications of high performance concrete

Over the last two decades, HPC has been largely developed and used. The first international conference on Utilisation of High Strength Concrete was held in Stavanger, Norway, in 1987. The first applications were started to use in northern Europe for longer bridges and high rise buildings as well as offshore structures. In the early 1990s it became mandatory in some countries. A publication, High performance concretes – a state-of-art report (1989-1994), summarised these developments (Zia et al, 1995).

2.1.6 Lightweight high performance concrete (LHPC)

Most or even all lightweight high performance concrete mixes used today include lightweight aggregates as the coarse aggregate and sand for the fine aggregate. When it grades greater than 55 MPa, it has a number of important characteristics such as excellent durability against freezing and thawing, internal curing, reduced self-weight and higher fire resistance. LHPC is defined by ACI 213 as concrete with an air-dry density in the range of 1361 to 1842 kg/m³, with some specifications allowing air-dry densities up to 1922 kg/m³, and a 28-day compressive strength greater than 69 MPa (ACI Committee, 2003).

2.1.7 Ultra-high strength concrete (UHSC)

Super high strength concrete has a compressive strength over 150 MPa and is generally made from the same components as HSC. However, by carefully selecting, proportioning, and mixing the components, large improvements in compressive strength, tensile strength and toughness can be achieved (Abu Lebdeh et al, 2011; Rui et al, 2007).

2.1.8 Mix design methods of HPC

Mix design of HPC is more complicated because it includes more materials like super plasticizer and supplementary cementations materials, e.g. silica fume, fly ash, fillers, etc. In addition, maintaining a low water-binder ratio with enough workability makes the design process more complicated (Zain et al, 2005). There are three aspects which were considered for the performance of a mix design: strength, workability and durability. The following subsections illustrate some currently used mix design methods for produce different types and grades of concrete, each having its own identity, unique procedure, advantages and disadvantages.

2.1.8.1 ACI 211-1 Standard practice for selecting proportions for normal, heavyweight and mass concrete

Comprehensive procedure for proportioning normal weight concrete of a maximum specified compressive strength of 40 MPa and a maximum slump of 180 mm was offered by ACI 211-1 Standard Practice for Selecting Proportions for Normal, Heavyweight and Mass Concrete (ACI, 2009). It essentially assumes that the concrete slump is affected by the maximum size of the coarse aggregate, and water/cement (W/C) ratio and the amount of entrained air are the only parameters affecting strength. Figure 2-1 shows the step-by-step procedure of mix design according to ACI 211-1.

The absolute volume method is applied to calculate the mix proportions based on the following assumption

$$\text{Absolute volume} = \text{mass}/\text{specific gravity}$$

The design procedure from this method is briefly summarised as follows:

- Step 1 Slump selection: In a special table, the slump values needed to cast concrete for different types of construction are suggested.
- Step 2 Determination of the maximum size of coarse aggregate (MSA): Based on the maximum and minimum dimensions of the structural member, different MSA values are suggested in the table. Large coarse aggregates have a lower specific surface than small coarse aggregates. For conventional concrete it is economical to use a large MSA. The MSA should not exceed one-fifth of the narrowest dimension between the sides of forms, one-third of the depth of slab, or three quarters of the minimum clear spacing between reinforcing bars, bundled bars or tendons.
- Step 3 Estimation of mixing water and air content: The amount of mixing water is obtained from the table for given MSA and slump values, both when the concrete is air-entrained and when it is not air-entrained.
- Step 4 Selection of W/C ratio: The W/C ratio can be determined from two tables, depending on the desired compressive strength within the 15 to 40 MPa range, and the required durability (exposure conditions).
- Step 5 Cement content: The mass of cement is calculated by dividing the mass of the free water by the W/C ratio.
- Step 6 Coarse aggregate content: The bulk volume of dry-rodded coarse aggregate per unit volume of concrete is determined from the table for a given fineness modulus of sand and a given MSA.
- Step 7 Fine aggregate content: To calculate the mass of the sand, the total volume of all ingredients is deducted from 1 m^3 .
- Step 8 Moisture adjustment: The mass of aggregates obtained in this procedure is for aggregate in an SSD state. Therefore their mass, along with mass of the mixing water, is adjusted for actual moisture conditions.
- Step 9 Trial batches: Trial batches are made, and the mixture proportioning is adjusted to meet the desired physical and mechanical characteristics of the concrete.

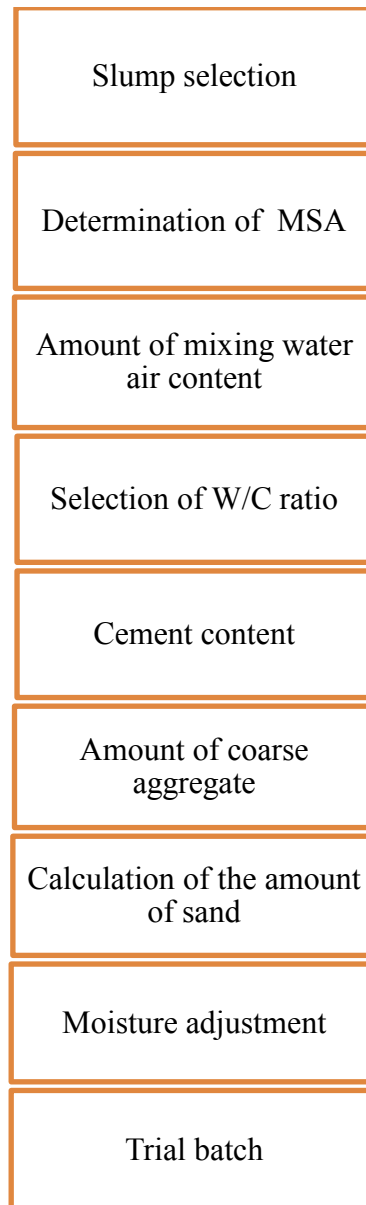


Figure 2-1 Step-by-step procedure of mix design according to ACI 211-1 (ACI, 2009)

2.1.8.2 The proposed method (Aitcin, 2004)

This method is very simple and follows the same approach as ACI 211–1 Standard Practice for Selecting Proportions for Normal, Heavyweight and Mass Concrete. It is a combination of empirical results and mathematical calculations based on the absolute volume method. The water contributed by the superplasticizer is considered as part of the mixing water. The proposed method is adopted for this research. A flow chart for this method is presented in Figure 2-2 (Aitcin, 2004).

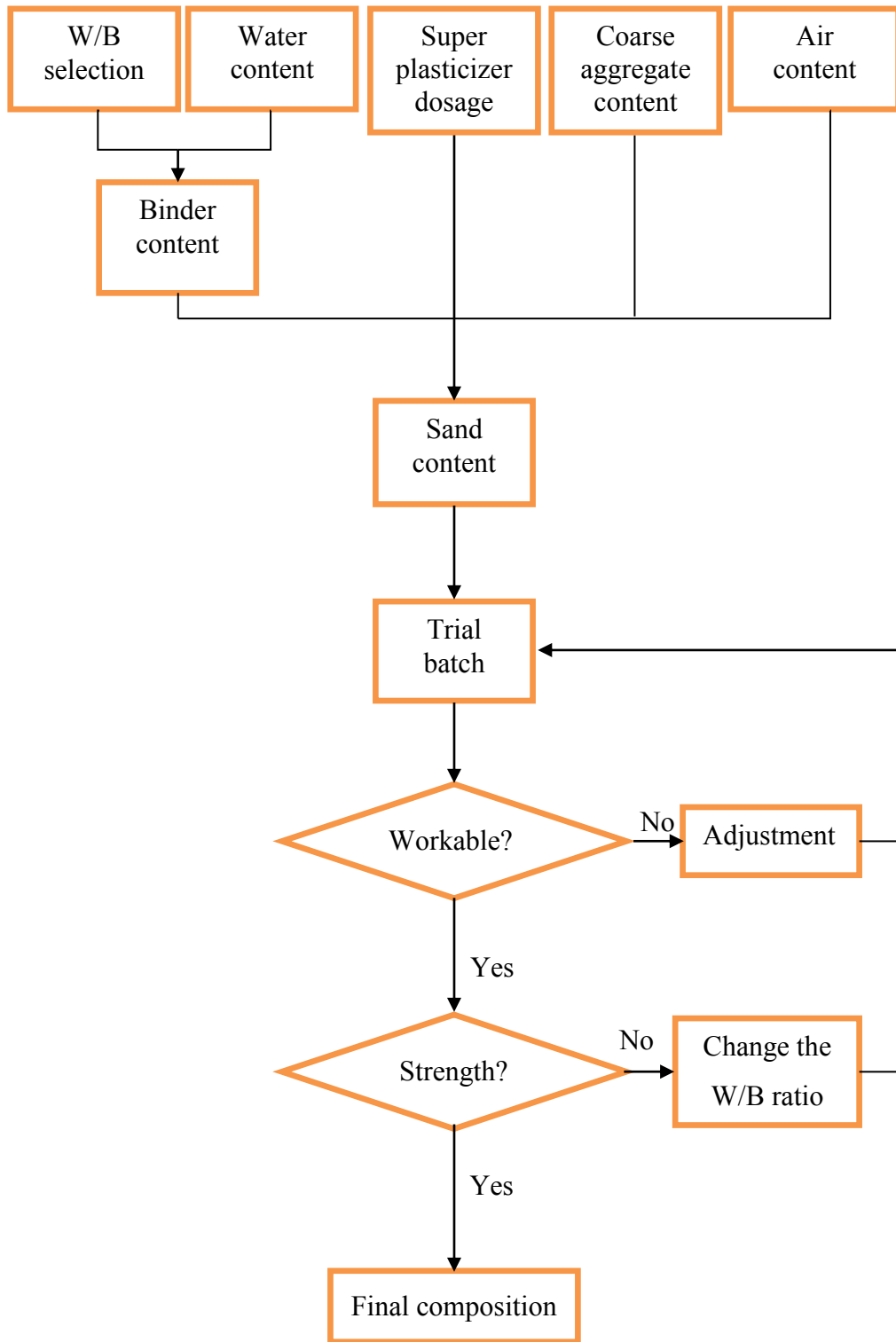


Figure 2-2 Proposed method (Aitcin, 2004)

Five different mix characteristics are selected to initiate the procedure in the following sequence:

- the water binder (W/B) ratio,
- the water content,

- the superplasticizer dosage,
- the coarse aggregate content,
- the entrapped air content (assumed value).

The procedure is initiated by selecting a number of mix characteristics or materials, e.g. the W/B ratio, the water content, the superplasticizer dosage, the coarse aggregate content, etc., and this is to be discussed in Appendix A (mix design).

2.1.8.3 Method suggested in ACI 363 Committee on high strength concrete

The steps of this method are given as follows:

- Step 1 Slump and required strength selection: It suggests two slump values for concretes: the first value made with superplasticizer and the second value without superplasticizer. The first value of the slump is between 25 and 50 mm for the concrete before adding the superplasticizers in order to ensure that sufficient water is used in the concrete (Aitcin, 2004).
- Step 2 Selection of the maximum size of the coarse aggregate (MSA): The method suggests using coarse aggregate depends on compressive strength, with an MSA of 19 or 25 mm for concrete made with f_c' lower than 65 MPa and 10 or 13 mm for concrete made with f_c' greater than 85 MPa. The method allows for the use of coarse aggregate with an MSA of 25 mm for concrete made with f_c' between 65 and 85 MPa when the aggregate is of high quality (Aitcin, 2004).
- Step 3 Selection of coarse aggregate content: This method suggests that the optimum content of coarse aggregate, expressed as a percentage of dry-rode unit weight (DRUW), can be 0.65, 0.68, 0.72 and 0.75 for nominal size aggregate of 10, 13, 20 and 25 mm, respectively. The DRUW is measured according to ASTM Standard C29 Standard Test Method for Unit Weight and Voids in Aggregate. These values are given for concrete made with a sand of fineness modulus 2.5 to 3.2 (Aitcin, 2004).
- Step 4 Estimation of free water and air content: The estimation of required water content and air content for concretes made with coarse aggregates of various nominal sizes is given by the table. These estimated water contents are given for a fine aggregate having a 35% void ratio. If this value is different from 35%, then the water content obtained from the table should be

adjusted by adding or subtracting 4.8 kg/m^3 for every 1% increase or decrease in sand air void (Aitcin, 2004).

- Step 5 Selection of W/B ratio: Two tables suggest W/B values for concretes made with and without superplasticizer, respectively, to meet the specified 28-day and 56-day compressive strengths. These values are based upon the MSA and f_c' of the concrete (Aitcin, 2004).
- Step 6 Cement content: The mass of cement is calculated by dividing the mass of the free water by the W/B ratio (Aitcin, 2004).
- Step 7 First trial mixture with cement: The first mixture using cement and no other cementations materials and sand content is then calculated using the absolute volume method as described in the previous method (Aitcin, 2004).

2.1.8.4 Larrard method (de Larrard, 1990)

This method is based on two semi-empirical mix design tools. The main idea of the method is to perform as many tests as possible on grouts for rheological tests and mortars for mechanical tests. The strength of the concrete is predicted by a formula where a limited number of mix design parameters are to be used (Aitcin, 2004):

$$f_c = \frac{k_g R_c}{\left[1 + \frac{3.1(w/c)}{1.4 - 0.4 \exp(-11s/c)} \right]^2} \quad (2.1)$$

where

f_c is the compressive strength of concrete cylinders at 28 days, in MPa,

w is the mass of water,

c is the cement unit for a unit volume of fresh concrete,

s is the silica fume for a unit volume of fresh concrete,

k_g is a parameter depending on the aggregate type, a value of 4.91 applied to common river gravels,

R_c is the strength of cement at 28 days, e.g. the strength of ISO mortar containing three parts of sand for each part of cement and one-half part of water, in MPa.

2.1.8.5 Mehta and Aïtcin simplified method

Mehta and Aïtcin (1990) proposed this simple mixture for normal weight concrete with compressive strength values between 60 and 120 MPa. The method is suitable for the maximum size of coarse aggregates between 10 and 15 mm, with slump values between 200 and 250 mm. A 2% non-air entrained high-performance concrete has an entrapped air volume of 2% and it is estimated that it can be increased to 5% to 6% when the concrete is air-entrained. The optimum volume of aggregate is suggested to be 65% of the volume of the high-performance concrete (Mehta and Aïtcin, 1990). The steps of this procedure are illustrated as follows:

- Step 1 Strength determination: Five grades of concrete with average 28 day compressive strength are listed on a table that ranging from 65 to 120 MPa.
- Step 2 Water content: For selecting the water content, the maximum size of the coarse aggregate and slump values are not considered since maximum sizes of 10 to 15 mm are only considered. The water content is specified for different strength levels.
- Step 3 Selection of the binder: The volume of the binding paste is assumed to be 35% of the total concrete volume. The volumes of the air content (entrapped or entrained) and mixing water are subtracted from the total volume of the cement paste to calculate the remaining volume of the binder. The binder is then assumed to be one of the following three combinations:
 - Option 1: 100% Portland cement to be used when absolutely necessary;
 - Option 2: 75% Portland cement and 25% fly ash or blast furnace slag by volume;
 - Option 3: 75% Portland cement, 15% fly ash, and 10% silica fume by volume.

A table lists the volume of each fraction of binder for each strength grade.

- Step 4 Selection of aggregate content: The total aggregate volume is equal to 65% of the concrete volume.
- Step 5 Batch weight calculation: By using the volume fractions of the concrete and the specific gravity values of each of the concrete constituents, the weights per unit volume of concrete can be calculated. Normal specific gravity values for Portland cement, fly ash, blast-furnace slag and silica fume

are 3.14, 2.5, 2.9 and 2.1, respectively. Those for natural siliceous sand and normal-weight gravel or crushed rocks can be taken as 2.65 and 2.70, respectively. The calculated mixture proportions of each concrete type and strength grade suggested in this method are listed in the table.

- Step 6 Superplasticizer content: It suggested that 1% superplasticizer solid content of binder for the first trial mixture and the mass and volume of a superplasticizer solution are then calculated by taking into account the percentage of solids in the solution and the specific gravity of the superplasticizer.
- Step 7 Moisture adjustment: The volume of the water included in the superplasticizer is calculated and subtracted from the amount of initial mixing water. Similarly, the masses of the aggregate and water are adjusted for moisture conditions and the amount of mixing water adjusted accordingly.
- Step 8 Adjustment of trial batch: Usually the first trial mixture will have to be modified to meet the desired workability and strength criteria. The aggregate type, proportions of sand to aggregate, type and dosage of superplasticizer, type and combination of supplementary cementations materials and the air content of the concrete can be adjusted to optimise the mixture proportioning.

2.2 Polymer Modified Cement, Mortar and Concrete

2.2.1 General

Over the past 25 years, polymers in concrete have received significant attention. Polymer-modified concrete (PMC) has been used mainly for repair and overlays. PMC started into use in the 1950s, but the users were very limited.

The first international congress on polymer in concrete (ICPIC) was held in London in 1975, and American Concrete Committee 548 on polymers in concrete was formed. Later RILEM committees were created to address specific areas in concrete with polymer composites. ICPIC conferences and ACI Symposia helped construction industry to use polymers material (Fowler, 1999).

The polymer is widely used in structural concrete due to its high bonding strength with most aggregates, outstanding stability in dimensions from low creep/shrinkage

during and after curing, low porosity and permeability, good thermal resistance, optimised chemical resistance, outstanding fatigue resistance and good electrical insulation. Polymer concrete has become a significant group of concretes that use polymers to supplement or replace cement as a binder. Figure 2-3 shows the Polymeric admixtures or modifiers. Polymer concrete is divided into three main categories (Ohama, 1997):

- Polymer modified mortar (PMM) and concrete (PMC),
- Polymer mortar (PM) and concrete (PC),
- Polymer impregnated concrete (PIC).

2.2.2 Polymer-modified mortar and concrete (PMM and PMC)

PMC consists of Portland cement concrete with a Polymer modifier such as acrylic or styrene-butadiene latex (SBR), polyvinyl acetate or ethylene vinyl acetate. The amount of polymer is usually in the range of 10-20% of the Portland cement binder weight. Polymer-modified concrete (mortar) comprises of repair systems for deteriorated reinforced concrete structures, strengthening (or retrofitting) methods and exfoliation (or delamination) prevention methods for existing reinforced concrete structures, liquid-applied membrane waterproofing systems, advanced polymeric admixtures such as high-grade dispersible polymer powders and hardener-free epoxy resins, intelligent repair materials, application of accelerated curing, semi flexible pavements, and drainage pavements with photo catalyst (Bhutta and Ohama, 2010). SBR has excellent bond strength to concrete, higher flexural strength, and lower permeability.

Acrylic latex is also useful for bonding ceramic tiles on floors. Acrylic PMC has the capacity to be colourfast, which makes it an attractive material for architectural finishes. Carboxylate SBR added to the concrete mixture causes a w/c reduction, an increase of porosity, delaying setting (for high amount of polymer) and shrinkage reduction. In general, polymer modification of cement matrix has good adhesion, higher tensile and flexural strength, and improved durability including resistance against chloride penetration, carbonation and freezing/thawing, and the costs are cheaper than those of PIC and PC (Chmielewska, 2008). Durability indicates the ability to remain fit for use during the design working life with proper maintenance.

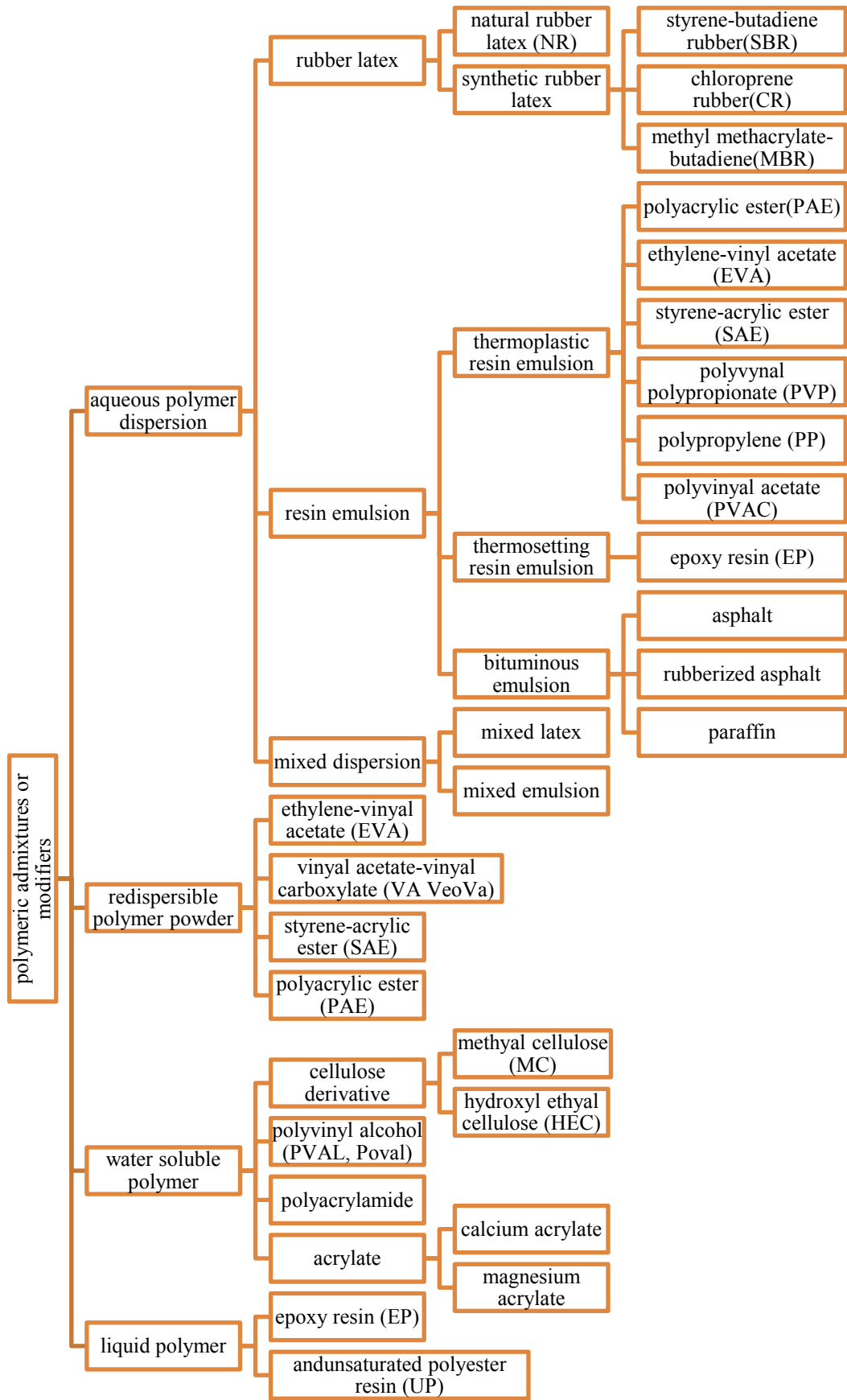


Figure 2-3 Polymeric admixtures or modifiers (Ohama, 1997)

SBR has been widely used for floor and bridge overlays. Acrylic latex has been used to produce mortars, which can be sprayed or trowelled on architectural finishes (Islam et al, 2011).

2.2.3 The workability of concrete modified with polymers

The term “workability” is largely defined to describe the property of fresh concrete, and there is no single test method for measuring all aspects of workability (Ferraris et al, 2008). According to ACI Cement and Concrete Technology, the workability is the property of freshly mixed concrete or mortar and is used to determine the degrees of ease and homogeneity with which it can be mixed, placed, consolidated and finished (http://www.concrete.org/technical/CCT/FlashHelp/ACI_terminology.htm). The advent of new high performance concrete mixtures that are susceptible to small changes in mixture proportions has made monitoring workability even more critical. A national ready-mixed concrete association survey identified the need for a better method to characterise the workability of high performance concrete (Ferraris et al, 2008).

An investigation on the fresh SBR-modified lightweight aggregate concretes showed that SBR modified lightweight aggregate concretes are more cohesive than unmodified lightweight aggregate concretes (Rossignolo and Agnesini, 2002). The SBR modified and unmodified lightweight aggregate concretes display very good workability for approximately 1h after the completion of mixing. The slump value decreases when the quantity of polymer increases. This implies that the polymer additive will reduce the workability of the concrete. This is because the polymer causes the concrete to become viscous and the solid particles of polymers which fill up the voids of the concrete will obstruct the concrete mix of slump. There is no slump value for 5% and 10% of polymer content, because the concrete mix became very harsh and sticky (Ferraris and Lobo, 1998).

The workability of the latex modified Portland cement paste decreases with increasing latex concentration. However this is dependent on the w/c ratio of the mixture. Using a suitable superplasticizer reduces the w/c ratio. In this case, the w/c ratio can vary from 0.33 to 0.28. These results show a progressive decrease in the water content required for obtaining enough workability (Colak, 2005).

The addition of polyvinyl acetate, copolymers of vinyl acetate-ethylene, styrene-butadiene, styrene-acrylic and acrylic and styrene butadiene rubber emulsions to cement mortar improves workability (Colak, 2005).

The addition of low-density polyethylene (LDPE), crushed polyethylene terephthalate (PET) and rubber from useless tires (TIRE) to concrete in the ratios 0.5%, 1.0%, 2.5%, 5.0% and 7.5% can reduce the workability of the fresh concrete (Galvao et al, 2011).

2.2.4 Compressive, tensile and flexural strengths

Portland cement pastes with and without super plasticizer show a high rate of increase in compressive strength up to 7 days. Their strengths continue to grow with the progress of hydration of cement. However, the addition of latex to the Portland cement paste results in a decrease in compressive strength of almost all pastes, except perhaps the pastes with a low concentration of latex (Yoshihiko, 1997). Significant differences exist not only in the strength values for these pastes but also in the rate of increase in strength as the latex concentration increases.

The use of super plasticizer in the latex modified Portland cement pastes tends to mask the debilitating effects of a superior latex concentration on the strength and the gain of strength with time. Nevertheless, curing in lime-saturated water begins to adversely affect the strengths of latex modified Portland cement pastes with and without super plasticizer from about 28 days onwards. This behaviour is just exactly the reverse of that normally shown by the Portland cement pastes with and without super plasticizer (Ohama, 2004).

It is likely that the increased solubility of the polymer leads to a poorer, probably more porous physical structure and consequent impairment of the strength. Addition of polyvinyl acetate, copolymers of vinyl acetate-ethylene, styrene-butadiene, styrene-acrylic and acrylic and styrene butadiene rubber emulsions increases flexural and compressive strength (Aggarwal et al, 2007). This new epoxy-hydraulic cement system provides an increase in the flexural strength (Ohama, 2004).

The application of the autoclave curing of SBR-modified concrete with a slag content of 40% and a polymer-binder ratio of 20% provides about three times higher tensile

strength and twice higher compressive strength than unmodified concrete (ordinary cement concrete) (Ohama, 2004).

The polymer-modified mortars or slurries for liquid-applied membrane waterproofing systems are prepared by polymer-cement ratios of 20 to 300% by using PAE and EVA emulsions, and have tensile strengths of 0.7 to 8.0 MPa and elongations of 25 to 400% (Ohama, 2004). The results of addition of polymer and silica fume to mortars indicate that the tensile bond strength was superior to those specified by the standard (Almeida and Sichieri, 2007).

The addition of 7.5% content of low-density polyethylene (LDPE), crushed polyethylene terephthalate (PET) and rubber from useless tires (TIRE) to concrete could reduce the compressive strength by 38.48% for TIRE, 26.24% for LDPE and 15.45% for PET (Galvão et al, 2011).

2.2.5 Durability

The resistance of plain and latex modified Portland cement pastes with and without super plasticizer against attack by salt solutions, such as sodium chloride and sodium sulphate, varies widely not only from paste to paste but in some cases within the different grades of a single paste. These salts may cause the degradation of Portland cement pastes with and without super plasticizer in several ways, dependent on the pH values of the aqueous solution and the solubility of the corrosion products formed during their reactions with hardened pastes. This is resulted from the plasticizing action of the absorbed salt solution by latex or from the partial removal of the added latex by leaching action. The magnitude of this effect is dependent on the latex concentration in the mixture. Higher concentration of latex generally increases the level and magnitude of corrosive attack. The effect becomes insignificant as the latex concentration decreases. These results strongly indicate that the presence of latex in paste composition has a profound effect on the chemical stability of the material (Yoshihiko, 1997).

According to Aggarwal, Thapliyal and Karade (Aggarwal et al, 2007), polyvinyl acetate, copolymers of vinyl acetate-ethylene, styrene-butadiene, styrene-acrylic and acrylic and styrene butadiene rubber emulsions may re-emulsify in humming alkaline

conditions. To overcome this problem, an epoxy emulsion based polymer system has been developed.

Addition of polyvinyl acetate, copolymers of vinyl acetate-ethylene, styrene-acrylic and styrene butadiene rubber emulsions decreases water absorption, carbonation and chloride ion penetration (Aggarwal et al, 2007).

Because of the two-component mixing of the conventional epoxy-modified mortars and concretes (epoxy resin and hardener), it has an inferior applicability, the toxicity of hardeners and the obstruction of cement hydration by the hardeners. The researchers found out that even without any hardeners the epoxy resin can harden in the presence of alkalis or hydroxide ions produced by the hydration of cement in the epoxy-modified mortars (Bhutta and Ohama, 2010). The new epoxy-hydraulic cement system provides improvements in the carbonation or chloride ion penetration resistance with increasing polymer-cement ratio up to 20% (Ohama, 2004).

Nitrite-type hydrocalumite provides excellent corrosion-inhibiting property to the reinforcing bars in reinforced concrete. Polymer-modified mortars with the nitrite-type hydrocalumite (calumite) have superior corrosion-inhibiting property and durability, and produce the attraction as effective repair materials for deteriorated reinforced concrete structures (Ohama, 2004). A calumite content of around 10% is recommended to make effective repair materials for deteriorated reinforced concrete structures (Ohama, 2004). The pavements are applied to heavy traffic roads, intersection pavements, bus stops, parking bays and airport runways because of their excellent rutting resistance, load spread ability, abrasion resistance, oil resistance and colourability (Ohama, 2004).

The addition of low-density polyethylene (LDPE), crushed polyethylene terephthalate (PET) and rubber from used tires (TIRE) to concrete increases the resistance to underwater erosion abrasion (Galvão et al, 2011).

The test results indicate that SBR modified lightweight aggregate concrete (LWAC) provides better performance in aggressive environments than the unmodified LWAC (Rossignolo and Agnesini, 2004).

2.2.6 Adhesion strength of SBR modified concrete

Styrene-butadiene rubber (SBR) is a polymer made from butadiene and styrene monomers. It has a good mechanical property and processing behaviour, and can be used as natural rubber (Peng, 2011).

According to Chmielewska (2008), the adhesion strength of the SBR enhanced concrete is between those of ordinary cement concrete (OCC) and selected repair materials (OCC, PCC-10%, PCC-20%). In addition to other factors influencing adhesion such as moisture of substrate's surface, direction of concreting in relation to the substrate's surface were observed.

To measure adhesion strength, there are three testing methods: pull-off test, shear test and wedge splitting test, as shown in Figure 2-4. The pull-off test brings 50 mm thick overlays and is poured on 100 mm thick plates. For the shear test, the 150 mm cubic samples were prepared. One half of such sample was made of OCC (substrate) and the second half was placed using the investigated material. The wedge splitting test was the third method used. Hardened concrete substrate and repair material are bonded with a notch placed in the plane of the bond. In the case of the last two methods, the following conditions were tested: concreting in the direction vertical to the dry substrate's surface or concreting in the direction parallel to the moist substrate's surface (Chmielewska, 2008).

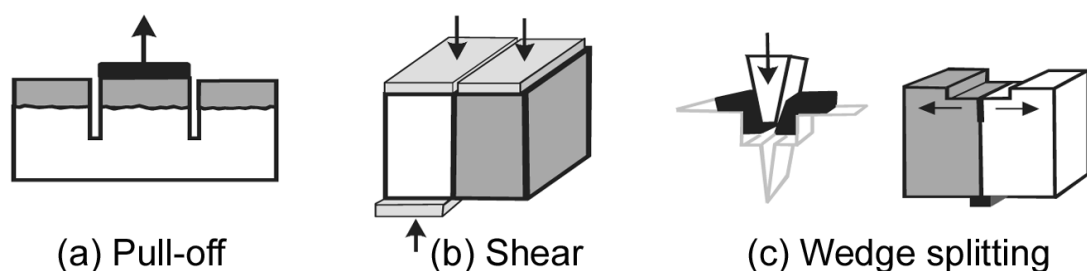


Figure 2-4 Shear testing methods (Chmielewska, 2008)

2.2.7 Polyethylene-vinyl acetate (EVA)

To improve the properties of mortars and concretes, such as elastic modulus, toughness, permeability and bond strength to various substrates as well as water retention capacity and plasticity in the fresh state, Polyethylene-vinyl acetate (EVA)

is added during mixing,. EVA polymer powder can be added to anhydrous cement and aggregates before mixing with water, or it can be added during the mixing as an aqueous dispersion. Due to improved adhesion by EVA, it is also used for the production of dry-set mortars for ceramic tile installation, especially for coating of façades, which are frequently exposed to severe environmental conditions (Silva and Monteiro, 2005).

2.2.8 Effects of vinyl acetate (VA/veova) powder on physical and mechanical properties of cement mortar

There are many effects of VA/veova powder on physical and mechanical properties of cement mortar, and VA/veova powder has good water reducing effect. It augments gradually with the increase of m_p/m_c , i.e. VA/veova powder to cement ratio by mass, where up to 35% when m_p/m_c is 15%. Also the VA/veova powder has a water-retention effect that rises considerably by 90% with the increase of m_p/m_c up to 7%. VA/veova powder has air entraining effect that increases the air content of fresh mortar and decreases the bulk density decrease. The compressive strength of cement mortar is depressed by VA/veova powder, but the flexural strength is not affected. The toughness of cement mortar needs to be improved significantly. VA/veova powder has shrinkage reducing effect in cement mortar when m_p/m_c is over 7%. VA/veova powder improves the hydrophobicity and water permeability of cement mortar. The water capillary adsorption decreases with the increase of m_p/m_c and to about 0.7 kg/m^2 at 24h when m_p/m_c increases to 7%. The water penetration depth decreases from 12 mm to 2 mm with the increase of m_p/m_c from 0% to 15% when the pressure is increased step by step to 1.5 MPa (Wang, 2011).

2.2.9 Effects of styrene-acrylic ester (SAE) on physical and mechanical properties of cement mortar

There are numerous effects of Styrene-Acrylic Ester (SAE) on physical and mechanical properties of cement mortar. SAE has fine water-reduction and water-retention effects that normally become more significant with m_p/m_c . The water-reduction rate reaches about 40% when m_p/m_c is 20%, and water-retention rate keeps 99% when m_p/m_c are higher than 10%. With 1% SAE addition, the air content of fresh mortar increases from 4.5% to 7.1% and the bulk density of the fresh mortar

decreases with the increase of m_p/m_c . The ratio of compressive strength to flexural strength decreases clearly with the increase in m_p/m_c . The shrinkage rate of the mortar is decreased with an addition of SAE latex by more than 10%. The waterproofing quality and anti-penetration capacity of the mortar are enhanced by the addition of the SAE latex. The water capillary adsorption decreases with the increase of m_p/m_c and the value at 24h is not higher than 0.7 kg/m^2 with m_p/m_c above 7%. When m_p/m_c is higher than 12%, no water penetrates into the mortar specimens with the pressure increasing to 1.5 MPa within 8 h (Wang, 2010).

2.2.10 Applications of latex blend modified concrete

Zhong and Chen (2002) found that there is relationship between the properties of polymer films formed from latex blends and the properties of the latex blend-modified mortars, using three types of latex blends SAE/SBR, SAE/PVDC and PVDC/SBR, and drew the following conclusions:

- The tensile strength of the latex blend films of SAE/PVDC blend and SAE/SBR blend showed approximately linear relation with the mass fraction of the component. This identified the good compatibility of the component in the case of blend films. However, tensile strength of the PVDC/SBR blend films was much lower than that of arithmetical addition. This shows the poor compatibility of PVDC and SBR.
- The mechanical properties were with similar behaviour by SAE/SBR blends and PVDC/SBR blend-modified mortars. In detail, the SAE/SBR blend-modified mortars showed good synergistic effect on the relationship between the mechanical properties of the mortars and the mass fraction of blends, while the PVDC/SBR blends showed antichloristic effect. If the mass ratio of SAE/SBR was between $2/3$ and 1.0, the flexural strength of the blend-modified mortars was 20-40% higher than that of the monol latex-modified mortar. Contrarily, the SAE/PVDC blend-modified mortars showed the behaviour opposite to the blend films. This may be attributed to the degradation of PVDC in the mortar.
- The compressive strength of latex blend-modified mortars increased with the increasing tensile strength of the latex blend films while the flexural strength

of the latex blend modified mortars was independent of the tensile strength of the latex blend films.

- With suitable mass ratio of the latex blends of SAE/SBR or PVDC/SBR, blend-modified mortars showed lower chloride diffusivity. Concretely, when PVDC with a mass fraction of 0.2 or SAE copolymer emulsion with a mass fraction of 0.4 was blended into SBR latex, the latex blend-modified mortars showed lower chloride diffusivity and also good mechanical properties.
- The chloride diffusivity of the latex blend-modified mortars decreased with decreasing of the compressive strength of the modified mortars while it was independent of the flexural strength of the modified mortars.
- The chloride diffusivity of the modified mortars increased approximately linearly with the increasing tensile strength of the latex blend films, and decreased with the increase of the elongation at rupture of the latex blend films. When the elongation at rupture of the latex blend films increased from 200-300% to more than 800%, the chloride diffusivity of the modified mortars decreased.

2.3 Fracture Characteristics of Concrete

2.3.1 History of fracture mechanics

Though the avoidance of brittle fracture had been practiced by keeping the structures members in compression, Leonardo Da Vinci was the first to keep records to study of materials through tests on iron wires in tension. The fracture energy was as a specific scientific regulation for less than 50 years old (Cotterell, 2002).

In the early elastic analysis in 1890, Love showed the important understanding of crack propagation. In 1920, the connection between fracture stress and flaw size was made by Griffith (Griffith, 1921). Orowan revealed that the limitation of Griffith approach for metals led to suggest the energy release rate as fracture criteria (Orowan, 1955). In 1968, Rice projected another fracture criterion to better characterise nonlinear behaviour of material ahead of the crack by assuming plastic deformation to be nonlinearly elastic (Rice, 1968).

The process of material fracture is presented in Figure 2-5, where L stands for linear, N stands for nonlinear and F stands for failure (Trussoni, 2009). In Figure 2-5(a), the fracture of materials displays a fundamentally linear elastic material behaviour, while the fracture process zone (FPZ) and nonlinear zone in the area of the crack explain this fracture behaviour as the subject of linear elastic fracture mechanics (LEFM). Figure 2-5(b) shows that nonlinear plastic fracture mechanics methodologies have been developed when a relatively large nonlinear zone which can be compared to the size of the specimen surrounds a small FPZ in front of the crack tip. Figure 2-5(c) shows the different situation in concrete from those for the linear and nonlinear fracture models. The difference is that the fracture zone is large and the zone with nonlinear behaviour is small, compared to the size of the specimen.

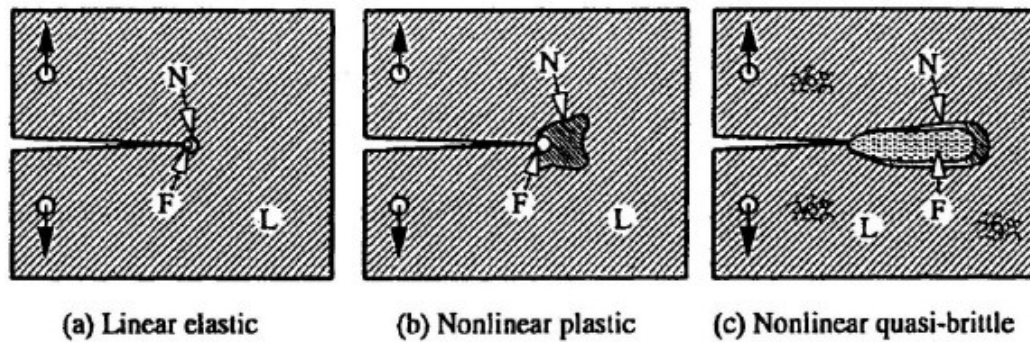


Figure 2-5 Linear, nonlinear and quasi-brittle fractures (Trussoni, 2009)

The difference in behaviour between these three categories of material behaviour, i.e. brittle, ductile and quasi-brittle, is shown in Figure 2-6 (Trussoni, 2009), and each is in uniaxial tensile stress field.

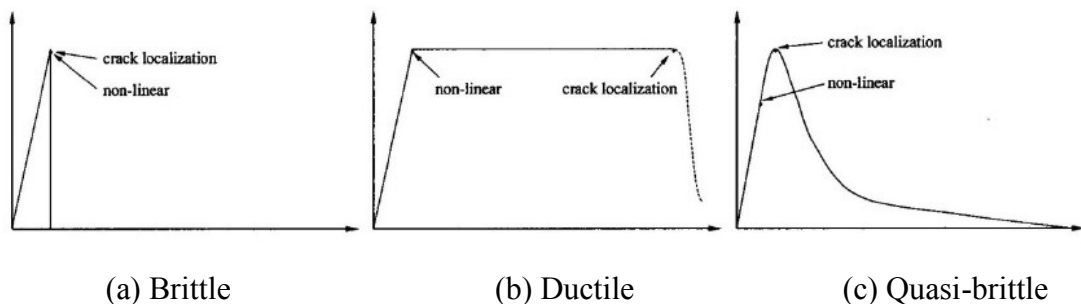


Figure 2-6 Different failure modes of engineering materials (Trussoni, 2009)

Figure 2-6(a) shows that the brittle material displays a linear-elastic relationship up to close to the peak load followed by a sudden crack development that propagates through the specimen cross-section, causing an almost instant unloading and fracture. In Figure 2-6(b), the yielding plateau characterises the ductile material and starts before the beginning of rapid crack expansion. Compared to the nonlinear zone FPZ, the ductile material remains comparatively small surrounding the crack tip, allowing the details of activity in the FPZ to be ignored. In Figure 2-6(c), the behaviour of quasi-brittle material starts before reaching the peak load associated with the process of micro cracking that occurs within the FPZ ahead of the crack tip. The response exhibits a negative slope after reaching the peak load. The softening portion of the curve provides important description of the fracture properties of concrete materials.

2.3.2 Linear elastic fracture mechanics (LEFM)

Griffith was the first researcher who showed that the stress field in the vicinity of the crack tip was critical to the load carrying capacity of material, and then initiated the linear elastic fracture (Griffith, 1921). Griffith developed the relationship in an infinite plate between the crack length, the surface energy connected with a traction-free crack surface, the modulus of elasticity and applied stress as follows:

$$\sigma^2 = \frac{E 2\gamma}{\pi a} \quad (2.2)$$

Irwin (Irwin, 1957) used the strain energy release rate G to replace the surface energy 2γ and showed that:

$$\sigma^2 = \frac{E G}{\pi a} \quad (2.3)$$

where

$$G = 2\gamma + G_p \quad (2.4)$$

where G_p is the plastic dissipation portion and it dominates during plastic fracture.

Irwin's equation for the strain energy release rate G shows that the purely elastic solution may be used to calculate the amount of energy available for fracture as following:

$$G = -\left[\frac{\partial U}{\partial a}\right]_P = \left[\frac{\partial U}{\partial a}\right]_U = \frac{\pi\sigma^2 a}{E} \quad (2.5)$$

where

U is the elastic energy,

a is the half crack length.

For mode I, Irwin showed that fracture the energy release rate G and the stress intensity factor K could be linked by:

$$G = G_I = \begin{cases} \frac{K_I^2}{E} & \text{for plane stress} \\ \frac{(1-\nu^2)K_I^2}{E} & \text{for plane strain} \end{cases} \quad (2.6)$$

where ν is the Poisson's ratio.

The best description of stress field, σ_{ij} , in front of a crack tip, is shown as follows:

$$\sigma_{ij} = \frac{K}{\sqrt{(2\pi r)}} f_{ij}\theta + C_1 + \dots \quad (2.7)$$

where

r is the distance,

θ is the angle,

$C_1 + \dots$ is the higher order terms.

Figure 2-7 (Trussoni, 2009) indicates that the stress varies with the distance r and the angle θ , while Figure 2-8 (Trussoni, 2009) illustrates the assumed shape of the crack tip and a typical stress distribution.

Griffith found from the geometry test that the critical stress intensity factor, K_{IC} for each crack tip becomes:

$$K_{IC} = \sigma\sqrt{\pi a} \quad (2.8)$$

with

$$G_C = \frac{K_{IC}^2}{E} \quad (2.9)$$

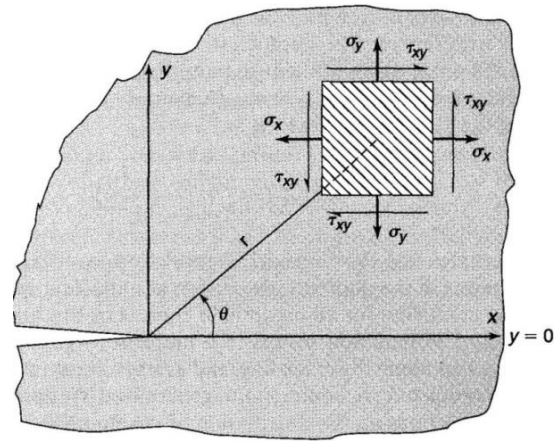


Figure 2-7 Stress near crack tip (Trussoni, 2009)

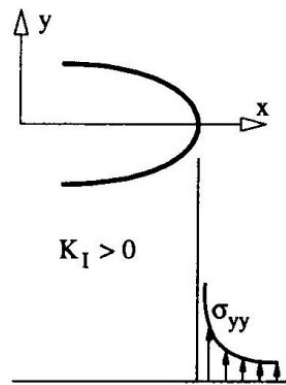


Figure 2-8 Crack tip and stress distribution (Trussoni, 2009)

2.3.3 Quasi-brittle fracture mechanics of concrete

For ideally brittle materials, the stress-strain curve is linearly elastic up to the maximum stress, while for quasi-brittle materials like concrete the stress-strain curve is non-linear before the maximum stress is reached. It is observed that the strain softening is under stable propagation of the crack. When the closed loop displacement controlled test machine is used both opening of the crack and unloading of the specimen for post peak part of the stress-strain curve can be observed (Shah et al, 1995).

Wang and Shrive (1995) showed that initial crack starts to propagate at the proportional limit, and keeps propagating in a steady behaviour until the peak stress, so new crack surfaces are formed by extension of cracks. Two fracture criteria, energy criteria and stress criteria, manage cracking of concrete.

The dimension and shape of the fracture process zone (FPZ) determines the difference between the brittle and ductile material. The toughening mechanism in the FPZ of a quasi-brittle material like concrete such as crack bridging, crack branching, crack deflection, crack face friction, crack tip blunting, and micro cracking arise the difficulties in applying fracture mechanics to quasi-brittle materials like concrete (Cox and Marshall, 1994). Kaplan was one of the first researchers to try to apply Linear Elastic Fracture Mechanics (LEFM) to concrete, by measuring the critical energy release rate G_c and the stress factor K_I (Kaplan, 1961).

The determination of critical energy release rate G_c depends on the size of the specimen and the results contradict the accepted thought that it was a uniform material property. In Figure 2-9, Tian, Huang and Liu showed this size dependency that the critical stress intensity factor K_I varies with specimen depth W , and K_{IC} reached a stabled value once the specimen becomes relatively large (Trussoni, 2009).

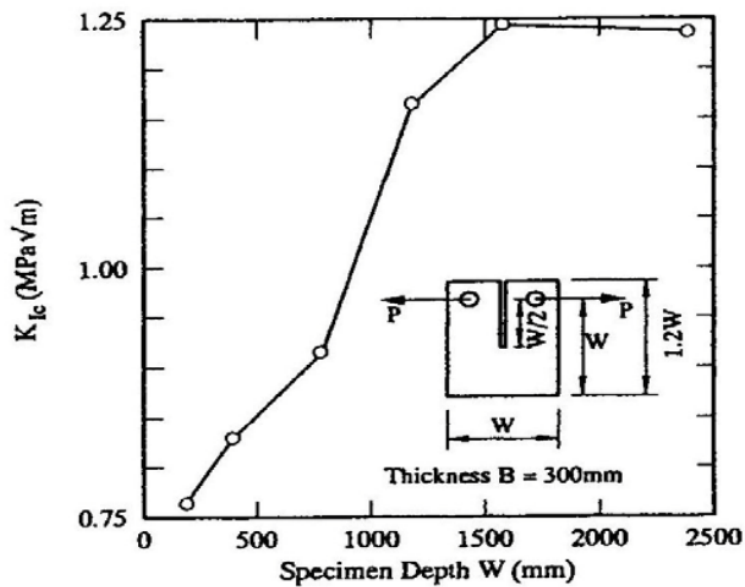


Figure 2-9 K_{IC} versus specimen depth W (Trussoni, 2009)

2.3.4 The fracture process zone

In the concrete matrix, stress concentrations form around aggregates, and flaws or air voids lead to formation of micro cracks. This stress occurs in the cement paste and aggregates interface and the increasing stress causes the micro cracks to coalesce into macro cracks. A number of researchers represented two main aspects of load-deflection curves in the FPZ. The first aspect is the distance between the failure point

and the peak load, and the second is the amount of deflection that occurs between the onset of non-linear behaviour and the sudden drop in load carrying capacity (Trussoni, 2009). Figure 2-10 illustrates the different stages of fracture occurrence of a crack tip, indicating that concrete specimen sustains Model I fracture. Micro cracking, aggregate bridging, crack branching and crack extension, as showed in Figure 2-11, exist as a result of development of FPZ in concrete and the evidence in the work carried out by Nemati et al supports this (Nemati et al, 1998).

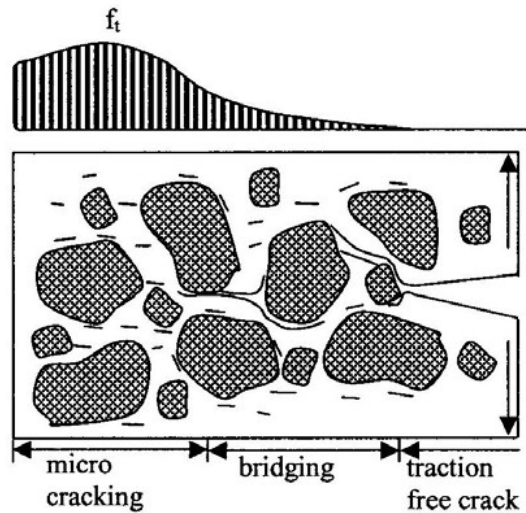


Figure 2-10 Enlarged fracture process zone (Trussoni, 2009)

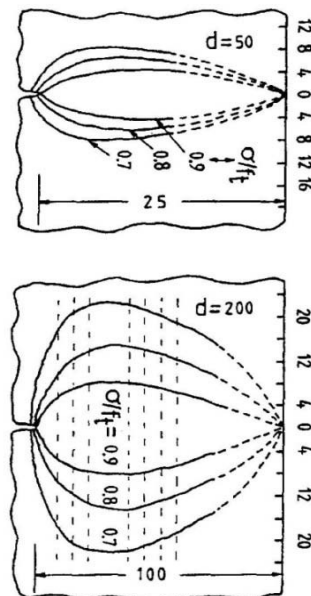


Figure 2-11 Varying sizes of FPZ (Nemati et al, 1998)

Figure 2-12 presents different estimated FPZ sizes for varying stress-to-tensile strength ratios with a relative notch depth of 0.5 for the beam. Figure 2-13 shows the edge effects in the FPZ in concrete, where the transition ligament exists (Hu and Wittmann, 1992). The length of the crack may be different along the width of the specimen and this may be due to the difference in plane stress and plane strain conditions taking place along the width of the specimen.

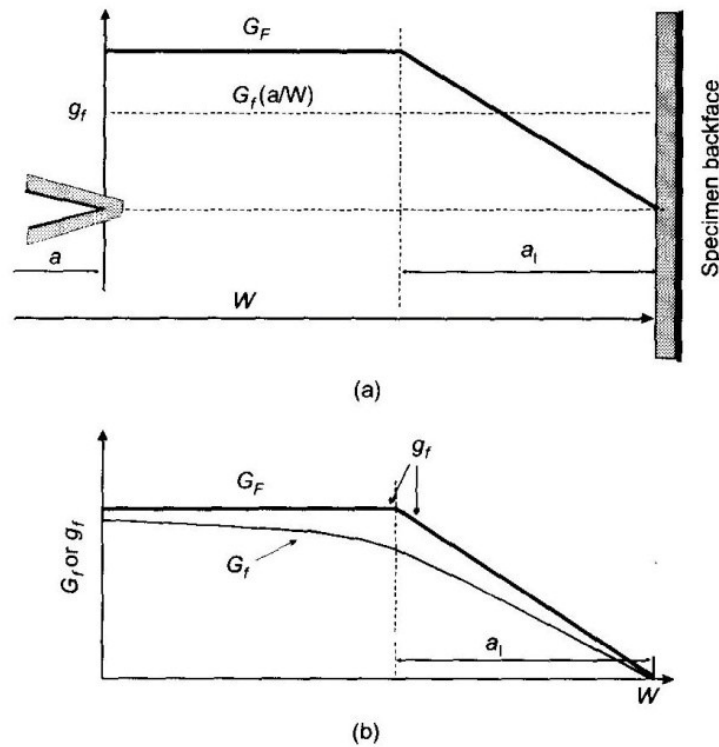


Figure 2-12 Edge effect on FPZ (Hu and Wittmann, 1992)

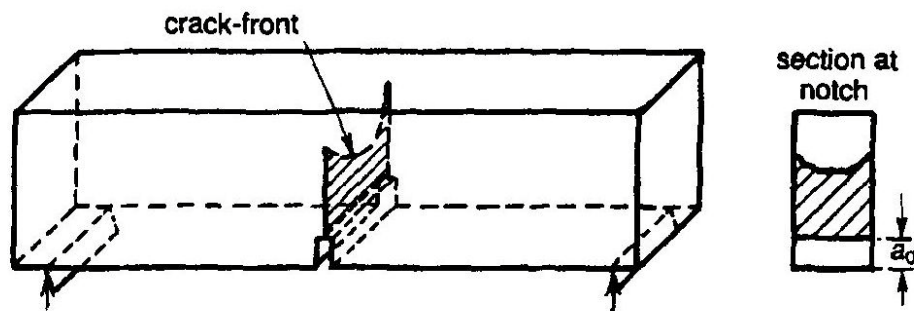


Figure 2-13 Plane stress – strain effects on fracture (Hu and Wittmann, 1992)

2.3.5 The fictitious crack model (FCM)

The fictitious crack model for fracture of concrete is suggested by Hillerborg et al (1976), when the pre-peak tensile response of concrete is ignored. The fictitious crack model (FCM) assumes that the crack initiates as soon as the tensile strength is reached. As described on the model in Figure 2-14, Hillerborg (1985) proposed a displacement controlled test on a concrete bar in tension and assumed that the fracture is located within zone D. The material in zones B, C and E is unloaded, but the deformation increases in zone D. The additional deformation due to the fracture in zone D is given as W .

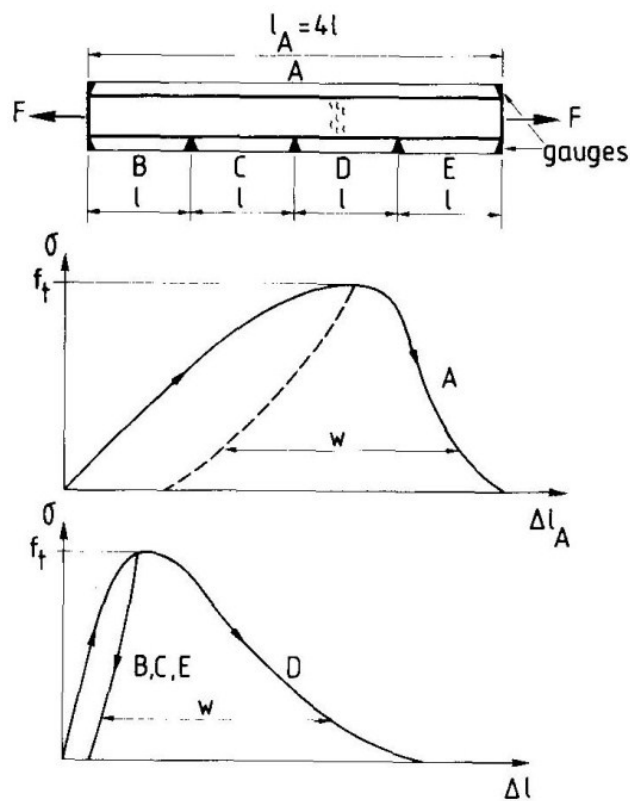


Figure 2-14 Tension test with deformation measurements (Hillerborg, 1985)

The elastic deformation of the specimen that does not contain the fracture zone can be expressed as:

$$\Delta l = \varepsilon l \quad (2.10)$$

where ε is the strain on the length that contains the fracture zone D (see Figure 2-14).

Also it contains an additional deformation W as:

$$\Delta l = \varepsilon l + W \quad (2.11)$$

It can be described that the tensile fracture behaviour of concrete is based on these curves with the modulus of elasticity of concrete (E), the tensile strength of concrete (f_t) and the fracture energy of the concrete (G_F). The modulus of elasticity (E) and the tensile strength (f_t) can be obtained from the curve in Figure 2-15 (Hillerborg, 1985).

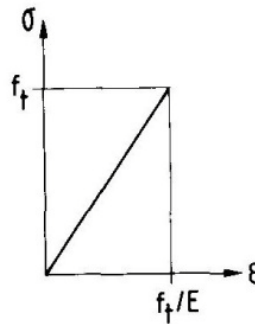


Figure 2-15 Linear approximation of a $\sigma - \varepsilon$ curve (Hillerborg, 1985)

The area under the curve is the most essential property that measures the total energy absorption and is called the fracture energy (G_F) as shown in Figure 2-16 (Hillerborg, 1985). Hillerborg considered the fracture as a material property, but Bažant showed the latter to be dependent on the specimen size. Figure 2-16 shows the relationship between f_t and G_F as a straight line (Bazant, 2002).

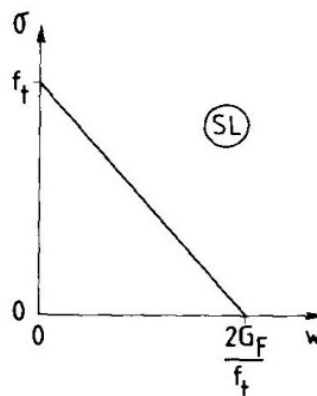


Figure 2-16 Linear approximation of a $\sigma - w$ curve (Hillerborg, 1985)

As shown in Figure 2-17, a bi-linear approximation of the $\sigma - w$ curve is proposed by Hillerborg to calculate the values of f_t and G_F for more accurate results than the linear approximation (Hillerborg, 1985).

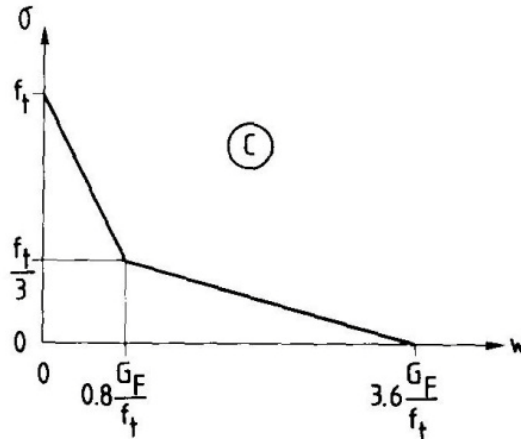


Figure 2-17 Bi-linear approximation of a $\sigma - w$ curve (Hillerborg, 1985)

The values of E , f_t and G_F with the assumption of linear $\sigma - \varepsilon$ and $\sigma - w$ curves define the properties that govern tensile fracture behaviour. As shown in Figure 2-18, it can be used to determine G_F by a three-point bending test (Hillerborg, 1985).

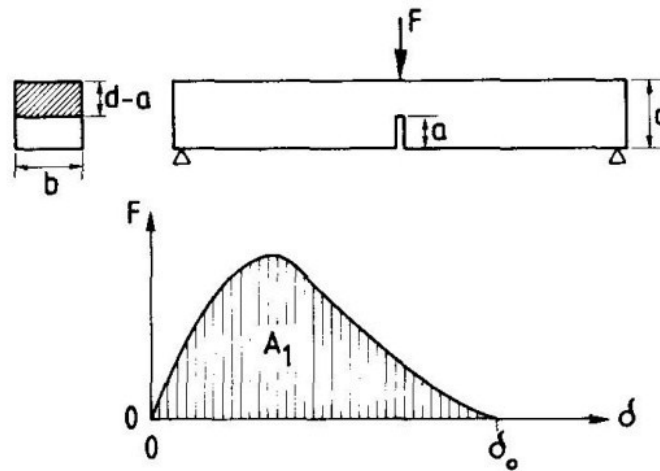


Figure 2-18 A three-point bending test (Hillerborg, 1985)

By including the specimen mass M and gravity g , G_F can be calculated from:

$$G_F = \frac{A_1 + M g \delta_0}{b(d-a)} \quad (2.12)$$

2.3.6 The size effect model

Bazant et al described the size effect model using an equivalent elastic approach to the nonlinearity of the load-deflection curve and considered the notch to depth ratio of the beam was held constant while the beam thickness was the same (Bazant et al, 1986). The stress at failure is calculated as:

$$\sigma_c = \frac{C_n P_c}{t H} \quad (2.13)$$

where

P_c is the critical load,

C_n is the geometry coefficient,

t is the beam thickness perpendicular to both the span and the load,

H is the depth of the beam parallel to loading.

The failure stress of a series of geometrically similar structures of different sizes is:

$$\sigma = B f t \left[\frac{H}{H_0} + 1 + L_1 \left(\frac{H}{H_0} \right)^{-1} + L_2 \left(\frac{H}{H_0} \right)^{-2} + \dots \right]^{-5} \quad (2.14)$$

where

B, H_0, L_1 and L_2 are constants,

f_c is the tensile strength of the material.

2.3.7 The two-parameter fracture model

In the two parameter fracture model (Jenq and Shah, 1985), there are two fracture criteria: the critical stress intensity factor K_{IC} and the critical crack tip opening displacement $CTOD_c$. Based on the effective-elastic crack approach, this includes the nonlinear behaviour of crack growth. The critical stress intensity factor K_{IC} can be determined from:

$$K_{IC}^s = \sigma_c \sqrt{(\pi a_c)} g_1 \left(\frac{a_c}{b} \right) \quad (2.15)$$

where σ_c is the critical stress, b is the beam width, and a_c is the critical crack length,

with

$$CMOD_c = \frac{4\sigma_c a_c}{E} g_2 \left(\frac{a_c}{b} \right) \quad (2.16)$$

The critical crack tip opening displacement is then determined by:

$$CTOD_c = CMOD_c \left(\frac{a_c}{b} \frac{a_0}{a_c} \right) \quad (2.17)$$

As shown in Figure 2-19, the critical crack length a_c can be obtained by equating the modulus of elasticity (E) of loading and unloading curves (Bordelon, 2005).

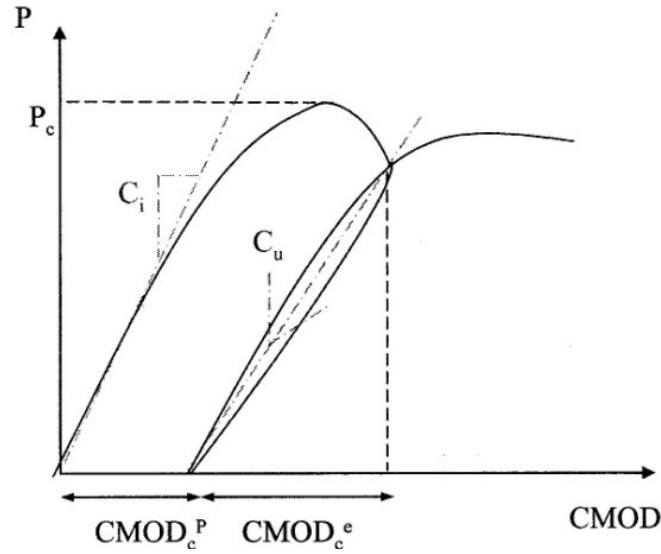


Figure 2-19 Typical unloading curve for two-parameter fracture model (Bordelon, 2005)

2.3.8 The effective crack model

Karihaloo and Nallathambi (1989) modified the fictitious crack model proposed by Hillerborg et al (1976) to obtain the critical stress intensity factor (K_{IC}). The main idea of the effective crack model is to replace the effect of various energy-consuming processes taking place in the fracture process zone (FPZ) by an equivalent energy-consuming process resulting in the formation of a supplementary traction-free crack. As shown in Figure 2-20, when the original notch length (a_0) is added to this supplementary traction-free crack, an effective notch length (a_c) can be obtained.

The effective depth of the stress-free crack is determined from the peak load P_c and the corresponding deflection δ_p . However the elastic modulus E can be obtained from the initial slope of the load-deflection curve based on the deflection equations. Consider a typical flexural load-deflection plot up to the peak load P_c and the corresponding deflection δ_p furthermore, and then consider an arbitrary load level P_i in the initial linear portion of the curve and a corresponding deflection δ_i , the mid-point deflection for a linear elastic (un-notched) beam can be determined from:

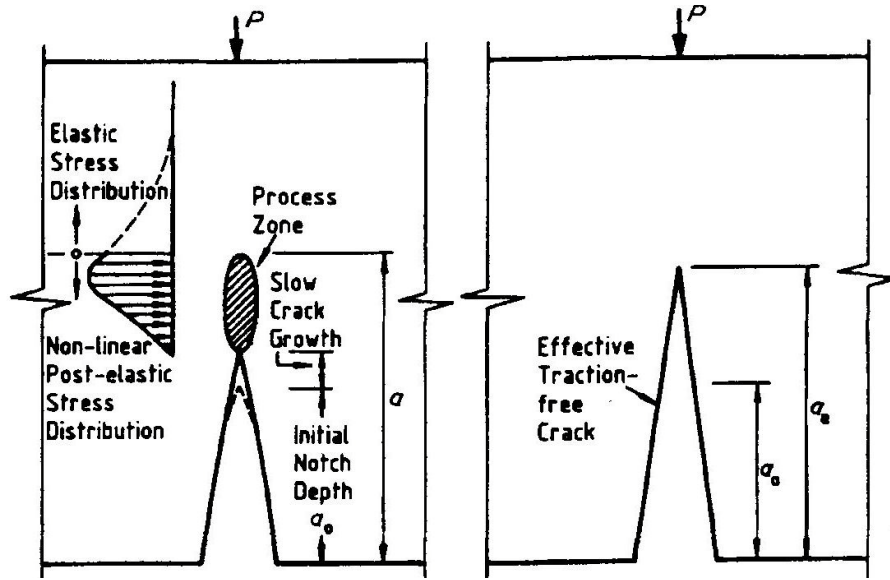


Figure 2-20 Effective notch concept (Karihaloo and Nallathambi, 1989)

$$\delta = \left(\frac{P}{E}\right) \frac{S^3 \left(1 + \left(\frac{5wS}{8P}\right)\right)}{4tW^3} + \frac{(1+\nu)S}{2ktW} \quad (2.18)$$

where

- t is the beam thickness,
- W is the beam depth,
- S is the span,
- P is the mid-span concentrated load,
- w is the self-weight of the beam per unit length,
- ν is the Poisson's ratio,
- k is the shear coefficient.

For rectangular cross section, $k = 10(1+\nu)/(12+11\nu)$ and including the shear deflection component into the equation extends its range of validity to beams with low span-to-depth ratios. The deflection of a beam containing an initial notch depth a_0 can be written as:

$$\delta = \frac{\lambda P}{E} \frac{S^3 \left(1 + \left(\frac{5SW}{8P}\right)\right)}{4tW^3 \left(1 - \frac{a_0}{W}\right)^3} + \frac{s(1+\nu)}{2ktH \left(1 - \frac{a_0}{W}\right)} \quad (2.19)$$

where λ is the correction factor relating the true deflection of the notched beam (calculated using finite-element analysis) to the deflection of un-notched beam with the same span and width but reduced depth ($H - a_0$).

The regression equation is given as:

$$\lambda = \eta'_1 \exp \left(\eta'_2 \left(\frac{a_0}{W} \right)^2 + \eta'_3 \left(\frac{a_0}{W} \right)^3 + \eta'_4 \left(\frac{a_0}{W} \right) \left(\frac{S}{W} \right) + \eta'_5 \left(\frac{a_0}{W} \right) \left(\frac{S}{W} \right)^2 + \eta'_6 \left(\frac{S}{W} \right) + \eta'_7 \left(\frac{S}{W} \right)^2 + \eta'_8 \left(\frac{S}{W} \right)^3 \right) \quad (2.20)$$

where $\eta'_1 = 1.0670$, $\eta'_2 = -0.652$, $\eta'_3 = -0.211$, $\eta'_4 = -0.3814$, $\eta'_5 = 0.0164$, $\eta'_6 = -0.0057$, $\eta'_7 = 0.0110$ and $\eta'_8 = 0.001$. The regression equation λ is valid for the ranges $2 \leq S / W \leq 9$ and $0.1 \leq a_0 / W \leq 0.6$.

The elastic modulus E is calculated by using Eq.(2.19) for the notched beam deflection and replacing P_c and δ_p with P_i and δ_i respectively. However, P_c and δ_p are useful for determining the effective notch depth a_e by imagining a fictitious beam containing a notch a_e whose stiffness remains unaltered and proportional to E of the real beam right up to the peak load as:

$$\delta = \frac{\lambda P_{\max}}{E} \frac{S^3 \left(1 + \left(\frac{5 S W}{8 P_{\max}} \right) \right)}{4 t W^3 \left(1 + \frac{a_e}{W} \right)^3} + \frac{S(1 + \nu)}{2 k t H \left(1 - \frac{a_e}{W} \right)} \quad (2.21)$$

The following regression equation gives the best fit for the data:

$$\left(\frac{a_e}{W} \right) = B_1 \left(\frac{\sigma_n}{E} \right)^{B_2} \left(\frac{a_0}{W} \right)^{B_3} \left(1 + \left(\frac{D_{\max}}{W} \right) \right)^{B_4} \quad (2.22)$$

where $B_1 = 0.121$, $B_2 = -0.192$, $B_3 = 0.467$, $B_4 = 0.215$, $\sigma_n = \frac{6M}{t W^3}$ and

$$M = \left(P_{\max} + \left(\frac{W S}{2} \right) \left(\frac{S}{4} \right) \right).$$

The elastic modulus E used here is determined from the load-deflection curve using Eq.(2.21) and the process described earlier. The effective notch depth a_e is then used in conjunction with the ASTM equation to calculate stress intensity factor at the end

of the effective crack. Karihaloo and Nallathabi (1989) show that there is no reason to suspect that the model is less accurate if the elastic modulus E used in Eq.(2.21) is determined from separate tests, say on cylindrical specimens.

Because of differing E values, the regression coefficients in Eq.(2.22) are changed. It is well known that different values of E result from using different strain measuring devices. For values of E measured on cylindrical specimens using electrical strain gauges with sufficient gauge length, usually at least three times the maximum aggregate size g , the regression Eq.(2.22) should be replaced by:

$$\left(\frac{a_e}{W}\right) = C_1 \left(\frac{\sigma_n}{E}\right)^{C_2} \left(\frac{a_0}{W}\right)^{C_3} \left(1 + \left(\frac{d_{\max}}{W}\right)\right)^{C_4} \quad (2.23)$$

where $C_1 = 0.249 \pm 0.029$, $C_2 = -0.120 \pm 0.015$, $C_3 = 0.643 \pm 0.015$ and $C_4 = 0.217 \pm 0.073$.

The fracture toughness K_{IC} is determined from the ASTM formula by using the effective crack model as (Karihaloo and Nallathambi, 1989):

$$K_{IC} = \sigma_n a_e^{1/2} \gamma(a_e/H) \quad (2.24)$$

where $\gamma(\alpha)$ is the correction function which is given by:

$$\gamma(\alpha) = 1.99 - \alpha(1 - \alpha) \left(2.15 - 3.93\alpha + 2.7\alpha^2\right) / (1 + 2\alpha)(1 - \alpha)^{3/2} \quad (2.25)$$

with $\alpha = a_e/H$.

2.3.9 Using three-point bending test to determinate fracture energy

For a beam in three-point bending (Figure 2-21), the load typically varies with load-point deflection, as shown in Figure 2-22. There are three stages of behaviour in the load versus displacement curve where the load either increases or decreases with the deflection. In the first stage the crack is opened but does not extend. In the second stage a fracture process zone develops where micro cracks form and slow crack growth is apparent. In the third stage, known as the strain softening zone, rapid crack growth is evident (Malver and Warren, 1988).

The specific fracture energy (G_F), according to the RILEM recommendation (RILEM, 1985), is the average energy given by dividing the total work of fracture by the projected fracture area which can be measured on a pre-cracked (notched) specimen. Commonly, a notched beam loaded in three-point bending is used for determination of K_{IC} and G_F (Figure 2-22).

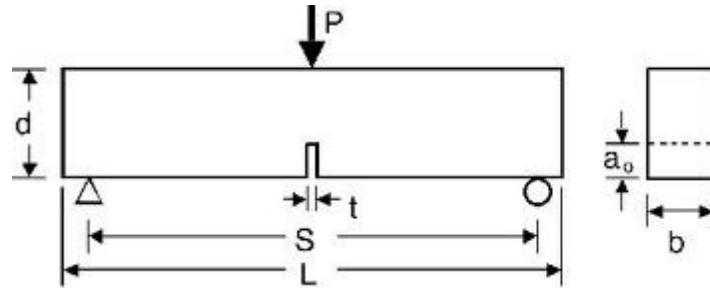


Figure 2-21 Three-point bending test on a notched beam specimen

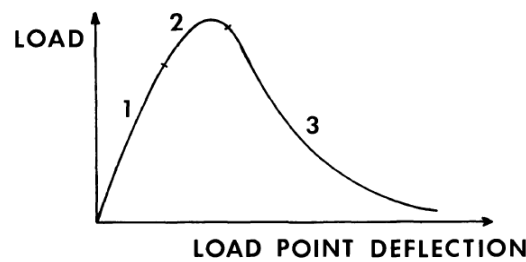


Figure 2-22 A typical load versus load-point deflection curve

The variation of the load (P) is plotted against the mid-span deflection of the specimen, and then the specific fracture energy G_F is calculated as:

$$G_F = \frac{1}{(W - a)B} \int P d\delta \quad (2.27)$$

where

W is the specimen depth,

B is the specimen width,

a is the notch depth,

P is the load.

Researchers have found that there exist size effects to a certain extent when three-point bending is used to determine the specific fracture energy of concrete, and as a material parameter, fracture energy should be independent of specimen size.

However, three-points bending test recommended by RILEM Committee FMC- 50 is widely used for the determination of fracture energy because it is simple to carry on testing (Farhat, 2004).

To overcome the effect of self-weight on the fracture properties, RILEM set up a committee in charge of proposing a test method based on compact specimens (Rossi et al, 1991). RILEM gives four standard specimen sizes (Table 2-1) that depend on the maximum aggregate size d_{max} and provides the rules for determining the dimensions of specimens larger than the largest standard one (Martin et al, 2007).

Table 2-1 Specimen dimensions specified by RILEM

d_{max} (mm)	d (mm)	b (mm)	L (mm)	l (mm)	A_{throat} (mm)	b/d	$(b/d)_{throat}$	l/d
1 to 16	100	100	840	800	5000	1.0	2	8.0
16.1 to 32	200	100	1190	1130	10000	0.5	1	5.7
32.1 to 48	300	150	1450	1385	22500	0.5	1	4.6
48.1 to 64	400	200	1640	1600	40000	0.5	1	4.0

2.3.10 Analytical models for test results

Several researchers investigated the current analytical models for concrete fracture and showed that none of the models can fully describe the fracture process of concrete. They found three fundamental concrete material behaviours at fracture that need to be described, i.e. the stress field in the vicinity of the crack tip at crack initiation, the energy absorbed during crack propagation and the material behaviour during fracture.

The FCM by Hillerborg is one fracture model that attempts to describe the three primary characteristics of fracture behaviour in concrete. These three properties according to the FCM are described as the tensile strength of the concrete (f_t), the fracture energy (G_F) and the elastic modulus (E).

To describe the stress field, the critical stress intensity factor (K_{IC}) equations were used. Shah (1988) observed that K_{IC} increases with an increase in the compressive strength of hardened cement paste for the two load rates tested as seen in Figure 2-23.

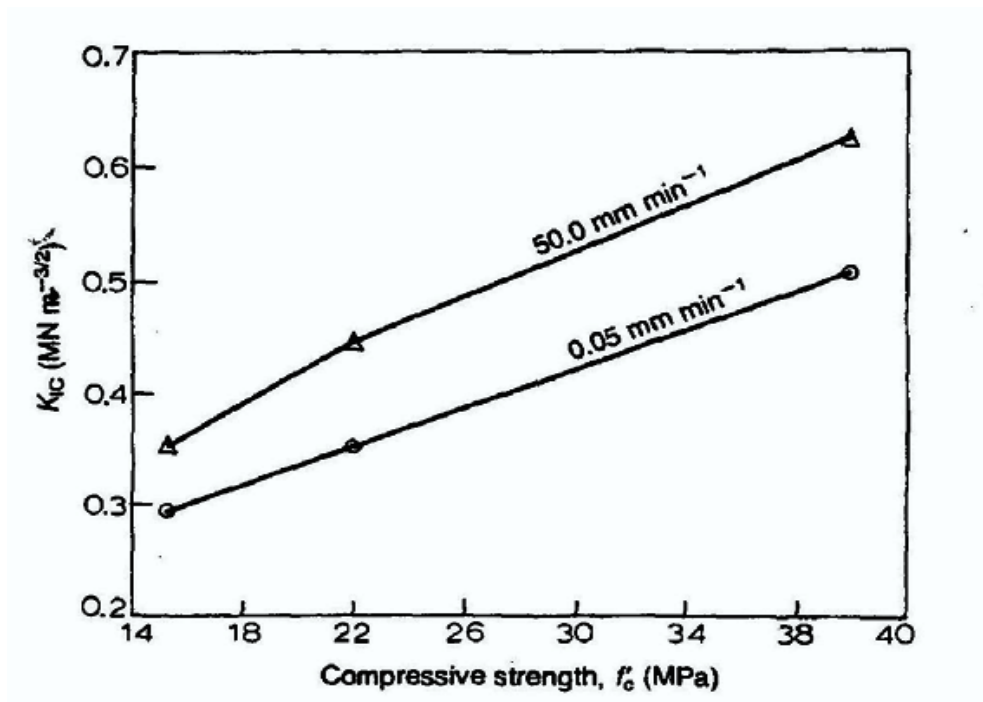


Figure 2-23 K_{IC} versus f'_c for hardened cement (Shah, 1988)

The fracture energy (G_F) is described as the energy absorbed per unit area for the formation of new crack surfaces (Hillerborg, 1985). Subsequent research reported that the fracture energy is a function of the size of the specimen (Bazant et al, 1986) and increases with an increase in the compressive strength of the concrete as shown in Figure 2-24 (Shah, 1988).

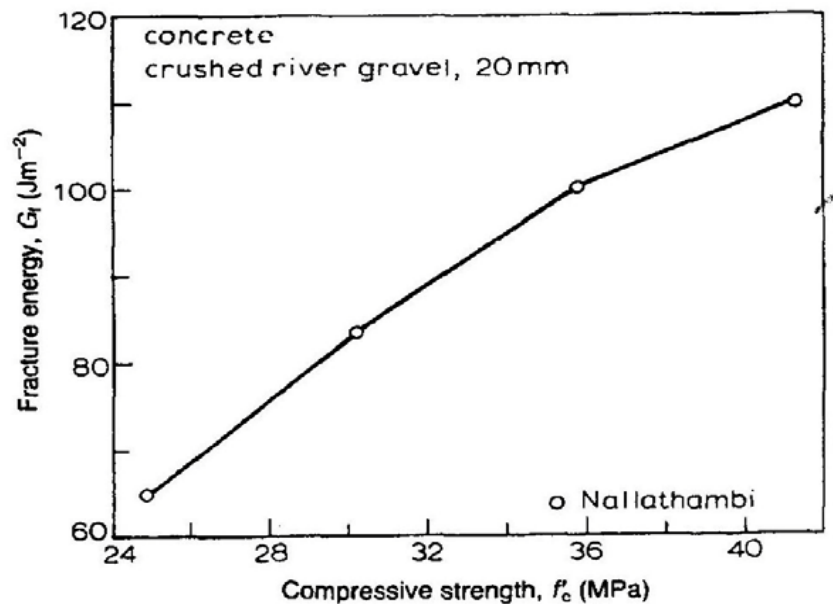


Figure 2-24 G_F versus f'_c for concrete (Shah, 1988)

Xie et al (1995) tested beam specimens by using the work-of-fracture method and obtained the average values for G_F that increased by 13% and 11% for increases of 53% and 29% in the compressive strength, respectively. Gettu et al (1990) compared results obtained for high-strength concrete and conventional concrete and verified that an increase of 160% in the compressive strength resulted in an increase of only 12% in the fracture energy.

2.3.11 Brittleness index for concrete

A complete load-displacement curve in flexure (Figure 2-25) comprises the initial stiffness K_0 , the ultimate load P_u , the cracking displacement Δ_c , the failure displacement Δ_f and other hardening and softening properties. Failure is defined as the point on the descending curve when load drops to zero (Zhang et al, 2002).

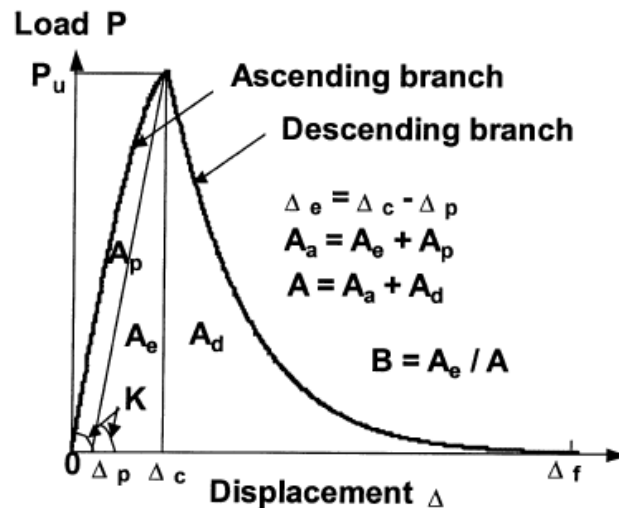


Figure 2-25 A complete load– displacement curve for a notched beam (Zhang et al, 2002)

The ratio of the elastic energy A_e stored at peak load to the total energy A at failure is defined as a brittleness index B :

$$B = \frac{\text{Elastic energy}}{\text{Total energy}} = \frac{A_e}{A} = \frac{A_e}{A_a + A_d} \quad (2.28)$$

where

A_e is the elastic energy on the ascending branch, and $A_e = A_a - A_p$,

A_a is the total energy on the ascending branch,

- A_p is the plastic energy on the ascending branch,
 A is the total energy over the complete fracture process, and $A = A_a + A_d$,
 A_d is the total energy on the descending branch,
 Δ_e is the elastic deformation on the ascending branch, and $\Delta_e = \Delta_c - \Delta_p$,
 Δ_c is the total deformation on the ascending branch,
 Δ_p is the plastic deformation on the ascending branch.

For an elastic-plastic material, $B = 0$, while for an elastic-brittle material, $B = 1$.

The two-function load-displacement relationship ($P - \Delta$) is proposed as follows:

$$P = \begin{cases} P_u \left[1 - (1 - \Delta/\Delta_c)^\alpha \right] & \text{for } 0 \leq \Delta \leq \Delta_c \\ P_u \exp \left[-\beta (\Delta - \Delta_c)^\gamma \right] & \text{for } \Delta_c < \Delta \leq \Delta_f \end{cases} \quad (2.29)$$

where

- α is a hardening index ($\alpha \geq 1$),
 β is a softening coefficient ($\beta > 0$),
 γ is a softening index ($\gamma > 0$).

Eq.(2.29) can be integrated to obtain A . If assuming that the unloading from the peak is linearly elastic with the same stiffness K_θ , then the brittleness index B can be obtained as:

$$B = \frac{1}{\frac{2\alpha^2}{\alpha+1} + \frac{2\alpha}{\beta \frac{1}{\gamma} \Delta_c} \left\{ \gamma \Gamma \left(1 + \frac{1}{\gamma} \right) - \Gamma \left[\frac{1}{\gamma}, \beta (\Delta_f - \Delta_c)^\gamma \right] \right\}} \quad (2.30)$$

where

$\Gamma(z) = \int_0^\infty x^{z-1} e^{-x} dx$ is the Euler gamma function,

$\Gamma(a, z) = \int_z^\infty x^{a-1} e^{-x} dx$ is the incomplete gamma function.

2.3.12 Factors influencing the brittleness of concrete

There are a number of factors which influence the brittleness of concrete. These factors can be classified into three categories based on the structural levels: micro, meso and macro levels.

2.3.12.1 Chemical bonds in cement paste

Setzer and Wittmann (1974) proposed that Chemical bonds provide 50% cement paste strength. From the theory of crystal structures, more complex structures and lower symmetry make the material more brittle.

2.3.12.2 Porosity in cement paste

Zhang (1987) found that the strength of cementations materials greatly depended on porosity. For cement paste, the brittleness monotonically decreased with the increasing total porosity, while for mortar, the brittleness first slightly increased with the increasing total porosity until a maximum value was reached, and then gradually decreased. This peak brittleness value corresponded to a total porosity of 20%.

2.3.12.3 Water-cement ratio (W/C)

Petersson (1980), based on his experimental results, showed that the characteristic length l_{ch} increased with the increasing water-cement ratio, which means the brittleness of concrete decreased.

2.3.12.4 Aggregate type

Petersson (1980) used the four aggregates to investigate the brittleness of concrete, crushed quartzite (Q), gravel (G), crushed limestone (LS) and expanded clay (EC). The results showed that:

$$l_{ch,G} > l_{ch,Q} > l_{ch,EC} > l_{ch,LS} \quad \text{or} \quad B_G < B_Q < B_{EC} < B_{LS}$$

This indicates that the worse the quality of aggregates, the higher the concrete brittleness. The test results by Zhang and Bicanic (2002) showed that the normal concrete had the largest l_{ch} or the smallest brittleness and the lightweight concrete had the lowest l_{ch} or the largest brittleness.

2.3.12.5 Aggregate size

Petersson and Zhou (Petersson, 1980; Zhou, 1988) found that the increase in the maximum aggregate size led to an increase in l_{ch} so as to decrease the brittleness of concrete. This can be explained from the crack zone model. The larger the maximum aggregate size, the larger the crack zone and the less brittle the concrete.

2.3.12.6 Aggregate-cement ratio (A/C)

The experimental results by Petersson (1980) showed that the brittleness of concrete increased with the increasing aggregate-cement ratio through decreasing of characteristic length l_{ch} . Also based on the test results by Zhou (1988), the increase in aggregate-cement ratio was equivalent to the decrease in cement-aggregate or the increase in water-cement ratio. Thus, the brittleness of concrete decreased accordingly.

2.3.12.7 Sand-cement ratio (S/C)

Zhang (1987) found that the change in the sand rate would change the strength and brittleness if water-cement ratio was kept constant for mortar. With the increase of sand-cement ratio, the brittleness of the mortar decreased.

2.3.12.8 Silica fume

The experimental results by Tasdemir et al (1996) showed that for the concretes without silica fume the fracture energy and characteristic length increased as the aggregate size increased. However, for the concretes with silica fume, the fracture energy G_F and characteristic length l_{ch} decreased, while the brittleness increased significantly especially for 20 mm maximum size of aggregate. Also for the concrete with silica fume, the cracks usually travel through the aggregates and fracture tends to be brittle in nature. However, for the concretes without silica fume, the cracks usually developed around the coarse aggregates, resulting in a more tortuous fracture path.

2.3.12.9 Polymers additives

Huang and Wu (1984) mixed polymer (polychlorobutadiene emulsion) with cement paste to form three different types of polymer mortar: 1:2.5 cement mortar, 1:2.5

PCC mortar with 15% and 20% of polychlorobutadiene emulsion. The results showed high tensile/compressive strength ratios, high fracture energy and low brittleness.

2.4 Elastic Modulus

The elastic modulus is a very important material property of concrete. A higher value of the elastic modulus leads to the stiffer behaviour of the material. The elastic modulus for high performance concrete is higher than that for normal strength concrete. Thereby this makes stiffer type of concrete. Although the stiffness is a desirable property for concrete, the deformations at fracture and creep increase in high strength concrete (Neville, 1973).

As the load is increased, the crack in the transition zone and the matrix is going to be bigger and failure finally occurs. However, until about 50 to 60 percent of ultimate load, micro cracks are considered stable and matrix cracking is minimal. According to Baalbaki et al (1992), due to the strong bond between the coarse aggregate and the matrix, the relationship between the elastic modulus E and the corresponding compressive strength f_c' of HPC is less consistent than that of normal strength concrete. Therefore the elastic modulus E of HPC should not be assumed to be a simple function of the compressive strength (Neville, 1995).

The elastic modulus, E , for the calculation of K_{IC} , can be obtained from the force – displacement curves in the three-point bending tests.

2.5 Summary

High performance concrete has very high strength and other desirable properties under some circumstances, such as high modulus of elasticity, high density, low permeability and high resistance to some forms of chemical attack. In spite of the superior characteristics of HPC, there are some problems which seem not to have been overcome, such as low tensile strength and low tensile strain. The design methods of high performance concrete include ACI 211-1 standard practice for selecting proportions for normal, heavyweight and mass concrete, the proposed

method in this study, the method suggested by ACI 363 Committee on high-strength, Larrard method (de Larrard, 1990) and Mehta and Aïteïn's simplified method.

The recent technical innovations in the construction industry have led to the active research and development of high-performance and multifunctional construction materials such as novel polymer-modified mortar and concrete. Polymer-modified mortar and concrete have been developed with a great interest in recent years. The effects of polymers on concrete are summary as follows:

- The addition of polyvinyl acetate, copolymers of polyvinyl acetate, styrene-acrylic and styrene butadiene rubber emulsions to cement mortar improves workability;
- The addition of low-density polyethylene (LDPE), crushed polyethylene terephthalate (PET) and rubber from useless tires (TIRE) to concrete in the weight ratios of 0.5%, 1.0%, 2.5%, 5.0% and 7.5% to cement reduces the workability of the fresh concrete;
- Portland cement pastes with and without super plasticizer show a high rate of increase in compressive strength up to 7 days;
- The addition of latex to the Portland cement paste results in a decrease in compressive strength of almost all pastes, except the pastes with a low concentration of latex;
- Addition of polyvinyl acetate, copolymers of vinyl acetate-ethylene, styrene-butadiene, styrene-acrylic and acrylic and styrene butadiene rubber emulsions increases flexural and compressive strength;
- The application of the autoclave curing of SBR-modified concrete with a slag content of 40% and a polymer-binder ratio of 20% provides about three times higher tensile strength and twice higher compressive strength than those for unmodified concrete (ordinary cement concrete);
- The addition of polymer and silica fume to mortars leads the bond strength to be superior to those specified by the standard;
- The addition of 7.5% low-density polyethylene (LDPE) in content, crushed polyethylene terephthalate (PET) and rubber from useless tires (TIRE) to concrete reduces the compressive strength by 38.48% for TIRE, 26.24% for LDPE and 15.45% for PET;

- The compressive strengths of these pastes are comparatively little affected by 62-day immersion of Na_2SO_4 solution as compared to those of the paste cured in lime saturated water for 90 days;
- Addition of polyvinyl acetate, copolymers of vinyl acetate-ethylene, styrene-acrylic and styrene butadiene rubber emulsions decreases water absorption, carbonation and chloride ion penetration;
- The addition of low-density polyethylene (LDPE), crushed polyethylene terephthalate (PET) and rubber from useless tires (TIRE) to concrete increases the resistance to underwater erosion abrasion;
- SBR modified lightweight aggregate concrete (LWAC) provides better performance in aggressive environments than the unmodified LWAC;
- Finally, VA/VeoVa powder has good water-reduction effects.

Here three methods to measure fracture parameters of concrete are extensively discussed, including the fictitious crack model, the two-parameter fracture model and the size effect model.

CHAPTER 3 CHARACTERISTICS OF MATERIALS FOR MANUFACTURING HIGH PERFORMANCE CONCRETE

3.1 Cement

The cement used in the test programme was Procem ordinary Portland cement, Class 52.5 N CEM I, and had grey colour and consistent strength which met all the conformity criteria in BS EN 197-1 (BSI 2011). It was compatible with admixtures such as air-entraining agents and workability succours, with cement replacement materials such as fly ash (PFA) and ground granulated blast furnace slag (GGBS), and with pigments. Trial mixes are recommended to determine the optimum mix proportions. It was packed in 25 kg bags. The physical and chemical compositions of the cement are given in Tables 3-1 and 3-2, according to the manufacturer (Procem, 2014).

Table 3-1 Chemical compositions of the cement used

Sulphate (SO ₃) %	Chloride (Cl) %	Alkali (EqNa ₂ O) %	Tricalcium Silicate (C ₃ S) %	Dicalcium Silicate (C ₂ S) %	Tricalcium Aluminate (C ₃ A) %	Tetracalcium Aluminoferrite (C ₄ AF) %
2.5-3.5	< 0.10%	< 1.0%	40.0-60.0	12.5-30.0	7.0-12.0	6.0-10.0

Table 3-2 Physical characteristics of the cement used

Mean particle size (µm)	Solubility in water (g/l) (T = 20 °C)	Density (g/cm ³)	Apparent density (ES) (g/cm ³)	pH (T = 20°C in water)	Boiling/melting point
5-30	1.0-1.5	2.75-3.20	0.9-1.5	11.0-13.5	> 1250°C

3.2 Silica Fume

The Silica fume is an extremely fine powder whose particles are smaller than cement. The silica fume is produced in electric arc furnaces as a by-product of the production of elemental silicon or alloys containing silicon and also known as very fine non-crystalline silica, condensed silica fume or microsilica (ACI, 2005). Detwiler and Mehta (1989) provided a summary on physical effects of silica fume in concrete indicating that the carbon black and plain cement mixes showed comparable strengths at both 7 and 28 days, even though the carbon black mixes contained 10 percent less cement by mass. Physical mechanisms do play a significant role, particularly at early ages. Because of the extremely fine particles, silica fume reduces the size and volume of voids near the surface of the aggregate. This so called interface zone has improved properties with respect to micro cracking and permeability (Neville, 1995). The siliceous and aluminous material does not possess adhesive value by itself physically, but chemically when reacting with calcium hydroxide at ordinary temperatures to form compounds (ACI, 2005). The Silica fume used was the Elkem microsilica grade 940-D Densified. 10% of the total cementitious material was substituted with silica fume. The physical properties and chemical composition of the silica fume used are given in Table 3-3.

Table 3-3 Physical Properties and chemical compositions of silica fume used

Physical properties		Chemical compositions	
Particle size (typical)	$< 4 \times 10^{-6}$ in (0.1 μm)	SiO ₂	more than 90%
Bulk density	8-27 lb/ft ³ (128-4324 kg/m ³)	H ₂ O	less than 1.0%
(slurry)	11-12 lb/gal (1.1-1.2 kg/litre)	Loss on Ignition (LOI)	less than 3.0%
(Densified)	30-45 lb/ ft ³ (480-720 kg/m ³)	Bulk density	500-700 kg/m ³
Specific gravity	2.2	Pozzolanic Activity (with cement)	120-210%
Surface area	60000-150000 ft ² /lb (12-30 kg/m ³)	Pozzolanic Activity (with lime)	1200-1660 psi (8.3-11.4 MPa)

3.3 Coarse Aggregate

The dry granite aggregates were used with 10 mm maximum particle size, water absorption $W_{abs} = 0.66\%$ and the specific bulk gravity $G_{SSD} = 2.9$ in the saturated surface condition. Figure 3-1 shows a sample of granite aggregate used in this study.

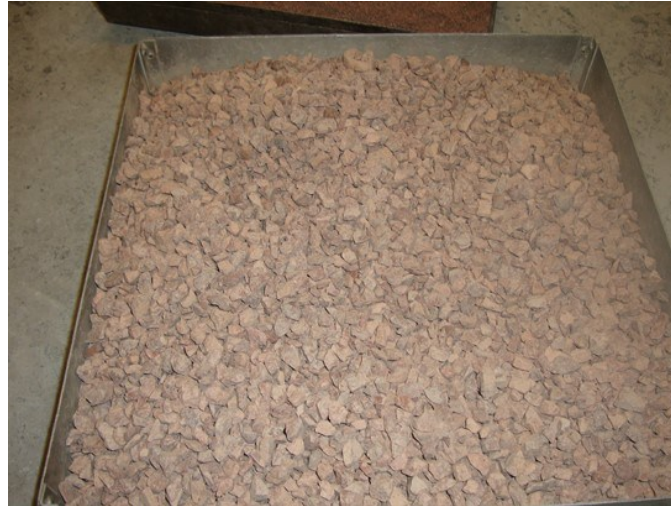


Figure 3-1 Sample of granite aggregate

3.3.1 Specific gravity and absorption of coarse aggregate

The bulk specific gravity (SSD condition) and the percentage of absorption can be calculated as follows:

$$\text{Bulk specific gravity (OD)} \quad G_{sb} = \frac{A}{B - C} = \frac{3326}{3348.06 - 2193.19} = 2.88 \quad (3.1)$$

$$\text{Bulk specific gravity (SSD)} \quad G_{SSD} = \frac{B}{B - C} = \frac{3348.06}{3348.06 - 2193.19} = 2.9 \quad (3.2)$$

$$\text{Absorption (\%)} \quad W_{abs} = \left(\frac{B - A}{A} \right) = \left(\frac{3348.06 - 3326}{3326} \right) = 0.66\% \quad (3.3)$$

where

A is the mass of the oven-dry (OD) sample in air,

B is the mass of the saturated surface-dry (SSD) sample in air,

C is the apparent mass of the saturated sample immersed in water.

3.3.2 Grading of coarse aggregates

Sieve analysis was carried out on coarse aggregates before use in the experimental work. The sieve analysis was used to find amounts of different sizes of aggregates in particular samples in accordance with BS 812-103.1 (BSI, 1985). Table 3-4 displays the results of the sieve analysis for a sample of coarse aggregates used in the study and compared with the grading limits for 10 mm aggregates, extracted from BS 882 (BSI, 1983). Figure 3-2 shows the grading of natural coarse granite aggregate compared with BS overall limits.

Table 3-4 Typical sieve analysis results of natural coarse granite aggregates

Weight of coarse aggregate sample = 2015.05 g					
Sieve size (mm)	Retained (g)	Percentage retained		Percentage by mass passing	Limits for single-sized aggregate (from BS 882)
		Individual	Cumulative		
16	0.00	0.00	0.00	100	100
14	2.17	0.10	0.10	99.90	95-100
12.5	5.07	0.25	0.35	99.65	95-100
10	114.18	5.70	6.05	93.95	85-100
8	563.32	27.90	33.95	66.05	85-100
6.3	661.92	32.84	66.79	33.20	0-50
4	518.29	25.70	92.49	7.51	0-25
2.36	78.17	3.87	96.36	3.64	0-5
1	16.11	0.79	97.15	2.85	
Pan	57.42	2.84	100.00	0.00	

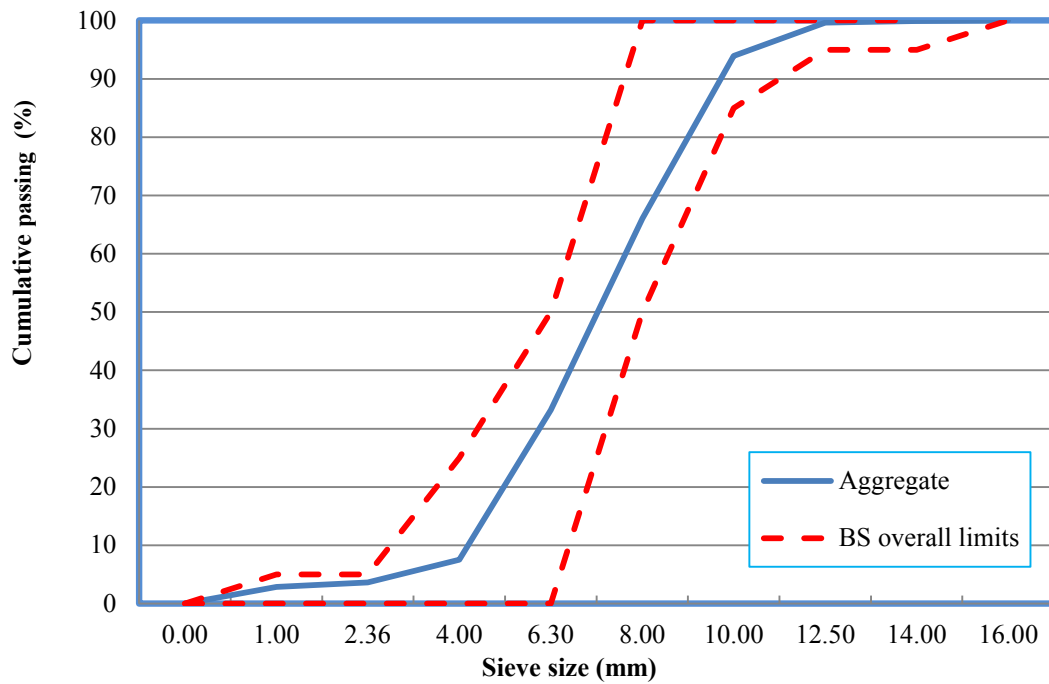


Figure 3-2 Grading of coarse granite aggregates

3.3.3 Aggregate impact value

The aggregate impact value (AIV) is used to assess if the material has ability to resist impact by evaluating the extent of particle crushing thereafter. The impact value is calculated by recording the fractions passing and retained in five sieves say 0.2 mm, 0.63 mm, 2 mm, 5 mm and 8 mm after the material has sustained 10 blows from a standard weight. This test is carried out to measure the resistance of a particular aggregate to sudden shock or impact. Table 3-5 shows analysis on the results of the impact value tests on the aggregates.

The AIV values were determined in a dry condition for aggregate, in accordance with BS EN 1097-2 (BSI 2010). A lower percentage indicates tougher and stronger aggregates. The mass retained on each of the five test sieves and in the pan for each test specimen is calculated as a percentage of the mass of the test sample before testing. From this the percentage masses passing the five sieves are calculated. Adding up the percentage masses passing each of the five test sieves will give the sum of percentage masses from BS EN 1097-2 (BSI 2010).

Table 3-5 Impact test results of aggregates

Sieve size in mm	Original mass: 638.95 g		
	Mass retained		Mass passing
	g	%	%
8	512.5	80.27	19.73
5	69.79	10.93	8.80
2	36.05	5.64	3.16
0.63	12.87	2.01	1.15
0.2	3.04	0.47	0.68
Pan	4.17	0.65	-
Sum	638.42	100.0	33.52

The impact value SZ , in percentage, is calculated from the following formula:

$$SZ = M / 5 \quad (3.4)$$

where M is the sum of the percentages of the mass passing each of the five test sieves.

In this case, $SZ = 33.52\% / 5 = 6.70\%$.

3.4 Fine Aggregate

Siliceous natural sand was used. The water absorption coefficient W_{abs} is measured as 3.72% with a bulk specific gravity in the saturated surface dry condition (SSD) as $G_{SSD} = 2.641$.

3.4.1 Specific gravity and absorption of fine aggregate

The specific gravity of the SSD fine aggregate and the percentage of absorption are calculated as follows:

Bulk specific gravity

$$G_{sb} = \frac{A}{(B+S-C)} = \frac{482.24}{(985.65+500.18-1296.47)} = 2.547 \quad (3.4)$$

Apparent specific gravity

$$G_{sa} = \frac{A}{(B + A - C)} = \frac{482.24}{(985.65 + 482.24 - 1296.47)} = 2.814 \quad (3.5)$$

Bulk SSD specific gravity

$$G_{SSD} = \frac{S}{(B + S - C)} = \frac{500.18}{(985.65 + 500.18 - 1296.47)} = 3.641 \quad (3.6)$$

Absorption (%)

$$W_{abs} = \frac{(S - A)}{A} \times 100 = \frac{(500.18 - 482.24)}{482.24} \times 100 = 3.72\% \quad (3.7)$$

where:

A is the mass of oven-dry sample in air,

B is the mass of pycnometer filled with water,

C is the mass of pycnometer with SSD sample and water,

S is the mass of SSD sample.

3.4.2 Grading of fine aggregate

Table 3-6 illustrates the sieve analysis test data of the fine aggregate sample used in the study and compared with the grading limits according to BS 882-1983 for fine aggregates (BSI, 1983). Figure 3-3 shows the grading of the fine concrete aggregate compared with the BS overall limits.

3.5 Superplasticizer

Superplasticizer is a chemical or mixture of chemicals in powder or liquid form. When added to a proportion of hydraulic binder content, it provides a very high workability while decreasing the water content. The Structuro 11180 is a new generation polycarboxylate (PC) polymer superplasticizer and a high range water reducer. It combines the effects of both steric and electrostatic repulsion, producing a product which outperforms conventional superplasticizers. The molecule of the Structuro 11180 has been engineered specifically towards the Precast Industry to give excellent performance at low dosage either in the production of low water/cement ratio, high strength mixes or high performance flowing concretes (Solutions, 2011).

Table 3-6 Typical sieve test results of fine aggregates

Weight of fine aggregate sample = 282.09 g					
Sieve size (mm)	Retained (g)	Percent retained		Percentage by mass passing	Limits for single-sized aggregate (from BS 882)
		Individual	Cumulative		
8	2.38	0.84	0.84	99.16	100
5	2.89	1.02	1.86	98.14	89-100
4	5.52	1.95	3.81	96.19	89-100
2	89.16	31.60	35.41	64.59	60-100
1	81.58	28.91	64.32	35.68	30-100
0.5	46.62	16.52	80.84	19.16	15-100
0.25	29.18	10.34	91.18	8.77	5-70
0.063	22.72	8.05	99.23	0.77	0-15
Pan	1.42	0.50	100	0.00	
Total	281.47				
Loss (g)	0.62				
Loss (%)	0.21				

The characteristics of the superplasticizer Structuro 11180 used are given in Table 3-7, together with the advantages of using Structuro 11180 as follows (Solutions, 2011):

- producing highly workable concretes and better consistence,
- enhancing more efficient mould usage,
- improving rheology of concrete by providing a blemish free surface finish and requiring less remedial work or ‘dressing’,
- improving productivity and earlier transfer of pre-stress and negating the need for accelerating admixtures during cold temperature working through early age compressive strength development,
- creating chloride free effect, ideal for concrete containing embedded steel.

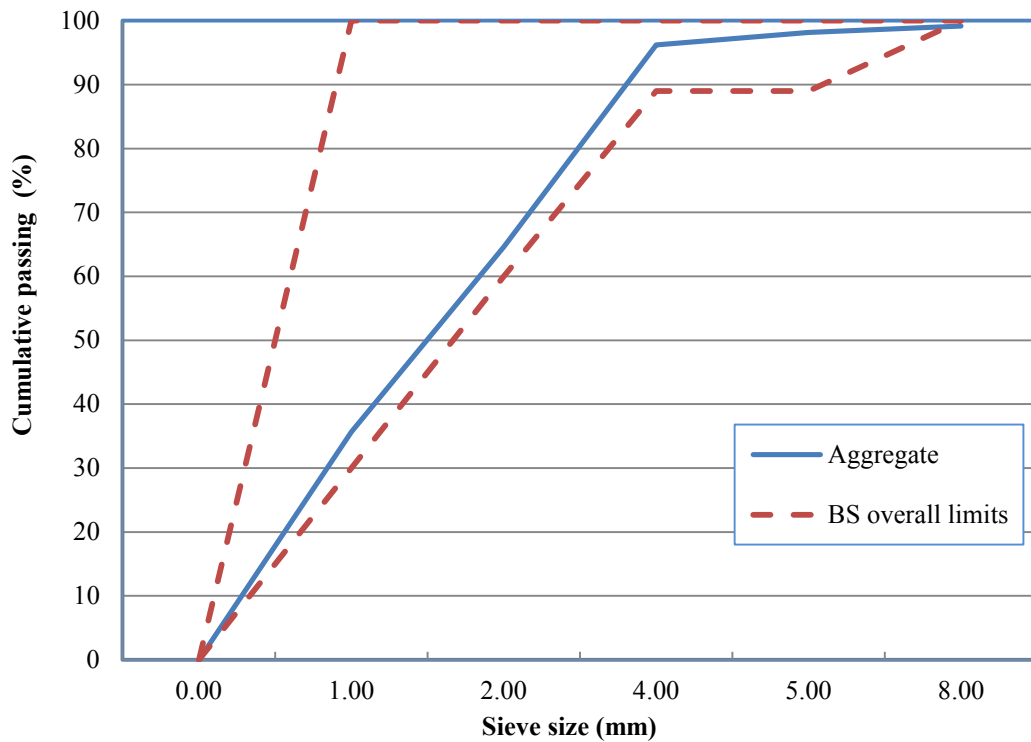


Figure 3-3 Grading of fine aggregates

Table 3-7 Characteristics of the superplasticizer Structuro 11180

Nature	Opaque liquid
Colour	Colourless, opaque light yellow
Specific gravity	1.10 kg/litre at 20°C
Total solid content	40%
pH at 10	6.5%
Chloride content	< 0.1 %
Na ² O equivalent	< 3.0%
Air entrainment	less than 2% additional air entrained at normal dosage

3.6 Polymers

The choice of polymer was classified to those which are manufactured and marketed under stringent conditions of quality control and therefore with well established material properties. Since Styrene butadiene rubber (SBR) and Polyvinylidene chloride (PVDC) are widely used in PMC, they were chosen due to the excellent

performance in the previous investigations. Linear low density Polyethylene LLDPE and high density Polyethylene HDPE were chosen to enable comparison between different properties of polymers and study systematic changes in composition.

3.6.1 Styrene-Butadiene Rubber (SBR) latex

SBR is a styrene-butadiene co-polymer emulsion which imparts beneficial property improvements to cementitious mixes. After appropriate dilution with water, the resultant liquid may be utilised to gauge the cementitious mix to the desired consistency.

Reduced water-cement ratio results in superior mechanical properties and resistance to moisture ingress. The advantages of using SBR latex include (Systems, 2012)

- producing plasticising effect,
- producing waterproofing effect,
- improving adhesion,
- reducing permeability,
- increasing mechanical strength,
- up-grading chemical resistance,
- being versatile and easy to use,
- being cost effective,
- improving freeze-thaw resistance,
- being compatible with many types of cement.

The chemical structure of SBR is shown in Figure 3-4. The formulations for emulsion polymerisation of typical SBR latexes as cement modifiers are listed in Table 3-8 (ACI, 1991), together with the physical and chemical properties of this SBR given in Table 3-9.

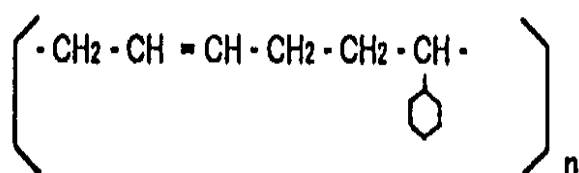


Figure 3-4 Chemical structure of SBR

Table 3-8 Formulations for emulsion polymerisation of typical SBR latexes as cement modifiers (ACI, 1991)

Material	Parts by weight
Styrene	64.0
Butadiene	35.0
Vinyl carboxylic acid	1.0
Non-ionic surfactant	7.0 ^a
Anionic surfactant	0.1 ^b
Ammonium persulfate	0.2
Water	105.0

^aThe non-ionic surfactants may be nonyl phenols reacted with 20-40 molecules of ethylene oxide.

^bThe low levels of anionic surfactant are used to control the rate of polymerisation.

Table 3-9 Physical and chemical properties of the SBR used

Description	Colour	Odour	pH	Relative density	Water solubility	Viscosity
Liquid	White	Aromatic	9-11	0.9-1.1	miscible in water	100-1000 mPa s

Wykamol SBR Latex shown in Figure 3-5 was used in this study. When used in cementitious mix, it

- provides special properties suitable for use in damp conditions,
- imparts high water/salt resistance when incorporated in a mix,
- improves adhesion,
- allows thinner screeds to be laid,
- improves workability,
- allows a reduction in water content,
- improves flexibility,
- reduces cracking, and
- improves resistance to abrasion and chemicals (Division, 2009).



Figure 3-5 SBR latex

3.6.2 Polyvinylidene Chloride (PVDC)

Polyvinylidene Chloride (PVDC) is in powder and contains Homopolymer and copolymers-usually with vinyl chloride (VC), or methyl acrylate (MA) (Mark, 1999). It is typically used in latex barrier coatings on cellophane, plastic film, paperboard and rigid food containers. Also the films of co-polymers are used as household cling wraps. It serves with other polymers in multilayer barrier films or containers mostly in packaging applications, and is also used in fibres and adhesives (Mark, 1999).

Using PVDC as a modified mortar increases the compressive and tensile strengths and gives excellent incombustibility values (Ohama, 1995). Figures 3-6 and 3-7 illustrate the chemical structure and packs of the used PVDC in this study. The physical and chemical properties of this PVDC are given in Table 3-10.

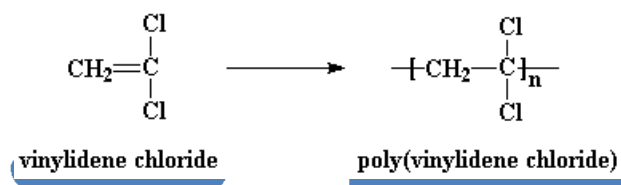


Figure 3-6 Chemical structure of the PVDC used in this study



Figure 3-7 PVDC Powder

Table 3-10 Physical and chemical properties of the PVDC used

Description	Colour	Density (g/cm ³)	Coefficient of friction	Water absorption – over 24h (%)	Hardness - Rockwell
Powder	White	1.36	0.24	0.1	R98-106

3.6.3 Linear Low Density Polyethylene (LLDPE)

Linear Low Density Polyethylene (LLDPE) is in powder. It is defined by a density ranging 0.915-0.925 g/cm³ and is produced using low-pressure in either a gas phase reactor or a solution process (Scheirs, 2009).

In this study, the LLDPE is used as a powder to get a good mix with concrete. LLDPE produced at low pressure through co-polymerisation (slurry or gas phase polymerisation) of ethylene with 1-alkenes (mainly 1-butene, also 1-hexene, 1-octene), see Figures 3-8 and 3-9 (Theunis and Franck, 2001).



Figure 3-8 Chemical structure of LLDPE



Figure 3-9 The LLDPE powder used in this study

LLDPE are mainly used to cast films for bags, shrink-wrap, packaging and injection moulding. Other applications include pipes and conduits, laminations, co-extrusions, and wire and cable coatings (Mark, 1999). The physical and chemical properties of this LLDPE are given in Table 3-11.

Table 3-11 Physical and chemical properties of the LLDPE used

Description	Colour	Density (g/cm ³)	coefficient of friction	Water absorption – over 24h (%)	Surface hardness
Powder	Green	0.935	0.24	0.01	SD48

3.6.4 High Density Polyethylene (HDPE)

High Density Polyethylene (HDPE) in powder form was used here as the modifier. HDPE is produced by pressure (25-50 bars) under a lower temperature in a reactor containing a liquid hydrocarbon diluent and Ziegler Natta catalysts, or gas phase polymerisation (Theunis and Franck, 2001). The specific gravity of HDPE was 0.95 g/cm³. Figures 3-10 and 3-11 illustrate the chemical structure and the feature of the HDPE. The physical and chemical properties of this HDPE are given in Table 3-12.

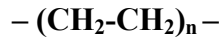


Figure 3-10 Chemical structure of HDPE

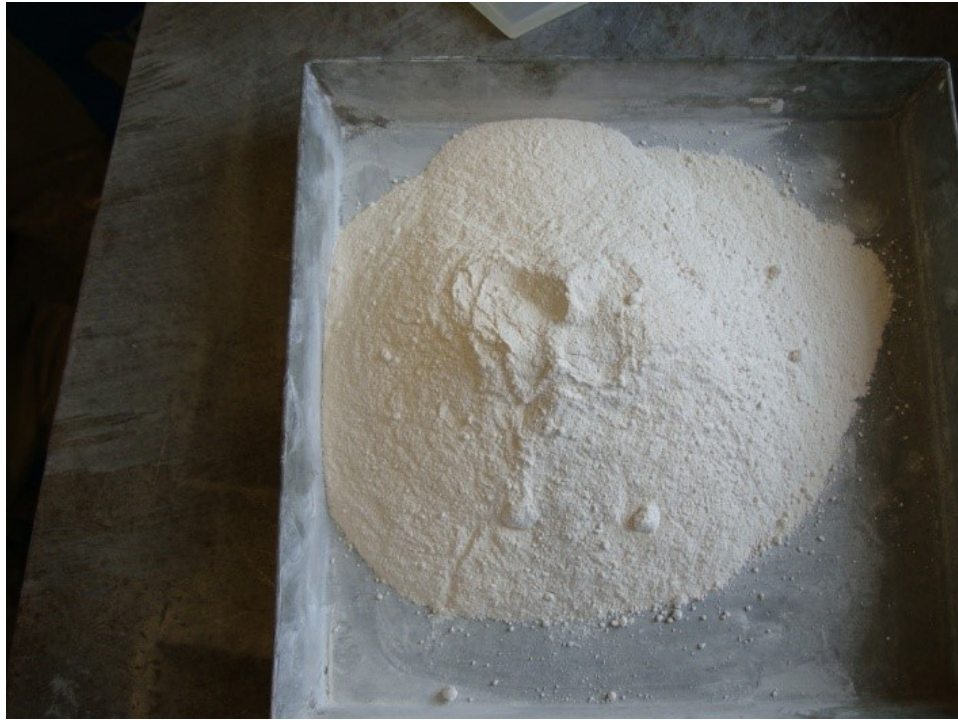


Figure 3-11 HDPE powder

Table 3-12 Physical and chemical properties of the HDPE used in this study

Description	Colour	Density (g/cm ³)	Coefficient of friction	Water absorption – over 24h (%)	Surface hardness
Powder	White	0.95	0.24	0.01	SD48

3.7 Water

The amount of water is designed based on the water-cement ratio. In general, the good quality of water used in concrete is usually fit for human consumption. It must be avoided to use water containing sufficient amounts of dissolved or solid impurities because they cause various effects on both fresh and hardened properties of concrete. Therefore the water used for high performance concrete was high quality tap water. The amount of water content in both concrete mixes is constant. For concrete with 110 MPa, the water-cement ratio is 0.25.

3.8 Summary

In this chapter, the materials used for producing high performance concrete together with their properties are described. Procem ordinary Portland cement, i.e. Class 52.5 N CEM I, was used, with the Elkem grade 940-D microsilica (Silica fume), granite aggregate, siliceous natural sand and superplasticizer (Structuro 11180 molecule). The selected four polymers for this study include Styrene-Butadiene Rubber (SBR) latex, Polyvinylidene Chloride (PVDC), Linear Low Density Polyethylene (LLDPE) and High Density Polyethylene (HDPE).

CHAPTER 4 MIX DESIGNS

4.1 Introduction

In recent years, the concrete properties have been improved by blending cements with pozzolanic and cementitious admixtures such as fly ash and silica fume. These materials when incorporating in concrete mixes improve the durability of concrete by refining its pore structure and reducing its porosity and permeability.

The aggressive substances such as chloride ions and carbon dioxide which cause corrosion of reinforced concrete structures are largely reduced. A higher concrete strength normally leads to a higher toughness but also increases the brittleness of concrete dramatically, which unavoidably causes concrete to fail very suddenly and even explosively. Therefore any attempt to alleviate the sudden failure implies designing and producing high performance concrete capable of withstanding the harsh environmental conditions.

A high performance mix design method was prepared according to the proposed method which follows the same approach as ACI 211-1 Standard Practice for Selecting Proportions for Normal, Heavyweight and Mass Concrete (ACI, 2009). It is a combination of empirical results and mathematical calculations based on the absolute volume method (Aitcin, 2004) as indicated in Figure 2-2 in Section 2.1.9.2. This method is further discussed in Appendix A for mix design.

In order to study the effects of additions of polymers on the materials and fracture properties of high performance concrete, four types of polymers, Styrene Butadiene Rubber (SBR) latex, Polyvinylidene Chloride (PVDC), Linear Low Density Polyethylene (LLDPE) and High Density Polyethylene (HDPE), were adopted, with contents of 1.5%, 3.0% and 5% in the mass of cementitious materials. These polymers are readily supplied in the market and some have been used in previous investigations by other researchers.

The polymer modified HPC cast in twenty six batches were used for the thirteen mixes with the original mix as the control mix without any addition of polymer. A

total of fifty-two beams and one hundred and fifty six cubes were produced. Each batch of concrete prepared for the fracture tests included four 500 mm × 100 mm × 100 mm beams and twelve 100 mm cubes. Table 4-1 summarises typical mixes with different amounts of polymers and other ingredients in weights for a volume of m³.

Table 4-1 Mix designs of polymers modified HPCs

Mix design with polymers (volume of mix per 1 m ³)									
Polymer	Volume (%)	Cement (kg)	Coarse aggregate (kg)	Sand (kg)	Water (l)	Silica fume (kg)	Superplasticizer (l)	Polymers	w/c ratio
Control	0.0	504	998	781	159	56	20	0.0	0.25
SBR	1.5	504	998	783	128	56	20	17.5 l	0.25
	3.0	504	998	761	119	56	20	35.0 l	0.25
	5.0	504	998	732	107	56	20	58.3 l	0.25
PVDC	1.5	504	998	768	139	56	20	8.4 kg	0.25
	3.0	504	998	755	141	56	20	16.8 kg	0.25
	5.0	504	998	737	165	56	20	28.0 kg	0.25
LLDPE	1.5	504	998	768	139	56	20	8.4 kg	0.25
	3.0	504	998	755	141	56	20	16.8 kg	0.25
	5.0	504	998	737	165	56	20	28.0 kg	0.25
HDPE	1.5	504	998	768	139	56	20	8.4 kg	0.25
	3.0	504	998	755	141	56	20	16.8 kg	0.25
	5.0	504	998	737	165	56	20	28.0 kg	0.25

4.2 Summary of the Proposed Method (Aitcin, 2004)

The procedure is initiated by selecting five different mix characteristics or material proportions in the following sequence.

4.2.1 Water/binder ratio

Water/binder ratio is suggested from the curve in Figure 4-1 for a given 28 day compressive strength. If the efficiency of the different supplementary cementitious materials is not known from prior experience, the average curve can be used to give an initial estimate of the mix proportions. In this study in order to reach a 110 MPa compressive strength the water/binder ratio should be 0.25.

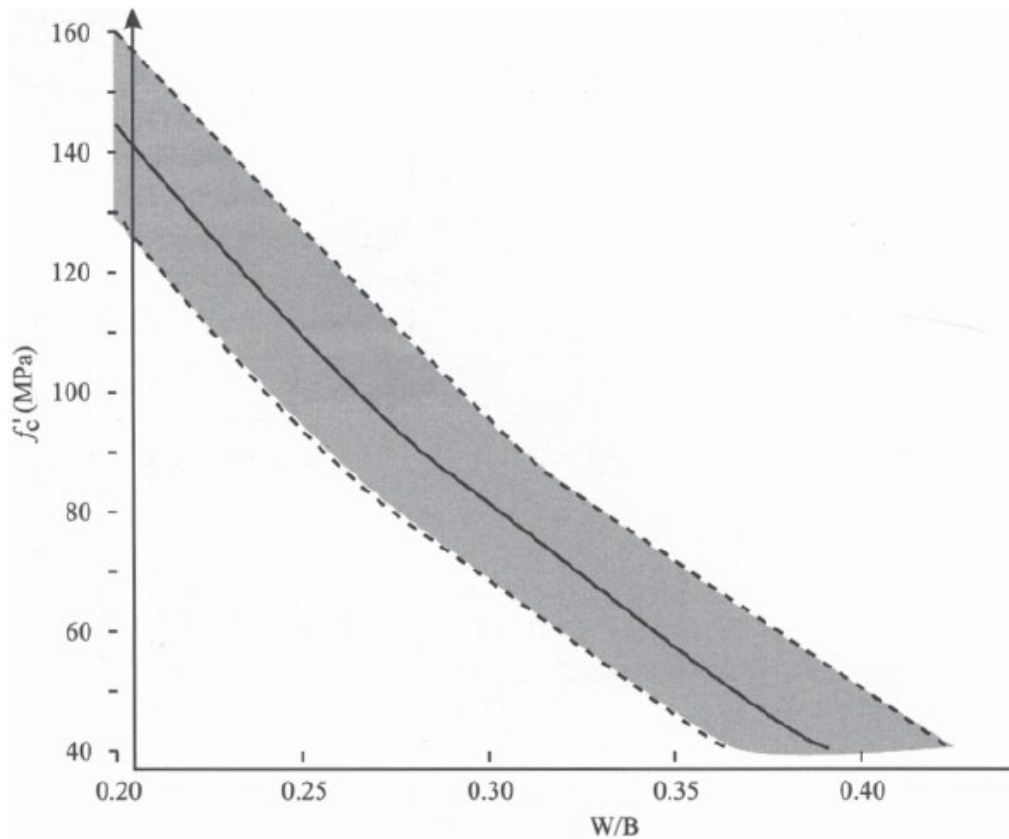


Figure 4-1 Proposed compressive strength – W/B relationship (Aitcin, 2004)

4.2.2 Water content

Because several factors affect the workability of the mix such as the amount of initial water, the reactivity of the cement, the amount of superplasticizer and its degree of compatibility with the particular cement, the determination of the water amount is difficult. A simplified approach based on the concept of the saturation point is given in Figure 4-2 from which it can be found that the water dosage for a saturation point of 1.0% should be between 135 and 145 l/m³. The dosage of 140 l/m³ for this trial batch is taken.

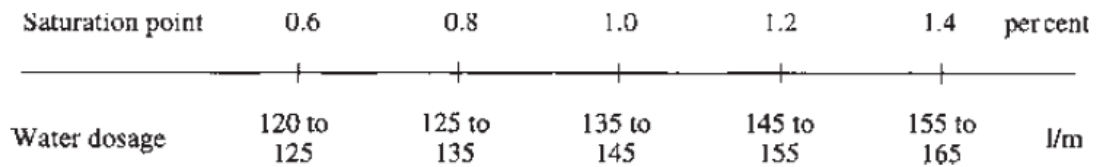


Figure 4-2 Determination of the minimum water dosage (Aitcin, 2004)

4.2.3 Super-plasticizer dosage

The amount of the superplasticizer can be deduced from the dosage at the saturation point. If the saturation point is not known, it is suggested to start with a trial dosage of 1.0%.

4.2.4 Coarse aggregate content

From Figure 4-3, it can be found that the coarse aggregate content is expressed as a function of the typical particle shape. If there is any doubt about the shape of the coarse aggregate or if its shape is not known, a content of 1000 kg/m³ of coarse aggregate can be used for trial tests.

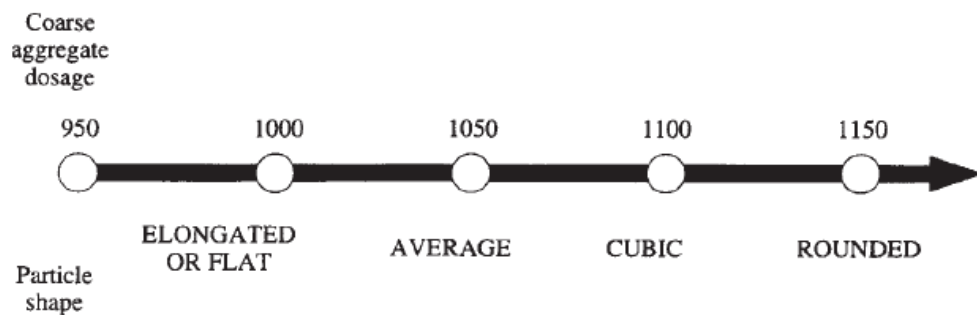


Figure 4-3 Coarse aggregate content (Aitcin, 2004)

4.2.5 Air content

From experience it has been found that it is difficult to achieve less than 1% entrapped air and that in the worst case the entrapped air contents can be as high as 3%. Therefore, 1.5% is suggested as an initial estimate of entrapped air content, and then it can be adjusted on the basis of the result obtained from the trial mix (Aitcin, 2004).

4.2.6 Calculations on the mix design sheet

Table 4-2 shows a mix design sheet with all the calculations needed to determine the mix proportions. It contains six main columns numbered in the top row. The initial data and calculations are reported in the first column. In the second column, the volume of fine aggregates is calculated. The SSD proportions are presented in the third column. In the fourth column, different water corrections are calculated. The proportions of the mix using the actual raw materials are given in the fifth column, and in the final sixth column the proportions of the trial batch can be calculated.

Table 4-2 Calculations on mix design sheet (Aitcin, 2004)

MIX DESIGN SHEET

Comp. Strength	Mpa
----------------	-----

Table A	Gc	%
Cement		

	%			
Aggregate	GSSD	Wabs	Wtot	Wh
coarse				
fine				

superplastizer	Msol=Bx d/100	Vlig=(Msol/SxGsup)	Vw = Vliq x Gsup x	Vsol=Vliq-Vw
sp.gravity		x 100	(100-s/100)	
solids dos				
(Gsup)	s(%)			
	15	E 24	F 21	G 11
				H

Materials	1		2	3	4	5		6	
	content		volume	SSD	water	composition			
	kg/m3			condition	correction	1m3	Trail batch		
water	2		2	2		23	25		
cement	W/B 1	3	4_1	8_1		4_1	4_1	26_1	
			4_2	8_2		4_2	4_2	26_2	
			4_3	8_3		4_3	4_3	26_3	
Coarse aggregate	5		9	5	18	17	27		
fine aggregate			13	14	20	19	28		
AIR	per cent		10	0					
	6								
Super-Plasticizer	7		11	15	21	24	Vliq	29	
TOTAL			12	16	22			30	

To complete this design sheet, the calculations are explained box by box as follows (Aitcin, 2004):

- Box 1: Record the water-binder ratio found from Figure 4-1;
- Box 2: Record the amount of water required, selected from Figure 4-2, and put it in columns 1, 2 and 3 where box 2 appears;
- Box 3: From the values appearing in boxes 1 and 2, calculate the necessary mass of binder;
- Boxes 4-1, 4-2 and 4-3: Calculate the mass of each of different materials according to the cementitious compositions selected appearing in Table A, and put it in columns 1, 3 and 5 where these boxes are found;
- Box 5: Fill in the mass of coarse aggregate, given by Figure 4-3, and put it in columns 1 and 3 in box 5;
- Box 6: Record the assumed air content;
- Box 7: Record the amount of superplasticizer needed, obtained from the saturation point value;
- Boxes 8-1, 8-2 and 8-3: Calculate the volumes of the different cementitious materials by dividing their masses, appearing in boxes 4-1, 4-2 and 4-3, by their respective specific gravities;
- Box 9: Calculate the volume of coarse aggregate by dividing its mass (appearing in box 5) by its SSD specific gravity;
- Box 10: Obtain the volume of entrapped air in l/m^3 by multiplying the air content (box 6) by 10;
- Box 11: Calculate the volume of the solids contained in the superplasticizer;
- Box 12: Put the total mix volume of $1000 l/m^3$ here;
- Box 13: Calculate the volume of the fine aggregate in l/m^3 by subtracting the volumes of all of the other ingredients (boxes 2, 8, 9, 10 and 11) from 1000;
- Column 3: Calculate the mass of fine aggregate and the unit mass of concrete;
- Box 14: Calculate the mass of fine aggregate by multiplying its volume appearing in box 13 by its SSD specific gravity;
- Box 15: Put the mass of solid in the superplasticizer, M_{sol} , here;
- Box 16: Sum up all the masses appearing in column 3 here to give the unit mass of the concrete;
- Box 17: Multiply the SSD mass of coarse aggregate by $(1 + W_h/100)$;

- Box 18: Subtract the value in box 17 from that in box 5 and enter the result;
- Box 19: Calculate the SSD mass of the fine aggregate;
- Box 20: Subtract the value in box 19 from that in box 14 and enter the result;
- Box 21: Write the amount of water brought to the mix by the superplasticizer from box G, the negative sign already appearing in this box;
- Box 22: Add algebraically all the water corrections;
- Column 5: Calculate the final composition of 1 m³ of concrete with the wet aggregates;
- Box 23: Add the water correction appearing in box 22 to the volume of water appearing in box 2;
- Box 24: Enter the superplasticizer dosage, V_{liq} , from box F;
- Column 6: Calculate the trial batch composition;
- Column 5: Multiply each number appearing in the column by a factor f and let it be equal to the desired mass of the trial batch in kg, divided by the mass in box 16, where the factor f can also be calculated on a volume basis, and if the trial batch has to have a certain volume, each number appearing in the column has to be multiplied by a factor corresponding to the volume of the trial batch in litres divided by 1000;
- Boxes 25: Calculate the value by multiplying the values in the adjacent to box 29 in column 5 by the factor f ;
- Box 30: Calculate the mass of the trial batch by adding the masses of the different concrete ingredients appearing in boxes 25 to 29;
- Box 30: Evaluate the calculation, multiply box 16 by f to check if the result is the same as that in box 30.

The mix design sheets are presented in Tables 4-3 to 4-15 for the total thirteen series. The mix design sheet for control mix of HPC is shown in Table 4-3. To help further understand the mix design, it is worthwhile to indicate the individual contents in detail.

The cement content was 504 kg/m³, and silica fume was used at a dosage of 10% binder contents in weight (56 kg/m³). The W/B ratio was 0.25, with the coarse aggregate of 998 kg/m³ and the sand of 781 kg/m³. The superplasticizer was 1.57% binder contents in weight (20 l/m³).

Table 4-3 Mix design sheet for the control mix of HPC

the amount of concrete to make the trial batch

	specimen		Total + 10% assuming a loss
	100*100*100 mm	100*100*500*mm	
Number	12	4	83
weight kg	2.3	12	
needed kg	28	48	

mix design sheet

comp strength	110 Mpa
---------------	---------

Table A	Gc	%
Cement	3.14	90
S.F	2.2	10

Aggregate	GSSD	%		
		Wabs	Wtot	Wh
coarse	2.9	0.66	0	-0.66
fine	2.641	3.22	0	-3.22

superplastizer		Msol=Bx d/100	Vliq=(Msol/SxGsup) x 100	Vw = Vliq x Gsup x (100-s/100)	Vsol=Vliq-Vw
sp.gravity (Gsup)	solids dos s(%)				
1.1	40	9	20	13	6.8

Materials	1		2	3	4	5	6
	content kg/m3	volume	SSD condition	water correction	composition		
water	water content	140	140	7	1m3	trail batch	
W/B= 0.25	140				159	5	
cement	Binder content	504	161		504	17	
silica fume	560	56	25		56	1.85	
Coarse aggregate	1005	347	1005	7	998	32.9	
fine aggregate		306	807	26	781	26	
AIR	percent	15	0				
	1.50						
Super Plasticizer	1.57	6.8	9	-13	Vliq 20	0.7	
TOTAL		694	2521	19		75.5	

Table 4-4 Mix design sheet for the HPC modified with 1.5% SBR

the amount of concrete to make the trial batch

	specimen		Total + 10% assuming a loss
	100*100 *100 mm	100*100*500*mm	
Number	12	4	83
weight kg	2.3	12	
needed kg	28	48	

mix design sheet 1.5% SBR

comp strength	110 Mpa
---------------	---------

Table A	Gc	%
Cement	3.14	90
S.F	2.2	10

Aggregate	GSSD	%		
		Wabs	Wtot	Wh
coarse	2.9	0.85	0	-0.85
fine	2.641	3.72	3.5	-0.22

superplastizer		Msol=Bx d/100	Vlig=(Msol/SxGsup) x 100	Vw = Vliq x Gsup x (100-s/100)	Vsol=Vliq-Vw
sp.gravity (Gsup)	solids dos s(%)				
1.1	40	8.8	20	13	6.8
SBR latex					
sp.gravity (GSBR)	solids dos (%)				
1.0	48	8.4	17.5	9.1	8.4

Materials	1		2	3	4	5	6
	content kg/m3		volume	SSD condition	water correction	composition	
						1m3	trial batch
water	water content 140		140	140		128	3.9
cement	W/B=					504	17
	0.25	Binder content	504	161		504	
silica fume		560	56	25		56	1.86
Coarse aggregate	1005		347	1005	7	998	33
fine aggregate			297	785	2	783	26
AIR	per cent 1.50		15	0			
Super Plasticizer	1.57		6.8	8.8	-13	vlig 20	0.7
SBR latex	1.5		8.4	8.4	-9.1	17.5	0.6
TOTAL			703	2507	-12		76

Table 4-5 Mix design sheet for the HPC modified with 3% SBR

the amount of concrete to make the trial batch

	specimen		Total + 10% assuming a loss
	100*100*100 mm	100*100*500*mm	
Number	12	4	83
weight kg	2.3	12	
needed kg	28	48	

mix design sheet with 3% SBR

comp strength	110 Mpa
---------------	---------

Table A	Gc	%
Cement	3.14	90
S.F	2.2	10

Aggregate	GSSD	%		
		Wabs	Wtot	Wh
coarse	2.9	0.85	0	-0.85
fine	2.641	3.72	3.5	-0.22

superplastizer		Msol=Bx d/100	Vliq=(Msol/SxGsup) x 100	Vw = Vliq x Gsup x (100-s/100)	Vsol=Vliq-Vw
sp.gravity (Gsup)	solids dos s(%)				
1.1	40	8.8	20	13	6.8
SBR latex					
sp.gravity (GSBR)	solids dos (%)				
1.0	48	16.8	35	18.2	16.8

Materials	1		2	3	4	5	6
	content kg/m3		volume	SSD condition	water correction	composition	
						1m3	trial batch
water	water content 140		140	140	-	119	3.6
W/B= 0.25	Binder content		504	504		504	17
cement	560		56	56		56	1.9
silica fume							
Coarse aggregate	1005		347	1005	7	998	33
fine aggregate			289	763	2	761	25.4
AIR	per cent 1.50		15	0			
Super Plasticizer	1.57		6.8	8.8	-13.2	Vliq 20	0.7
SBR latex	3		16.8	16.8	-18.2	35	1.17
TOTAL			711	2494	-21		76

Table 4-6 Mix design sheet for the HPC modified with 5% SBR

the amount of concrete to make the trial batch

	specimen		Total + 10% assuming a loss
	100*100 *100 mm	100*100*500*mm	
Number	12	4	83
weight kg	2.3	12	
needed kg	28	48	

mix design sheet

comp strength	110 Mpa
---------------	---------

Table A	Gc	%
Cement	3.14	90
S.F	2.2	10

Aggregate	GSSD	%		
		Wabs	Wtot	Wh
coarse	2.9	0.85	0	-0.85
fine	2.641	3.72	3.5	-0.22

superplastizer		Msol=Bx d/100	Vliq=(Msol/SxGsup) x 100	Vw = Vliq x Gsup x (100-s/100)	Vsol=Vliq-Vw
sp.gravity (Gsup)	solids dos s(%)				
1.1	40	8.8	20	13	6.8
SBR latex					
sp.gravity (GSBR)	solids dos (%)				
1.0	48	28	58.3	30.3	28.0

Materials	1		2	3	4	5		6	
	content kg/m3		volume	SSD condition	water correction	composition 1m3		trail batch	
water	water content 140		140	140		107	3.3		
cement	W/B= 0.25	Binder content	504	161		504	504	15	
			56	25		56	56	1.7	
silica fume	560								
Coarse aggregate	1005		347	1005	7	998	30		
fine aggregate			278	733	2	732	22.3		
AIR	per cent 1.50		15	0					
Super Plasticizer	1.57		6.8	8.8	-13	Vliq 20	0.6		
SBR latex	5		28.0	28	-30.3	58.3	1.78		
TOTAL			722	2475	-33		76		

Table 4-7 Mix design sheet for the HPC modified with 1.5% PVDC

the amount of concrete to make the trial batch

	specimen		Total + 10% assuming a loss
	100*100*100 mm	100*100*500*mm	
Number	12	4	83
weight kg	2.3	12	
needed kg	28	48	

mix design sheet 1.5% pvdc

comp strength	110 Mpa
---------------	---------

Table A	Gc	%
Cement	3.14	90
S.F	2.2	10
PVDC	1.63	1.5

Aggregate	GSSD	%		
		Wabs	Wtot	Wh
coarse	2.9	0.85	0	-0.85
fine	2.641	3.72	3.5	-0.22

superplastizer	Msol=Bx d/100	Vliq=(Msol/SxGsup) x 100	Vw = Vliq x Gsup x (100-s/100)	Vsol=Vliq-Vw
sp.gravity (Gsup)				
1.1	9	20	13	6.8

Materials	1		2	3	4	5		6
	content kg/m3	volume	SSD condition	water correction	composition		1m3	trail batch
water	water content 140		140	142	7	139		4
W/B= 0.25	Binder content 504		161	504		504		15
cement	56		25	56		56		1.7
silica fume								
Coarse aggregate	1005		347	1005	7	998		30
PVDC powder	8.4		5	8.4		8.4		0.252
fine aggregate			301	794	26	768		23.8
AIR	per cent 1.50		15	0				
Super Plasticizer	1.57		6.8	9	-13	vlig 20	0.6	
TOTAL			699	2518	-3			76

Table 4-8 Mix design sheet for the HPC modified with 3% PVDC

the amount of concrete to make the trial batch

	specimen		Total + 10% assuming a loss
	100*100 *100 mm	100*100*500*mm	
Number	12	4	83
weight kg	2.3	12	
needed kg	28	48	

mix design sheet

comp strength	110 Mpa
---------------	---------

Table A	Gc	%
Cement	3.14	90
S.F	2.2	10
PVDC	1.63	3

Aggregate	GSSD	%		
		Wabs	Wtot	Wh
coarse	2.9	0.85	0	-0.85
fine	2.641	3.72	3.5	-0.22

superplastizer		Msol=Bx d/100	Vliq=(Msol/SxGsup) x 100	Vw = Vliq x Gsup x (100-s/100)	Vsol=Vliq-Vw
sp.gravity (Gsup)	solids dos s(%)				
1.1	40	9	20	13	6.8

Materials	1		2	3	4	5		6
	content kg/m3	volume	SSD condition	water correction	composition		1m3	trial batch
water	water content 140		140	144	7	141		4.2
cement	Binder content	504	161	504		504		15
		56	25	56		56		1.7
560								
Coarse aggregate	1005	347	1005		998		30	
PVDC powder	16.8	10	16.8		16.8		0.5	
fine aggregate		295	780	25	755		23.4	
AIR	per cent		15	0				
	1.50							
Super Plasticizer	1.57	6.8	9	-13	Vliq 20	0.6		
TOTAL		705	2515	-3			76	

Table 4-9 Mix design sheet for the HPC modified with 5% PVDC

the amount of concrete to make the trial batch

	specimen		Total + 10% assuming a loss
	100*100 *100 mm	100*100*500*mm	
Number	12	4	
weight kg	2.3	12	
needed kg	28	48	83

mix design sheet

comp strength 110 Mpa

Table A	Gc	%
Cement	3.14	90
S.F	2.2	10
PVDC	1.63	5

Aggregate	GSSD	%		
		Wabs	Wtot	Wh
coarse	2.9	0.85	0	-0.85
fine	2.641	3.72	3.5	-0.22

superplastizer	Msol=Bx d/100	Vliq=(Msol/SxGsup) x 100	Vw = Vliq x Gsup x (100-s/100)	Vsol=Vliq-Vw
sp.gravity (Gsup)	solids dos s(%)			
1.1	40	9	13	6.8

Materials	1	2	3	4	5		6
					composition		
	content kg/m3	volume	SSD condition	water correction	1m3	trail batch	
water	water content						
	140	140	147		167	5.5	
cement	Binder content						
	504	161	504		504	17	
silica fume	560						
	56	25	56		56	1.9	
Coarse aggregate	1005		347	1005	9	996	33
PVDC powder	28		17	28		28	0.927
fine aggregate			289	762	25	737	24.4
AIR	per cent			0			
	1.50		15				
Super Plasticizer	1.57		6.8	9	-13	Vliq 20	0.7
TOTAL			711	2511	20		83

Table 4-10 Mix design sheet for the HPC modified with 1.5% LLDPE

the amount of concrete to make the trial batch

	specimen		Total + 10% assuming a loss
	100*100 *100 mm	100*100*500*mm	
Number	12	4	
weight kg	2.3	12	
needed kg	28	48	83

mix design sheet

comp strength	110 Mpa
---------------	---------

Table A	Gc	%
Cement	3.14	90
S.F	2.2	10
LLDPE	0.94	1.5

Aggregate	GSSD	%		
		Wabs	Wtot	Wh
coarse	2.9	0.85	0	-0.85
fine	2.641	3.72	3.5	-0.22

superplastizer	Msol=Bx d/100	Vliq=(Msol/SxGsup) x 100	Vw = Vliq x Gsup x (100-s/100)	Vsol=Vliq-Vw
sp.gravity (Gsup)				
1.1	9	20	13	6.8

Materials	1		2	3	4	5		6
	content kg/m3		volume	SSD condition	water correction	composition		
						1m3	trial batch	
water	140		140	142	-	152	5.0	
cement	560	504	161	504		504	17	
silica fume		56	25	56		56	1.9	
Coarse aggregate	1005		347	1005	7	998	33	
LLDPE	8.4		9	8.4		8.4	0.279	
fine aggregate			297	784	16	768	25.5	
AIR	per cent			0				
	1.50		15					
Super Plasticizer	1.57		6.8	9	-13	Vliq 20	0.7	
TOTAL			703	2508	10			83

Table 4-11 Mix design sheet for the HPC modified with 3% LLDPE

the amount of concrete to make the trial batch

	specimen		Total + 10% assuming a loss
	100*100 *100 mm	100*100*500*mm	
Number	12	4	
weight kg	2.3	12	
needed kg	28	48	83

mix design sheet

comp strength 110 Mpa

Table A	Gc	%
Cement	3.14	90
S.F	2.2	10
LLDPE	0.94	3

Aggregate	GSSD	%		
		Wabs	Wtot	Wh
coarse	2.9	0.85	0	-0.85
fine	2.641	3.72	3.5	-0.22

superplastizer	Msol=Bx d/100	Vliq=(Msol/SxGsup) x 100	Vw = Vliq x Gsup x (100-s/100)	Vsol=Vliq-Vw
sp.gravity (Gsup)	solids dos s(%)			
1.1	40	9	13	6.8

Materials	1		2	3	4	5		6
	content kg/m3		volume	SSD condition	water correction	composition		
						1m3	trial batch	
water	water content 140		140	144		143	4.8	
cement	Binder content 504		161	504		504	17	
silica fume	560		56	56		56	1.9	
Coarse aggregate	1005		347	1005	7	998	33	
LLDPE	16.8		18	16.8		16.8	0.560	
fine aggregate			288	760	5	755	25.2	
AIR	per cent 1.50		15	0				
Super Plasticizer	1.57		6.8	9	-13	Vliq 20	0.7	
TOTAL			712	2495	-1		83	

Table 4-12 Mix design sheet for the HPC modified with 5% LLDPE

the amount of concrete to make the trial batch

	specimen		Total + 10% assuming a loss
	100*100 *100 mm	100*100*500*mm	
Number	12	4	
weight kg	2.3	12	
needed kg	28	48	83

mix design sheet

comp strength 110 Mpa

Table A	Gc	%
Cement	3.14	90
S.F	2.2	10
LLDPE	0.94	5

Aggregate	GSSD	%		
		Wabs	Wtot	Wh
coarse	2.9	0.85	0	-0.85
fine	2.641	3.72	3.5	-0.22

superplasticizer	Msol=Bx d/100	Vliq=(Msol/SxGsup) x 100	Vw = Vliq x Gsup x (100-s/100)	Vsol=Vliq-Vw
sp.gravity (Gsup)				
1.1	9	20	13	6.8

Materials	1		2	3	4	5		6
	content kg/m3	volume	SSD condition	water correction	composition		1m3	trial batch
water	water content							
	W/B= 0.25	140	140	147		132	4.4	
cement	Binder content	504	161	504		504	17	
silica fume	560	56	25	56		56	1.9	
Coarse aggregate	1005	347	1005	7	998	33		
LLDPE	28	30	28		28	0.940		
fine aggregate		276	729	-8	737	24.7		
AIR	per cent			0				
	1.50	15						
Super Plasticizer	1.57	6.8	9	-13	Vliq 20	0.7		
TOTAL		724	2477	-15		83		

Table 4-13 Mix design sheet for the HPC modified with 1.5% HDPE

the amount of concrete to make the trial batch

	specimen		Total + 10% assuming a loss
	100*100 *100 mm	100*100*500*mm	
Number	12	4	
weight kg	2.3	12	
needed kg	28	48	83

mix design sheet

comp strength	110 Mpa
---------------	---------

Table A	Gc	%
Cement	3.14	90
S.F	2.2	10
HDPE	0.94	1.5

Aggregate	GSSD	%		
		Wabs	Wtot	Wh
coarse	2.9	0.85	0	-0.85
fine	2.641	3.72	3.5	-0.22

superplastizer		Msol=Bx d/100	Vliq=(Msol/SxGsup) x 100	Vw = Vliq x Gsup x (100-s/100)	Vsol=Vliq-Vw
sp.gravity (Gsup)	solids dos s(%)				
1.1	40	9	20	13	6.8

Materials	1		2	3	4	5	6
	content kg/m3		volume	SSD condition	water correction	composition	
						1m3	trial batch
water	140		140	142		152	5.0
cement	560	504	161	504		504	17
silica fume		56	25	56		56	1.9
Coarse aggregate	1005		347	1005		7	998
HDPE	8.4		9	8.4		8.4	0.279
fine aggregate			297	784	16	768	25.5
AIR	per cent			0			
	1.50		15				
Super Plasticizer	1.57		6.8	9	-13	Vliq 20	0.7
TOTAL			703	2508	10		83

Table 4-14 Mix design sheet for the HPC modified with 3% HDPE

the amount of concrete to make the trial batch

	specimen		Total + 10% assuming a loss
	100*100 *100 mm	100*100*500*mm	
Number	12	4	83
weight kg	2.3	12	
needed kg	28	48	

mix design sheet

comp strength 110 Mpa

Table A	Gc	%
Cement	3.14	90
S.F	2.2	10
HDPE	0.94	3

Aggregate	GSSD	%		
		Wabs	Wtot	Wh
coarse	2.9	0.85	0	-0.85
fine	2.641	3.72	3.5	-0.22

superplastizer	Msol=Bx d/100	Vlig=(Msol/SxGsup) x 100	Vw = Vliq x Gsup x (100-s/100)	Vsol=Vliq-Vw
sp.gravity (Gsup)	solids dos s(%)			
1.1	40	9	13	6.8

Materials	1		2	3	4	5		6	
	content kg/m3		volume	SSD condition	water correction	composition		trail batch	
water	water content					1m3			
	140		140	144		143	4.8		
cement	Binder content		504	161		504	504	17	
silica fume	560		56	25		56	56	1.9	
Coarse aggregate	1005		347	1005	7	998	33		
HDPE	16.8		18	16.8		16.8	0.560		
fine aggregate			288	760	5	755	25.2		
AIR	per cent		15	0					
	1.50								
Super Plasticizer	1.57		6.8	9	-13	Vliq 20	0.7		
TOTAL			712	2495	-1		83		

Table 4-15 Mix design sheet for the HPC modified with 5% HDPE

the amount of concrete to make the trial batch

	specimen		Total + 10% assuming a loss
	100*100 *100 mm	100*100*500*mm	
Number	12	4	
weight kg	2.3	12	
needed kg	28	48	83

mix design sheet

comp strength 110 Mpa

Table A	Gc	%
Cement	3.14	90
S.F	2.2	10
HDPE	0.94	5

Aggregate	GSSD	%		
		Wabs	Wtot	Wh
coarse	2.9	0.85	0	-0.85
fine	2.641	3.72	3.5	-0.22

superplastizer	Msol=Bx d/100	Vliq=(Msol/SxGsup) x 100	Vw = Vliq x Gsup x (100-s/100)	Vsol=Vliq-Vw
sp.gravity (Gsup)	solids dos s(%)			
1.1	40	9	13	6.8

Materials	1		2	3	4	5	6
	content kg/m3		volume	SSD condition	water correction	composition 1m3 trail batch	
water	water content 140		140	147		132	4.4
cement	Binder content 504		161	504		504	17
silica fume	560		56	56		56	1.9
Coarse aggregate	1005		347	1005		7	998
HDPE	28		30	28		28	0.940
fine aggregate			276	729	-8	737	24.7
AIR	per cent 1.50		15	0			
Super Plasticizer	1.57		6.8	9	-13	Vliq 20	0.7
TOTAL			724	2477	-15		83

The mix design sheet for HPC with 1.5% SBR is shown in Table 4-4. The cement content was 504 kg/m^3 , and silica fume was used at a dosage of 10% binder contents in weight (56 kg/m^3). The superplasticizer was 1.57% binder contents in weight (20 l/m^3). The W/B ratio was 0.25, with the coarse aggregate of 998 kg/m^3 and the sand of 783 kg/m^3 . The SBR modified HPC had liquid polymer of 1.5% binder contents in weight (17.5 l/m^3).

The mix design sheet for HPC with 3% SBR is shown in Table 4-5. The cement content was 504 kg/m^3 , and silica fume was used at a dosage of 10% binder contents in weight (56 kg/m^3). The W/B ratio was 0.25, with the coarse aggregate of 998 kg/m^3 and the sand of 761 kg/m^3 . The superplasticizer was 1.57% binder contents in weight (20 l/m^3). The SBR modified HPC had a liquid polymer of 3% binder contents in weight (35 l/m^3).

The mix design sheet for HPC with 5% SBR is shown in Table 4-6. The cement content was 504 kg/m^3 , and silica fume was used at a dosage of 10% binder contents in weight (56 kg/m^3). The W/B ratio was 0.25, with the coarse aggregate of 998 kg/m^3 and the sand of 732 kg/m^3 . The superplasticizer was 1.57% binder contents in weight (20 l/m^3). The SBR modified HPC had liquid polymer of 5% binder contents in mass (58.3 l/m^3).

The mix design sheet for HPC with 1.5% PVDC is shown in Table 4-7. The cement content was 504 kg/m^3 , and silica fume was used at a dosage of 10% binder contents in weight (56 kg/m^3). The W/B ratio was 0.25, with the coarse aggregate of 998 kg/m^3 and the sand of 768 kg/m^3 . The superplasticizer was 1.57% binder contents in weight (20 l/m^3). The PVDC modified HPC had solid polymer of 1.5% binder contents in weight (8.4 kg/m^3).

The mix design sheet for HPC with 3% PVDC is shown in Table 4-8. The cement content was 504 kg/m^3 , and silica fume was used as a dosage of 10% binder contents in weight (56 kg/m^3). The W/B ratio is 0.25, with the coarse aggregate of 998 kg/m^3 and the sand of 755 kg/m^3 . The superplasticizer was 1.57% binder contents in weight (20 l/m^3). The PVDC modified HPC had solid polymer of 3% binder contents in weight (16.8 kg/m^3).

The mix design sheet for HPC with 5% PVDC is shown in Table 4-9. The cement content was 504 kg/m^3 , and silica fume was used at a dosage of 10% binder contents

in weight (56 kg/m^3). The W/B ratio was 0.25, with the coarse aggregate of 998 kg/m^3 and the sand of 737 kg/m^3 . The superplasticizer was 1.57% binder contents in mass (20 l/m^3). The PVDC modified HPC had solid polymer of 5% binder contents in weight (28 kg/m^3).

The mix design sheet for HPC with 1.5% LLDPE is shown in Table 4-10. The cement content was 504 kg/m^3 , and silica fume was used at a dosage of 10% binder contents in mass (56 kg/m^3). The W/B ratio was 0.25, with the coarse aggregate of 998 kg/m^3 and the sand of 768 kg/m^3 . The superplasticizer was 1.57% binder contents in weight (20 l/m^3). The LLDPE modified HPC had solid polymer of 1.5% binder contents in weight (8.4 kg/m^3).

The mix design sheet for HPC with 3% LLDPE is shown in Table 4-11. The cement content was 504 kg/m^3 , and silica fume was used at a dosage of 10% binder contents in weight (56 kg/m^3). The W/B ratio was 0.25, with the coarse aggregate of 998 kg/m^3 and the sand of 755 kg/m^3 . The superplasticizer was 1.57% binder contents in weight (20 l/m^3). The LLDPE modified HPC had solid polymer of 1.5% binder contents in weight (16.8 kg/m^3).

The mix design sheet for HPC with 5% LLDPE is shown in Table 4-12. The cement content was 504 kg/m^3 , and silica fume was used at a dosage of 10% binder contents in weight (56 kg/m^3). The W/B ratio was 0.25, with the coarse aggregate of 998 kg/m^3 and the sand of 737 kg/m^3 . The superplasticizer was 1.57% binder contents in weight (20 l/m^3). The LLDPE modified HPC had solid polymer of 5% binder contents in weight (28 kg/m^3).

The mix design sheet for HPC with 1.5% HDPE is shown in Table 4-13. The cement content is 504 kg/m^3 . Silica fume was used in a dosage of 10% binder contents in weight (56 kg/m^3). The W/B ratio was 0.25, with the coarse aggregate of 998 kg/m^3 and the sand of 768 kg/m^3 . The superplasticizer was 1.57% binder contents in weight (20 l/m^3). The LLDPE modified HPC had solid polymer of 1.5% binder contents in weight (8.4 kg/m^3).

The mix design sheet for HPC with 3% HDPE is shown in Table 4-14. The cement content was 504 kg/m^3 , and silica fume was used at a dosage of 10% binder contents in weight (56 kg/m^3). The W/B ratio was 0.25, with the coarse aggregate of 998 kg/m^3 and the sand of 755 kg/m^3 . The superplasticizer was 1.57% binder contents in

weight (20 l/m^3). The LLDPE modified HPC had solid polymer of 3% binder contents in weight (16.8 kg/m^3).

Finally, the mix design sheet for HPC with 5% HDPE is shown in Table 4-15. The cement content was 504 kg/m^3 , and silica fume was used at a dosage of 10% binder contents in weight (56 kg/m^3). The W/B ratio was 0.25, with the coarse aggregate of 998 kg/m^3 and the sand of 737 kg/m^3 . The superplasticizer was 1.57% binder contents in weight (20 l/m^3). The LLDPE modified HPC had solid polymer of 5% binder contents in weight (28 kg/m^3).

4.3 Specimens

ACI committee 446 has determined several provisions that should be met when the concrete specimens are cast (ACI, 2009). A minimum of three beam specimens should be cast. Whenever practical, all the specimens should be cast from the same concrete batch. In this study, four beam specimens were produced and they should be prismatic beams of rectangular cross-section with a sawn central notch.

Beam depth H shall be at least 6 times greater than the maximum aggregate size d_{max} , i.e. $H \geq 6d_{max}$. The preferred depth H is 150 mm if $d_{max} \leq 25$ mm. In this study, H was adopted as 100 mm. Beam width B should be at least 6 times greater than the maximum aggregate size d_{max} , i.e. $B \geq 6 d_{max}$. The preferred width B is 150 mm if $d_{max} \leq 25$ mm. In this study B was adopted as 100 mm. The loading span S should be equal to three times the beam depth, i.e. $3H$, within $\pm 5\%$. In this study S was adopted 400 mm to allow the pre-cut notch to develop steadily. The total length L of the specimen should be at least 50 mm longer than three times the beam depth H , i.e. $L \geq 3H + 50$ mm. In this study L was controlled at 500 mm. The nominal notch depth a_0 should be equal $H/3$. In this study a_0 was adopted as 50 mm.

One day before the three-point bending tests, the beam specimens were removed from the water tank and were notched using a diamond saw under water cooling, see Figure 4-4. To avoid any damage to concrete the pressure of the saw was maintained as low as possible and the specimens were handled carefully to avoid any damages.

Besides beam specimens, 100 mm cubes were used for compression and tension tests (Figure 4-5).



Figure 4-4 Beam samples with notches at mid-span

4.4 Batching and Curing

Mixing method based on several concrete mixing trials was piloted in the lab by Swamy and Bouikni (1990). The coarse aggregate and sand were mixed first with one third of the required water to allow the aggregate and sand to absorb water, and then the cement, silica fume and polymer were added and mixed for another 30 seconds. Superplasticizer and the remaining water were slowly added in to the mixed materials. If the polymer is liquid like SBR, it will be added in with the water and superplasticizer together. The mixing continued with the addition of water and superplasticizer until thorough mixing was achieved. Before casting all the beams and cubes the moulds had been oiled. Each specimen was well compacted on the vibration table. A slump test was performed and the concrete used for the slump was put back into the mixer before casting all specimens. Due to limited numbers of

moulds (4 steel beam moulds and 12 cube moulds) and the capacity of the mixer, two batches of concrete were produced per mix on each casting day.

When all the moulds were filled up with concrete, the specimens were then covered with wet papers to maintain moisture, and left in the casting room for 24 hours until demoulding next day. With the addition of SBR, PVDC, LLDPE and HDPE, however, the specimens needed another 24 hours in air for polymer based composites to complete the polymerising process and thereafter were immediately taken to the curing room. Figure 4-5 shows the specimens after 24 hours that needed another 24 hours to complete the polymerisation process. At 7 days, three cubes for each mix were tested in compression to obtain the 7-day compressive strengths. At 28 days, compressive and tensile tests were conducted, together with dynamic elastic module tests on six cubes. Also three-point bending tests were conducted on four notched beam specimens.



(a) In the first 24 hours



(b) In the second 24 hours

Figure 4-5 Typical cube specimens of polymer modified concrete for first 24 hours after casting and second 24 hours to complete the polymerisation process

As indicated above, along with the beam specimens, a total of one hundred and fifty six cubes of 100 mm × 100 mm × 100 mm were cast for all concrete mixes. These

cubes were tested at seven, twenty-eight and ninety days, and the compressive strengths at 28 days were 110 MPa or over for all thirteen groups of polymer modified concretes.

4.5 Summary

The mix designs for all thirteen HPCs with four types of polymers, i.e. Styrene Butadiene Rubber (SBR) latex, Polyvinylidene Chloride (PVDC), Linear Low Density Polyethylene (LLDPE) and High Density Polyethylene (HDPE), with contents of 1.5%, 3.0% and 5% in the mass of cementitious materials are presented in detail. The proposed method in this study is very simple and it follows the approach recommended by ACI 211-1 Standard Practice for Selecting Proportions for Normal, Heavyweight and Mass Concrete. It is a combination of empirical results and mathematical calculations based on the absolute volume method. The water contributed by the superplasticizer is considered as part of the mixing water. Three-points bending tests recommended by International Union of Laboratories and Experts in Construction Materials RILEM Committee FMC-50 are to be widely used for the determination of the fracture energy because it is simple to carry on testing.

Twenty six of batches of concrete were used for the thirteen mixes and for moulding fifty two beams. The dimensions of all the beams were 100 mm × 100 mm × 500 mm and the beams were tested at twenty-eight days. Before testing the beam specimens, a notch of half depth was produced using a diamond saw at the mid-section of the beam. Along with the beam specimens, a total of one hundred and fifty six cubes of 100 mm × 100 mm × 100 mm were cast for all concrete mixes and tested at seven, twenty-eight and ninety days, with the compressive strengths of 110 MPa or over at 28 days for all thirteen groups of polymer modified concretes.

CHAPTER 5 THE EXPERIMENTAL PROGRAMME

5.1 Introduction

The experimental programme carried out in this study on the modified high performance concrete with SBR, PVDC, LLDPE and HDPE would aim to eventually achieve high strength, high performance and low brittle concrete. In this chapter, the experimental programme is described and specimen casting is discussed, where the tests are carried out on different concrete mixes, curing regimes and mix proportions.

5.2 Fundamental Mechanical Tests

5.2.1 Workability testing

The workability of fresh concrete was determined by conducting the conventional slump testing prior to concrete placement in the forms. The concrete used for slump and density testing was put back into the mixer for further mixing prior to specimen casting. The slump test is most famous and widely used test method to assess the workability of fresh concrete. The test method is widely standardised throughout the world, including ASTM C143/C143M in the United States (ASTM, 2010) and EN 12350-2 in Europe (BSI, 2009). The slump testing equipment consists of a hollow slump cone with a diameter of 200 mm at the bottom, a diameter of 100 mm at the top and a height of 300 mm. The slump cone is filled with concrete in three layers of equal volume. Each layer is compacted with 25 strokes using a tamping rod as shown in Figure 5-1. Thereafter, the difference between the cone and the highest spot of the concrete will be regarded as the slump.

5.2.2 Compression testing

Figure 5-2 shows the 3000 kN Avery motorised compression testing machine, with the computer control unit, to test 100 mm cubes under compression.



Figure 5-1 Slump testing



Figure 5-2 The 3000 kN Avery Denison testing machine

Standard concrete cube specimens of 100 mm × 100 mm × 100 mm were casted and tested to obtain the compressive strength at 7, 28 and 90 days, respectively. This happened after the high performance concrete modified with various types and dosages of polymer materials gained certain strength.

The strength characteristics of the cubes were tested under compression at a loading rate between 0.2 and 1.0 MPa per second in the 3000 kN Avery Denison Universal Testing Machine (Figure 5-3).

Three cubes for every mix at every specified curing age were crushed, and the average compressive strengths were determined.



Figure 5-3 Compression tests

5.2.3 Splitting tensile testing

Due to difficulties associated with the direct tension testing, indirect tension testing method has been used to determine the tensile strength of concrete. The splitting testing is well known as an indirect testing used for determining the tensile strength of concrete, sometimes referred to as the splitting tensile strength of concrete, see Figures 5-4 and 5-5. The splitting tensile strengths of plain concrete and polymer modified concrete were determined at 28 days on cubes of 100 mm × 100 mm × 100 mm, which had been cured in the water tank until the date of testing. Three specimens of each mix were tested and the mean value was recorded. The splitting tensile strength f'_t was calculated from the following equation:

$$f'_t = \frac{2F_t}{\pi a^2} \quad (5.1)$$

where

- f'_t is the splitting tensile strength in MPa,
- F_t is the maximum splitting load in N,
- a is the length of the specimen in mm.

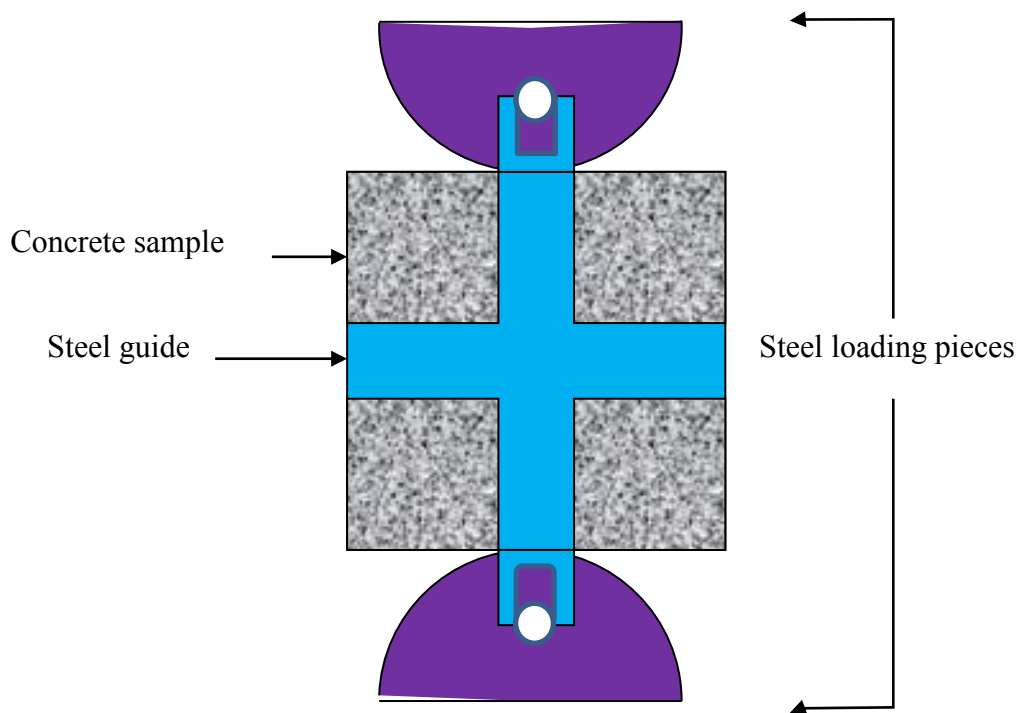


Figure 5-4 Arrangement of splitting tensile testing



Figure 5-5 Splitting tensile testing

5.2.4 Dynamic and static elastic modulus testing

The technique of ultrasonic pulse velocity provides a method for measuring dynamic elastic modulus and studying the quality of concrete by monitoring the properties of different concrete mixtures with time and the effect of curing conditions. This technique is very sensitive to the development of internal micro cracking.

As shown in Figure 5-6, the Pundit device, with 4 digits on the screen and a 12 mm reflective LCD at a data-recording rate of 2 sets per second, is the leading portable ultrasonic pulse velocity (U.P.V.) test instrument for non-destructive testing on concrete samples. It measures the time taken for a pulse of ultrasound to pass through the detected length of a material between two transducers. By taking a number of readings, it is possible to detect the presence of cracks and voids in the concrete, and to determine the dynamic elastic modulus and strength of concrete and other imperfections within the concrete.

The elastic modulus reveals the progressive change in the strength of a concrete specimen and is related to the structural stiffness and deformation process of concrete structures. It is also very sensitive to cracking and can be used to monitor the effect of drying and in alkali-silica reaction structures.



Figure 5-6 Pundit ultrasonic tester for measuring the dynamic elastic modulus

In this study two methods were used to determine the elastic modulus of concrete. The first method was conducting the ultrasonic testing on cube specimens. However, this model was found to be less accurate. The second method was using a force-displacement diagram obtained during a three-point bending test, and this method can determine the elastic modulus E more consistently in conjunction with the effective crack model for determining the critical fracture stress intensity K_{IC} .

The dynamic elastic modulus E_d was determined from the ultrasonic testing on cube specimens based on Eq.(5.2) as follows:

$$E_d = \rho_c V \quad (5.2)$$

where

E_d is the dynamic elastic modulus of concrete in GPa,

ρ_c is the concrete density in kg/m^3 ,

V is the velocity of the ultrasonic wave in m/s, and $V = L/t$,

L is the length of specimen in m,

t is the time the ultrasonic wave travelling through the specimen length in s.

The static elastic modulus E of concrete was determined from three-point bending tests based on Eq.(5.3) as follows:

$$E = \frac{K L_{eff}^3}{48I \alpha \beta} \quad (5.3)$$

where

K is the bending stiffness of a beam and can be determined from a force-displacement curve obtained from a three-point bending test,

L_{eff} is the effective beam span,

I is the second moment of area for the beam, and $I = Bh^3/12$,

α is a geometric parameter which is dependent on the relative notch length a , based the regression analysis

$$\alpha = -2.3617a^4 + 6.587a^3 - 5.2356a^2 + 0.0815a + 0.9277 \quad (5.4)$$

a is the relative notch length of the beam, and $a = a_0/h$,

a_0 is the notch length of the beam,

h is the depth of the beam,

β is another geometric parameter which is dependent on the relative notch width b , based the regression analysis

$$\beta = 14.981b^2 - 4.587b + 1.1053 \quad (5.5)$$

b is the relative notch width of the beam, and $b = w_a/L_{eff}$,

w_a is the notch width on the beam.

5.2.5 Unit weight (density) testing

The apparatus for measuring density is shown in Figure 5-7, which consists of an electronic balance and a basket attached to the balance. Below this basket is a tank filled with potable water and the basket can be raised and lowered. The cube sample is put into the basket and weighed in air. The tank of water is subsequently raised until the cube sample is completely submerged in water and the sample is re-weighed. The volume of the sample is taken from the difference between the weights in air and in water. Therefore, from these two figures, the densities for the control concrete cubes and polymer modified concrete cubes can be simply determined.



Figure 5-7 Density testing apparatus (weight-in-air/weight-in-water method)

The density of hardened concrete cubes was measured just before crushing, by using the weight and relative density apparatus as shown in Chapter 4 in accordance with ACI code. The unit weight or density of the hardened concrete ρ_c was measured at different ages and calculated from:

$$\rho_c \text{ (kg/m}^3\text{)} = W_{air} / (LBH) \quad (5.6a)$$

or

$$\rho_c \text{ (kg/m}^3\text{)} = W_{air} / (W_{air} - W_{water}) \quad (5.6b)$$

where:

W_{air} is the mass of concrete in the air in kg,

W_{water} is the mass of concrete in the water in kg,

L is the length of specimen in m,

B is the width of specimen in m,

H is the depth of specimen in m.

5.3 Fracture Testing

The machine used for three point-bending testing was the 100 kN 5500R Instron electro-mechanic testing machine manufactured by Instron Corporation in USA (Figure 5-8). RILEM recommends minimum machine stiffness of 57000 lb/in (10

kN/mm) for tests to be carried out on the smallest recommended specimen sizes in order to obtain stable failure (Malvar and Warren, 1987). The required stiffness of the machine increases as the specimen size increased. The specimens used in this research are the minimum sizes recommended.



Figure 5-8 Fracture toughness testing in the 5500 R Instron testing machine

The size-effect method described in Section 2.3.6 is used to determine reliable fracture characteristics of polymers modified high performance concrete with a very simple experimental setup.

This research utilises three-point bending tests to obtain the fracture properties of polymer modified high performance concrete in order to determine which polymer will be more appropriate. The procedures used to obtain the fracture properties from

these tests have been discussed and compared before. The fundamental material properties of the polymers used in this research have been presented in Chapter 3. As described above, the samples that were prepared for the fracture tests used different types and amounts of polymers to modify high performance concrete.

5.3.1 Test apparatus and data acquisition

The linear variable differential transducers (LVDTs) were used to measure the net deflection at the loading point relative to the supports (see Figure 5-9). To measure the beam deflections, two LVDTs were used, one on each side of the specimen at the load point. The loading head was positioned directly above the original notch location. The 100 kN load cell in the 5500R Instron testing machine was used to determine the load applied during testing. With the LVDTs and the load cell, the load and displacements were automatically recorded and stored in the desktop computer using the data acquisition device and hardware. The data collected were displayed in EXCEL sheets for further analysis.



Figure 5-9 The linear variable differential transducer (LVDT)

5.3.2 Three-point bending testing

Three-point bending test is the most widely used test for obtaining the fracture properties of cementitious materials (Figure 5-10). The standard was established in 1985 and updated in 2000 by the RILEM committee (Trussoni, 2009). RILEM

specifies that the ratio of the notch depth to the total depth, d_{notch}/d , is 0.5, the width/depth ratio is 1.0, and the span/total-depth ratio varies between 4 and 8.

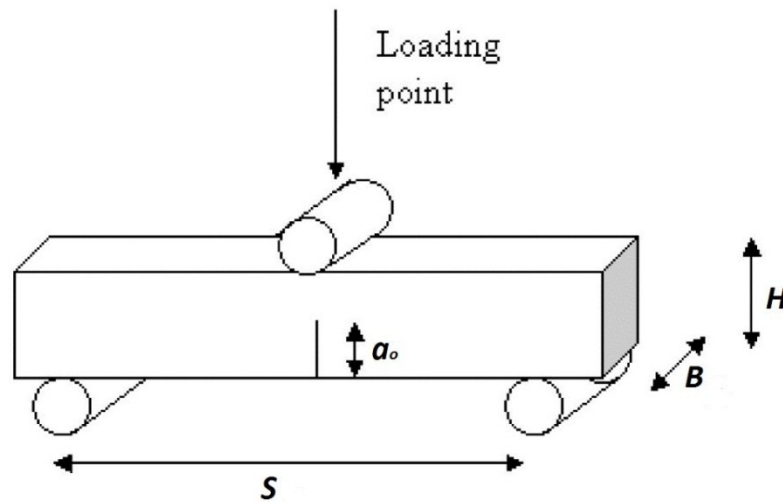


Figure 5-10 Illustration of three-point bending test set-up

For the current tests, the same geometries were used for the notched beam specimens. Specimen dimensions were chosen from the RILEM specifications, to satisfy the laboratory configuration requirements. In addition to geometry, the influence of aggregate type on fracture energy was also investigated. Thirteen different concrete mixes were used. The beams were fabricated using steel moulds of 500 mm \times 100 mm \times 100 mm. The laboratory apparatus used for the fracture energy testing was adapted from a standard three-point loading flexural strength test setup defined in ASTM C78 (2002) as shown in Figures 5-11 and 5-12. The notch in the beam specimen was set to face down and the beam was simply supported on a roller at one end and on a ball bearing on the other side.



Figure 5-11 Three-point bending test set-up



Figure 5-12 A notched beam during three-point bending testing

5.3.3 Testing for modulus of rupture

The modulus of rupture was obtained from three-point loading testing, which produces a constant bending moment between the loading points. The tests were carried out according to BS 1881: Part 118 Method for determining the flexural strength (BSI, 1983). The modulus of rupture was determined at 28 days on the beam specimens of 500 mm × 100 mm × 100 mm which had been cured in water until the date of testing. Four specimens for each mix were tested and the mean value was adopted. The modulus of rupture, f_r , was calculated from the following equation:

$$f_r = \frac{6M}{bh^2} \quad (5.7)$$

where:

- M is the maximum bending moment at mid span,
- b is the width of the beam,
- h is the depth of the beam.

By comparing Eq.(5.7) for bending with Eq.(5.1) for tension, both equations reflect the tensile capacity of the concrete but the former shows a higher value because of partial tension. However, the induction of notches makes the situation more complex.

5.3.4 Testing for fracture energy

The fracture energy G_F was determined from the analysis on the complete load-deflection curves obtained from three-point bending tests. A total of 52 three-point bending tests were conducted to determine G_F on the same notched HPC beams for determining f_r . The calculation procedures used for analysis have been described before. Figure 5-13 shows a typical load versus deflection curve ($P - \Delta$ curve) from the three-point bending test on a notched HPC beam (Figure 5-14).

The following equations were used to calculate the area under the $P - \Delta$ curves. The equations were applied to each load versus deflection curve which was put into an Excel spreadsheet with relevant data, including the ultimate load P_c , the notch depth a_o , the total specimen depth H , the specimen thickness W , etc. Using Eqs.(5.8) to (5.14), these data were used appropriately for each test method to determine K_{IC} , G_F and B_f .

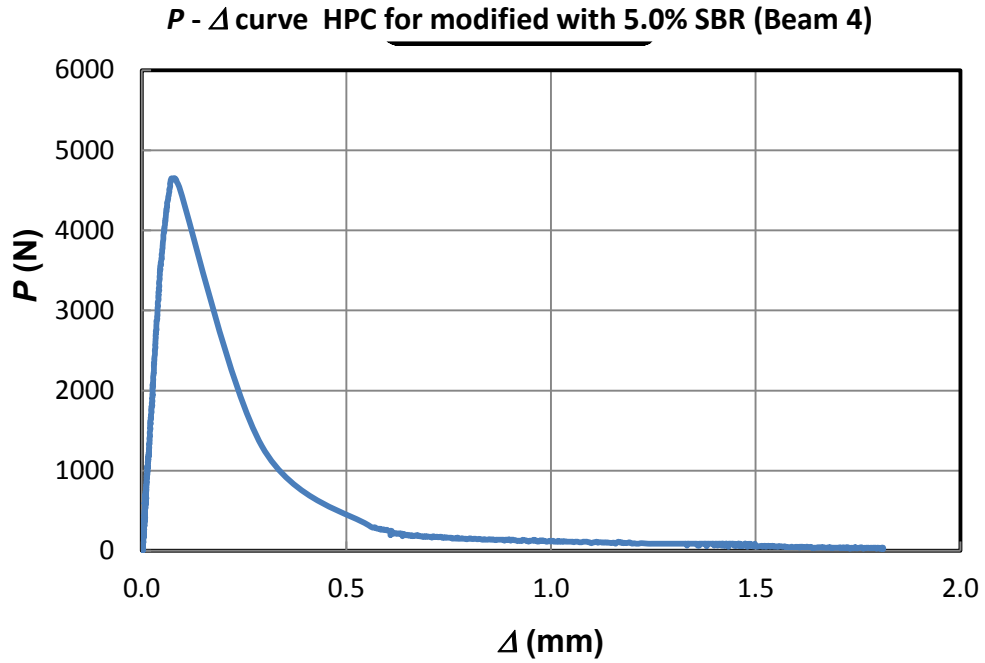


Figure 5-13 A typical load versus deflection curve

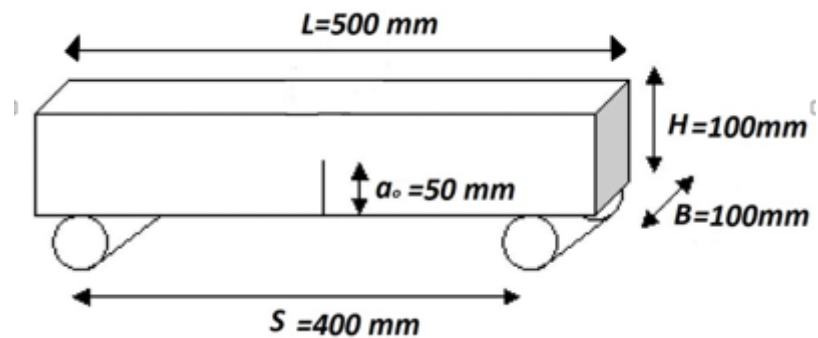


Figure 5-14 Standard three-point-bending notched concrete beam

The fracture energy G_F , defined as the total energy dissipated over a unit area of the cracked ligament, was obtained on the basis of the work done by the force, i.e. the area under a load-displacement curve in three-point bending on a centrally notched beam, associated with the gravitational work done by the self-weight of the beam. The fracture energy was calculated based on the following equation:

$$G_F = \frac{W_P + W_G}{A_{lig}} \quad (5.8)$$

where

$$W_P = \int_0^{\Delta_{max}} P(\Delta) d\Delta \quad (5.9)$$

$$W_G = m g \left(\frac{L}{S} \right) \left(2 - \frac{L}{S} \right) \Delta_{\max} \quad (5.10)$$

$$A_{lig} = B (H - a_0) \quad (5.11)$$

Failure pattern of a typical HCP beam at the end of the three-point bending test is shown in Figure 5-15. The failure was due to principal crack propagation from the notch towards the loading point.

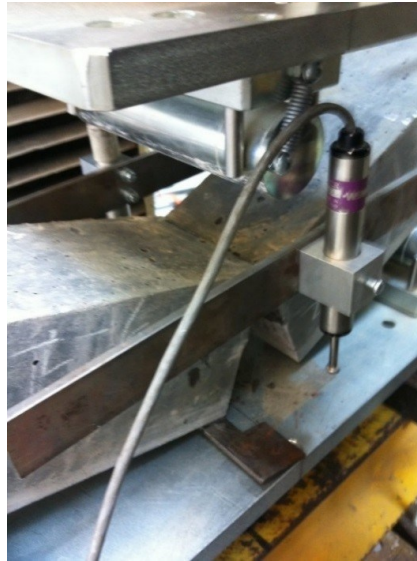


Figure 5-15 Typical failure pattern in a three-point bending test

5.3.5 Fracture energy related fracture toughness

The determination of the critical stress intensity fracture K_{IC} was described in Section 2.3.8. The fracture toughness K_{IC} is calculated using the effective crack model, it is determined from the ASTM formula (Karihaloo and Nallathambi, 1989). The fracture toughness K_{IC} can also be calculated from the following equation

$$K_{IC} = \sqrt{G_F E} \quad (5.12)$$

where

G_F is the fracture energy,

E is the Young's modulus that was calculated using Eq.(5.3).

5.3.6 Brittleness

The brittleness is a parameter in fracture mechanics as described in Section 2.3.11 and it is very interesting to researchers that the brittleness is a measure of the nature of the fracture behaviour of the concrete during loading, i.e. more brittle or more ductile. The equation for the brittleness index is given in Eq.(5.13) for this purpose (Zhang et al, 2002):

$$B_f = \frac{\Delta_e}{\Delta_f} \quad (5.13)$$

$$\Delta_e = \frac{P_u(N)}{K(N/mm)} \quad (5.14)$$

where

Δ_e is the elastic displacement in mm,

P_u is the ultimate load in N,

K is the initial stiffness in N/mm,

Δ_f is the failure displacement in mm.

5.4 Summary

This chapter has described the experimental programme designed to determine the fracture characteristics of HPC modified with polymers. The tests carried out on different concrete mixes, curing regimes, mix proportions and specimen productions have been discussed, including mix proportions, preparation of test specimens, batching and curing, testing machines, the test details for workability, compression, tension, dynamic elastic modulus, unit weight (density) and modulus of rupture, etc. The description of the fracture testing has included test apparatus and data acquisition, three-point bending testing and experimental measurements of G_F , K_{IC} and B_f . Detailed test results and the corresponding discussions will follow next.

CHAPTER 6 TEST RESULTS AND DISCUSSION

The mechanical and fracture properties that are intended to use and to show the effects of polymers on the fracture behaviour of high performance concrete are compressive strength, tensile strength, flexural strength, modulus of elasticity, static and dynamic modulus of elasticity, critical stress intensity factor K_{IC} , specific fracture energy G_F and the brittleness. These parameters are dependent variables and follow normal distributions around the mean values based on the load and deflection measurements on the beam specimens under three-point bending. The coefficients of variance (CoV) for all tests ranged from approximately 2% to 10%.

6.1 Workability

The slump measurement of all high performance concrete mixes studied was investigated by conducting the slump tests using the slump cone immediately after mixing the concrete. Table 6-1 illustrates the results of the slump tests on the HPC modified with different types and amounts of polymers.

For concrete mix with a constant W/C of 0.25 and a constant content of superplasticizer for all mixes, there were some changes in slump with the addition of different types and amounts of polymers. For the concrete mix with 1.5% SBR, the slump increased to 30 mm from 28 mm for the control mix, to 35 mm with 3% SBR, and to 40 mm with 5% SBR. For the concrete mix with 1.5% PVDC, the slump increased to 30 mm, to 45mm with 3% and 5% PVDC. For the concrete mix with 1.5% LLDPE, the slump increased to 45 mm, to 47 mm with 3% LLDPE and to 50 mm with 5% LLDPE, respectively. For the concrete mix with 1.5 HDPE, the slump increased to 35mm, to 40 mm with 3% HDPE and to 60 mm with 5% HDPE. Figure 6-1 shows the slump measurements on the high performance concrete modified with different types and amounts of polymers.

In general, the slump increased when the quantity of polymer increased. This means that the polymer additive could slightly enhance the workability of the high performance concrete. This was because the polymer causes the high performance

concrete to become more viscous and the particles of polymer which fill up the voids of the concrete will enhance the concrete slump.

Table 6-1 Slumps of concrete mixes investigated

Mix	Water/binder ratio	Polymer and SF (kg/m ³)	Superplasticizer (l/m ³)	Slump (mm)
Control	0.25	0.0 polymer + 55 SF	20	28
1.5% SBR	0.25	17.5 l SBR + 55 SF	20	30
3% SBR	0.25	35.0 l SBR+ 55 SF	20	35
5% SBR	0.25	58.3 l SBR+ 55 SF	20	40
1.5% PVDC	0.25	8.4 PVDC + 55 SF	20	40
3% PVDC	0.25	16.8 PVDC + 55 SF	20	45
5% PVDC	0.25	28.0 PVDC + 55 SF	20	45
1.5% LLDPE	0.25	8.4 LLDPE + 55 SF	20	45
3% LLDPE	0.25	16.8 LLDPE + 55 SF	20	47
5% LLDPE	0.25	28.0 LLDPE + 55 SF	20	50
1.5% HDPE	0.25	8.4 HDPE + 55 SF	20	35
3% HDPE	0.25	16.8 HDPE + 55 SF	20	40
5% HDPE	0.25	28.0 HDPE + 55 SF	20	60

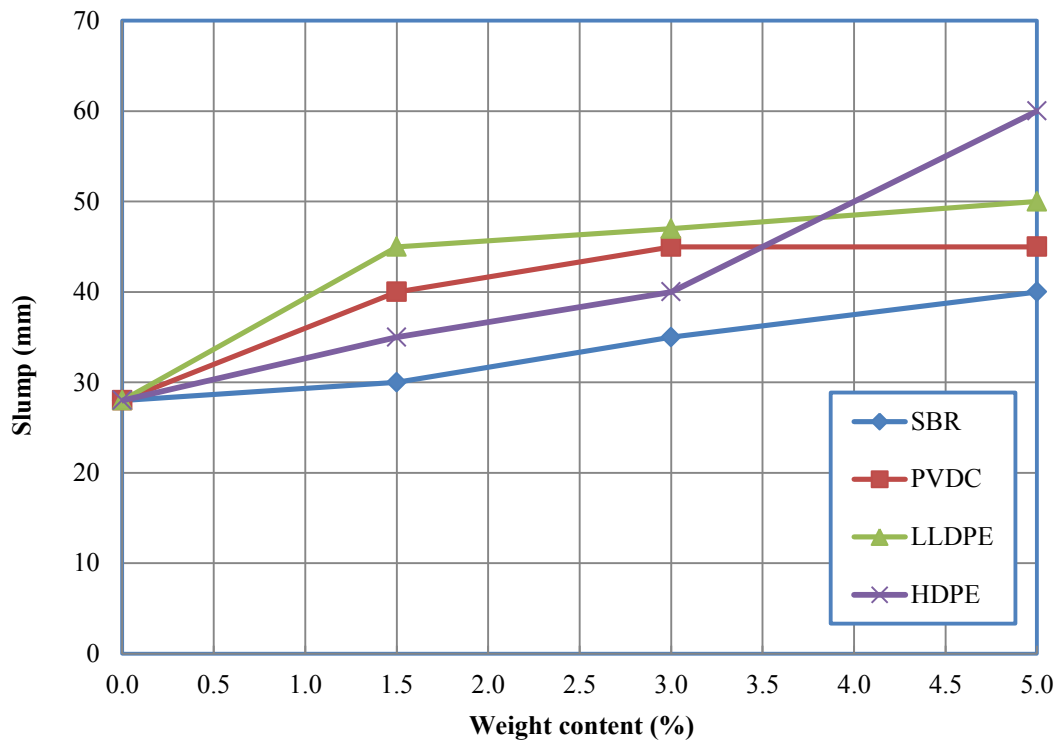


Figure 6-1 Measured slump values for the HPC modified with different types and contents of polymers

6.2 Unit Weight (Density)

The range of concrete density for normal weight concrete is between 2200-2600 kg/m³. Typically it is about 2400 kg/m³ (Neville, 1995). The measured densities of the high performance concrete modified by polymers were slightly more or less than those average values frequently obtained. The results are presented in Table 6-2. The test results for the concrete density at 28 days are shown in Figure 6-2, which clearly indicates that polymers modified unmodified high performance concrete.

As indicated in Figure 6-2, the densities of high performance concrete samples with 1.5% and 5% of SBR latex are slightly higher than that of the control mix, whereas the density for the HPC with 3% SBR additives slightly decreased.

The densities of high performance concrete samples with different percentages of PVDC powder are slightly higher than that of the control mix.

For the concrete modified with LLDPE, the concrete density monotonically decreased with the increasing polymer contents. The additions of 1.5%, 3% and 5%

of LLDPE decreased the density of high performance concrete by 0.4%, 1.0% and 2.2%. Similarly, the additions of 3% and 5% of HDPE also resulted in a decrease in the density of high performance concrete by 1.4% and 1.9%, respectively.

Table 6-2 Density test results at 28 days

Mixture		Density of cubes ρ_c (kg/m ³)				Standard deviation (SD)	Coefficient of variation (CoV %)
		Cube 1	Cube 2	Cube 3	Average		
Control mix		2447.5	2438.5	2427.0	2437.7	10.3	0.42
SBR	1.5%	2478.0	2450.0	2461.5	2463.2	14.1	0.57
	3.0%	2439.5	2443.0	2411.0	2431.2	17.6	0.72
	5.0%	2439.0	2462.0	2464.0	2455.0	13.9	0.57
PVDC	1.5%	2472.0	2486.5	2432.0	2463.5	28.2	1.15
	3.0%	2492.5	2444.5	2457.0	2464.7	24.9	1.01
	5.0%	2473.0	2424.5	2431.5	2443.0	26.2	1.07
LLDPE	1.5%	2434.5	2417.0	2434.0	2428.5	10.0	0.41
	3.0%	2408.0	2392.0	2440.5	2413.5	24.7	1.02
	5.0%	2375.0	2385.0	2395.0	2385.0	10.0	0.42
HDPE	1.5%	2438.5	2436.5	2452.0	2442.5	8.4	0.35
	3.0%	2430.0	2385.0	2395.0	2403.5	23.6	0.98
	5.0%	2408.5	2395.0	2374.5	2392.5	17.1	0.72

Meanwhile, it can be seen that the densities of the HPC with 1.5% SBR and 1.5% PVDC were higher than those of the HPC with other two polymers at the same content. For 3% polymer content, the concrete density with PVDC was higher than those of the HPC modified with the rest three polymers at the same content. The densities of the HPC with 5% LLDPE and 5% HDPE were lower than those of the HPC with other two polymers at the same content.

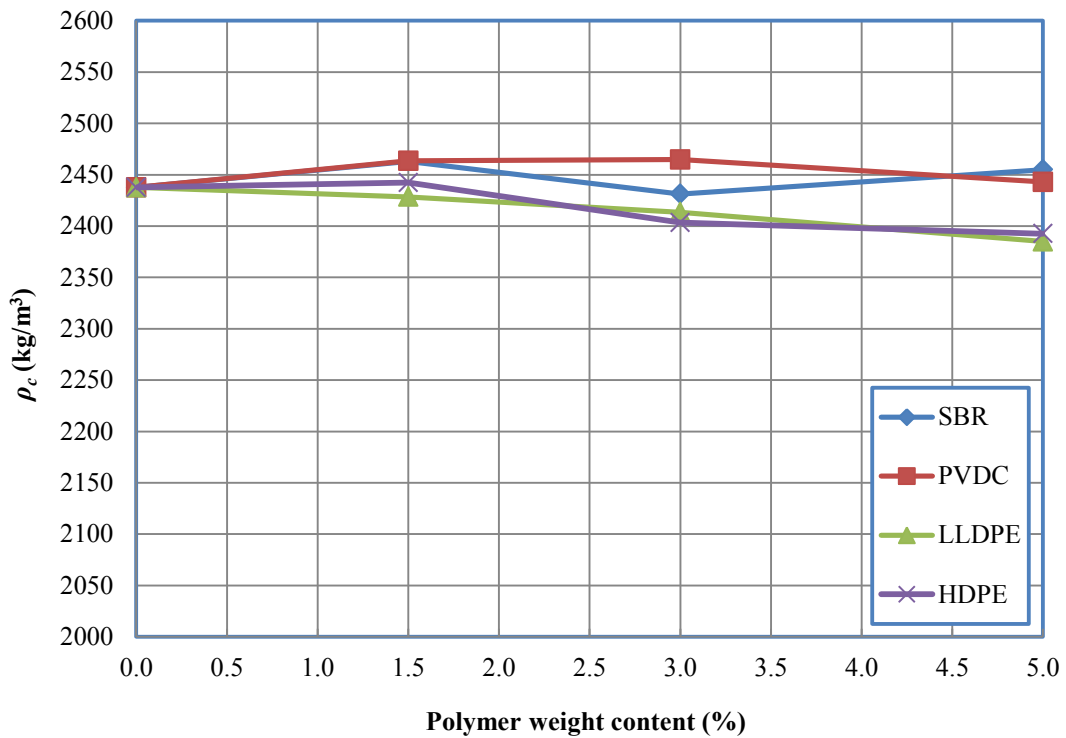


Figure 6-2 Densities of the HPC modified with different types and contents of polymers at 28 days

6.3 Compressive Strength

The results for compressive strength demonstrate the effect that is expected with the addition of different types and amounts of polymers on the high performance concrete. Differences in the compressive strength between concrete mixtures modified with the different types and amounts of polymers are reported. The compressive strength development of mixtures at 7, 28 and 90 days for different dosages of polymers has been illustrated in Tables 6-3, 6-4 and 6-5, respectively. Big bangs were heard at failure in all cases.

Fracture angles were often between 30° and 60° to the central vertical axis as showed in Figures 6-3 to 6-6. The cracking pattern within the cubes yielded a double pyramid shape after failure. The concrete cubes sustained a sudden rupture combined with a dense columnar cracking. The crack patterns in the cube specimens observed after the compressive tests are shown in Figures 6-3 to 6-6. It was found that there was a dense columnar cracking in the bulk of the specimen. The fracture process was provoked by a stress concentration near the cube corners. Inclined micro-cracks appeared and coalesced near the corners and provoked the crack patterns observed.



(a) With 1.5% SBR



(b) With 3% SBR



(c) With 5% SBR

Figure 6-3 Shapes of the crushed SBR modified HPC cubes at failure



(a) With 1.5% PVDC



(b) With 3% PVDC



(c) With 5% PVDC

Figure 6-4 Shapes of the crushed PVDC modified HPC cubes at failure



(a) With 1.5% LLDPE



(b) With 3% LLDPE



(c) With 5% LLDPE

Figure 6-5 Shapes of the crushed LLDPE modified HPC cubes at failure



(a) With 1.5% HDPE



(b) With 3% HDPE



(c) With 5% HDPE

Figure 6-6 Shapes of the crushed HDPE modified HPC cubes at failure

6.3.1 Compression test results at 7 days

At 7 days, the test results of the compressive strength of the polymer-modified high performance concrete are presented in Table 6-3 and also illustrated in Figure 6-7. It can be seen that the compressive strength sustained similar trends with various types and amounts of polymers. In general, the compressive strength of the HPC generally decreased with the increasing polymer dosage, except for the 5% HDPE dosage.

Table 6-3 Compression test results at 7 days

Mixture	Compressive strength f_{cu} (MPa)				Standard deviation (SD)	Coefficient of variation (CoV) %
	Cube 1	Cube 2	Cube 3	Average		
Control mix	104.66	106.39	107.80	106.29	1.57	1.48
1.5% SBR	95.15	90.59	94.71	93.49	2.51	2.69
3% SBR	94.87	95.53	96.76	95.72	0.96	1.00
5% SBR	81.94	88.90	85.75	85.53	3.49	4.07
1.5% PVDC	97.28	102.00	104.45	101.25	3.64	3.60
3% PVDC	101.21	106.45	101.91	103.20	2.84	2.76
5% PVDC	90.53	95.08	93.97	93.20	2.37	2.55
1.5% LLDPE	106.67	101.41	108.04	105.38	3.50	3.32
3% LLDPE	98.14	100.77	101.78	100.23	1.88	1.87
5% LLDPE	85.07	84.12	90.25	86.49	3.30	3.81
1.5% HDPE	100.76	100.86	112.09	104.57	6.51	6.23
3% HDPE	90.69	100.40	93.54	94.88	4.99	5.26
5% HDPE	105.18	104.84	99.66	103.23	3.09	3.00

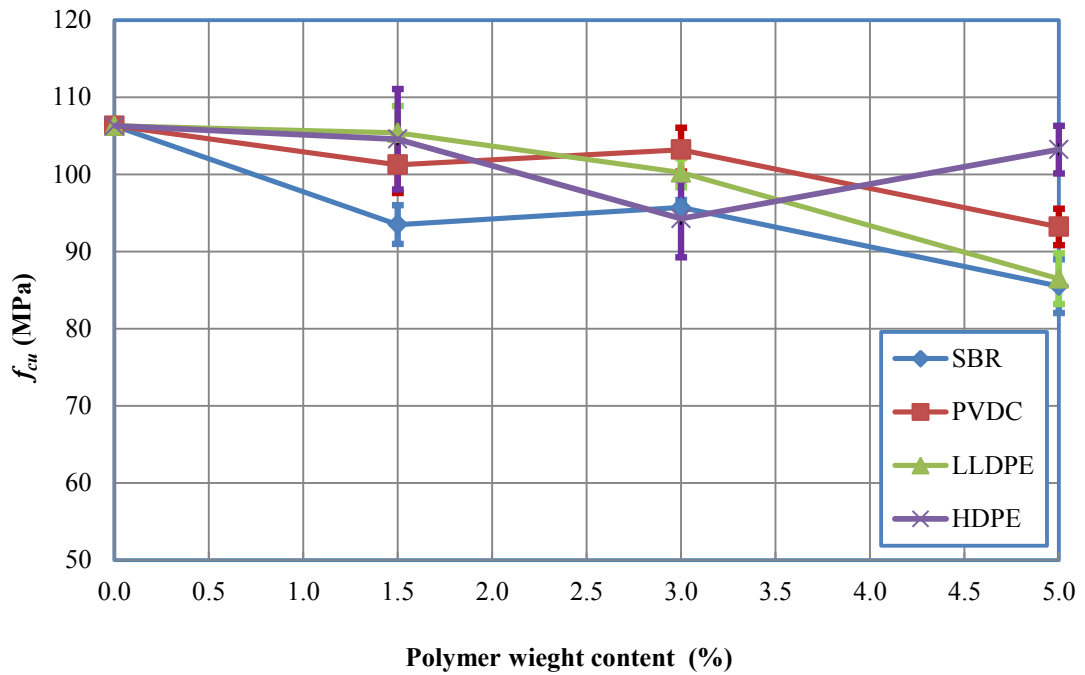


Figure 6-7 Compressive strength of the HPC modified with different types and contents of polymers at 7 days with standard deviations

The compressive strength of the HPC at 7 days decreased with the addition of SBR latex. When the addition of SBR increased from 0.0% to 1.5%, the compressive strength decreased from 106.29 MPa to 93.49 MPa. When the addition of SBR increased to 3%, the compressive strength slightly recovered back to 95.72 MPa. When the addition of SBR continuously increased to 5%, the compressive strength declined again, down to 85.53 MPa.

The decrease tendency of compressive strength with the increasing addition of PVDC powder is similar to that of the SBR latex modified concrete. However, the decrease was slower than that for the SBR latex modified concrete. When the content of PVDC increased from 0.0% to 1.5%, the compressive strength decreased from 106.29 MPa to 101.25 MPa. When the addition of PVDC increased to 3%, the compressive strength slightly recovered back to 103.20 MPa. When the addition of PVDC increased 5%, the compressive strength dropped down to 93.20 MPa.

The compressive strength of the HPC at 7 days fell with the addition of LLDPE powder. When the addition of LLDPE increased from 0.0% to 1.5%, the compressive strength decreased slightly from 106.29 MPa to 105.38 MPa. When the addition of LLDPE increased to 3%, the compressive strength decreased slightly to 100.23 MPa.

When the addition of LLDPE increased to 5%, the compressive strength further declined to 86.49 MPa.

The decrease tendency of the compressive strength with the increasing addition of HDPE powder is different with those of the HPC modified with SBR latex, PVDC and LLDPE. When the HDPE content increased from 0% to 1.5%, the compressive strength slightly decreased from 106.29 MPa to 104.57 MPa. When the addition of HDPE increased to 3%, the compressive strength decreased further to 94.88 MPa. When the addition of PVDC increased to 5%, the compressive strength slightly recovered to 103.23 MPa.

6.3.2 Compression test results at 28 days

The test results of the compressive strength at 28 days of the polymers modified high performance concrete are listed in Table 6-4 and also illustrated in Figure 6-8. The compressive strengths of the high performance concrete samples with 1.5% and 3% SBR latex at the 28-day curing age were higher than those of the control mix. The additions of 1.5% and 3% of SBR resulted in an increase in the concrete strength of 15.6% and 5.8%, respectively. From Figure 6-8, it can be seen that the 5% SBR additive did not largely help to enhance the compressive strength of the high performance concrete. For 5% SBR additive, the results showed a slight decrease in the compressive strength by 1.4%.

The compressive strengths of the high performance concrete samples with different percentages of PVDC powder at the 28-day curing age were all higher than that of the control mix. The addition of 1.5%, 3% and 5% of PVDC to the mix increased the compression strength by 13.6%, 13.1% and 10.9%, respectively.

The additions of 8.4 kg and 16.8 kg LLDPE used as the volume fraction of 1.5% and 3% improved the compressive strength of the high performance concrete by 12.5% and 9.7%, respectively, compared with the control mix. When 5% LLDPE was used, a decrease of 2.3% in the compressive strength was noticed.

The additions of 1.5% and 3% of HDPE resulted in an increase in the concrete compressive strength by approximately 19.7% and 12.7%, respectively, while the addition of 5% HDPE resulted in a slight decrease in the compressive strength by 2.9%.

Table 6-4 Compression test results at 28 days

Mixture	Compressive strength f_{cu} (MPa)				Standard deviation (SD)	coefficient of variation (CoV) %
	Cube 1	Cube 2	Cube 3	Average		
Control mix	110.32	113.72	114.56	112.87	2.25	1.99
1.5% SBR	127.55	127.95	136.26	130.59	4.92	3.76
3% SBR	115.43	123.09	119.66	119.40	3.84	3.21
5% SBR	107.74	111.84	114.41	111.34	3.36	3.02
1.5% PVDC	125.46	132.05	127.21	128.24	3.41	2.55
3% PVDC	130.26	122.75	129.99	127.61	3.38	3.43
5% PVDC	121.98	124.21	129.42	125.21	3.82	3.05
1.5% LLDPE	125.47	127.30	128.27	127.02	1.42	1.12
3% LLDPE	122.23	122.68	126.49	123.80	2.32	1.89
5% LLDPE	111.53	112.78	106.52	110.28	3.31	3.00
1.5% HDPE	131.64	135.83	137.72	135.07	3.11	2.30
3% HDPE	127.19	129.15	125.24	127.20	1.96	1.54
5% HDPE	104.50	110.49	113.93	109.65	4.77	4.33

For the highest addition of polymer contents say 5%, a decrease in the compressive strength of the high performance concrete occurred. For the four types of polymer materials, the ideal content in the mixture was observed as 1.5% in weight, the HDPE having the best performance, with 135.07 MPa, followed by the other three polymer materials, SBR, PVDC and LLDPE, with convergent values of 130.59 MPa, 128.24 MPa and 127.02 MPa, respectively.

The lowest compressive strength was recognised for 5% of polymer contents, in percentage weight, the PVDC having the best performance, with 125.21 MPa, followed by the other three materials, SBR, LLDPE and HDPE, with very similar compressive strengths of 111.34 MPa, 110.28 MPa and 109.65 MPa, respectively.

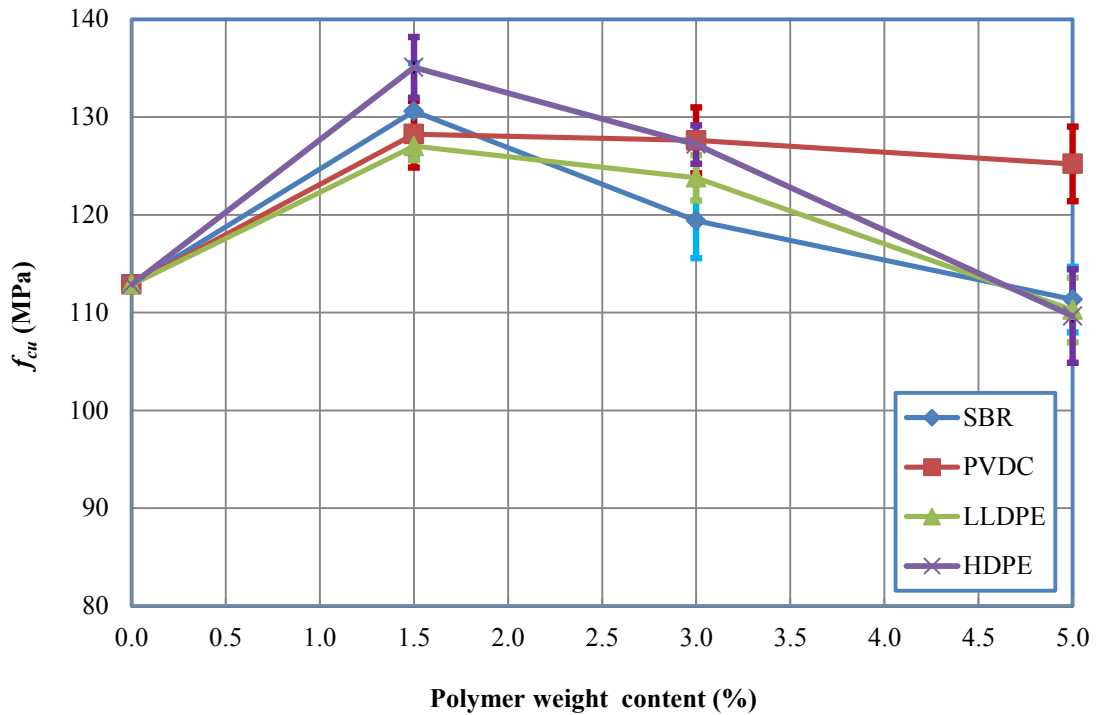


Figure 6-8 Compressive strength of the HPC modified with different types and contents of polymers at 28 days with standard deviations

6.3.3 Compression test results at 90 days

The test results of the compressive strengths at 90 days of the polymers modified high performance concrete are listed in Table 6-5 and also illustrated in Figure 6-9.

The compressive strengths of the high performance concrete samples modified with 1.5% and 3% SBR latex at the 90-day curing age were higher than that of the control mix. The additions of 1.5% and 3% of SBR resulted in an increase in the compressive strength of approximately 6.4% and 5.6%, respectively. From Figure 6-9, it can be seen that the 5% SBR additive did not help enhancing the compressive strength of the high performance concrete, the corresponding compressive strength slightly decreased by 4.0%.

The compressive strengths of the high performance concrete samples with different percentages of PVDC powder at the 90-day curing age were higher than that of the control mix. The additions of 1.5%, 3% and 5% PVDC to the mix increased the compression strength by 16.0%, 4.7% and 2.5% respectively.

Table 6-5 Compression test results at 90 days

Mixture	Compressive strength f_{cu} (MPa)				Standard deviation (SD)	Coefficient of variation (CoV) %
	Cube 1	Cube 2	Cube 3	Average		
Control mix	117.67	130.59	129.19	125.82	7.09	5.64
1.5% SBR	131.82	135.54	134.29	133.89	1.89	1.42
3% SBR	131.07	134.57	133.00	132.88	1.75	1.32
5% SBR	124.25	119.99	117.94	120.73	3.22	2.67
1.5% PVDC	138.53	153.08	146.03	145.89	7.28	4.99
3% PVDC	137.37	130.61	127.09	131.69	5.22	3.97
5% PVDC	126.88	126.16	133.96	129.00	4.31	3.34
1.5% LLDPE	130.71	132.47	138.87	134.02	4.29	3.21
3% LLDPE	131.07	127.31	126.25	128.21	2.53	1.97
5% LLDPE	115.43	113.92	116.03	115.13	1.09	0.95
1.5% HDPE	136.37	141.57	144.50	140.81	4.12	2.92
3% HDPE	140.39	137.52	132.01	136.64	4.26	3.12
5% HDPE	118.84	125.71	117.03	120.53	4.58	3.80

The additions of 1.5% and 3% of LLDPE increased the compression strength by approximately 6.5% and 2%, respectively, while the addition of 5% LLDPE resulted in a decrease of 8.5%.

The additions of 1.5% and 3% of HDPE resulted in an increase of 11.9% and 8.6% in the compressive strength, respectively, while the 5% HDPE addition resulted in a slight decrease of 4.2% in the compressive strength.

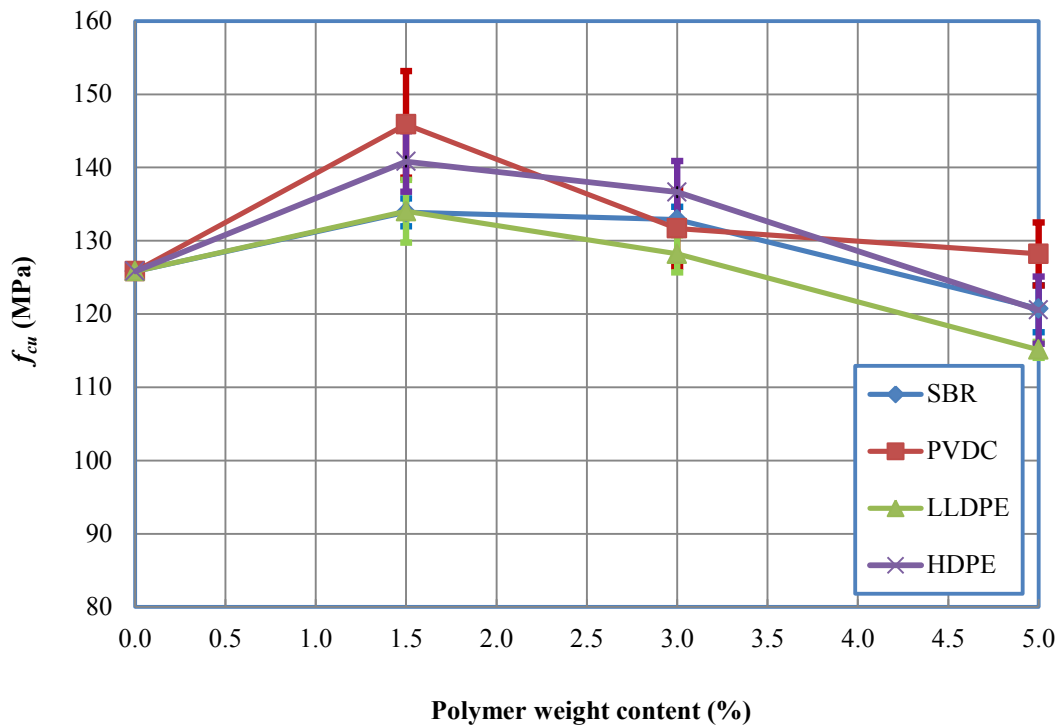


Figure 6-9 Compressive strength of the HPC modified with different types and contents of polymers at 90 days with standrad deviations

From Figures 6-7, 6-8 and 6-9, in general, the experimental results evidently indicate that the characteristic compressive strength of the polymer modified high performance concrete increased with the increase of polymer dosage to 1.5%, and after this optimum percentage dosage, the compressive strength started to decrease. It was shown that high polymer contents did not help to enhance the compressive strength of the high performance concrete. This is due to the weakened bonding between the cement paste and aggregates. This phenomenon is similar to the the findings in previous research done by Ismail et al (2011) who used polymer additives in concrete. Abdurrahman et al (2008) showed that this is likely due to polymerisation of the latex monomers that form a latex film filling pores in the internal structure of concrete.

6.4 Splitting Tensile Strength

The splitting tensile strengths were measured at 28 days and the results are presented in Table 6-6 and Figure 6-10, from which it can be seen that tensile the strength increased with the additions of SBR latex, PVDC, LLDPE and HDPE powders.

Table 6-6 Indirect tension test results at 28 days

Mixture	Splitting tensile strength f_t' (MPa)				Standard deviation (SD)	Coefficient of variation (CoV) %
	Cube 1	Cube 2	Cube 3	Average		
Control mix	5.50	6.18	6.12	5.93	0.34	6.40
1.5% SBR	7.22	7.40	7.25	7.29	0.10	1.34
3.0% SBR	9.85	9.83	11.01	10.23	0.68	6.60
5.0% SBR	6.80	7.24	7.91	7.32	0.56	7.61
1.5% PVDC	8.01	8.34	7.76	8.04	0.29	3.6
3% PVDC	8.59	8.89	7.68	8.39	0.63	7.50
5% PVDC	8.57	7.93	8.44	8.31	0.34	4.02
1.5% LLDPE	10.49	11.76	10.40	10.88	0.76	6.98
3% LLDPE	8.47	9.70	9.82	9.33	0.75	7.99
5% LLDPE	8.85	9.24	8.63	8.91	0.31	3.46
1.5% HDPE	8.36	7.79	8.28	8.14	0.31	3.79
3% HDPE	7.93	8.32	7.65	7.97	0.34	4.22
5% HDPE	8.30	9.08	8.53	8.64	0.40	4.64

The splitting tensile strengths of the high performance concrete modified with different percentages of SBR latex at the 28-day curing age was higher than that of the control mix. The additions of 1.5%, 3% and 5% of SBR to the mix could increase the splitting tensile strengths by 22.9%, 72.5% and 23.4%, respectively. The ideal content of SBR latex in the mix was found to be 3% in weight, which produced the best performance, with an average tensile strength of 10.23 MPa.

The additions of 1.5%, 3% and 5% of PVDC resulted in increases in the splitting tensile strength of the high performance concrete by 35.6%, 41.5% and 40.1%, respectively. The most optimum content of PVDC powder in the mix was found to be 3% in weight, which produced the best performance, with 8.39 MPa.

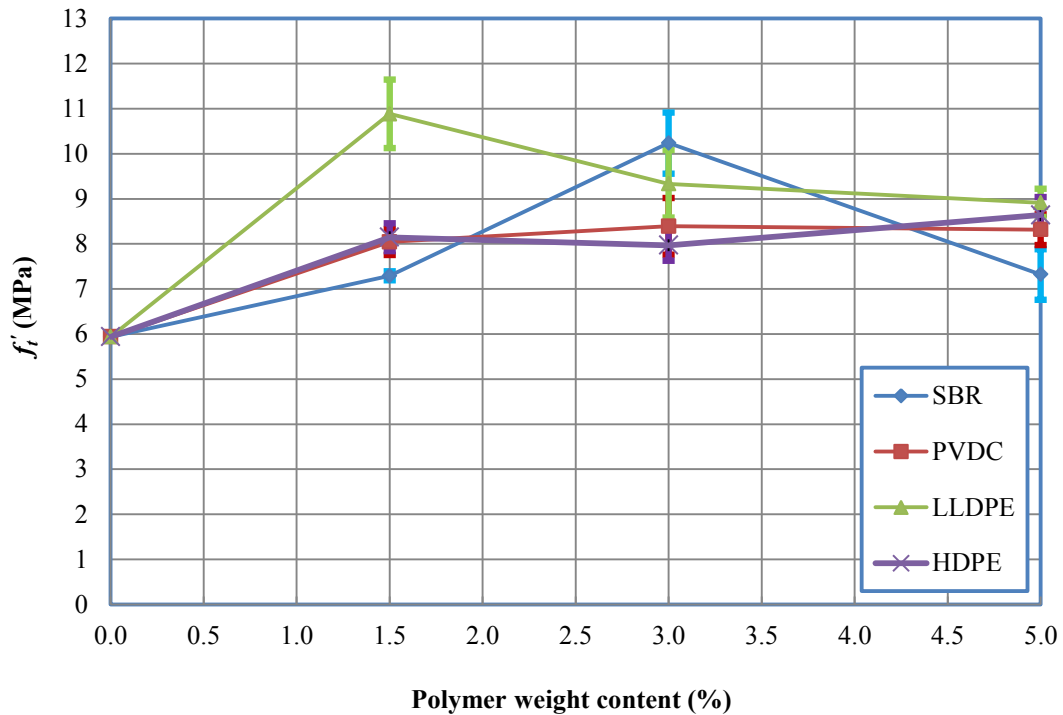


Figure 6-10 Splitting tensile strengths of the HPC modified with different types and contents of polymers at 28 days with standrad deviations

With the additions of 1.5%, 3% and 5% LLDPE to the concrete mix, the tensile strength increased by up to 83.5%, 57.3% and 50.3%, respectively, which is excelent.

The trend of the splitting tensile strength with the additon of HDPE is similar to that of the splitting tensile strength with the additon of PVDC. When the polymer additive increased from 0% to 1.5%, the splitting tensile strength increased by 37.3%, with 3% of HDPE increased by 34.4%, and with 5% of HDPE the splitting tensile strength increased by 45.7%.

In general, the tensile strengths were substantially improved when adding the four selected types of polymers with different amounts. Ismail et al (2008) showed that the enhancement may be due to the function of the polymer additive in the concrete which possesses high tensile strength (Ismail et al, 2011).

Figures 6-11 to 6-14 illustrate the fractured surfaces of the tested samples, indicating that the failure was through the aggregate particles. At the end of splitting tensile tests, the principal cracks for all types and amounts of polymers started at the centre of the specimen where the tensile stresses were high, as shown in Figure 6-15.



(a) With 1.5% SBR



(b) With 3% SBR



(c) With 5% SBR

Figure 6-11 Fracture surfaces of the HPC samples modified with SBR in splitting



(a) With 1.5% PVDC



(b) With 3% PVDC

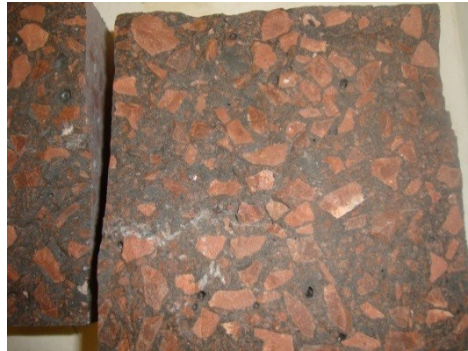


(c) With 5% PVDC

Figure 6-12 Fracture surfaces of the HPC samples modified with PVDC in splitting



(a) With 1.5% LLDPE



(b) With 3% LLDPE



(c) With 5% LLDPE

Figure 6-13 Fracture surfaces of the HPC samples modified with LLDPE in splitting



(a) With 1.5% HDPE



(b) With 3% HDPE



(c) With 5% HDPE

Figure 6-14 Fracture surfaces of the HPC samples modified with HDPE in splitting



Figure 6-15 Failure patterns of the HPC specimens under splitting tension

6.5 Modulus of Rupture

The results of the modulus of rupture are presented in Table 6-7 and shown in Figure 6-16. It can be seen that the polymer additive did not help enhancing the modulus of rupture of the high performance concrete.

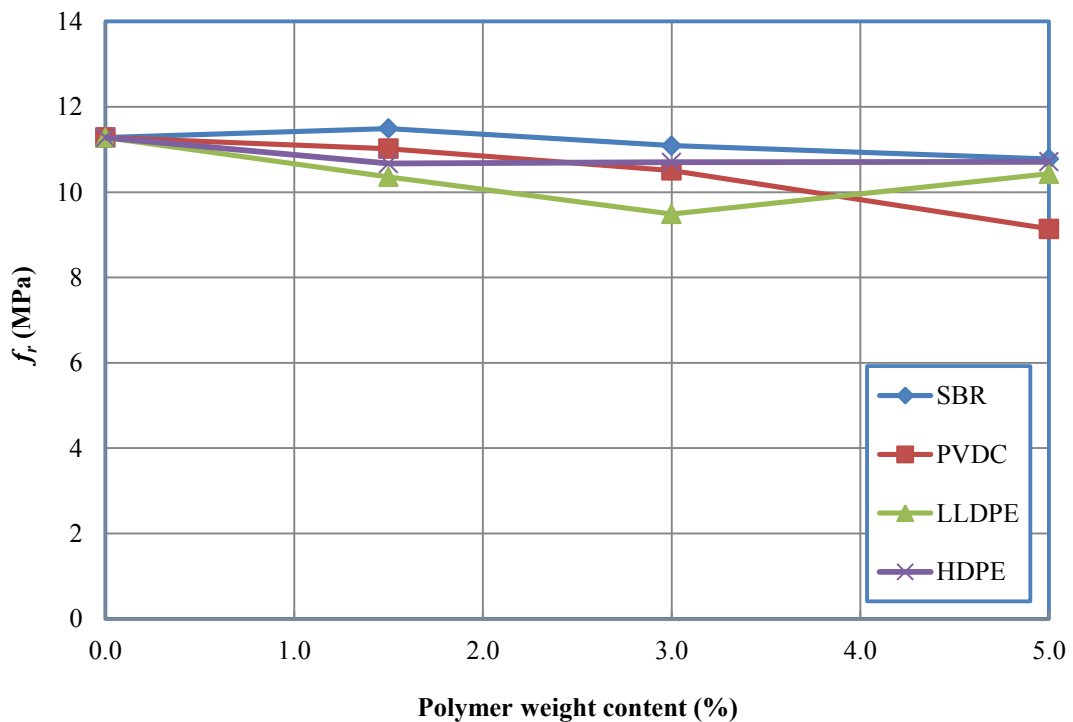


Figure 6-16 Modulus of rupture of the HPC modified with different types and contents of polymers at 28 days

It can be seen from Figure 6-16 that the modulus of rupture increased slightly with the addition of 1.5% SBR by 1.9%, while with the additions of 3% and 5% SBR it

only decreased by 1.7% and 4.4%, respectively. 1.5% SBR additive achieved the best performance, with 11.49 MPa, followed by 3% SBR.

Table 6-7 Modulus of rupture test results at 28 days

Mixture	Modulus of rupture f_r (MPa)					Standard deviation (SD)	Coefficient of variation (CoV) %
	Beam 1	Beam 2	Beam 3	Beam 4	Average		
Control mix	11.59	11.52	10.75	11.26	11.28	0.38	3.37
1.5% SBR	11.23	11.87	11.09	11.77	11.49	0.39	3.37
3% SBR	10.584	12.024	10.8	10.96	11.09	0.65	5.77
5% SBR	10.680	10.44	10.85	11.16	10.78	0.30	2.81
1.5% PVDC	10.61	10.61	11.71	11.16	11.02	0.53	4.79
3% PVDC	10.34	10.32	10.44	10.92	10.51	0.28	2.67
5% PVDC	8.64	8.66	9.58	9.70	9.14	0.57	6.24
1.5%LLDPE	10.44	10.37	10.91	9.72	10.36	0.49	4.71
3% LLDPE	9.31	9.79	9.67	9.17	9.49	0.29	3.12
5% LLDPE	10.32	10.09	10.19	11.10	10.43	0.46	4.41
1.5% HDPE	11.28	10.51	10.82	10.08	10.67	0.51	4.74
3% HDPE	10.41	10.20	11.21	10.99	10.70	0.48	4.44
5% HDPE	10.59	10.55	10.86	10.49	10.71	0.23	2.12

With the additions of 1.5%, 3% and 5% PVDC to the mix, the modulus of rupture decreased by 2.3%, 6.8% and 19.0%, respectively. The lowest modulus of rupture was captured for the addition of 5% PVDC and the highest modulus of rupture was corresponding to the addition of 1.5% PVDC.

With the additions of 1.5%, 3% and 5% LLDPE to the mix, the modulus of rupture decreased by 8.2%, 15.9% and 7.5%, respectively. The 1.5% LLDPE and 5% LLDPE additives led to the best performance. The trends for the modulus of rupture

with the addition of 1.5%, 3% and 5% HDPE were quite similar, with a decrease of approximately 5% in the modulus of rupture.

Finally, comparing the test results in Table 6-7 with those in Table 6-6 indicates that the modulus of rupture were generally larger than the tensile strength for all concrete mixes, as expected, except for the concrete modified with 1.5% LLDPE.

6.6 Fracture Toughness

In general, all the HPC mixes modified with SBR, PVDC, LLDPE and HDPE had slightly lower values of the fracture toughness compared to the control high performance concrete mix with the same treatment. Tables 6-8 to 6-11 illustrate the test results of the fracture toughness for all thirteen batches used to produce HPC samples for the testing procedures in this research. The results of the fracture toughness are listed according to the mix type, including the standard deviation for each test set as well as the corresponding coefficient of variation. The load versus deflection curve for each test is illustrated in Appendix B. Figure 6-17 shows the variations of the fracture toughness K_{IC} with different contents of SBR, PVDC, LLDPE and HDPE. Figure 6-18 shows the variations of the fracture toughness K_{IC} with the standard deviations.

Table 6-8 Fracture toughness results of the SBR modified high performance concrete

	Specimen	Control	SBR		
		0.0%	1.5%	3.0%	5.0%
K_{IC} (MN/m ^{1/2})	Beam 1	3.52	3.54	2.95	3.42
	Beam 2	3.44	3.44	3.23	2.95
	Beam 3	3.48	3.20	3.16	3.17
	Beam 4	3.44	3.65	3.18	3.29
	Average	3.47	3.46	3.13	3.21
	SD	0.04	0.19	0.12	0.20
	CoV (%)	1.09	5.54	3.97	6.21

Table 6-9 Fracture toughness results of the PVDC modified high performance concrete

	Specimen	Control 0.0%	PVDC		
			1.5%	3.0%	5.0%
K_{IC} (MN/m ^{1/2})	Beam 1	3.52	3.20	2.82	2.55
	Beam 2	3.44	3.15	2.90	2.75
	Beam 3	3.48	3.41	3.03	2.83
	Beam 4	3.44	3.03	3.15	2.42
	Average	3.47	3.20	2.98	2.64
	SD	0.04	0.16	0.14	0.19
	CoV (%)	1.09	4.92	4.81	7.05

Table 6-10 Fracture toughness results of the LLDPE modified high performance concrete

	Specimen	Control 0.0%	LLDPE		
			1.5%	3.0%	5.0%
K_{IC} (MN/m ^{1/2})	Beam 1	3.52	3.62	3.65	3.17
	Beam 2	3.44	3.50	3.09	3.04
	Beam 3	3.48	3.66	3.06	3.23
	Beam 4	3.44	3.52	2.98	3.27
	Average	3.47	3.57	3.20	3.18
	SD	0.04	0.08	0.31	0.10
	CoV (%)	1.09	2.10	9.58	3.20

Table 6-11 Fracture toughness results of the HDPE modified high performance concrete

Specimen	Control	HDPE			
	0.0%	1.5%	3.0%	5.0%	
Beam 1	3.52	3.01	3.08	3.10	
Beam 2	3.44	2.87	3.24	3.09	
Beam 3	3.48	2.86	3.23	3.09	
Beam 4	3.44	2.81	3.20	2.95	
K_{IC} (MN/m ^{1/2})	Average	3.47	2.89	3.19	3.06
	SD	0.04	0.08	0.07	0.07
	CoV (%)	1.09	2.93	2.31	2.40

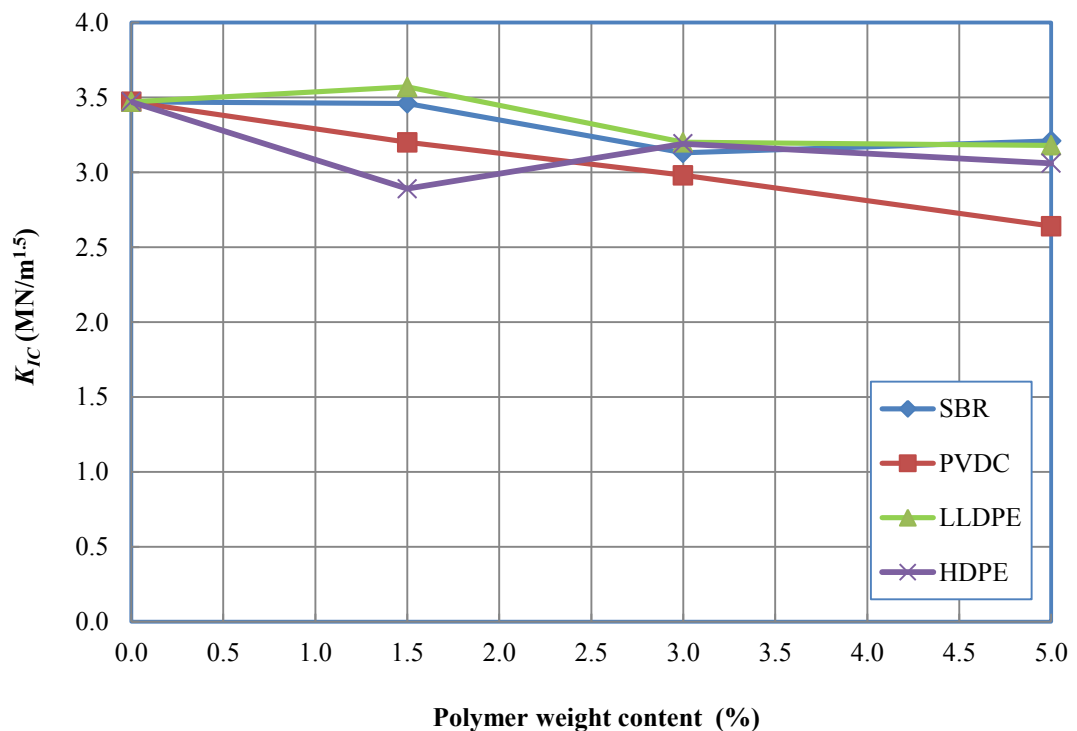


Figure 6-17 Fracture toughness of the HPC modified with different types and contents of polymers

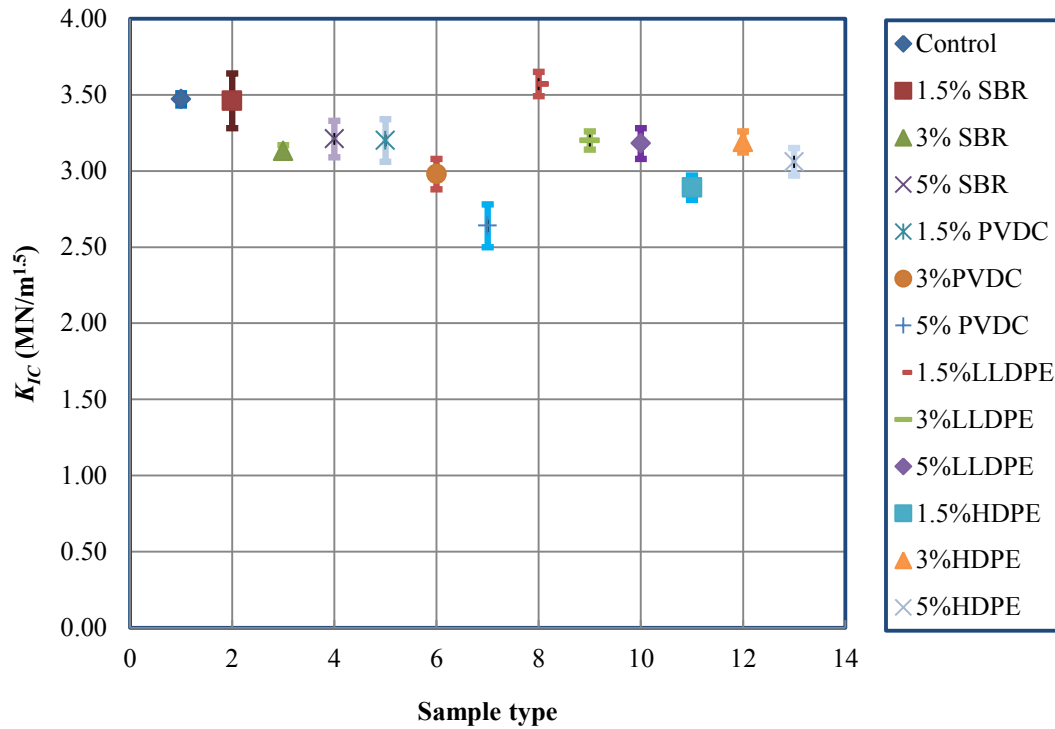


Figure 6-18 Fracture toughness with the standard deviations

The results show that the use of SBR latex as additive to the HPC slightly lowered the fracture toughness K_{IC} . All the mixtures containing SBR had lower values compared to the control mix with the same treatment. The test results show that the use of 1.5%, 3% and 5% SBR additives in the high performance concrete mix decreased the critical stress intensity factor or fracture toughness K_{IC} by 0.3%, 9.8% and 7.5%, respectively. This indicates that the addition of 3% SBR to the high performance concrete produced the lowest fracture toughness.

It can also be seen that the fracture toughness K_{IC} decreased by 7.8%, 14.1% and 23.9% with adding 1.5%, 3% and 5% PVDC powder into the high performance concrete mix by weight.

The test results show that the use of 1.5% LLDPE additive in the high performance concrete mix slightly increased the fracture toughness K_{IC} by 2.9%, while the additions of 3% and 5% LLDPE decreased K_{IC} by 7.8% and 8.4%, respectively.

With the additions of 1.5%, 3% and 5% HDPE to the HPC mix, K_{IC} decreased by 16.7%, 8.1% and 11.8%, respectively. The results also show that the addition of 1.5% HDPE to the high performance concrete mix produced the lowest fracture toughness.

6.7 Fracture Energy

Tables 6-12 to 6-15 illustrate the test results of the fracture energy for the thirteen mixes of polymer modified high performance concrete for the testing procedures used in this research. The fracture energy results are listed according to the mixture type, including the standard deviation for each test set as well as the coefficient of variation.

The EXCEL spreadsheets were developed to calculate the fracture energy values. The load versus deflection curves for all tests are presented in Appendix B. Figure 6-19 illustrates the variations of the fracture energy G_F for the high performance concrete with different contents of SBR latex, PVDC powder, LLDPE powder and HDPE powder. Figure 6-20 shows the variations of the fracture energy G_F with the standard deviations.

Table 6-12 Fracture energy results of the SBR modified high performance concrete

	Specimen	Control	SBR		
		0.0%	1.5%	3.0%	5.0%
G_F (N/m)	Beam 1	274.45	276.77	217.86*	290.93
	Beam2	261.07	286.00	254.11	224.34*
	Beam 3	262.06	262.35	250.29	277.88
	Beam 4	265.40	342.47*	258.20	284.10
	Average	265.75	275.04	254.20	284.30
	SD	6.09	11.92	3.96	6.53
	CoV (%)	2.29	4.33	1.56	2.30

* Values not included for computing the average G_F .

Table 6-13 Fracture energy results of the PVDC modified high performance concrete

	Specimen	Control	PVDC		
		0.0%	1.5%	3.0%	5.0%
G_F (N/m)	Beam 1	274.45	262.51	213.46	192.36
	Beam 2	261.07	261.68	220.55	201.68
	Beam 3	262.06	279.20	240.28	216.07
	Beam 4	265.40	239.25*	259.85	166.05*
	Average	265.75	267.80	223.54	203.37
	SD	6.09	9.88	20.89	11.95
	CoV (%)	2.29	3.69	8.95	5.87

* Values not included for computing the average G_F .

Table 6-14 Fracture energy results of the LLDPE modified high performance concrete

	Specimen	Control	LLDPE		
		0.0%	1.5%	3.0%	5.0%
G_F (N/m)	Beam 1	274.45	322.49	342.94*	273.55
	Beam 2	261.07	328.07	257.49	268.63
	Beam 3	262.06	347.36	253.01	285.94
	Beam 4	265.40	323.71	250.33	319.12
	Average	265.75	330.41	253.61	286.81
	SD	6.09	11.55	3.62	22.74
	CoV (%)	2.29	3.50	1.43	7.93

* Values not included for computing the average G_F .

Table 6-15 Fracture energy results of the HDPE modified high performance concrete

	Specimen	Control	HDPE		
		0.0%	1.5%	3.0%	5.0%
G_F (N/m)	Beam 1	274.45	210.15	247.47	249.05
	Beam 2	261.07	204.26	264.14	199.89*
	Beam 3	262.06	207.70	267.01	249.63
	Beam 4	265.40	202.12	260.89	241.83
	Average	265.75	206.06	259.88	246.84
	SD	6.09	3.57	8.64	4.35
	CoV (%)	2.29	1.73	3.33	1.76

* Values not considered for computing the average G_F .

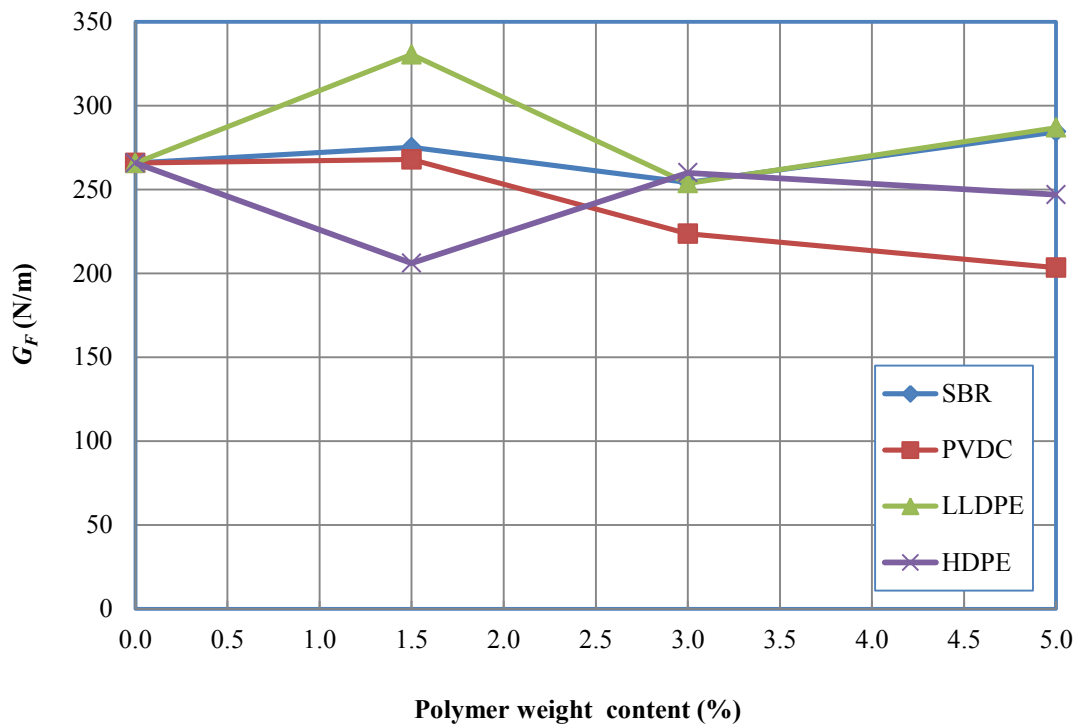


Figure 6-19 Fracture energy of the HPC modified with different types and contents of polymer

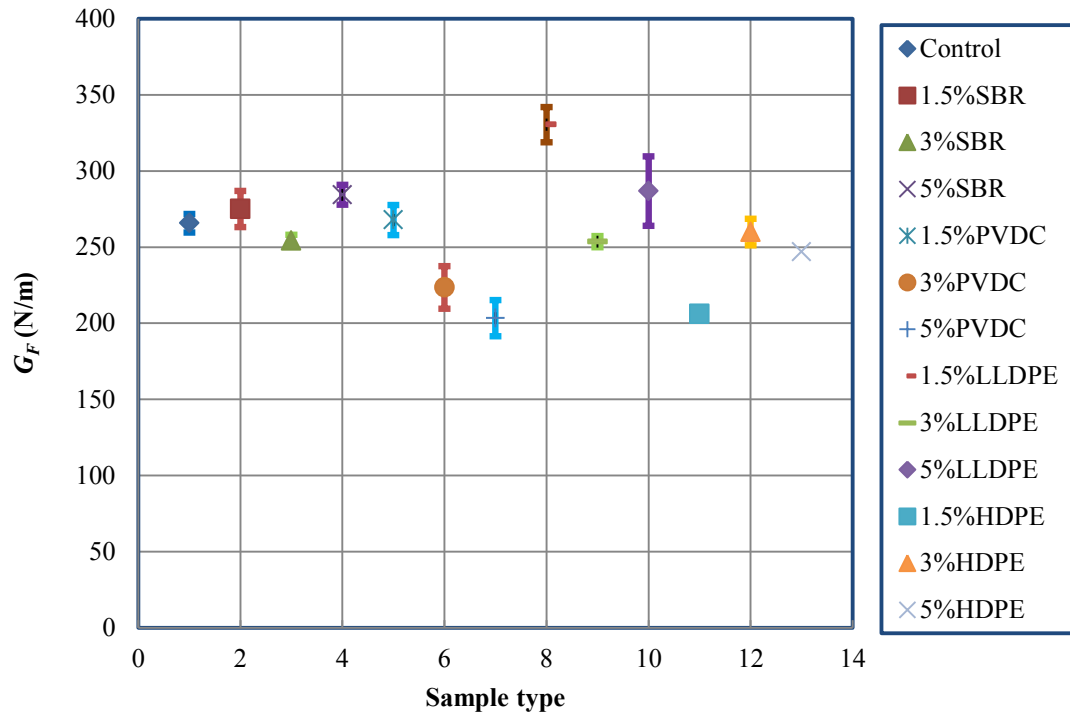


Figure 5-20 Fracture energy with the standard deviations

As seen in Figure 6-19, when the addition of SBR increased from 0.0% to 1.5%, the fracture energy slightly increased from 265.75 N/m to 275.04 N/m. When the addition of SBR increased 3%, the fracture energy decreased to 254.20 N/m, while the addition of SBR increased to 5%, the fracture energy rose again to 284.30 N/m. The test results show that the addition of 5% SBR latex produced the best performance for the fracture energy while the addition of 3% SBR latex led to the worst performance for the fracture energy.

The tendency of fracture energy varied with the increasing addition of PVDC. When the PVDC content increased from 0.0% to 1.5%, the fracture energy slightly increased from 265.75 N/m to 267.80 N/m. When the addition of PVDC increased to 3%, the fracture energy decreased to 224.76 N/m, while the addition of PVDC increased to 5%, the fracture energy further decreased to 203.37 N/m. The addition of 1.5% PVDC powder produced the best performance for the fracture energy while adding 5% PVDC powder led to the worst performance for the fracture energy.

The fracture energy slightly fell for the addition of 3% LLDPE powder, while for the additions of 1.5% and 5% LLDPE powder opposite trends occurred. When the addition of LLDPE increased from 0.0% to 1.5%, the fracture energy increased from

265.75 N/m to 330.41 N/m, while the addition of LLDPE powder increased to 3%, G_F decreased back to 253.61 N/m. When the addition of LLDPE powder increased to 5%, the fracture energy increased again to 286.81 N/m. The addition of 1.5% LLDPE powder produced the best performance for the fracture energy while adding 3% LLDPE powder led to the worst performance for the fracture energy.

The fracture energy of the HPC modified with HDPE slightly decreased by 22.5%, 2.2% and 7.1% when adding 1.5%, 3% and 5% HDPE powder. This variation tendency is different with those of the HPC modified with SBR latex, PVDC powder and LLDPE powder. When the HDPE powder content increased from 0% to 1.5%, the fracture energy decreased from 265.75 N/m to 206.06 N/m. When the HDPE powder content increased to 3%, the fracture energy recovered back to 259.88 N/m. When the addition of HDPE powder increased to 5%, the fracture energy further decreased to 246.84 N/m.

Compared with previous results indicated in Section 2.3.10, the results obtained in the present study did not follow this trend. For all four polymer modified high performance concretes, various trends between the fracture energy and compressive strength can be observed. Nevertheless, the test results confirm a slight decrease tendency in G_F with the increasing compressive strength.

6.8 Static Elastic Modulus

Tables 6-16 to 6-19 present the test results of the static elastic modulus for the thirteen mixes of polymer modified concrete used for the testing procedures in this program. The elastic modulus results are listed according to the mixture type, including the standard deviation for each test set as well as the corresponding coefficient of variation.

The load versus deflection for each test is included in Appendix B. Elastic modulus is an important parameter to indicate the stiffness of materials and structures. Even though concrete has nonlinear stress-strain behaviour, the modulus of elasticity is still very useful for designing and analysing concrete structures. Figure 6-21 shows the variations of the static elastic modulus E with the standard deviations. Figure 6-22 shows the relationships between E and f_{cu} for all the polymer modified concretes, but they are very inconclusive.

Table 6-16 Elastic modulus results of the SBR modified high performance concrete

	Specimen	Control 0.0%	SBR		
			1.5%	3.0%	5.0%
<i>E</i> (GPa)	Beam 1	45.12	45.35	40.07	40.20
	Beam 2	45.45	41.40	41.17	38.68
	Beam 3	46.16	39.07	39.84	36.21
	Beam 4	44.47	38.99	39.10	38.06
	Average	45.30	41.20	40.04	38.29
	SD	0.70	2.98	0.86	1.65
	CoV (%)	1.56	7.24	2.14	4.32

Table 6-17 Elastic modulus results of the PVDC modified high performance concrete

	Specimen	Control 0.0%	PVDC		
			1.5%	3.0%	5.0%
<i>E</i> (GPa)	Beam 1	45.12	39.20	37.33	33.70
	Beam 2	45.45	37.95	38.24	37.46
	Beam 3	46.16	41.57	38.14	36.97
	Beam 4	44.47	38.57	38.24	35.38
	Average	45.30	39.32	37.99	35.88
	SD	0.70	1.59	0.44	1.70
	CoV (%)	1.56	4.03	1.16	4.75

Table 6-18 Elastic modulus results of the LLDPE modified high performance concrete

	Specimen	Control	LLDPE		
		0.0%	1.5%	3.0%	5.0%
<i>E</i> (GPa)	Beam 1	45.12	40.59	38.89	36.79
	Beam 2	45.45	37.39	37.15	34.34
	Beam 3	46.16	38.47	37.12	36.58
	Beam 4	44.47	38.22	35.44	33.45
	Average	45.30	38.67	37.15	35.29
	SD	0.70	1.36	1.41	1.65
	CoV (%)	1.56	3.52	3.79	4.69

Table 6-19 Elastic modulus results of the HDPE modified high performance concrete

	Specimen	Control	HDPE		
		0.0%	1.5%	3.0%	5.0%
<i>E</i> (GPa)	Beam 1	45.12	44.13	38.40	38.61
	Beam 2	45.45	40.45	39.76	37.32
	Beam 3	46.16	39.52	39.18	38.16
	Beam 4	44.47	39.12	39.33	35.90
	Average	45.30	40.56	39.17	37.50
	SD	0.70	1.80	0.57	1.19
	CoV (%)	1.56	4.45	1.45	3.18

As indicated in Figure 6-21, as the polymer content in the high performance concrete increased, the elastic modulus decreased. This is explained by Ohama by indicating that the polymer films formed in the concrete may effectively halt propagating micro cracks through their high tensile strength (Ohama, 1995).

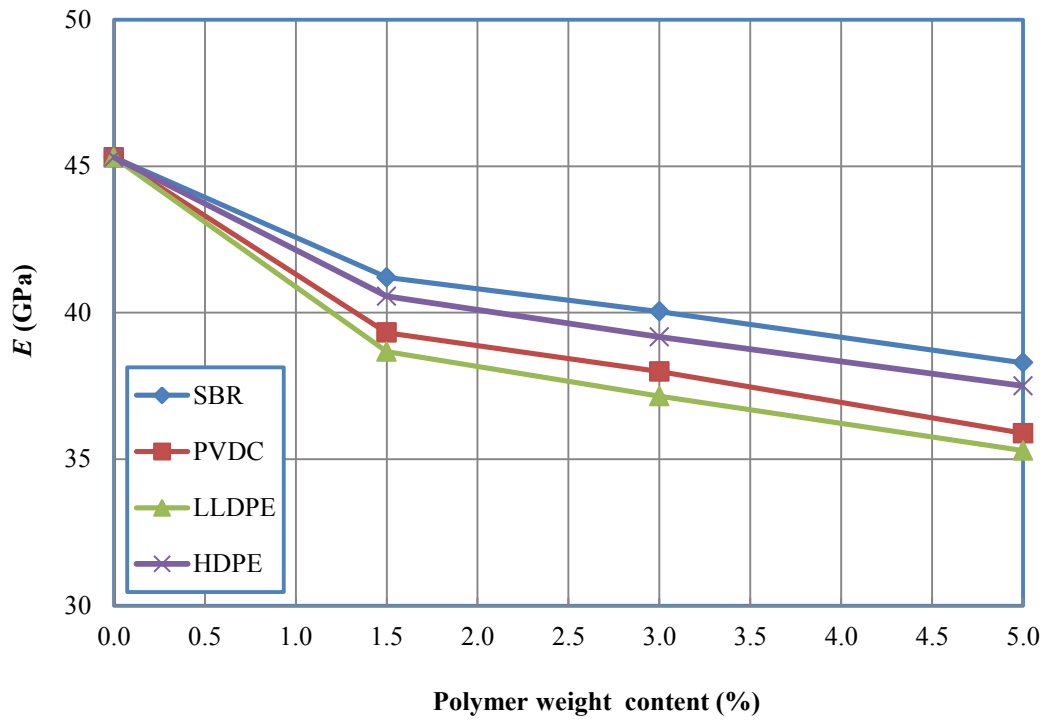


Figure 6-21 Static elastic modulus of the HPC modified with different types and contents of polymers

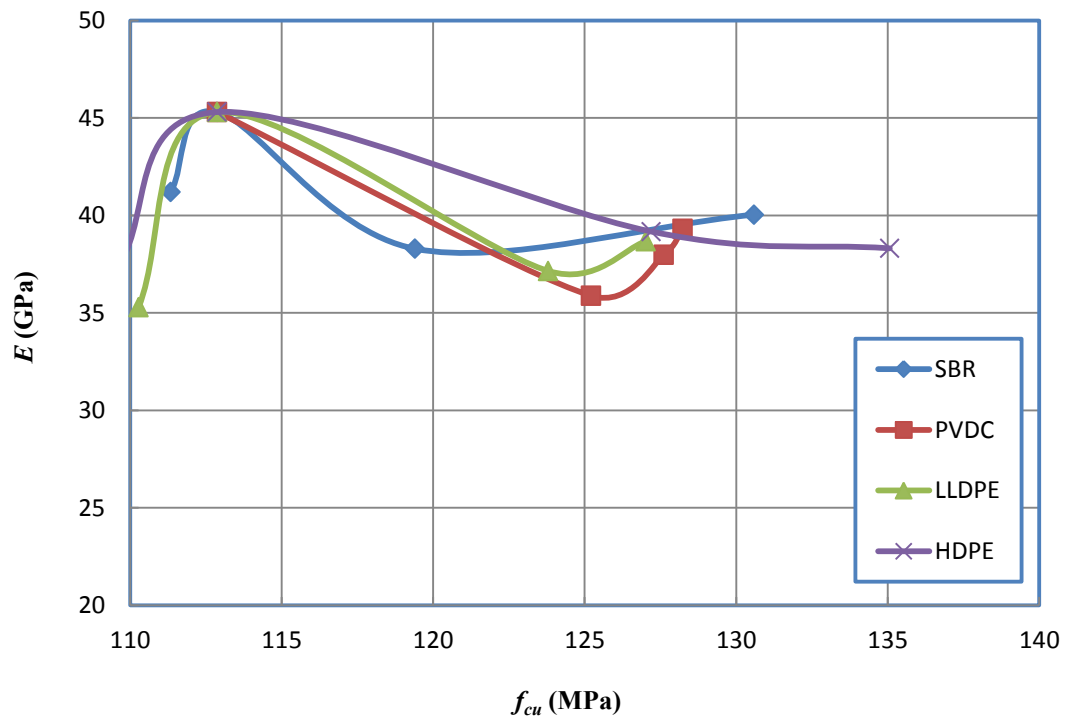


Figure 6-22 Static elastic modulus E versus compressive strength f_{cu}

Figure 6-21 also indicates that the static elastic modulus had monotonic decrease trends with the increasing polymer contents for all four types of polymer modified high performance concrete.

All the concrete mixes containing SBR had lower values compared to the control mix. The results show that the use of 1.5%, 3% and 5% SBR additives in the high performance concrete mixes decreased the static elastic modulus E by 9.1%, 11.6% and 15.5%, respectively. The static elastic modulus E reduced by 13.2%, 16.1% and 20.8%, respectively, with adding 1.5%, 3% and 5% PVDC powder by weight. For the additions of 1.5%, 3% and 5% LLDPE additives in the high performance concrete mix, the static elastic modulus E decreased by 14.6%, 18.0% and 22.1%, respectively. Finally, with the additions of 1.5%, 3% and 5% HDPE to the HPC mix, the static elastic modulus E decreased by 10.5%, 13.5% and 17.2%, respectively. In general, for the same polymer content, the high performance concrete modified with SBR sustained the smallest decrease in E , while the HPC modified with LLDPE sustained the largest drop in E .

6.9 Brittleness

The brittleness of concrete was investigated by conducting three-point bending tests on notched concrete beams. Based on Eqs.(5.13) and (5.14) for the parameters including elastic displacement, Δ_e , and the failure displacement, Δ_f , the brittleness index B can be determined using Eq.(5.13). Tables 6-20 to 6-31 illustrate the elastic displacement, failure displacement and brittleness for the thirteen concrete mixes used for the testing procedures used in this research program. The brittleness results are listed according to the mixture type. For ideal elastic-plastic materials, $B_f = 0$; and for ideal elastic-brittle materials, $B_f = 1$. In general, B_f varies between 0 and 1.

Figures 6-23 and 6-24 illustrate the elastic displacement Δ_e and the failure displacement Δ_f of the high performance concrete with different types and contents of polymers. Figure 6-25 illustrates the brittleness of the high performance concrete with different contents of polymers.

Table 6-20 Elastic displacements of the SBR modified high performance concrete

	Specimen	Control	SBR		
		0%	1.5%	3.0%	5.0%
Δ_e (mm)	Beam 1	0.048	0.046	0.050	0.050
	Beam 2	0.048	0.054	0.050	0.051
	Beam 3	0.044	0.048	0.051	0.056
	Beam 4	0.048	0.047	0.053	0.055
	Average	0.047	0.049	0.051	0.053
	SD	0.002	0.003	0.001	0.003
	CoV (%)	4.39	6.83	2.64	5.96

Table 6-21 Elastic displacements of the PVDC modified high performance concrete

	Specimen	Control	PVDC		
		0%	1.5%	3.0%	5.0%
Δ_e (mm)	Beam 1	0.048	0.051	0.052	0.058
	Beam 2	0.048	0.052	0.051	0.058
	Beam 3	0.044	0.050	0.051	0.049
	Beam 4	0.048	0.046	0.054	0.051
	Average	0.047	0.050	0.052	0.054
	SD	0.002	0.003	0.001	0.005
	CoV (%)	4.39	5.49	2.43	8.81

Table 6-22 Elastic displacements of the LLDPE modified high performance concrete

	Specimen	Control 0%	LLDPE		
			1.5%	3.0%	5.0%
Δ_e (mm)	Beam 1	0.048	0.048	0.052	0.053
	Beam 2	0.048	0.052	0.049	0.055
	Beam 3	0.044	0.053	0.049	0.052
	Beam 4	0.048	0.048	0.060	0.062
	Average	0.047	0.050	0.053	0.056
	SD	0.002	0.003	0.005	0.005
	CoV (%)	4.39	5.40	9.80	8.35

Table 6-23 Elastic displacements of the HDPE modified high performance concrete

	Specimen	Control 0%	HDPE		
			1.5%	3.0%	5.0%
Δ_e (mm)	Beam 1	0.048	0.049	0.051	0.053
	Beam 2	0.048	0.049	0.049	0.053
	Beam 3	0.044	0.051	0.054	0.053
	Beam 4	0.048	0.048	0.052	0.055
	Average	0.047	0.049	0.052	0.054
	SD	0.002	0.001	0.002	0.001
	CoV (%)	4.39	2.78	3.78	1.51

Table 6-24 Failure displacements of the SBR modified high performance concrete

	Specimen	Control	SBR		
		0%	1.5%	3.0%	5.0%
Δ_f (mm)	Beam 1	1.839	1.492	1.151	1.795
	Beam 2	1.424	1.496	2.083	1.067
	Beam 3	1.456	1.672	1.315	1.720
	Beam 4	1.623	1.607	1.934	1.811
	Average	1.586	1.567	1.621	1.598
	SD	0.190	0.088	0.457	0.356
	CoV (%)	12.00	5.62	28.18	22.30

Table 6-25 Failure displacements of the PVDC modified high performance concrete

	Specimen	Control	PVDC		
		0%	1.5%	3.0%	5.0%
Δ_f (mm)	Beam 1	1.839	1.572	1.628	1.790
	Beam 2	1.424	1.662	1.302	1.5960
	Beam 3	1.456	1.569	1.401	1.213
	Beam 4	1.623	1.529	1.957	1.660
	Average	1.586	1.583	1.572	1.565
	SD	0.190	0.056	0.291	0.248
	CoV (%)	12.00	3.55	18.49	15.85

Table 6-26 Failure displacements of the LLDPE modified high performance concrete

	Specimen	Control	LLDPE		
		0%	1.5%	3.0%	5.0%
Δ_f (mm)	Beam 1	1.839	1.782	2.582	2.770
	Beam 2	1.424	2.438	1.794	2.3260
	Beam 3	1.456	1.628	2.429	2.039
	Beam 4	1.623	1.683	1.737	2.616
	Average	1.586	1.883	2.136	2.438
	SD	0.190	0.376	0.432	0.323
	CoV (%)	12.00	19.95	20.25	13.26

Table 6-27 Failure displacements of the HDPE modified high performance concrete

	Specimen	Control	HDPE		
		0%	1.5%	3.0%	5.0%
Δ_f (mm)	Beam 1	1.839	1.884	1.651	1.713
	Beam 2	1.424	1.797	1.595	1.191
	Beam 3	1.456	1.219	1.245	1.591
	Beam 4	1.623	1.239	1.452	1.295
	Average	1.586	1.535	1.486	1.448
	SD	0.190	0.355	0.181	0.245
	CoV (%)	12.00	23.13	12.19	16.93

Table 6-28 Brittleness values of the SBR modified high performance concrete

	Specimen	Control 0%	SBR		
			1.5%	3.0%	5.0%
B_f	Beam 1	0.0262	0.0312	0.0431	0.0278
	Beam 2	0.0334	0.0359	0.0240	0.0474
	Beam 3	0.0300	0.0287	0.0386	0.0327
	Beam 4	0.0293	0.0292	0.0272	0.0303
	Average	0.0297	0.0313	0.0332	0.0345
	SD	0.0030	0.0033	0.0091	0.0088
	CoV (%)	9.96	10.47	27.35	25.48

Table 6-29 Brittleness values of the PVDC modified high performance concrete

	Specimen	Control 0%	PVDC		
			1.5%	3.0%	5.0%
B_f	Beam 1	0.0262	0.0323	0.0320	0.0324
	Beam 2	0.0334	0.0316	0.0389	0.0363
	Beam 3	0.0300	0.0319	0.0366	0.0401
	Beam 4	0.0293	0.0301	0.0274	0.0310
	Average	0.0297	0.0315	0.0337	0.0349
	SD	0.0030	0.0010	0.0051	0.0041
	CoV (%)	9.96	3.05	15.17	11.73

Table 6-30 Brittleness values of the LLDPE modified high performance concrete

	Specimen	Control 0%	LLDPE		
			1.5%	3.0%	5.0%
B_f	Beam 1	0.0262	0.0270	0.0201	0.0190
	Beam 2	0.0334	0.0213	0.0275	0.0237
	Beam 3	0.0300	0.0326	0.0201	0.0256
	Beam 4	0.0293	0.0283	0.0345	0.0238
	Average	0.0297	0.0273	0.0256	0.0230
	SD	0.0030	0.0047	0.0069	0.0028
	CoV (%)	9.96	17.09	27.06	12.28

Table 6-31 Brittleness values of the HDPE modified high performance concrete

	Specimen	Control 0%	HDPE		
			1.5%	3.0%	5.0%
B_f	Beam 1	0.0262	0.0260	0.0311	0.0310
	Beam 2	0.0334	0.0271	0.0307	0.0445
	Beam 3	0.0300	0.0421	0.0430	0.0335
	Beam 4	0.0293	0.0390	0.0361	0.0423
	Average	0.0297	0.0336	0.0352	0.0378
	SD	0.0030	0.0082	0.0057	0.0065
	CV (%)	9.96	24.38	16.30	17.30

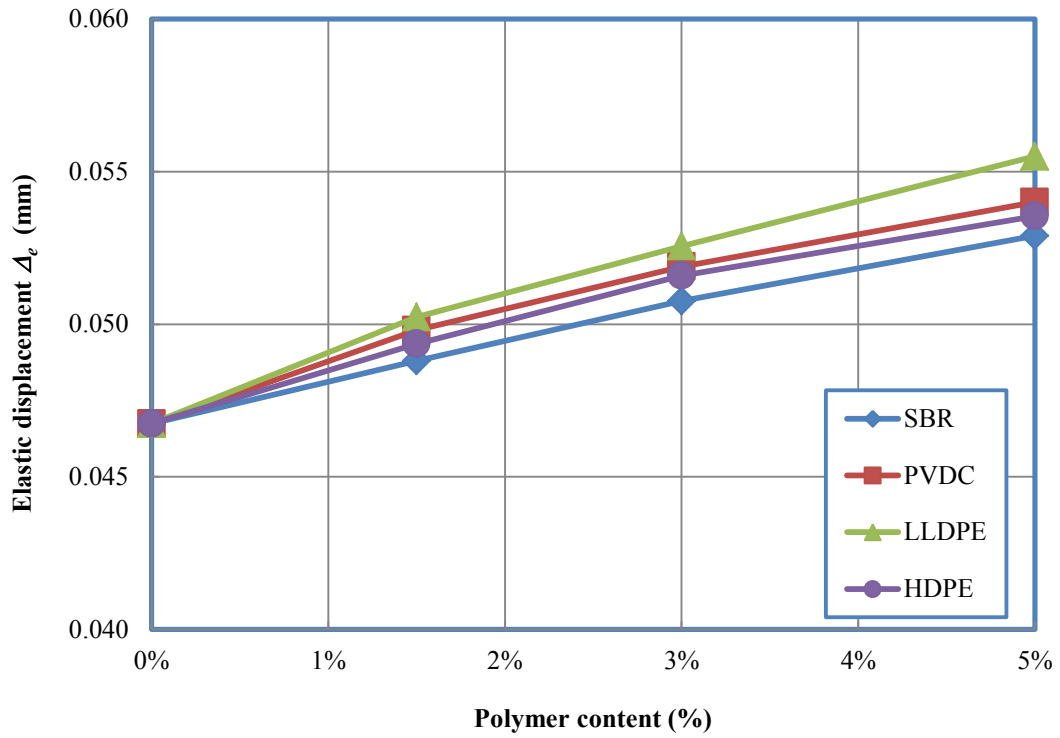


Figure 6-23 Elastic displacement of the HPC modified with different types and contents of polymers

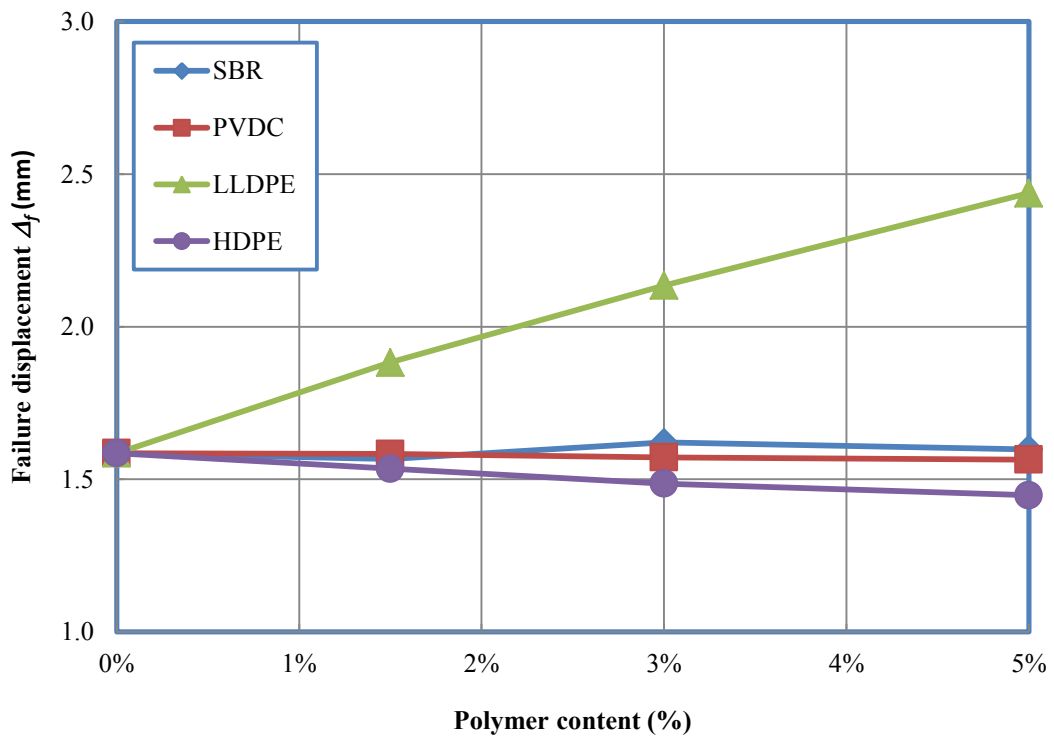


Figure 6-24 Failure displacement of the HPC modified with different types and contents of polymers

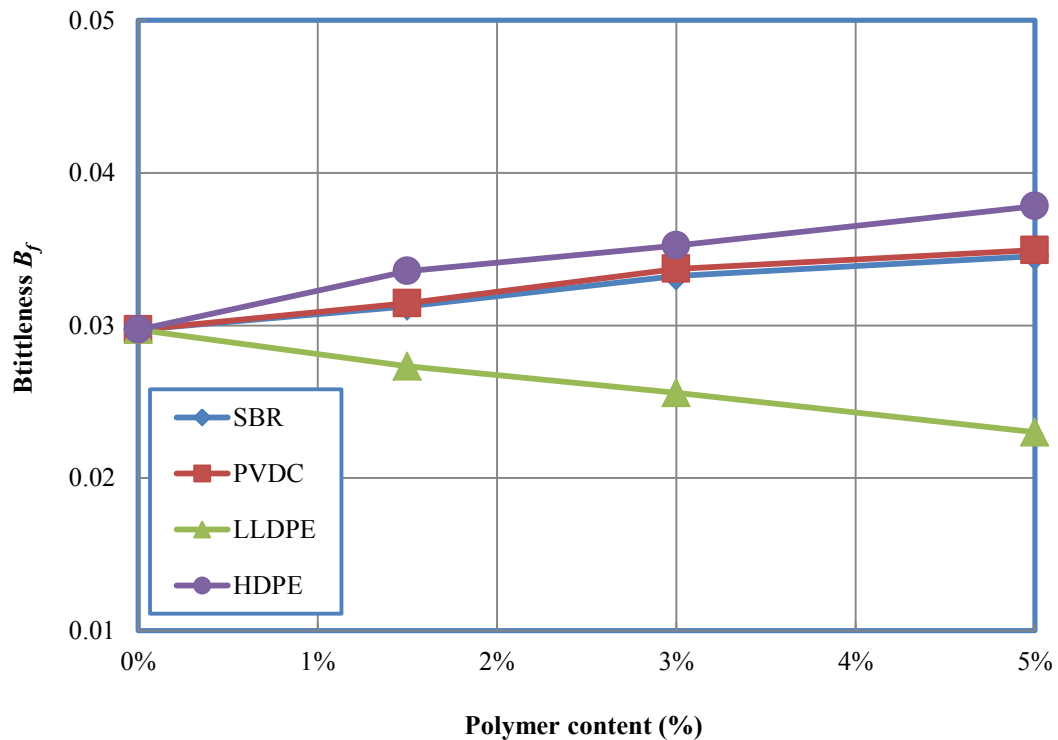


Figure 6-25 Brittleness of the HPC with different types and contents of polymers

In Figure 6-25, the experimental data show that B_f decreased gradually with increasing amount of LLDPE powder, while B_f increased with increasing amounts of SBR latex, PVDC powder and HDPE powder. This indicates that the increasing LLDPE gradually decreased the brittleness of the high performance concrete, but the increasing amounts of other polymers increased the brittleness of the high performance concrete.

Furthermore, the experimental data show that brittleness B_f increased gradually with the increasing SBR latex additive put in the high performance concrete. When the addition of SBR latex increased from 0% to 1.5%, the brittleness B_f increased from 0.0297 to 0.0313, up by 5.4%. With the increasing SBR latex to 3%, the brittleness B_f increased to 0.0332, up by 11.8%, and with 5% SBR latex the brittleness B_f increased to 0.0345, up by 16.2%.

The analysis indicates that the brittleness B_f increased gradually with the increasing PVDC powder additive in the high performance concrete. When the addition of PVDC powder increased from 0% to 1.5%, the brittleness B_f increased from 0.0297 to 0.0315, up by 6.1%, and with the increasing PVDC to 3%, the brittleness B_f

increased to 0.0337, up by 13.5%. With the addition of 5% PVDC powder, the brittleness B_f increased to 0.0349, up by 17.5%.

The brittleness B_f decreased gradually with the increasing LLDPE powder additive in the high performance concrete. When the addition of LLDPE powder increased from 0% to 1.5%, the brittleness B_f decreased from 0.0297 to 0.0273, down by 8.1%, and with the increasing LLDPE powder to 3%, the brittleness B_f decreased to 0.0256, down by 13.8%. With the addition of 5% LLDPE, the brittleness B_f decreased to 0.0230, down by 22.6%.

Finally, the analysis show that brittleness B_f increased gradually with the increasing HDPE powder additive in the high performance concrete. When the addition of HDPE powder increased from 0% to 1.5%, the brittleness B_f increased from 0.0297 to 0.0336, up by 13.1%, and with the increasing HDPE powder to 3%, the brittleness B_f increased to 0.0352, up by 18.5%. With the addition of 5% HDPE powder, the brittleness B_f increased to 0.0378, up by 27.3%.

6.10 Summary

Various mechanical and fracture tests were performed to determine the potential use of polymers as additive materials in the high performance concrete. The effects of polymers on the fracture characteristics of the high performance concrete were evaluated. On the basis of the test results of the present study, the following fundamental findings can be summarised.

The density of the polymer modified high performance concrete varied slightly compared with the unmodified high performance concrete. The basic mechanical properties of the high performance concrete, namely the compressive strengths, were substantially improved with the addition of 1.5% polymers and slightly improved with the addition of 3% polymers, but with the addition 5% SBR, LLDPE and HDPE there were no obvious improvements. The tensile strengths were substantially improved when adding four different types of polymers with various amounts. In general, the modulus of rupture decreased slightly for the high performance concrete modified with all types of polymers and with different amounts, while with the addition of 1.5% SBR it increased by approximately 2%. All the HPC mixes modified with SBR, PVDC, LLDPE and HDPE had lower values of fracture

toughness compared to the unmodified high performance concrete mix, except that with the addition of 1.5% LLDPE additive in the high performance concrete mix the fracture toughness slightly increased by around 6%. The fracture energy slightly increased with the additions of 1.5% and 5% SBR, 1.5% PVDC, 1.5% and 5% LLDPE but decreased with the additions of 3% SBR, 3% and 5% PVDC, 3% LLDPE, and 1.5%, 3% and 5% HDPE. The elastic modulus continuously decreased with the increasing contents of all four polymers. The brittleness of the high performance concrete monotonically decreased with the increasing contents of LLDPE, but increased with the increasing amounts of SBR, PVDC and HDPE.

CHAPTER 7 CONCLUSIONS AND FUTURE WORK

7.1 Conclusions

This research was intended to investigate the effects of polymer materials on the fundamental mechanical and fracture characteristics of the high performance concrete through the extensive experimental testing and analysis on the test results in order to find the ways to enhance these properties and to eventually design and manufacture high performance concrete with high strength, high performance and low brittleness. In this study, an extensive and comprehensive review was first carried out on high performance concrete, polymer modified cement, mortar and concrete, and fracture characteristics of concrete. It was confirmed that the published data on improving the fracture characteristic in high performance concrete were rather limited. Therefore, information on the performance of high performance concrete without and with polymer materials needed to be further studied, including the fracture characteristic of high performance concrete in addition to the compressive and tensile strengths, modulus of rupture and elasticity modulus. This research could add new knowledge to these aspects. Also the significance, aims, objectives and methodologies of the research were presented.

Four types of conventional polymers were used as additives with different contents in weight as proportions of cementitious materials to the high performance concrete, including Styrene Butadiene Rubber (SBR) latex, Polyvinylidene Chloride (PVDC), Linear Low Density Polyethylene (LLDPE) and High Density Polyethylene (HDPE). A total of thirteen high performance concretes with different types and amounts of polymers were designed based on the proposed method which largely followed the approach recommended by ACI 211-1 Committee. Special curing conditions were adopted in this research to significantly enhance the properties of the polymer modified high performance concrete. The conventional concrete material properties studied included the density, compressive and tensile strengths, modulus of rupture and elastic modulus. The fracture characteristics of concrete studied included the fracture energy, fracture toughness and brittleness. Three-point bending tests were conducted to obtain these fracture properties by following the RILEM methods. Most

concrete samples were tested at 28 days except the compression tests which were conducted at 7 days, 28 days and 90 days to monitor the development of the concrete performance. The compressive strength of the high performance concrete with control mix was 112.87 MPa at 28 days.

In general, the workability was enhanced by utilising polymer materials. The slump values increased when the quantity of polymer increased because the polymer made the high performance concrete more viscous and the particles of polymers filling up the voids of the concrete would enhance the concrete slump. The density of the polymer enhanced concrete slightly decreased with the increasing polymer because the densities of the adopted polymer materials were lighter.

The compressive strength of the high performance concrete modified with the specified proportions of four polymers generally increased with the increasing curing age. In particular at 28 days, the compressive strengths of the high performance concrete with 1.5% and 3% SBR latex were higher than those of the control mix by 15.6% and 5.8%, respectively. For the 5% SBR addition to the HPC, however, a slight reduction of 1.4% in the compressive strength was observed. The enhancements on the compressive strength were 13.6%, 13.1% and 10.9% for the high performance concrete with the addition of 1.5%, 3% and 5% PVDC, respectively. Adding 1.5% and 3% LLDPE improved the compressive strength of the high performance concrete by 12.5% and 9.7%, respectively. When 5% LLDPE was used, a decrease of 2.3% in the compressive strength was observed. The additions of 1.5%, 3% and 5% HDPE all resulted in the increases in the concrete compressive strength by 19.7%, 12.7% and 2.9%, respectively. For the four types of polymer materials, the ideal content in the mixture was found to be 1.5% in weight, the HDPE having the best performance, followed SBR, PVDC and LLDPE. The lowest compressive strength was generally recognised for the HPC with 5% polymer contents, the PVDC having the best performance, followed by SBR, LLDPE and HDPE.

In general, the tensile strengths were substantially improved when adding four types of polymers with different proportions. The tensile strengths of the high performance concrete modified with different proportions of SBR latex at 28 days were higher than that of the control mix by 22.9%, 72.5% and 23.4% for the additions of 1.5%, 3.0% and 5% of SBR to the HPC mix, respectively. The ideal content of SBR latex

in the mix was found to be 3% in weight, which produced the best performance, with an average tensile strength of 10.23 MPa, compared with the corresponding tensile strength of 5.93 MPa for the control mix. The additions of 1.5%, 3% and 5% of PVDC resulted in the increases of 35.6%, 41.5% and 40.1% in the tensile strength of the high performance concrete. The most optimum content of PVDC powder in the mix was found to be 3% in weight, which produced the best performance, with 8.39 MPa. With the additions of 1.5%, 3% and 5% LLDPE to the concrete mix, the tensile strength increased by up to 83.5%, 57.3% and 50.3%, respectively, the most optimum content of LLDPE in the mix was found to be 3% in weight, which produced a highest tensile strength of 10.88 MPa in the whole testing programme. The trend of the tensile strength with the addition of HDPE is similar to that with the addition of PVDC. When the polymer additive increased to 1.5%, 3% and 5%, the tensile strength increased by 37.3%, 34.4% and 45.7%, respectively.

The modulus of rupture for the high performance concrete was not enhanced by adding polymer materials. The modulus of rupture only slightly increased with the addition of 1.5% SBR by 1.9%, while the additions of 3% and 5% SBR decreased the modulus of rupture by 1.7% and 4.4%, respectively. The 1.5% SBR additive achieved the best performance, with 11.49 MPa, compared with 11.28 MPa for the control mix. With the additions of 1.5%, 3% and 5% PVDC to the mix, the modulus of rupture decreased by 2.3%, 6.8% and 17.0%, respectively. When adding 1.5%, 3% and 5% LLDPE to the mix, the modulus of rupture decreased by 8.2%, 15.9% and 7.5%, respectively. The trend for the modulus of rupture with the addition of 1.5%, 3.0% and 5% HDPE was quite similar, with a decrease of about 5% in the modulus of rupture on average.

In this study, the dynamic elastic modulus was measured on all cube specimens at different ages. Because the test results were very scattered, they were not included in the thesis. Instead, the values of the static elastic modulus which were obtained from the analysis on the complete load-deflection curves on the beams under three-point bending were very stable and meaningful so the results for the static elastic modulus were only presented here. In general, the static elastic modulus had monotonic decrease trends with the increasing polymer contents for all four types of polymer modified high performance concretes. All the concrete mixes with SBR had lower values compared to the control mix. The additions of 1.5%, 3% and 5% SBR in the

high performance concrete mixes reduced the elastic modulus by 9.1%, 12.5% and 15.5%, respectively. The static elastic modulus dropped by 13.2%, 16.1% and 20.8% with adding 1.5%, 3% and 5% PVDC into the high performance concrete by weight. For the additions of 1.5%, 3% and 5% LLDPE additives in the high performance concrete mix, the static elastic modulus decreased by 14.6%, 18.0% and 22.1%, respectively. With the additions of 1.5%, 3% and 5% HDPE to the HPC mix, the static elastic modulus decreased by 10.5%, 13.5% and 17.2%, respectively. In general, for the same polymer content, the high performance concrete modified with SBR sustained the smallest decreases in the elastic modulus, while the HPC modified with LLDPE had the largest drops.

The fracture toughness of the high performance concrete modified with polymers varied in a similar way as the rupture of modulus. The use of SBR latex as additives in the high performance concrete slightly lowered the fracture toughness. The additions of 1.5%, 3% and 5% SBR in the high performance concrete decreased the fracture toughness by 0.3%, 9.8% and 7.5%, respectively. The fracture toughness decreased by 7.8%, 14.1% and 23.9%, respectively, when adding 1.5%, 3% and 5% PVDC in the high performance concrete. The additions of 1.5% LLDPE in the high performance concrete slightly increased the fracture toughness by 2.9%, while the additions of 3% and 5% LLDPE caused the reductions of 7.8% and 8.4%, respectively. With the additions of 1.5%, 3% and 5% HDPE to the high performance concrete, the fracture toughness decreased by 16.7%, 8.1% and 11.8%, respectively.

As for the fracture energy, when adding 1.5% and 5% SBR in the HPC, the fracture energy slightly increased by 3.5% and 7.0%, respectively, from 265.75 N/m for the control mix, while the addition of 3% SBR slightly decreased the fracture energy by 4.3%. When the PVDC content increased to 1.5%, the fracture energy slightly increased by 0.8%, while the additions of 3% and 5% PVDC led to the decreases in the fracture energy of 15.9% and 23.5%, respectively. The fracture energy slightly decreased by 4.6% for the addition of 3% LLDPE, while for the additions of 1.5% and 5% LLDPE the fracture energy increased by the highest 24.3% and 7.9%, respectively. The fracture energy of the high performance concrete modified with HDPE decreased by 22.5%, 2.2% and 7.1% when adding 1.5%, 3% and 5% HDPE in the HPC.

Finally the concrete brittleness was assessed by using a brittleness parameter which is defined as the ratio of the elastic displacement at the peak load to the failure displacement. The experimental data illustrated that the brittleness of the high performance concrete decreased gradually with increasing proportions of LLDPE powder, but increased with the increasing proportions of SBR latex, PVDC powder and HDPE powder. This indicates that the increasing LLDPE proportion would help decrease the brittleness of the high performance concrete, but the increasing proportions of other polymers would increase the brittleness of the high performance concrete. In this study, the additions of 1.5%, 3% and 5% SBR latex increased the brittleness of the high performance concrete by 5.4%, 11.8% and 16.2%, respectively. The additions of 1.5%, 3% and 5% PVDC powder increased the brittleness of the high performance concrete by 6.1%, 13.5% and 17.5%, respectively. Furthermore, the additions of 1.5%, 3% and 5% HDPE powder increased the brittleness of the high performance concrete by 13.1%, 18.5% and 27.3%, respectively. This means that the additions of HDPE powder proportions would largely increase the brittleness of the high performance concrete. Inversely, the additions of 1.5%, 3% and 5% LLDPE powder would decrease the brittleness of the high performance concrete by 8.1%, 13.8% and 22.6%, respectively.

To sum up, the utilisations of the four adopted polymers in the high performance concrete could indeed largely enhance the compressive and tensile strengths. LLDPE could also decrease the brittleness of concrete. The fracture characteristics did not sustain significant improvements and the elastic modulus of the concrete decreased with the increasing polymer contents.

7.2 Future Work

This research has extensively investigated the mechanical and fracture characteristics of the high performance concrete modified with polymer materials, but other irregular properties, e.g. the time dependent properties including shrinkage and creep, permeability, durability, sustainability, and their applications to plain, reinforced and prestressed concrete structures need to be further explored.

The previous research indicated that curing conditions may help improve the material properties and structural performance of the high performance concrete modified

with polymer materials. In this study, only conventional curing methods were used to cure the concrete samples, and it is worthwhile to try other unconventional curing methods to cure the concrete, e.g. steam curing, hot water curing, electric curing, etc.

It is well understood that the mechanisms of the improvement on macroscopic mechanical and fracture properties of high performance concrete modified with polymer materials should be explored by investigating the physical and chemical properties of concrete ingredients, e.g. cement paste, aggregates, additives, bonding, etc., at microscopic and mesoscopic levels, including chemical elements and compositions, porosity and pore size distribution, etc. Due to the limits of time and testing facilities during this study, only macroscopic properties of the high performance concrete modified with polymer materials were investigated, and it is worthwhile to further explore the microscopic and mesoscopic characteristics of the polymer modified concrete.

In this study, four conventional polymer materials including Styrene Butadiene Rubber (SBR) latex, Polyvinylidene Chloride (PVDC) powder, Linear Low Density Polyethylene (LLDPE) powder and High Density Polyethylene (HDPE) powder have been utilised for modifying the high performance concrete and improving the concrete brittleness. There are many other types of polymer materials available in the market which may more effectively improve the fracture properties and brittleness. It is worthwhile to try other types of polymer materials for this purpose.

Previous research has confirmed that the introduction of polymer materials could improve the material and fracture properties of normal strength concrete, and this study has further confirmed that the use of polymer materials could also enhance the material and fracture properties of high strength concrete, e.g. the compressive and tensile strengths. It is worthwhile to investigate the effects of polymer materials on the material and fracture properties of concrete with the strength between normal and high values, say 70-80 MPa, because this range of the concrete strength has been largely used for special concrete constructions, e.g. marine structures, tall reinforced concrete buildings, long span reinforced and prestressed concrete bridges, nuclear power station protection shell structures, etc.

REFERENCES

- Abdalla HM and Karihaloo BL** (2003) Determination of size-independent specific fracture energy of concrete from three-point bend and wedge splitting tests, *Magazine of Concrete Research*, 55, 133–141.
- Abdulrahman M, Moncef N and Aiham A** (2008) Recycling waste latex paint in concrete with added value, *ACI Materials Journal*, 105(4), 367-374.
- Abu-Lebdeh T, Hamoush S, Heard W and Zornig B** (2011) Effect of matrix strength on pullout behavior of steel fiber reinforced very-high strength concrete composites, *Construction and Building Materials*, 25, 39-46.
- ACI** (1991) *ACI Committee 548 Polymers in Concrete*, Detroit, American Concrete Institute (ACI), USA.
- ACI** (2003) *ACI 213R-03 Guide for Structural Lightweight-Aggregate Concrete*, American Concrete Institute (ACI), USA.
- ACI** (2005) *ACI 116R-00 Cement and Concrete Terminology*, American Concrete Institute (ACI), USA.
- ACI** (2009) *ACI Committee 2 Standard Practice for Selecting Proportions for Normal, Heavyweight, and Mass Concrete* (reapproved 2009), American Concrete Institute (ACI), USA.
- ACI** (2009) *ACI 446 Fracture Toughness Testing of Concrete*, American Concrete Institute (ACI), USA.
- Aggarwal L, Thapliyal P and Karade S** (2007) Properties of polymer-modified mortars using epoxy and acrylic emulsions, *Construction and Building Materials*, 21, 379–383.
- Aitcin P** (2003) The durability characteristics of high performance concrete: a review, *Cement & Concrete Composites*, 4, 409–420.
- Aitcin P** (2004) *High-Performance Concrete*, E & FN SPON, New York, USA.

Almeida AE and Sichieri EP (2007) Experimental study on polymer-modified mortars with silica fume applied to fix porcelain tile, *Building and Environment*, 42, 2645–2650.

Ansari A (1989) Mechanics of microcrack formation in concrete, *ACI Material Journal*, 5, 459-464.

ASTM (2002) *ASTM C78 Standard Test Method for Flexural Strength of Concrete Using Simple Beam with Third-Point Loading*, ASTM International, West Conshohocken, USA.

ASTM (2010) *ASTM C143/C143M Standard Test Method for Slump of Hydraulic-Cement Concrete*, ASTM International, West Conshohocken, USA.

Baalbaki W, Aicin PC and Ballivy G (1992) On predicting modulus of elasticity in high-strength concrete, *Materials Journal*, 89(5), 517-520.

Barbuta M and Leqadatu D (2008) Mechanical characteristics investigation of polymer concrete using mixture design of experiments and response surface method, *Journal of Applied Sciences*, 8(12), 2242-2249.

Bazant ZP (2002) Concrete fracture models: testing and practice, *Engineering Fracture Mechanics*, 69, 165-205.

Bazant ZP, Kim FA and Pfeiffer PA (1986) Nonlinear fracture properties from size effect tests, *Journal of Structural Engineering*, 112, 289-307.

Bentur A and Mindess S (1986) The effect of concrete strength on crack patterns, *Cement and Concrete Research*, 16, 59-66.

Bharatkumar BH, Raghuprasad BK, Ramachandramurthy DS, Narayanan R and Gopalakrishnan S (2005) Effect of fly ash and slag on the fracture characteristics of high performance concrete, *RILEM Journal of Materials and Structures*, 38(275), 63-72.

Bhutta MA and Ohama Y (2010) Recent status of research and development of concrete-polymer composites in Japan, *Concrete Research Letters*, 1(4), 125-130.

- Bordelon AC** (2005) *Fracture Behaviour of Concrete Materials for Rigid Pavement Systems*, PhD thesis, University of Illinois at Urbana-Champaign.
- BSI** (1983) *BS 822 Specification for Aggregates from Natural Sources for Concrete*, British Standards Institution (BSI), London, UK.
- BSI** (1985) *BS 812-103.1 Testing Aggregates, Method for Determination of Particle Size Distribution Sieve Tests*, British Standards Institution (BSI), London, UK.
- BSI** (1986) *BS 410 Specification for Test Sieves*, British Standards Institution (BSI), London, UK.
- BSI** (2009) *BS EN 12350-2 Testing fresh concrete, Slump-test*, British Standards Institution (BSI), London, UK.
- BSI** (2010) *BS EN 1097-2 Tests for Mechanical and Physical Properties of Aggregates Methods for the Determination of Resistance to Fragmentation*, British Standards Institution (BSI), London, UK.
- BSI** (2011) *BS EN 197-1 Cement, Composition, Specifications and Conformity Criteria for Common Cements*, British Standards Institution (BSI), London, UK.
- Cheyrezy M, Maret V and Frouin L** (1995) Microstructure analysis of RPC (reactive powder concrete), *Cement and Concrete Research*, 25, 1491-1500.
- Chmielewska B** (2008) Adhesion strength and other mechanical properties of SBR modified concrete, *International Journal of Concrete Structures and Materials*, 2(1), 3-8.
- Colak A** (2005) Properties of plain and latex modified Portland cement pastes and concretes with and without superplasticizer, *Cement and Concrete Research*, 35, 1510-1521.
- Cotterell B** (2002) The past, present, and future of fracture mechanics, *Engineering Fracture Mechanics*, 69, 533–553.
- Cox BN and Marshall DB** (1994) Concepts for bridged cracks in fracture and fatigue, *Acta Metallurgica et Materialia*, 42, 341-36.

De Larrard F (1990) A method for proportioning high-strength concrete mixtures, *Cement Concrete and Aggregates*, 12(1), 47–52.

Detwiler RJ and Mehta PK (1989) Chemical and physical effects of silica fume on the mechanical behaviour of concrete, *ACI Materials Journal*, 86, 609-614.

Division WW (2009) *SBR Latex*, Burnley, Wykamol.

Domone PL and Soutsos MN (1995) Properties of high strength concrete mixes containing pfa and ggbs, *Magazine of Concrete Research*, 47(173), 355-367.

Einsfeld RA and Velasco MS (2006) Fracture parameters for high-performance concrete, *Cement and Concrete Research*, 36, 576-583.

Farhat FA (2004) *Performance of Concrete Structures Retrofitted with CARDIFRC after Thermal Cycling*, PhD Thesis, School of Engineering, Cardiff University, Cardiff, UK.

Ferraris CF and Lobo CL (1998) Processing of HPC, *Concrete International*, 20(4), 61-64.

Ferraris CF, Koehler E, Amziane S, Crockett NJ, Khayat KH and Sobolev K (2008) *ACI Committee 238 Report on Measurements of Workability and Theology of Fresh Concrete*, American Concrete Institute (ACI), USA.

Fosroc Limited (2011) *Structuro 11180*, Tamworth, UK.

Fowler D (1999) Polymers in concrete: a vision for the 21st century, *Cement and Concrete Composites*, 21, 449-452.

Galvão JC, Portella KF, Joukoski A, Mendes R and Ferreira ES (2011) Use of waste polymers in concrete for repair of dam hydraulic surfaces, *Construction and Building Materials*, 25, 1049-1055.

Gettu R, Bazant ZP and Karr ME (1990) Fracture properties and brittleness of high-strength concrete, *ACI Materials Journal*, 87, 608-618.

Griffith A (1921) The phenomena of rupture and flow in solids, *Philosophical Transactions of the Royal Society of London*, 221, 163-198.

Hale W M, Freyne S and Russell B (2009) Examining the frost resistance of high performance concrete, *Construction and Building Materials*, 23, 878-888.

Hillerborg A, Modeer M and Petersson PA (1976) Analysis of crack formation and crack growth in concrete by means of fracture mechanics and finite elements, *Cement and Concrete Research*, 6, 773-782.

Hillerborg A (1985) The theoretical basis of a method to determine the fracture energy G_F of concrete, *Materials and Structures*, 18(4), 291-296.

Hinshlogl S and Agar E (2004) Use of waste high density polyethylene as bitumen modifier, *Materials Letters*, 58, 267– 271.

Houst YF, Bowen P, Perche F, Kauppi A, Borget P and Galmiche L (2008) Design and function of novel superplasticizers for more durable high performance concrete (superplast project), *Cement and Concrete Research*, 38(10), 1197–1209.

Hu XZ and Wittmann FH (1992) Fracture energy and fracture process zone, *Materials and Structures*, 25, 319-326.

Huang YY and Wu KR (1984) The mechanism of modification in mechanical behaviour of PCC, PIC and PI (PCC), *The 4th International Congress on Polymers in Concrete*, Darmstadt, 429-433.

Ince R and Alyamac KE (2008) Determination of fracture parametres based on water-cement ratio, *Indian Journal of Engineering and Materials Sciences*, 15, 14-22.

Irwin G (1957) Ananalysis of stresses and strains near the end of a crack traversing a plate, *Journal of Applied Materials*, 24, 361-364.

Islam M, Rahman M and Ahmed M (2011) Polymer-modified concrete: world experience and potential for Bangladesh, *The Indian Concrete Journal*, 4, 55-63.

Ismail M, Muhammad B, Mohdyatim J, Noruzman AH and Soon YW (2011) Behaviour of concrete with polymer additive at fresh and hardened states, *Procedia Engineering*, 14, 2230-2237.

Jenq Y and Shah SP (1985) Two parameter fracture model for concrete, *ASCE Journal of Engineering Mechanics*, 111(10), 1227–1241.

- Jiang R, Jia J-Q and Xu X-L** (2007) Seismic ductility of very-high-strength-concrete short columns subject to combined axial loading and cyclic lateral loading, *Journal of Chongqing University*, 6(3), 205-212.
- Kaplan MF** (1961) Crack propagation and the fracture of concrete, *Journal of the American Concrete Institute*, 58, 591-610.
- Karihaloo BL** (1995) *Fracture Mechanics and Structural Concrete*, Addison Wesley Longman, Lonon, UK.
- Karihaloo BL and Nallathambi P** (1989) Fracture toughness of plain concrete from three point bend specimens, *Materials and Structure*, 22, 185-193.
- Khan MI** (2006) *Properties of High Performance Concrete*, King Saud University, Ryadh, Saudi Arabia.
- Lemaitre J** (2001) *Handbook of Behavioural Material Models*, Academic Press, San Diego, USA.
- Malvar LJ and Warren GE** (1987) Fracture energy for three point bend tests on single edge notched beams: proposed evaluation, *Materials and Structures*, 20(6), 440-447.
- Malvar J and Warren G** (1988) Fracture energy for three point bend tests on single edge notched beams, California, Naval Civil Engineering Laboratory.
- Mark JS** (1999) *Polymer Data Handbook*, Oxford University Press Inc., Oxford, UK.
- Martin A, Stanton J, Mitra N and Lowes L** (2007) Experimental testing to determine concrete fracture energy using simple laboratory test setup, *ACI Materials Journal*, 104, 575-584.
- Mehta PK and Aïtcin PC** (1990) Principles underlying production of high performance concrete, *Cement, Concrete and Aggregates*, 12(2), 70-78.
- Mojumdar SC** (2005) Thermal properties, environmental deterioration and applications of macro-defect-free cements, *Research Journal of Chemistry and Environment*, 9, 23-27.

- Morin V, Moevus M and Gartner E** (2011) Effect of polymer modification of the paste-aggregate interface on the mechanical properties of concrete, *Cement and Concrete Research*, 5, 459-466.
- Nawy EG** (2001) *Fundamentals of High Performance Concrete*, John Wiley & Sons, New York, USA.
- Nemati KM, Monteiro PJ and Scrivener KL** (1998) Analysis of compressive stress-induced cracks in concrete, *ACI Materials Journal*, 95, 617-630.
- Neville A** (1995) *Properties of Concrete*, 4th Ed, Longman Group, UK.
- Neville A** (1997) Aggregate bond and modulus of elasticity of concrete, *ACI Material Journal*, 94, 71-74.
- Neville A and Aitcin PC** (1998) High performance concrete - an overview, *Materials and Structures*, 31, 111-117.
- Newman K** (1965) The structure and properties of concrete-an introductory review, In *The Structure of Concrete and its Behaviour under Load* by Brooks A and Newman K, Cement and Concrete Association, London, UK.
- Ohama Y** (1995) *Handbook of Polymer-Modified Concrete and Mortars Properties and Process Technology*, Noyes Publications, New Jersey, USA.
- Ohama Y** (1997) Recent progress in concrete-polymer composites, *Advanced Cement Based Materials*, 5(2), 31-40.
- Ohama Y** (2004) Recent progress in research and development activities of polymer-modified mortar and concrete in Japan, *Slovenski Kolokvij Obetonih – Gradnja Zbetoni Visokih Zmogljivosti*, 4, 11-16, Ljubljana, Slovenia.
- Orowan E** (1955) Energy criteria for fracture, *Welding Journal*, 34, 1575-1581.
- Paco Systems** (2012) *SBR*, Newton Abbot Devon, UK.
- Peng J** (2011) *Styrene-Butadiene Rubber (SBR) Encyclopedia of Chemical Processing*, Taylor and Francis.
- Petersson PE** (1980) Fracture energy of concrete: method and determination, *Cement and Concrete Research*, 10, 78-89.

Procem PD (2014) *Portland Cement (CEM I 52,5N) Product Data Sheet*, Retrieved from Lafarge Tarmac.

Ramakrishnan V (1995) Concrete fibre composites for the twenty-first century, In *Real World Concrete* by Singh G, 111-144, Elsevier Science Ltd, UK.

Reinhardt HW (1995) Relation between the microstructure and structural performance of concrete, In *Concrete Technology: New Trends, Industrial Applications* by Aguado A, Gettu R and Shah SP, 19-32, E&FN Spon, London, UK,

Rice JR (1968) A path independent integral and the approximate analysis of strain concentration by notches and cracks, *Journal of Applied Mechanics*, 35, 379-386.

RILEM (1985) Determination of the fracture energy of mortar and concrete by means of the three-point bend tests on notched beams, *RILEM Materials and Structures*, 18, 1501-1511.

Rossello C and Elices M (2004) Fracture of model concrete: types of fracture and crack path, *Cement and Concrete Research*, 17, 1441–1450.

Rossi P, Brihwiler E, Chhuy S, Jenq YS and Shah SP (1991) Fracture properties of concrete as determined by means of wedge splitting tests and tapered double cantilever beam tests, In *Fracture Mechanics Test Methods for Concrete* by Shah SP and Carpinteri A, 87-128, Chapman & Hall, London.

Rossignolo JA and Agnesini MV (2004) Durability of polymer-modified lightweight aggregate concrete, *Cement and Concrete Composites*, 26, 375–380.

Rossignolo JA and Agnesini MV (2002) Mechanical properties of polymer-modified lightweight aggregate concrete, *Cement and Concrete Research*, 32, 329-334.

Sabir BB (1995) High strength condensed silica fume concrete, *Magazine of Concrete Research*, 47(172), 219-226.

Scheirs J (2009) *Report on LLDPE and MDPE Resins: Their Physical Characteristics, Production Methods, Functional Attribute and Commercial Attributes*, Australia: Australian Customs and Border Production Service.

- Setzer MJ and Wittmann FH** (1974) Surface energy and mechanical behaviour of hardened cement paste, *Applied Physics*, 3(5), 403-409.
- Shah SP** (1988) Fracture toughness of cement-based materials, *RILEM Materials and Structures*, 21, 145-150.
- Shah SP, Swartz SE and Ouyang C** (1995) *Fracture Mechanics of Concrete*, John Wiley and Sons Inc., New York, USA.
- Silva D and Monteiro P** (2005) Hydration evolution of C3S–EVA composites analyzed by soft X-ray microscopy, *Cement and Concrete Research*, 35(2), 351–357.
- Struble L, Skalny J and Mindess S** (1980) A review of the cement-aggregate bond, *Cement and Concrete Research*, 10, 277-286.
- Swamy RN and Bouikni A** (1990) Some engineering properties of slag concrete as influenced by mix proportioning and curing, *ACI Materials Journal*, 87, 210-220.
- Swartz SE and Go CG** (1984) Validity of compliance calibration to cracked concrete beams in bending, *Experimental Mechanics*, 24, 129-134.
- Tasdemir C and Tasdemir MA** (1995) Microstructural effects on the brittleness of high strength concretes, In *Fracture Mechanics of Concrete* by Wittmann FH, 125-134, Aedificatio Publishers, Freiburg, Germany.
- Tasdemir C, Tasdemir MA, Lydon FA and Barr BI** (1996) Effects of silica fume and aggregate size on the brittleness, *Cement and Concrete Research*, 26(1), 63-68.
- Theunis J and Franck S** (2001) *Greenhouse Gas Emissions and Material Flows*.
- Torgal P and Jalali S** (2009) Sulphuric acid resistance of plain, polymer modified, and fly ash cement concretes, *Construction and Building Materials*, 23, 3485–3491.
- Trussoni M** (2009) *Fracture Properties of Concrete Mixtures Containing Expanded Polystyrene Aggregate Replacement*, PhD Dissertation, University of Miami, Florida, USA.
- Wang EZ and Shrive NG** (1995) Brittle fracture in compression: mechanisms, models and criteria, *Engineering Fracture Mechanics*, 52, 1107-1126.

- Wang R and Wang P** (2010) Function of styrene-acrylic ester copolymer latex in cement mortar, *Materials and Structures*, 43, 443–451.
- Wang W and Wang P** (2011) Action of redispersible vinyl acetate and versatate copolymer powder in cement mortar, *Construction and Building Materials*, 8, 1-5.
- Wu KR, Chen B, Wu Y and Zhang D** (2001) Effect of coarse aggregate type on mechanical properties of high-performance concrete, *Cement and Concrete Research*, 31, 1421–1425.
- Xie J, Elwi AE and MacGregor JG** (1995) Mechanical properties of three high-strength concretes containing silica fume, *ACI Materials Journal*, 92(2), 135-145.
- Yoshihiko O** (1997) Recent progress in concrete-polymer composites, *Advanced Cement Based Materials*, 5(2), 31-40.
- Zain MF, Islam MN and Basri H** (2005) An expert system for mix design of high performance concrete, *Advances in Engineering Software*, 36, 325–337.
- Zeng S** (1996) *Polymer Modified Cement: Hydration, Microstructure and Diffusion Properties*, PhD thesis, University of Aston in Birmingham, Birmingham, UK.
- Zhang B** (2011) Effects of moisture evaporation (weight loss) on fracture properties of high performance concrete subjected to high temperatures, *Fire Safety Journal*, 46, 453-549.
- Zhang B and Bicanic N** (2002) Residual fracture toughness of normal- and high-strength gravel concrete after heating to 600C, *ACI Material Journal*, 99(3), 217-226.
- Zhang B, Bicanic N, Pearce CJ and Phillips DV** (2002) Relationship between brittleness and moisture loss of concrete exposed to high temperatures, *Cement and Concrete Research*, 32, 363-371.
- Zhang XH** (1987) PhD Thesis, Tongji University, Shanghai, China.
- Zhong S and Chen Z** (2002) Properties of latex blends and its modified cement mortars, *Cement and Concrete Research*, 32(10), 1515–1524.

Zhou FP, Barn B and Lydon F (1995) Fracture properties of high strength concrete with varying silica fume content and aggregates, *Cement and Concrete Research*, 25, 543-552.

Zhou JH (1988) *Influence of the Interfacial Bonding Between Coarse Aggregates and Hardened Cement Paste on the Mechanical Behaviour of Concrete and Computing Analysis*, PhD Thesis, Tongji University, Shanghai, China.

Zia P, Ahmad S and Leming M (1995) *High-Performance Concretes A State-of-Art Report (1989-1994)*, FHWA-RD-97-030, US Department of Transportation, USA.

APPENDIX A MIX DESIGN

All mixes in this study were designed in accordance with the proposed method which followed the same approach as ACI 211-1 Standard Practice for Selecting Proportions for Normal, Heavyweight and Mass specified. It is a combination of empirical results and mathematical calculations based on the absolute volume method (Aitcin, 2004).

a) Mix design calculations

All the calculations needed to find the mix proportions are presented on the mix design sheet.

i. Water/binder ratio

In order to reach a 110 MPa compressive strength, the water/binder ratio (Figure A-1) should be 0.25, which will be put in Box 1.

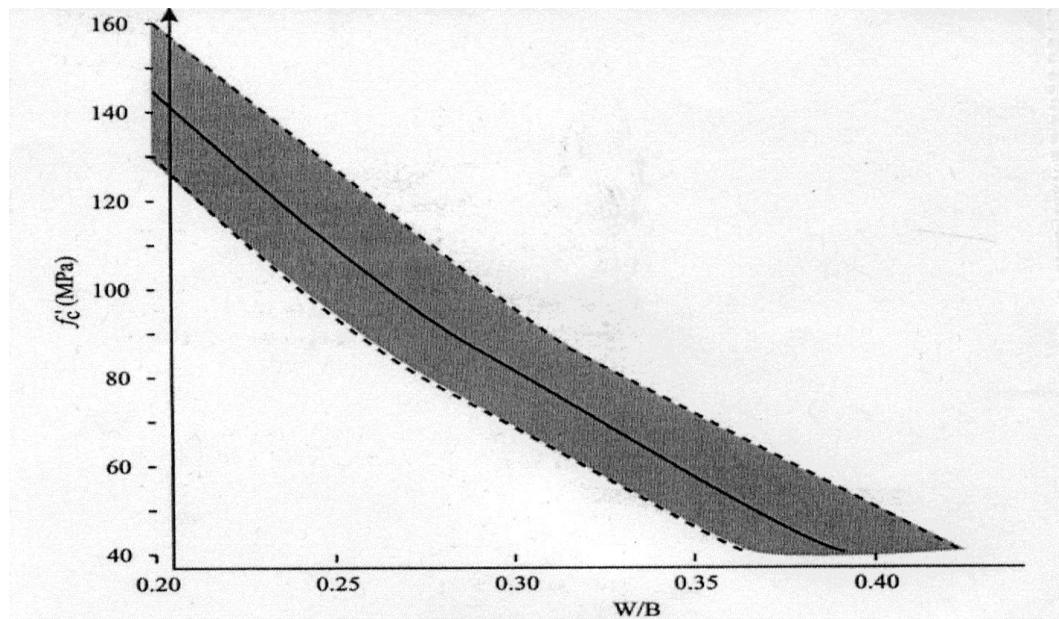


Figure A-1 Proposed W/B – compressive strength relationship

ii. Water content

From Figure A-2, it can be found that the water dosage for a saturation point of 1.0% should be between 135 and 145 l/m³. A dosage of 140 l/m³ is for this trial batch, which will be written it in Box 2.

Saturation point	0.6	0.8	1.0	1.2	1.4	percent
Water dosage	120 to 125	125 to 135	135 to 145	145 to 155	155 to 165	l/m

Figure A-2 Determination of the minimum water dosage

iii. Binder content

The binder content is equal to:

$$B = \frac{140}{0.25} = 560 \text{ kg/m}^3$$

which will be put in Box 3.

iv. Silica fume content

Suppose that a 110 MPa concrete has to be made with silica fume as replacement of 10% the total cementations material and it is to be used with its specific gravity of 2.20, i.e. 56 kg. Here 55 kg is taken and put in Box 4-2.

v. Cement content

The cent content will then be $560 - 55 = 505 \text{ kg/m}^3$ which is put in Box 4-1.

vi. Content of coarse aggregate

1000 kg/m^3 , given by (Figure A-3), should be put in Box 5.

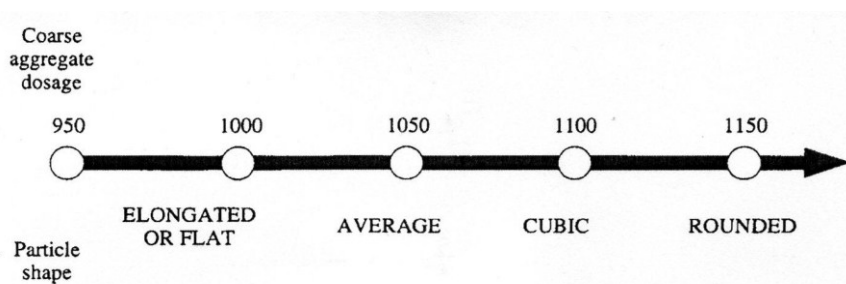


Figure A-3 Coarse aggregate content

vii. 1.5% volume of entrapped air is put in Box 6.

viii. A dosage of superplasticizer of 10% for the saturation point is put in Box 7.

ix. The volume of the cement is calculated as:

$$505/3.14 = 160.8 \approx 160 \quad (\text{Box 8-1})$$

x. The volume of silica fume is:

$$55/2.2 = 25 \quad (\text{Box 8-2})$$

xi. The volume of coarse aggregate is:

$$1000/2.9 = 344.8 \approx 345 \quad (\text{Box 9})$$

xii. The volume of entrapped air is:

$$1.5 \times 10 = 15 \quad (\text{Box 10})$$

xiii. The sum of all the numbers appearing in Column 2 is:

$$140 + 160 + 25 + 345 + 15 + 3.5 = 688.5 \quad (\text{Box 12})$$

xiv. The volume of the sand will be:

$$1000 - 688.5 = 311.5 \quad (\text{Box 13})$$

xv. The SSD mass of the sand is:

$$311.5 \times 2.641 = 822 \text{ kg/m}^3 \quad (\text{Box 14})$$

xvi. Add the values appearing in Column 3:

$$140 + 505 + 55 + 1000 + 822 + 6 = 2528 \text{ kg/m}^3 \quad (\text{Box 16})$$

xvii. Water corrections

When the aggregate to be used is not in the SSD condition and it is dry, it will absorb certain amount of water from the mix. The mass M_c of the dry coarse aggregate to be weighed is:

$$M_c = \text{the content of coarse aggregate} \times [1 - (W_{abs}/100)]$$

where W_{abs} is the absorbed water in the aggregate in percentage. Thus,

$$M_c = 1000 \times [1 - (0.75/100)] = 992 \text{ kg} \quad (\text{Box 17})$$

The dry coarse aggregate will absorb $1000 - 992 = 8$ kg water; so +8 is put in Box 18.

As the fine aggregate is wet, a mass greater than 822 kg must be weighed and the water added has to be subtracted from the total amount of water. As $w_h = 2.3\%$,

$$M_f = 822 \times (1 + 2.3/100) = 841 \quad (\text{Box 19})$$

This mass of fine aggregate will bring to the mix: $841 - 822 = 19$ kg, so -19 is put in Box 20.

The total will be: $+8 - 19 - 9 = -20$ (Box 22)

This gives the final composition of 1 m^3 concrete with aggregates.

The necessary volume of mixing water to be measured is:

$$140 - 20 = 120 \quad (\text{Box 23})$$

Suppose that to test the concrete, the following specimens are needed:

- three 100 mm cube for tests at 7, 28 and 91 days in compression, respectively;
- three 100 mm cube for tests at 28 days in splitting tension;
- four notched beams of 500 mm × 100 mm × 100 mm for three-point bending tests to determine the fracture parameters.

A slump test, an air content test and a unit mass test will be done on the fresh concrete. Except for the air content test, the concrete used for these tests will be recovered.

Knowing that:

a 100 mm cube weighs about 2.3 kg, and

a 500 mm × 100 mm × 100 mm weighs about 12 kg,

the amount of concrete to make this trial batch can be calculated.

Here assume 10% extra materials to compensate for losses:

Table A-1 The amount of concrete to make the trial batch

Specimen			Total
	100 mm cubes	500 mm × 100 mm × 100 mm beams	
Number	12	4	
Mass needed (kg)	28	48	76

Assuming a loss of 10% it will be necessary to mix 84 kg of concrete which represents $84/2528 \approx 0.03 \text{ m}^3$. All the numbers in Column 5 have to be multiplied by this factor to obtain the mass of each ingredient to be weighed to make the trial batch:

Mixing water	$120 \times 0.03 = 3.65$	(Box 25)
Cement	$505 \times 0.03 = 15.1 \approx 15 \text{ kg}$	(Box 26–1)
Silica fume	$55 \times 0.03 = 1.65 \text{ kg}$	(Box 26–2)
Coarse aggregate	$992 \times 0.03 = 29.8 \text{ kg}$	(Box 27)
Fine aggregate	$813 \times 0.03 = 24.43 \text{ kg}$	(Box 28)
Superplasticizer	$13 \times 0.03 = 0.39 = 0.4 \text{ kg}$	(Box 29)

In order to check the final composition, the values appearing in Boxes 25 to 28 are added: $3.65 + 15 + 1.65 + 29.8 + 24.43 = 74.53 \text{ kg}$ (Box 30)

This is close to the value of 60 kg calculated earlier.

b) Mix design sheet

Table A-2 Mix design sheet of abbreviations

Comp. Strength MPa 110	%				
	Aggregate	G _{SSD}	W _{abs}	W _{tot}	W _h
	coarse	2.80	0.8	0.0	-0.8
	fine	2.65	1.2	3.5	2.3

$$M = M_{SSD} (1+W_h) \quad W_h = W_{tot} - W_{abs}$$

Table A	G _C	%
Cement	3.14	90
Silica fume	2.2	10

superplasticizer		M _{sol} =C*d/ 100	V _{liq} = $\frac{M_{sol}}{s * G_{sup}} *$ 100	V _w =V _{liq} *G _s up*($\frac{100-s}{100}$)	V _{sol} =V _{liq} -V _w =[1* $(\frac{100-s}{100}) * G_{sup}$]
Spec. gravity (GSUP)	Solids dosage (%)				
1.2	40	15	24	21	11
		6	13	9	3.5
		E	F	G	11

	1	2	3	4	5	6	
Materials	Content kg/m3		Volum e l/m3	Dosage SSD conditions kg/m3	Water correcti on l/m3	composition	
						Lm3	Trial batch
Water	2		2	2		23	25
w/c=0.25 cement	140		140	140		120	3.6
	3 560	4-1	8-1	4-1		4-1	26-1
505		160	505	505		3.6	
4-2		8-2	4-2	4-2		26-2	
Silica fume	55	25	55	55		1.65	

Table A-2 Mix design sheet of abbreviations (cont.)

Coarse aggregate	5 1000	9 345	5 1000	18 +8	17 992	27 29.8
Fine aggregate		13 311.5	14 822	20 -19	19 841	28 25
air	percent	10 15				
	6 1.5					
Superplastezier	7 1.1%	11 3.5	15 6	21 -9	24 Vliq 13	29 Vliq 0.4
total		12 688.5	16 2528	22 -20		30 75.6

c) Mix design calculations from trial batch proportions for 1 m³ composition (SSD conditions)

Water (L)	Cement (kg)	Silica fume (kg)	Aggregates (kg)		Superplasticizer (l)
			Coarse	Fine	
3.6	15	1.65			0.6
			29.8	25	

The slump test is 28 mm. The materials used to make this trial batch have the following properties:

aggregate	G _{SSD}	W _{abs}	W _{tot}
coarse	2.9	0.66	0
fine	2.641	3.72	0

The silica fume used has a specific gravity of 2.20.

The superplasticizer is Structuro 11180 with a specific gravity, G_{sup} , of 1.10 and a solid content of 40%.

Let us start by put 3.6 kg, 15 kg, 1.65 kg, 29.8 kg, 25 kg, 0.6 and 1.5% in the appropriate boxes in Column 1.

The SSD mass of coarse aggregate is

$$\frac{\text{mass of coarse aggregate}}{1 + W_h / 100}$$

where $W_h = W_{tot} - W_{abs}$

$$\frac{29.8}{1 + (-0.66 / 100)} = 30.0 \text{ kg} \quad (\text{Box 7})$$

The SSD mass of fine aggregate is

$$\frac{25.0}{1 + (0.78 / 100)} = 24.8 \text{ kg} \quad (\text{Box 8})$$

The mass of water absorbed by the coarse aggregate is equal to -0.2 kg, which is put in Box 9.

The amount of water added to the mix by the fine aggregate is $30 - 29.8 = 0.2$ kg, which is put in Box 10.

The amount of water contained in the superplasticizer is equal to:

$$V_w = V_{lig} G_{sup} \left(\frac{100-s}{100} \right) = 0.6 \times 1.10 \times \left(\frac{100-40}{100} \right) = 0.396. \quad (\text{Box 11})$$

The total water correction to be made is $(-0.2 + 0.2 + 0.396) = +0.396$. (Box 12)

The actual volume of effective water in the mix is $(3.6 + 0.396) = 3.996$. (Box 13)

The volume of cement used is equal to $15/3.14 = 4.77$ (Box14-1)

The volume of silica fume used is equal to $1.65/2.2 = 0.75$ (Box14-2)

The volume of coarse aggregate is equal to $30/2.9 = 10.344$ (Box15)

The volume of fine aggregate is equal to $24.8/2.641 = 9.39$ (Box16)

The volume of the solids in the superplasticizer is

$$V_{sol} = V_{lig} \left[1 - \left(\frac{100-s}{100} \right) G_{sup} \right] = 0.6 \times \left[1 - \left(\frac{100-40}{100} \right) \times 1.10 \right] = 0.204. \quad (\text{Box 17})$$

The sum of these volumes represents 98.5% of the total volume of the trial batch:

$$3.996 + 4.77 + 0.75 + 10.344 + 9.39 + 0.204 = 29.454 \quad (\text{Box 18})$$

Therefore the actual volume of concrete in this trial batch becomes:

$$29.454 / (1 - 1.5/100) = 29.90 \quad (\text{Box 19})$$

In order to make 1 m^3 concrete, the proportions of the materials will have to be multiplied by: $1000/29.90 = 33.44$ (Box 20)

The compositions of 1 m³ of concrete now become:

Water	$3.996 \times 33.44 = 133.626 \rightarrow 134 \text{ l/m}^3$	(Box 21)
Cement	$15 \times 33.44 = 501.6 \rightarrow 502 \text{ kg/m}^3$	(Box 22-1)
Silica fume	$1.65 \times 33.44 = 55.176 \rightarrow 55 \text{ kg/m}^3$	(Box 22-2)
Coarse aggregate	$30 \times 33.44 = 1003.2 \rightarrow 1005 \text{ kg/m}^3$	(Box 23)
Fine aggregate	$24.8 \times 33.44 = 829.312 \rightarrow 830 \text{ kg/m}^3$	(Box 24)
Superplasticizer	$0.6 \times 33.44 = 20.064 \rightarrow 20.1 \text{ l/m}^3$	(Box 25-1)

The mass of the solids is:

$$20.1 \times 1.1 \times 0.40 = 8.844 \rightarrow 9 \text{ kg} \quad (\text{Box 25-2})$$

The unit mass of this concrete is:

$$134 + 502 + 55 + 1005 + 830 + 9 = 2535 \text{ kg/m}^3 \quad (\text{Box 26})$$

The binder mass is: $502 + 55 = 557$ (Box 27)

The actual water/binder ratio is: $134/557 = 0.24$ (Box 28)

Table A-3 Mix design sheet of abbreviations

	G_c	$V_{mix} = \frac{V_s + V_w}{1 - a/100}$	$\%$				
cement	3.14		aggregate	G_{SSD}	W_{abc}	W_{tot}	W_h
			Coarse				
			fine				

V_s volume of solids

V_w volume of water

a air content %

$$W_h = W_{tot} - W_{abs} \quad M = M_{SSD} (1 + W_h)$$

superplasticizer		$V_w = V_{lig} \times G_{sup} \times \left(\frac{100-s}{100}\right)$	$V_{sol} = V_{lig} \left[1 - \left(\frac{100-s}{100}\right) \times G_{sup}\right]$	$M_{sol} = V_{liq} \times G_{sup} \times \frac{s}{100}$
Spec. gravity (G_{sup})	Solids content s%			

Table A-3 Mix design sheet of abbreviations (cont.)

	1	2	3	4	5	
Materials	used	SSD conditions	Water correction 1	Volume 1	Dosage SSD conditions kg/m ³	
Water	1 3.6l			13 3.996	21 134	
Cement	2.1 15 kg			14.1 4.77	22.1 502	²⁸ w/c = 0.25
silica fume	2.2 1.65kg			14.2 0.75	22.2 55	27 557
	2.3			14.3	22.3	
coarse aggregate	3 29.8 kg	7 30 kg	9 -0.2	15 10.344	23 1005	
fine aggregate	4 25 kg	8 24.8 kg	10 0.2	16 9.39	24 830	
Super. plastisizer	5 0.6 l		11 0.396	17 0.204	25.1 20.1 l/m ³ 25.2 9 kg of solids	
Air	percent 6 1.5 %				18 volume of solids + water 29.454	6 1.5 %

Table A-3 Mix design sheet of abbreviations (cont.)

	TOTAL	¹² Water correction 0.396	¹⁹ 29.90	²⁶ 2535
	Mult.factor	²⁰ 33.44		

W/C	Water (L)	Cement (kg)	Silica fume (kg)	Aggregate (kg)		Superplasticizer (l)
				Coarse	Fine	
0.25	134	505	55	996	830	20

APPENDIX B LOAD VERSUS DISPLACEMENT CURVES

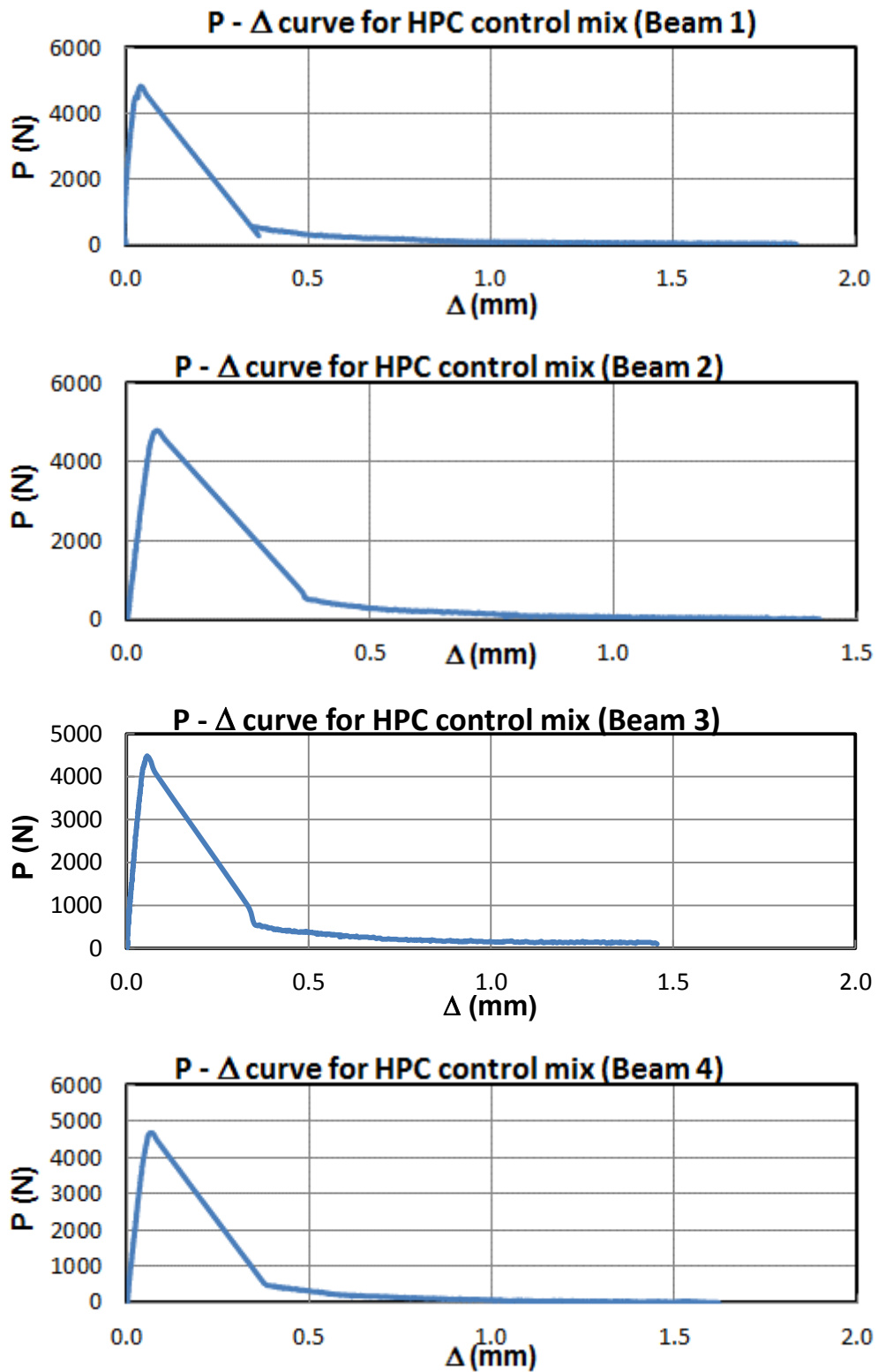


Figure B-1 Load – displacement curves for the HPC control mix

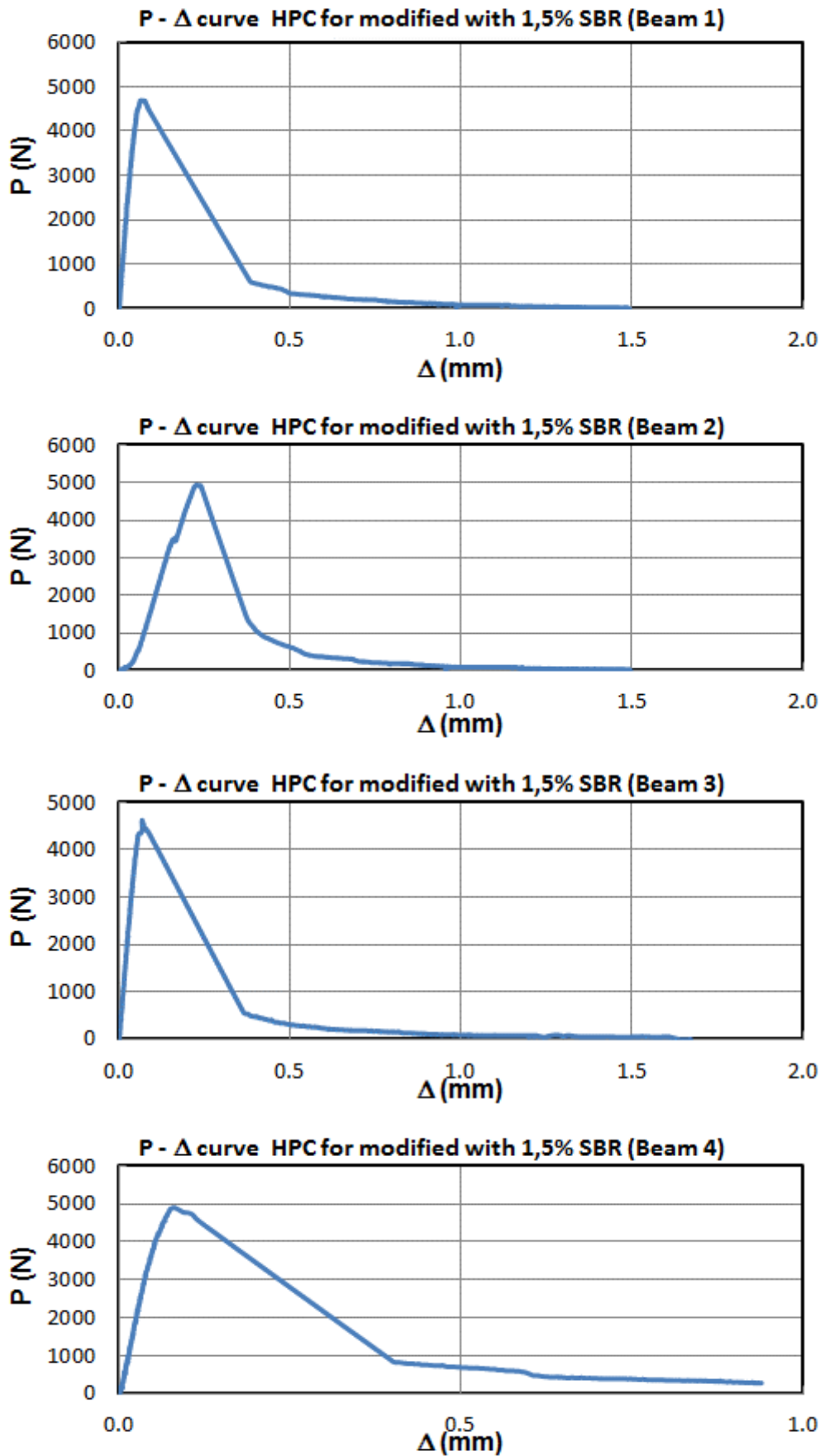


Figure B-2 Load – displacement curves for the HPC modified with 1.5% SBR

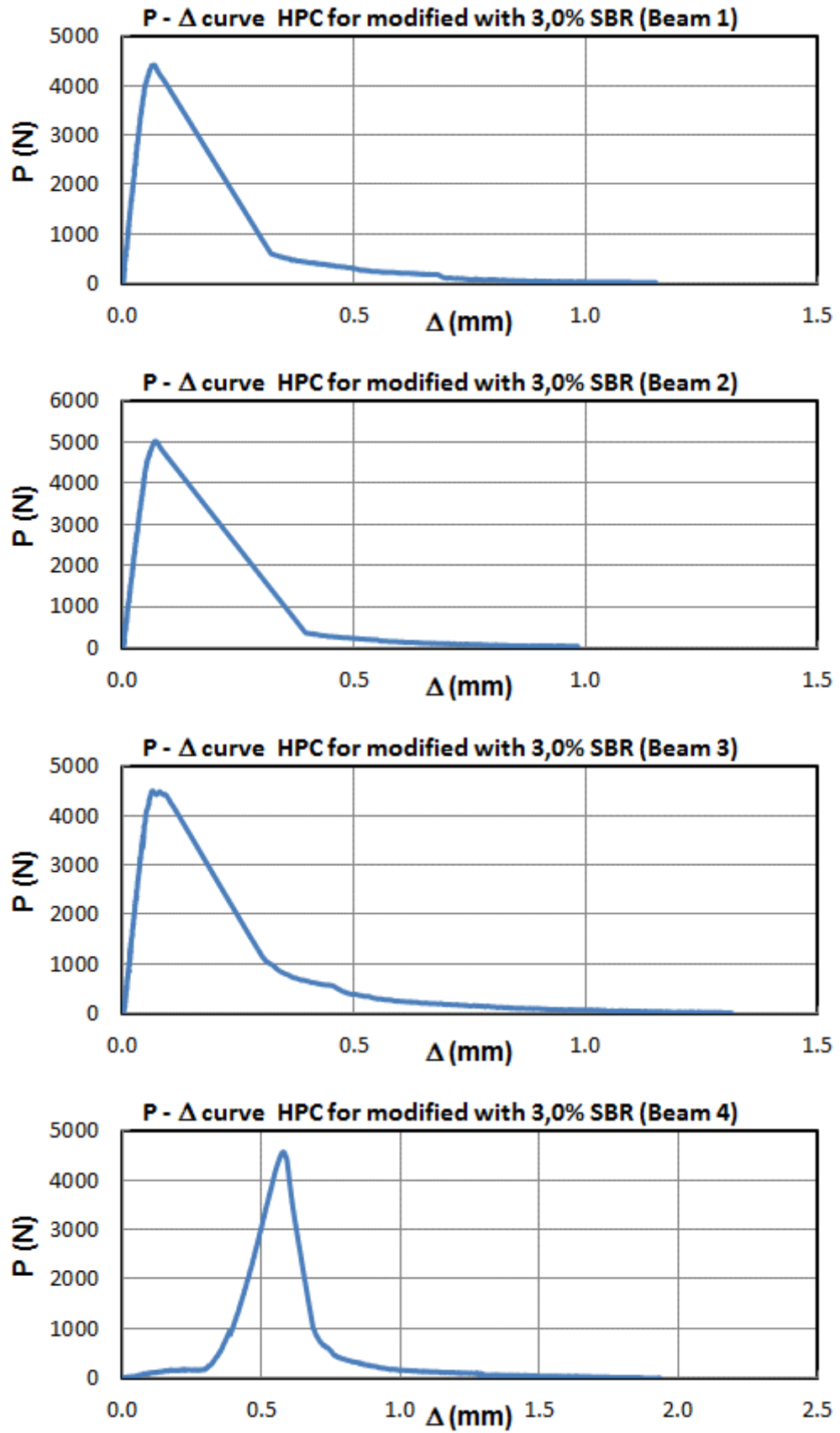


Figure B-3 Load – displacement curves for the HPC modified with 3.0% SBR

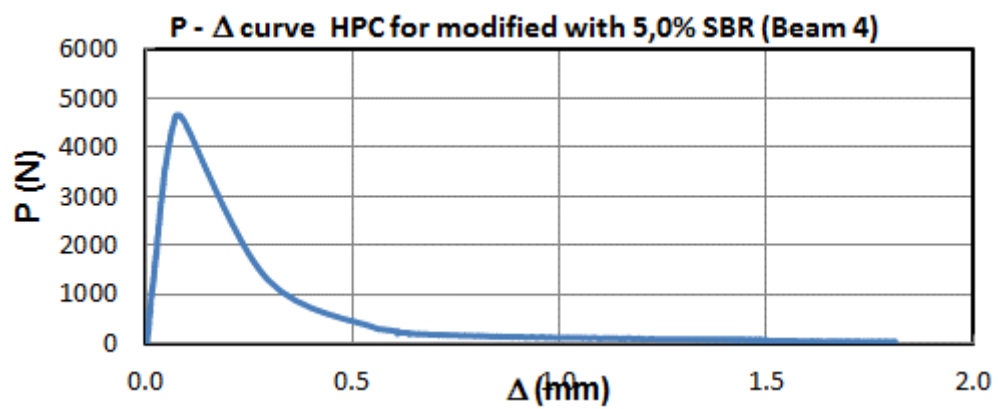
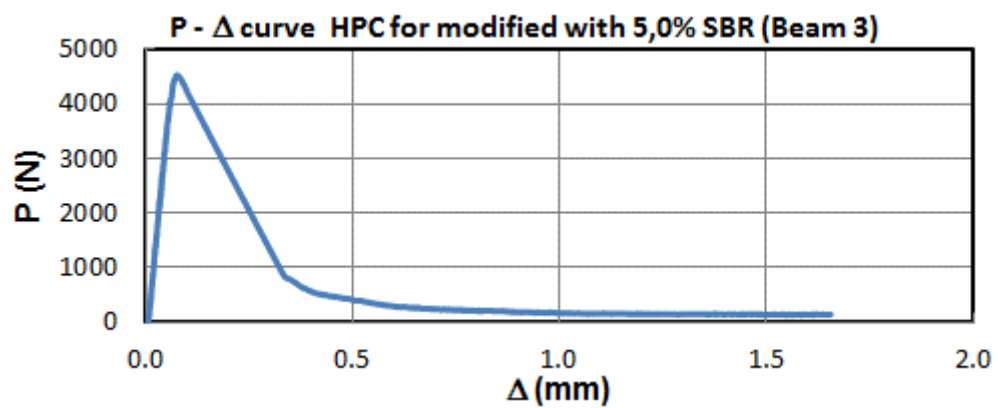
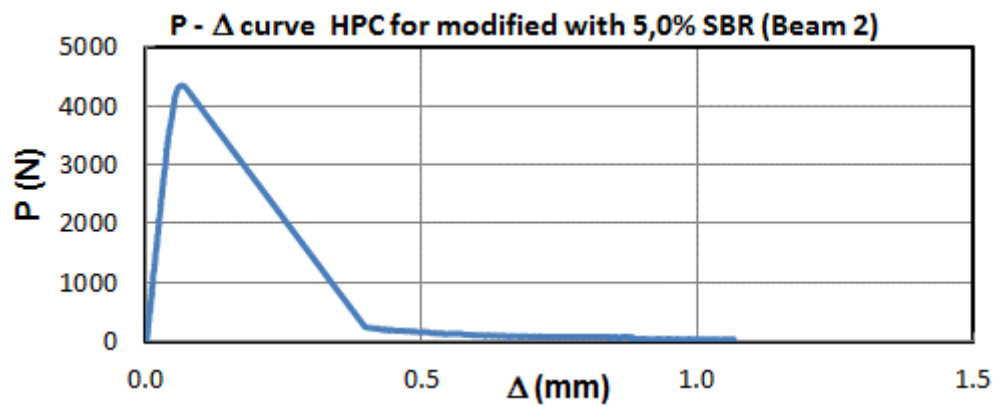
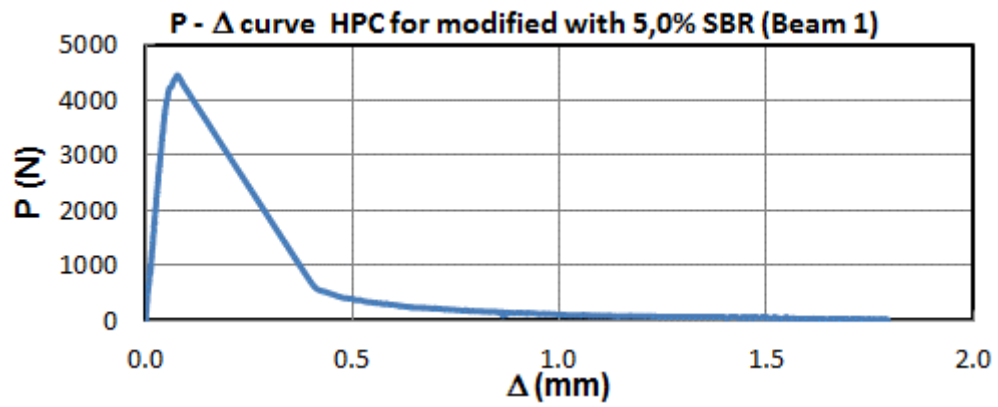


Figure B-4 Load – displacement curves for the HPC modified with 5.0% SBR

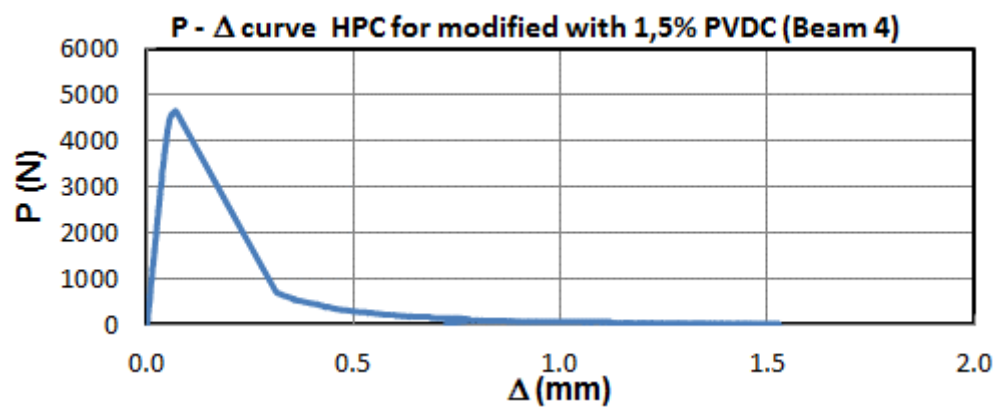
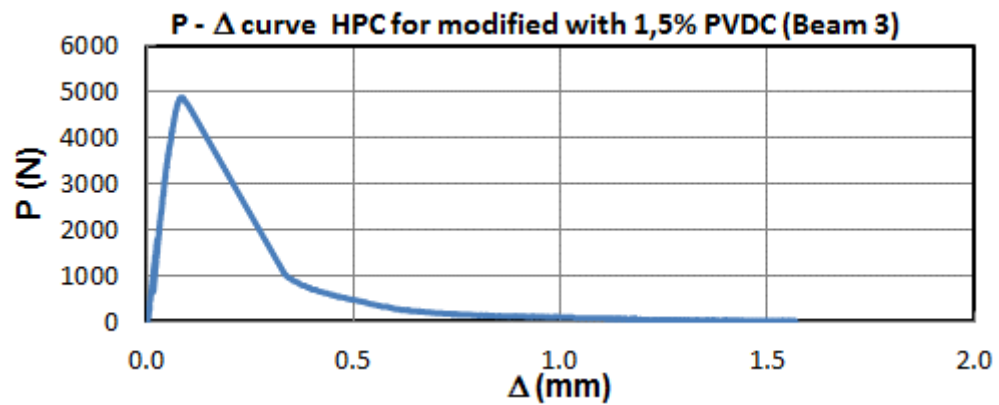
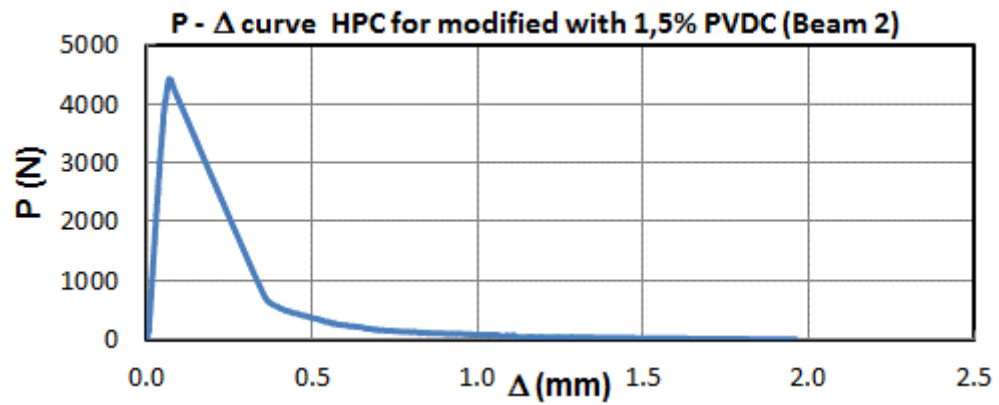
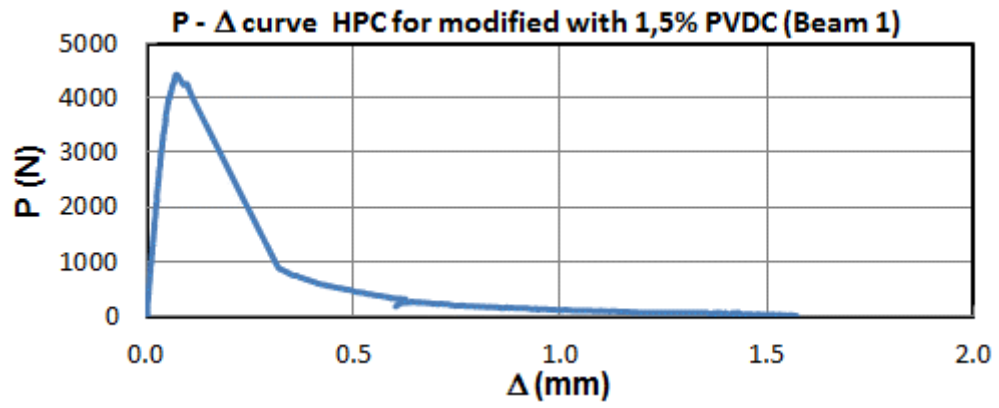


Figure B-5 Load – displacement curves for the HPC modified with 1.5% PVDC

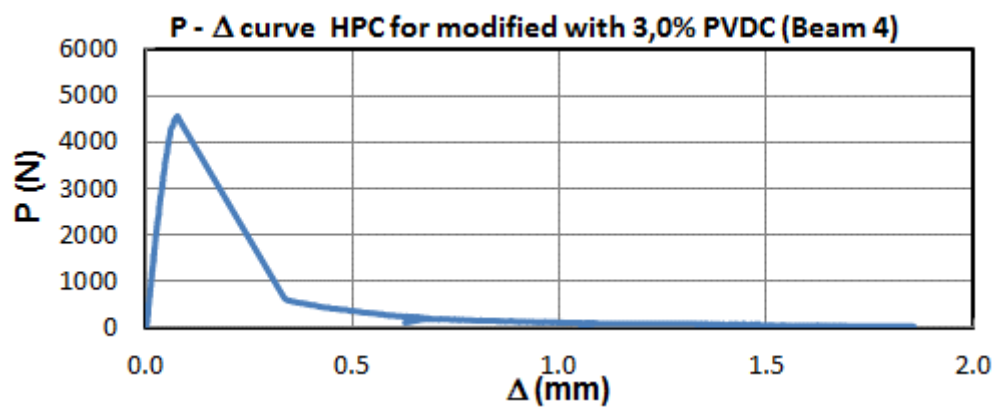
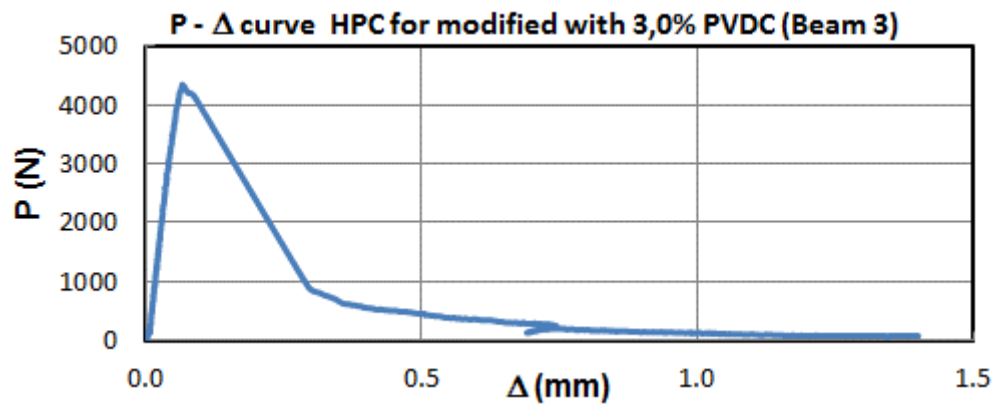
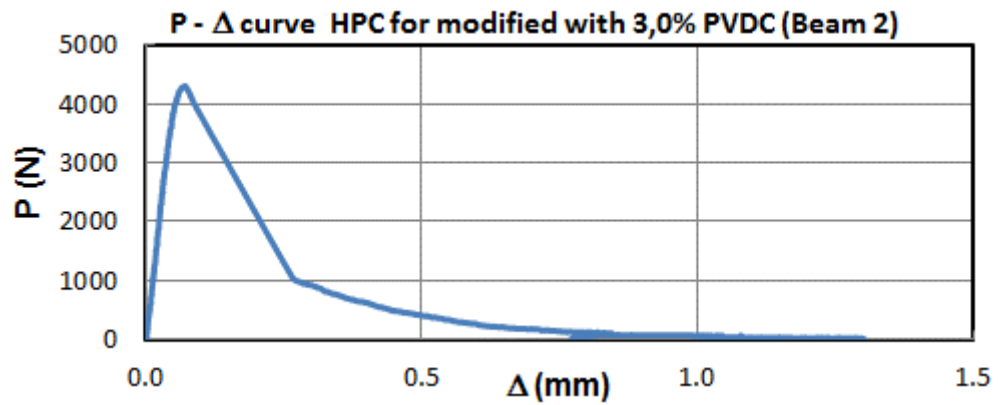
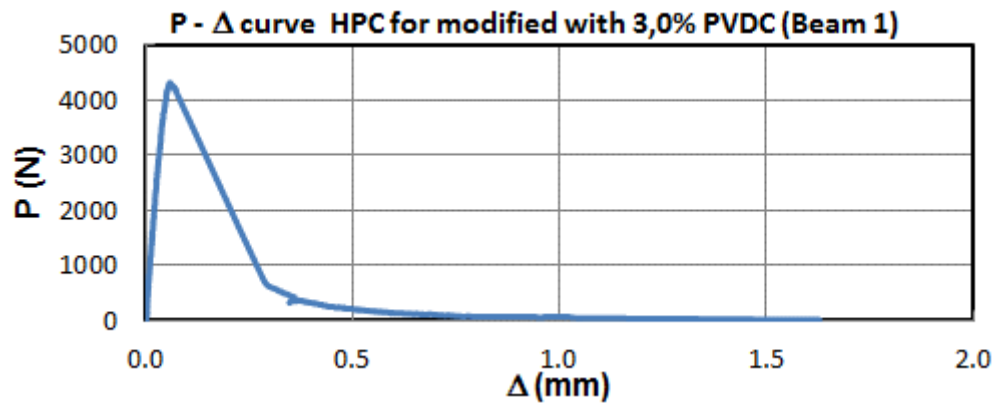


Figure B-6 Load – displacement curves for the HPC modified with 3.0% PVDC

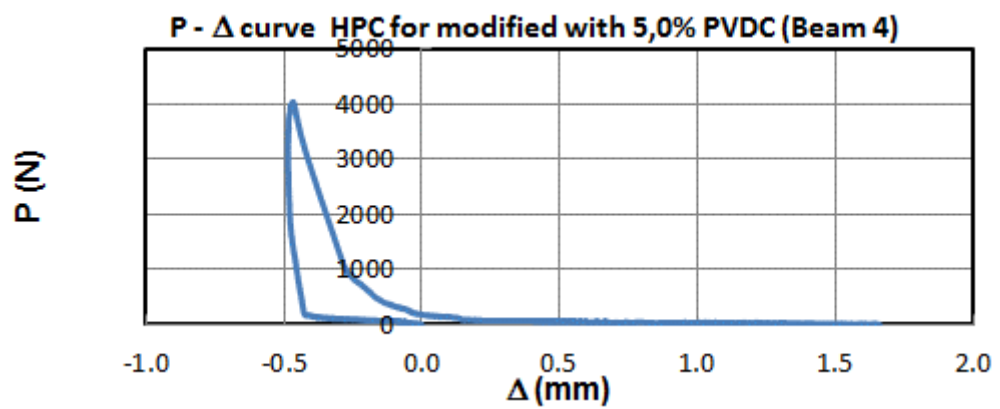
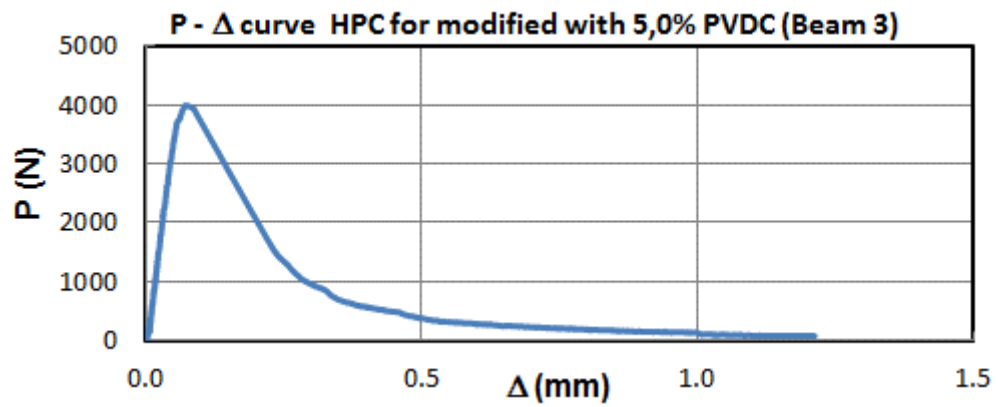
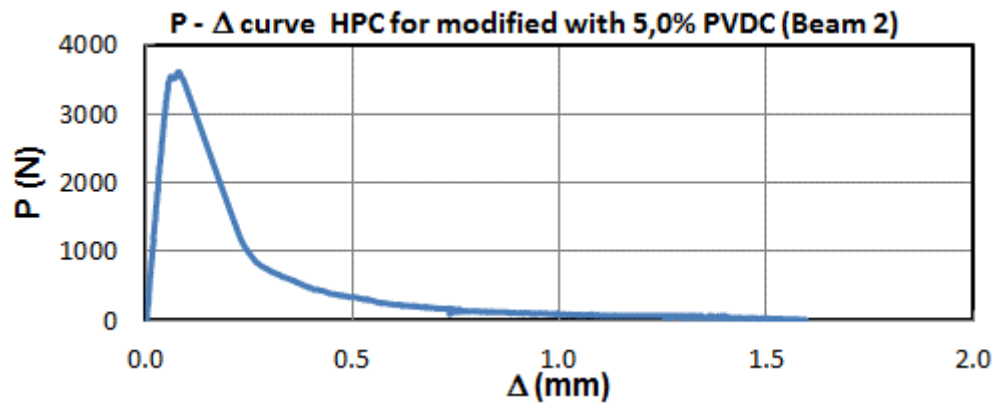
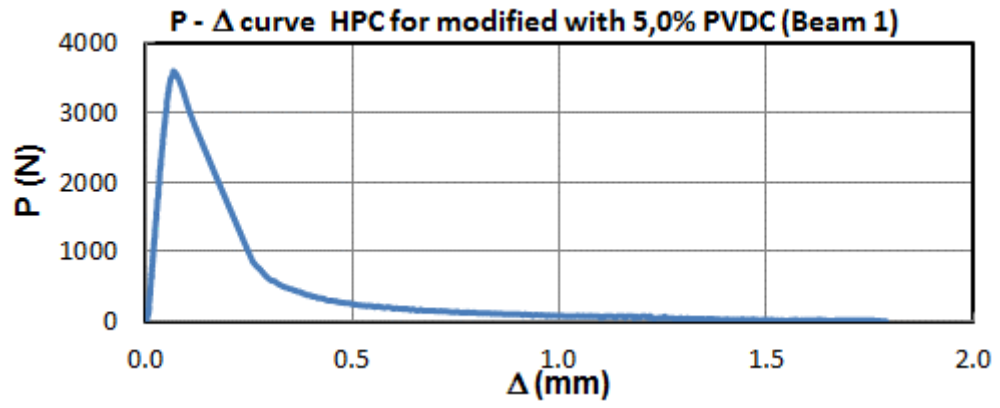


Figure B-7 Load – displacement curves for the HPC modified with 5.0% PVDC

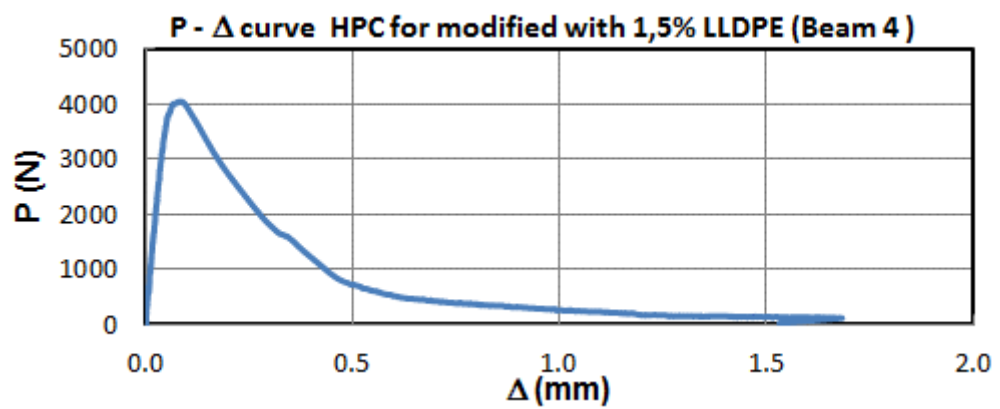
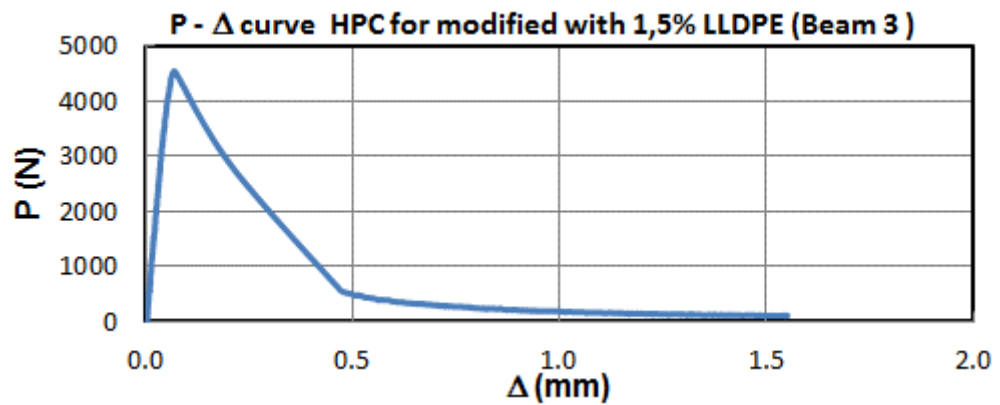
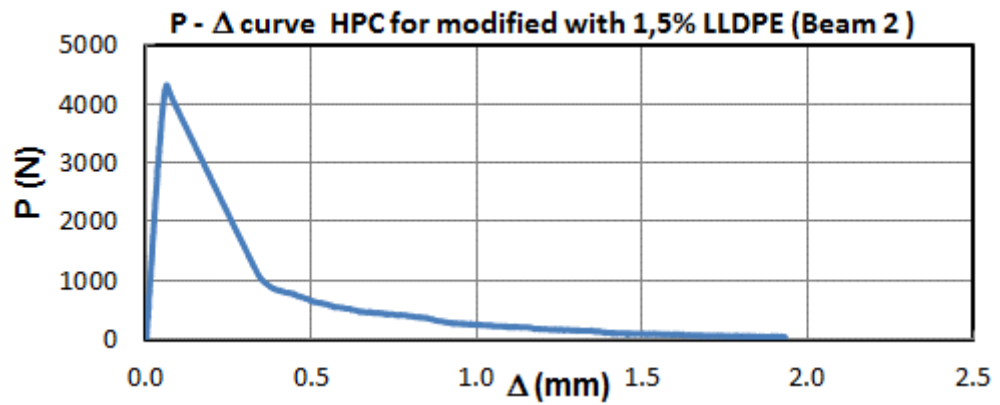
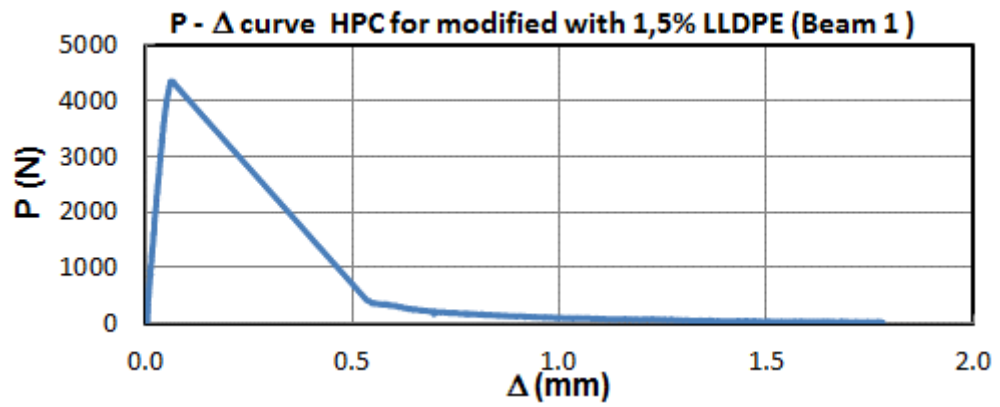


Figure B-8 Load – displacement curves for the HPC modified with 1.5% LLDPE

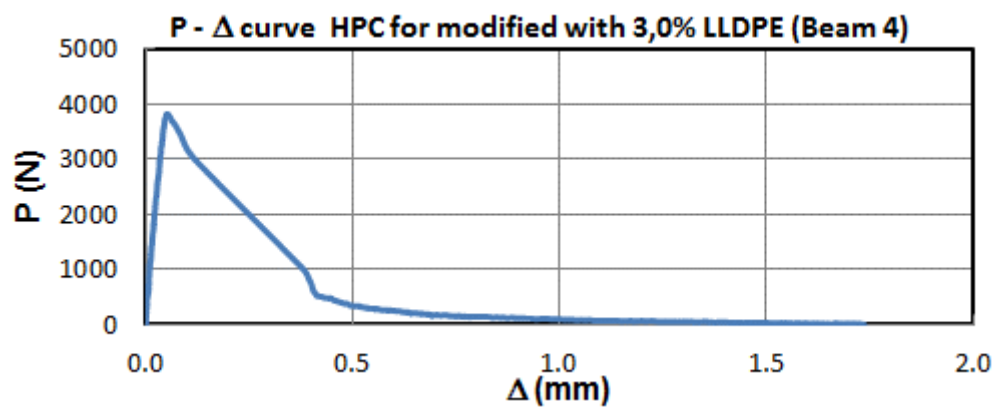
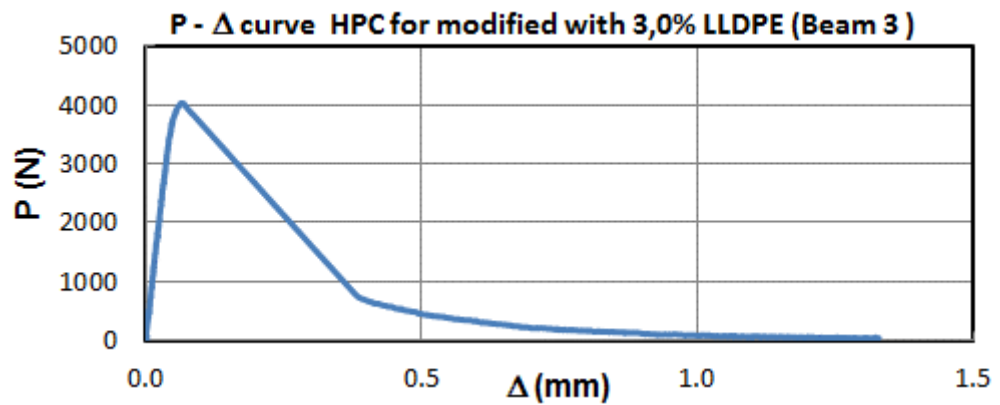
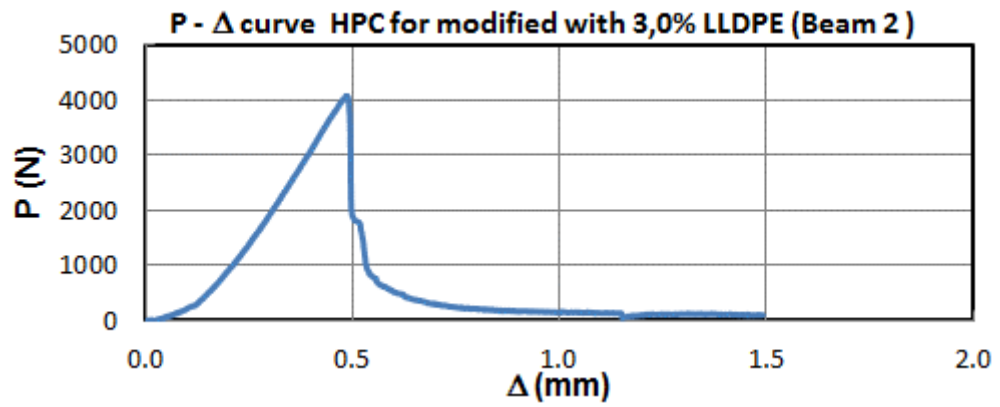
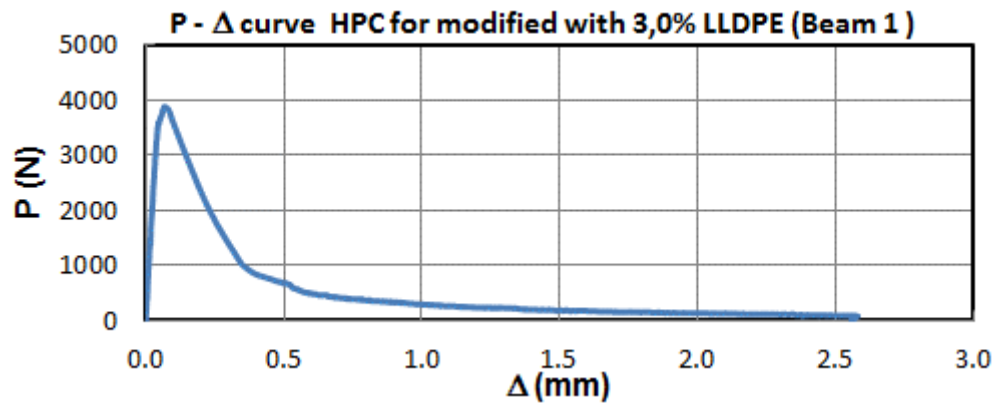


Figure B-9 Load – displacement curves for the HPC modified with 3.0% LLDPE

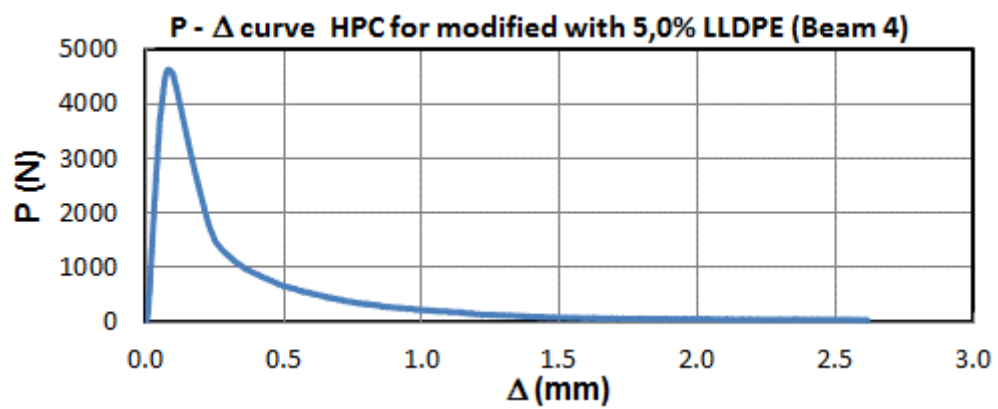
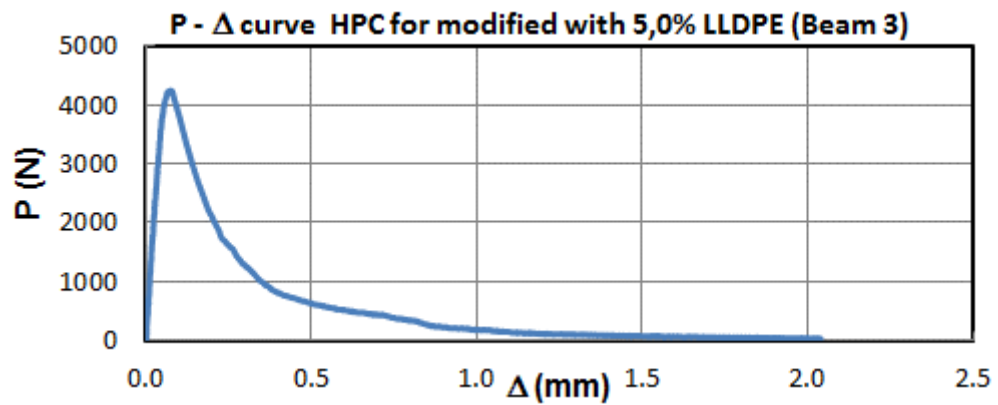
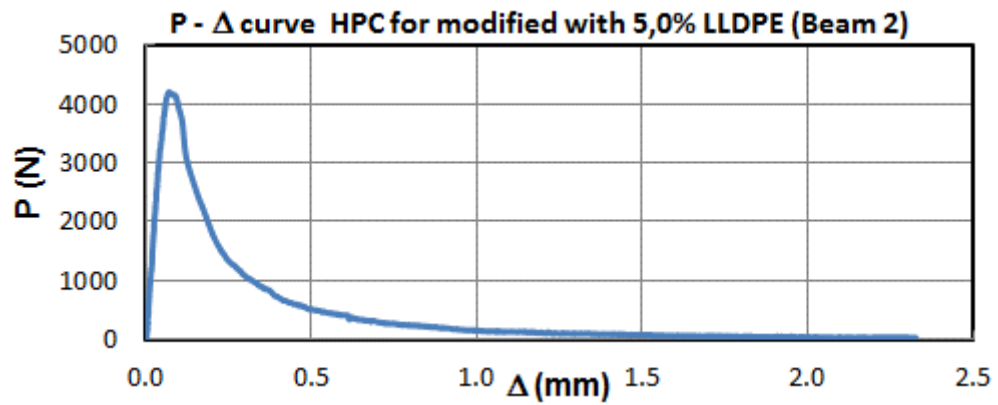
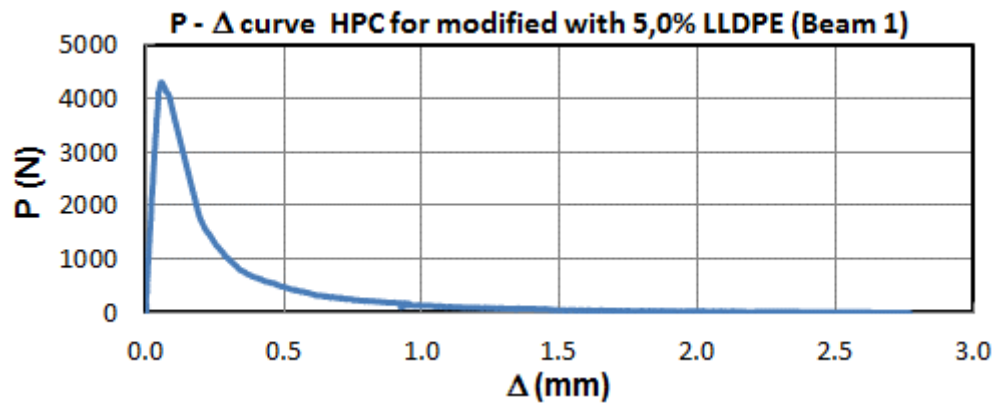


Figure B-10 Load – displacement curves for the HPC modified with 5.0% LLDPE

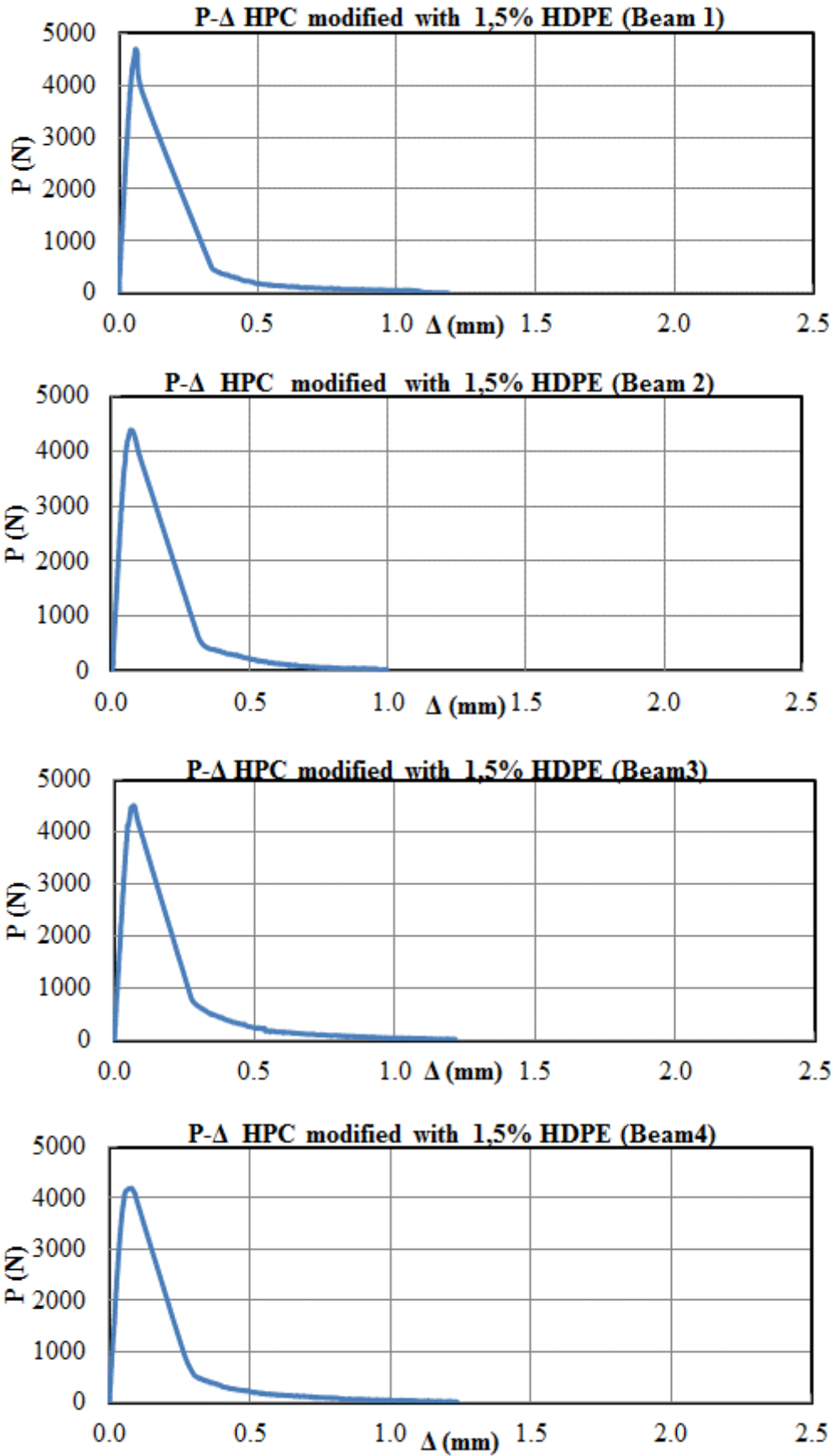


Figure B-11 Load – displacement curves for the HPC modified with 1.5% HDPE

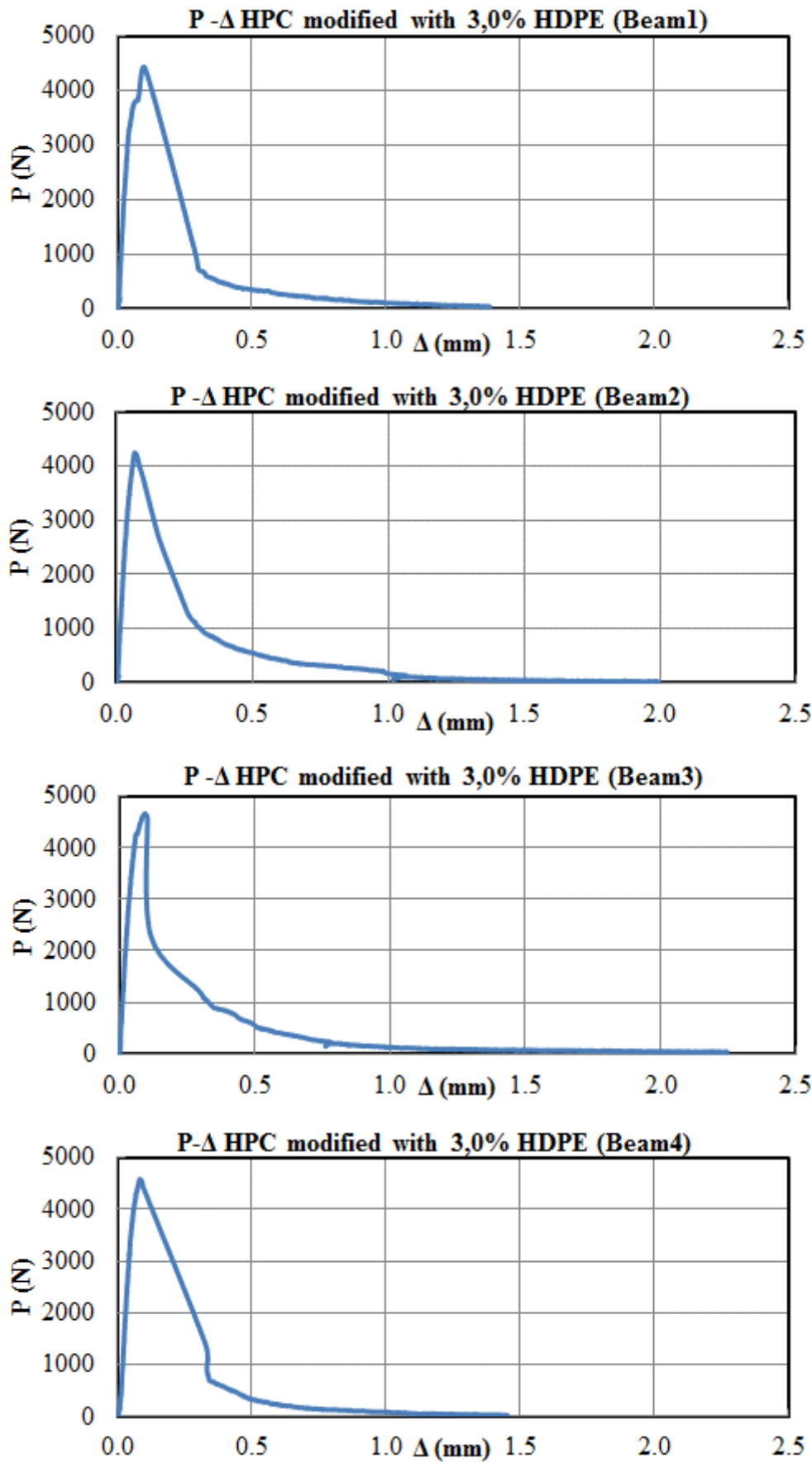


Figure B-12 Load – displacement curves for the HPC modified with 3.0% HDPE

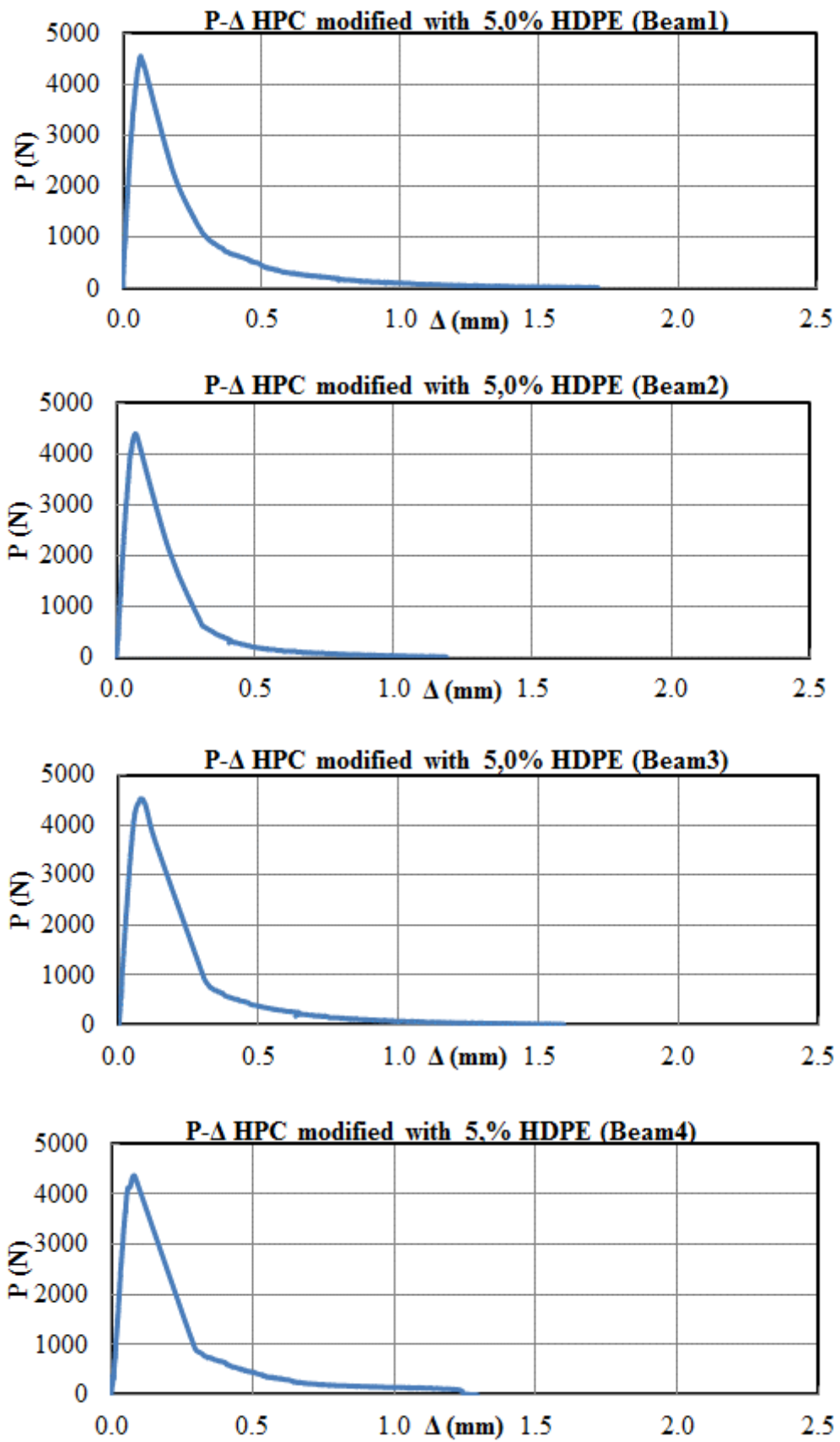


Figure B-13 displacement curves for the HPC modified with 5.0% HDPE